Development of novel monolithic matrices for drug delivery using conventional and non-conventional polymer processing technologies

being a thesis submitted for the degree of

Doctor of Philosophy

to the

Higher Education and Training Awards Council

by

John G. Lyons, BEng.,

Based on the research carried out under the supervision

of

Dr. Clement L. Higginbotham and Mr. Paul Blackie

Centre for Nanotechnology and Materials Research,
Department of Polymer Engineering,
Athlone Institute of Technology,
Athlone.

February, 2007

Declaration

I hereby declare that this thesis submitted to the Higher Education and Training Awards Council for the degree of Doctor of Philosophy, is a result of my own work and has not in the same or altered form, been presented to this institute or any other institute in support for any degree other than for which I am now a candidate.

John Lyons (Date)

"If we knew what it was we were doing,
it would not be called research, would it?"

Albert Einstein *1879-1955*

Acknowledgements

Firstly, and most importantly, I would like to take this opportunity to thank Dr. Clement Higginbotham and Mr. Paul Blackie for stepping in and taking over as my supervisors. Paul's expertise, advice and technical know how were invaluable and very much appreciated (and I think he took up the hill walking to get away from me). I'd like to thank Clem for his friendship and leadership while I completed this thesis. I would never have got this far without him and I can only hope this experience hasn't put him off supervising PhD students for life!

I would like to thank Dr. Sinéad Devery, Oilbhe Lawlor and Dominic Kirf for performing cytotoxicity and genotoxicity testing.

Thank you to the technicians and support staff throughout the college, but particularly Eddie and Michael for their help, hindrance, comic relief, arguments, shouting matches and out of date booze.

Special thanks to the employees of Pharmaplaz Ltd, particularly Mark McGoldrick and Dr. Joe Geever for all their help.

I would like to thank all the postgrad students at A.I.T., both past and present, who have helped or encouraged me throughout my (extended) stay in the college. I would especially like to thank my colleagues, Mark Hallinan, James Kennedy, Luke Geever, Thomas O Gloinn and Declan Devine (PUCK!), who have made my time here both enjoyable and at times excruciating. Their humour, camaraderie and friendship made the time I spent in Athlone pass quickly and enjoyably (which is probably why it took me so long to finish the PhD), cheers lads!

I would like to thank all my family, especially my parents John and Maureen for helping me through college, the gruesome twosome that are my sisters Christine and Lisa for all their encouragement, my grandmother Eileen for years of love and support, and of course my Aunt and Uncle; Bernie and Francis for their help (financial and otherwise!!!) throughout my time in college.

I would like to thank my girlfriend Mary for her unconditional love, and support (and for not having me committed despite the many provocations I have given her over the last couple of years). You are amazing, I love you.

Finally, I would like to thank Dr. Alan Brazier, Alan started my research in A.I.T., his presence, friendship, humour and expertise has been sorely missed these last few years. May he rest in peace.

Table of Contents

Chapter 3: Results and Discussion

Chapter 4: Conclusions

References

Appendices

Relevant publications

Abstract

The aim of this study was to produce a range of polymer based monolithic matrices for controlled oral drug delivery using conventional polymer processing equipment. Poly (ethylene oxide) (PEO) was chosen as the primary matrix forming polymer for the work described herein. The molecular weight of the matrix forming polymer was found to play a substantial role not only in the processing of the polymer but also in modulating the release rate of an active agent from the dosage form. PEO was found to be thermally and chemically stable when exposed to both multiple processing operations in conventional extrusion equipment and extended storage.

PEO was melt blended with poly(e-caprolactone) (PCL) to investigate the effect of the addition of a second biodegradable polymer to the monolithic matrix. Dissolution studies indicated that the drug release from PEO / PCL blends could be modulated by altering the ratio of PEO to PCL present in the blend. PCL was found to improve the processability of the matrix. The processing parameters used during manufacture of the monolithic matrices were seen to have little effect on the end properties of the drug delivery devices. Blends of PEO and Eudragit were melt processed using a supercritical fluid (SCF) assisted process. The use of SCF in the extrusion of monolithic matrices was found to have several benefits when compared to conventional extrusion. Dissolution analysis showed that the use of supercritical CO_2 during the extrusion process resulted in a faster dissolution of drug when compared with unassisted extrusion. μTA also showed that the use of SCF in the processing operation had an effect on the morphology of the resultant polymer matrix. The supercritical CO_2 incorporation also resulted in reduced viscosity during processing, therefore allowing for quicker throughput and productivity.

The effect of novel filler materials on monolithic matrices produced from hot melt extrusion was also investigated. Agar and microcrystalline cellulose were used as the filler materials in varying ratios, to examine the effect of filler content as well as filler type on the properties of hot melt extruded matrices. Rheological analysis concluded that the fillers used resulted in an increase in the matrix viscosity. Thermal analysis showed negligible effects on the melting behaviour of the matrix as a result of the filler inclusion. Dissolution analysis showed that the presence of the fillers resulted in a slower release rate of an active pharmaceutical ingredient (API) than for the matrix alone. Initial cytotoxic and genotoxic testing carried out indicated that the agar filler systems were suitable for biological contact. In addition to agar and microcrystalline cellulose, an organically modified layered silicate was also investigated as a filler material at various levels of inclusion. Mechanical analysis indicated that the nanoclay filler incorporation resulted in an increase in all of the mechanical properties of the matrix. Dissolution analysis showed that the presence of the filler particles resulted in a slower release rate of API than for the matrix alone.

Finally, matrices were manufactured using micro-moulding equipment and compared to matrices produced by ram injection moulding and by extrusion alone. Processing of the matrices selected showed that not all of the materials were capable of being processed in conventional screw-type injection moulding equipment. However, all of the materials could be processed using ram-type injection moulding equipment. Different drug release profiles were successfully achieved using the various materials, including pH sensitive and pH insensitive drug release. These matrices could easily be combined within a single capsule to deliver a range of release profiles for a single API or to deliver more than one API to targeted regions along the GI tract.

Abbreviations

μMDTA	Micro modulated thermal analysis
μTA	Micro thermal analysis
μTMA	Micro thermomechanical analysis
ΔH	Heat of fusion
AFM	Atomic force microscopy
API	Active pharmaceutical ingredient
AUC	Area under the curve
BrdU	Bromodeoxyuridine
CAB	Cellulose acetate butyrate
CPM	Chloropheniramine maleate
ddH_2O	Double distiled water
DMEM	Dubecco's modified essential medium
DMSO	Dimethyl sulfoxide
DNA	(Deoxy) ribonucleic acid
DSC	Differential scanning calorimetry
ECACC	European Cell and Culture Collection
EDTA	ethylenediaminetetraacetic acid
ETC	Environmental test chamber
EVAC	Poly (ethylene-co-vinyl acetate)
FCS	Foetal calf serum
FTIR	Fourier transform Infrared spectroscopy
GI	Gastrointestinal

HDT	Heat distortion temperature
HLB	Hydrophilic-lipophilic balance
HPMA	Hydroxypropyl methacrylamide
HPMC	Hydroxy propyl methyl cellulose
ISO	International standards organisation
LDH	Lactate dehydrogenase
LFM	Lateral force microscopy
LMP	Low melting point
LUD	Left ventricular dysfunction
MCC	Microcrystalline cellulose
MDSC	Modulated differential scanning calorimetry
MI	Myocardial infarction
MMT	Montmorillonite
MTT	3-(4,5-dimethylthiazol-2yl)-2,5-diphenyl-2H-tetrazoliumbromid
Mw	Weight average molecular weight
OMLS	Organically modified layered silicate
PA	Poly (amide)
PBS	Phosphate buffered saline
P_c	Critical pressure
PCL	Poly(e-caprolactone)
PDLA	Poly(D-lactic acid)
PE	Poly(ethylene)
PEG	Poly(ethylene glycol)
PEO	Poly(ethylene oxide)

PET	Poly(ethylene terephthalate)
PLA	Poly(lactic acid)
PMMA	Poly(methylmethacrylate)
PTFE	Poly(tetrafluroethylene)
PVA	Poly(vinyl alcohol)
PVAc	Poly(vinyl acetate)
PVC	Poly(vinyl chloride)
RPM	Revolutions per minute
SEM	Standard error of mean
SMA	Styrene–co-maleic anhydride copolymer
SPM	Scanning probe microscopy
T_c	Critical temperature
T_g	Glass transition temperature
T_m	Melting temperature
TPGS	Alpha-tocopheryl polyethylene glycol succinate
UDS	Unscheduled DNA synthesis
USP	United States pharmacopia
UV	Ultra violet

List of Figures

Chapter 1: Introduction

Chapter 2: Experimental Details

Chapter 3: Results and Discussion

List of Tables

Chapter 1: Introduction

Chapter 2: Experimental Details

Chapter 3: Results and Discussion

Chapter 1

Introduction

1.1 Biomaterials

The term biomaterial has been used to describe materials derived from biological sources or to describe materials used for therapies in the human body other than food or drugs (Egan and Waterman, 1998). A biomaterial is a non-viable material used in a medical device intended to interact with biological systems. They may be distinguished from other materials in that they possess a combination of properties, including chemical, mechanical, physical and biological properties that render them suitable for safe, effective and reliable use within a physiological environment (Williams, 1987). Biomaterial applications date back thousands of years with the Romans, Chinese and more recently the Aztec, all commonly using gold in dentistry. Furthermore, artificial eyes, ears, teeth and noses were found on Egyptian mummies (Williams and Cunningham, 1979).

The use of biomaterials did not become practical until aseptic surgical techniques were developed by Joseph Lister in 1865 (cited in Das, 2000). The presence of biomaterial implants can exacerbate infections as the implant can provide a region inaccessible to the body's immunologically competent cells. Work to counteract this response has been carried out by Modak *et al.* (1990) and has led to a patent that enables medical devices to have anti-infective agents to be impregnated onto their surfaces. The earliest successful implants were in the skeletal system and this still accounts for a large portion of modern biomaterial implants. Bone plates were introduced in the early 1900s to aid the fixation of fractures. Many of these early plates broke as a result of unsophisticated mechanical design. It was also discovered that materials such as vanadium steel corrode rapidly in the body despite initially being chosen because of their superior mechanical properties (Ratner, 1996).

Biomaterials uses include the replacement of body parts that have lost functionality due to disease or trauma, to assist in healing, to improve function, and to correct abnormalities. Advances in many areas of medicine have influenced the role of biomaterials considerably. For example, with the advent of antibiotics, infectious disease is less of a threat than in former times, so that degenerative disease assumes a greater importance. Moreover, advances in surgical technique have permitted materials to be used

in ways that were not possible previously (Park and Lakes, 1992). Table 1.1 outlines a selection of commercially available biomaterials and their uses.

Table 1.1 *Selected biomaterials and their uses.*

Material	Principal Applications
Metals and alloys	
316L stainless steel	Fracture fixation, stents, surgical instruments
Cp-Ti, Ti-Al-V, Ti-Ai-Nb, Ti-13Nb-13Zc, Ti-Mo-Zr-Fe	Bone and joint replacement, fracture fixation, dental implants, pacemaker encapsulations
Co-Cr-Mo, Cr-Ni-Cr-Mo	Bone and joint replacement, fracture fixation, dental implants, dental restorations, heart valves
Ni-Ti	Bone plates, stents, orthodontic wires
Gold alloys	Dental restorations
Silver product	Antibacterial agents
Platinum and Pt-Ir	Electrodes
Hg-Ag-Sn amalgam	Dental restorations
Ceramics and glasses	
Alumnia	Joint replacements, dental implants
Zirconia	Joint replacements,
Calcium phosphates	Bone repair and augmentation, surface coatings on metals
Bioactive glasses	Bone replacements
Porcelain	Dental restorations
Carbons	Heart valves, percutaneous devices, dental implants
Polymers	
Poly(ethylene)	Joint replacements
Poly(propylene)	Sutures
Poly(ethylene terephthalate)	Sutures, Vascular prosthesis
Poly(amide)	Sutures
Poly(tetrafluroethylene)	Soft-tissue augmentation, vascular prosthesis
Poly(ester)	Vascular prosthesis, drug delivery systems
Poly(urethane)	Blood contacting devices
Poly(vinyl chloride)	Tubing
Poly(methyl methacrylate)	Dental restorations, intraocular lenses, joint replacements (bone cement)
Silicones	Soft-tissue replacements, opthalmology
Hydrogels	Opthalmology, drug delivery systems
Composites	
BIS-GMA-quartz/silica filler	Dental restorations
Poly(methyl methacrylate)-glass fillers	Dental restorations (dental cements)

Polymers remain the most versatile class of biomaterials, being extensively applied in medicine and biotechnology as well as the food and cosmetics industries (Williams, 1987). The use of polymers in the medical field began almost at the birth of the field of polymer science; many early synthetic polymers were employed in experimental surgical studies soon after their invention and many have endured to become staples of clinical practice. In the early 1940s the use of nylon sutures were reported and polymers such as nylon, poly(methylmethacrylate) (PMMA), Dacron poly(ester), and poly(vinyl chloride) (PVC) were reviewed in prominent medical journals for their use in surgery (cited by Rehman *et al*. 1996).

Whereas the original uses of polymers in surgery centred primarily on replacements for connective tissues, a host of new applications are emerging as a result of major advances in the medical sciences. Polymers are now selected so that they serve both the purposes of tissue engineering [degradable] and biosensors [stable] as well as implants [degradable/stable] (Dimitriu, 1996). Current applications for polymers include surgical devices, supporting materials and implants such as the total hip replacement device depicted in Figure 1.1 (Piskin and Hoffman, 1986; Tarcha, 1991; Atala and Mooney, 1997), drug delivery systems with different routes of administration and design (Piskin and Hoffman, 1986; Bickerstaff, 1997), carriers of immobilised enzymes (Young, 1988) and cells (Williams, 1990; Goosen, 1993), components of diagnostic arrays, bioadhesives, and ocular devices.

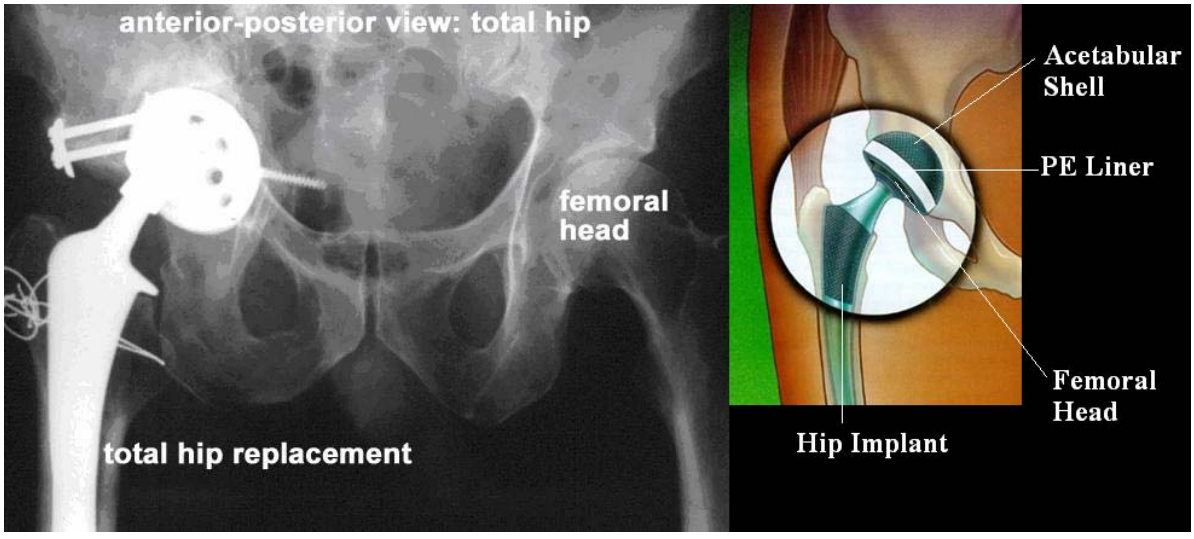

Figure 1.1 *Diagram detailing a device for total hip replacement (adapted from the national health museum resource centre).*

Polymers used as biomaterials can be synthesised to have appropriate chemical, physical, interfacial and bio-mimetic characteristics which permit various specific applications. Compared with other biomaterials such as metals and ceramics, polymers offer the advantage that they can be prepared with a wide variety of structures and properties. Polymers used as biomaterials can be naturally occurring, synthetic or a combination of both.

1.2 Biocompatibility

Biocompatibility is a multidimensional concept, which escapes easy definition. In general, an ideal biomaterial would not induce an inflammatory response, would resist bacterial colonisation and would promote normal differentiation in the surrounding tissues. Specific requirements for biocompatibility vary with the application and site of implantation and may conflict. For stable tissue integration, surface modification to promote cell adhesion is desirable. For fluid contacting applications, the reverse is true: biocompatibility may be significantly impaired by cell adhesion (Williams, 1987).

Polymer biocompatibility refers to the reaction of polymers with blood, tissue and biological bodily fluids, depending on the site and purpose of use. A response in a host organism is generally unfavourable unless vascularistion is required to support living cells. For blood contacting applications, biocompatibility is determined largely by specific interactions with blood and its components. For applications not involving blood contact (e.g. dental work) the choice of biomaterial generally depends on its tissue biocompatibility. Indeed, a material may be biocompatible in one application and bio-incompatible in another (Langer, 1990). For sustained release drug delivery applications the polymer biomaterials used are generally biocompatible and biodegradable.

1.3 Biodegradable Polymers

Over the past decade the use of biodegradable polymers for the administration of pharmaceuticals and implantation of biomedical devices has increased dramatically. The most important biomedical applications of biodegradable polymers are in the areas of controlled drug delivery systems (Holy and Fialkov, 2003) and in the forms of implants and devices for bone and dental repairs (Chasin and Langer, 1990; Ma and Zhang 2001).

Biodegradable polymers can be either natural or synthetic. In general, synthetic polymers offer greater advantages than natural ones in that they can be tailored to give a wider range of properties (Uhrich, 1999). The general criteria for selecting a polymer for use as a degradable biomaterial are to match the mechanical properties and the degradation rate to the needs of the application. Historically, homopolymers such as the poly(ester)s were first in the discovery process for synthetic biomaterials due to their availability (Miller and Shanks, 2001). As properties are defined and utilised from homopolymer systems, copolymer systems emerge that combine and merge desired function for more effective systems.

Poly(D-lactic acid) (PDLA) is a biodegradable polymer with extensive medical applications due to its biodegradable properties and its proven nontoxic effects in the human body. PDLA has been used as a substrate material for potential applications in nerve regeneration in the field of tissue engineering. Poly(e-caprolactone) (PCL), an aliphatic poly(ester), is one of the most important biodegradable polymers in medicine. Due to the chiral nature of lactic acid, several distinct forms of polylactide exist. Copolymers based on poly(lactic acid) and poly(glycolic acid) also offer tuned degradability and have therefore found extensive use in the fabrication of tissue seeded constructs (Tarcha, 1991). Some of the applications of PCL are sutures and biocompatible medical devices. Poly(vinyl alcohol) (PVA) is used in a wide range of applications such as adhesives, fibres, textile, paper-sizing, and water-soluble packaging. It is also used to modify the degradation profile of other polymers (Armani and Liu, 2000; Kishida, 2002). Polymer hydrogel materials (three-dimensional, hydrophilic, polymeric networks capable of imbibing large amounts of water or biological fluids) have also found extensive use in the medical field in a variety of applications including diagnostic, therapeutic, and implantable devices; for example controlled release drug delivery systems (Graham, 1990; Bazel and Peppas, 1996; McNair, 1996; Aikawa *et al*. 1998; Grass *et al.* 2000; Ruel-Gariépy *et al.* 2000) and tissue engineering (Nguyen and West, 2002).

Biodegradable materials possess chemical functionalities that are unstable within living environments, e.g. anhydride, ester or amide bonds. The most common routes of biodegradation *in vivo* are hydrolysis and enzymatic cleavage resulting in scission of the polymer backbone. Biodegradable polymers with ‘hydrolysable’ groups incorporated in the

backbone chain, which are susceptible to degradation to low molecular weight non-toxic products, have also been extensively investigated for drug delivery applications (Blaine, 1946; Williams and Cunningham, 1979; Park and Lakes, 1992). Biodegradation is frequently a desirable property for controlled release applications because metabolism and excretion of the polymer results in its complete removal. Poly(ester)s, poly(anhydride)s, poly(amide)s, and natural polymers, as well as networks, copolymers, blends and microcapsules based on these polymers have all found use as biodegradable matrices for the release of bioactive substances (Piskin and Hoffman, 1986; Tarcha, 1991; Bickerstaff, 1997; Miller and Shanks, 2001).

1.4 Polymer based controlled drug delivery

Controlled drug delivery occurs when a polymer, whether natural or synthetic, is judiciously combined with a drug or other active agent in such a way that the active agent is released from the material in a pre-designed manner (Peppas, 1997). Traditionally, delivery systems have not incorporated means of controlled release. The problem, however, is that with each dose of a non-controlled release drug, the concentration of drug available to the body immediately peaks and then declines rapidly.

With conventional dosage forms, high peak blood concentrations may be reached soon after administration with possible adverse effects related to the transiently high concentration. An example is hypotension in patients taking rapid-release nifedipine products. Recently, the development of tablets which can be swallowed and thereafter slowly release the drug in the gastrointestinal tract has gained great interest. There are currently many different nomenclatures available for the aforementioned dosage forms, such as slow release, prolonged release, sustained release and extended release. The term extended release has been adopted by the European Pharmacopiea as the denominator for this type of device. Various release profiles from such devices are depicted in Figure 1.2. The release pattern may vary from continuous to two or more pulses (Alderborn and Aulton, 2002).

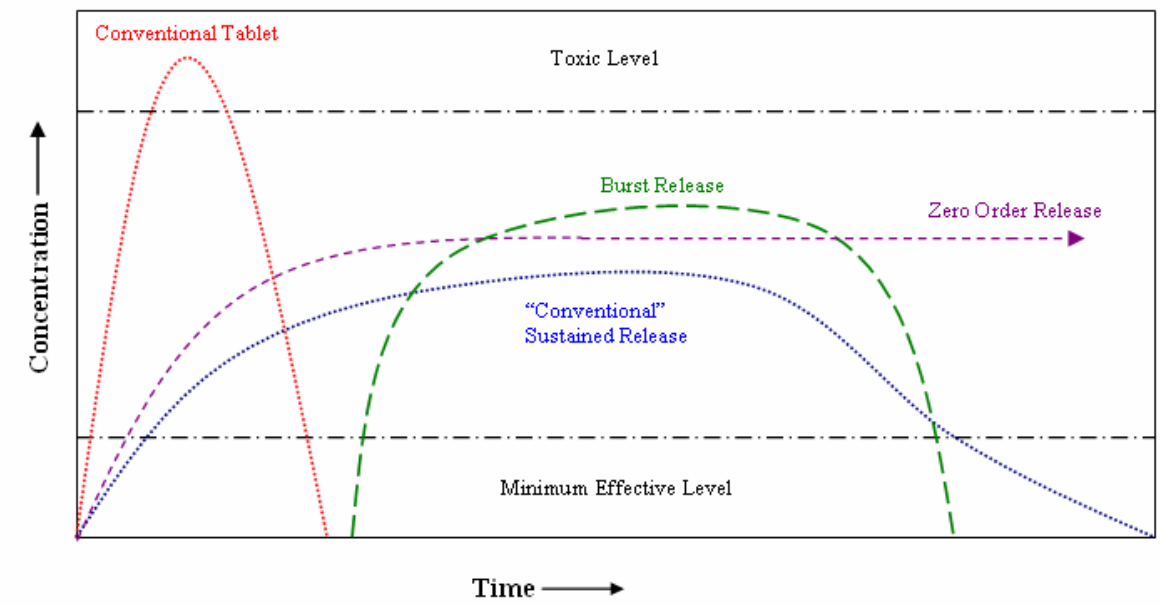

Figure 1.2 *Graph showing the concentration of active agent in blood plasma as a function of time.*

The use of an extended-release product avoids the high initial blood concentrations which cause the sudden reduction in blood pressure and other significant haemodynamic changes such as reflex tachycardia. Another example is the transient nausea at sub-toxic concentrations which results from the local irritation caused by high intestinal concentrations of some conventional-release products such as theophylline. It is desirable to release drugs at a constant rate, thereby maintaining drug concentration within the therapeutic range and eliminating the need for frequent dosages. The goal of an extended-release dosage form is to maintain therapeutic blood or tissue levels of the drug for an extended period and have a zero order release pattern (the amount of drug released is independent of the amount of drug in the system), while simultaneously allowing control over the spatial targeting of the drug. Providing control over the drug delivery can be the most important factor at times when traditional methods of drug delivery cannot be used. These include situations requiring the slow release of water soluble drugs, the fast release of low solubility drugs, drug delivery of two or more agents with the same formulation, and systems based on carriers that can dissolve or degrade and be readily eliminated.

Oral controlled delivery systems are often broadly classified in terms of the mechanism of drug release. Several modes of drug release from oral controlled drug delivery systems exist.

A) Polymer–drug conjugates

In this type of controlled drug delivery system, the active agent is covalently bound to the macromolecular backbone through a labile bond. This type of delivery system is particularly attractive because it is designed on a molecular basis. However, despite the high degree of versatility this approach offers, it is difficult to find marketed products mainly because these conjugates are viewed as new drug molecules and the path needed for regulatory approval is arduous and expensive. The conjugation sites may be at one or both ends of the macromolecule or they may be pendant to the main chain, with the sites repeating along the backbone (Hoffman, 1998).

B) Pendant chain systems

This type of delivery system requires that the active agent molecules are covalently attached to the main polymer chain via degradable spacer linkages to sterically facilitate hydrolysis and the release of the active agent or to provide groups that allow an enzymatic specific recognition. The original polymeric carrier, or the final residue, must be, in general, water-soluble and clearable by normal bodily processes. It is now accepted that chains with molecular weights below 30–50,000 (depending on the nature of the polymer) are amenable to renal elimination (Seymour, 2002). The support must also be non toxic and non immunogenic. Numerous conjugated systems have been designed and investigated. Particularly relevant are two conjugates, based on the work of Duncan and Kopecek (1984) and Maeda *et al*. (1992), currently used in clinics, based on hydroxypropyl methacrylamide (HPMA) and styrene–co-maleic anhydride (SMA) copolymer, respectively.

C) End-group systems

This approach finds important applications in protein pegylation, that is, the conjugation of poly(ethylene glycol) (PEG) to protein drugs to protect them from recognition by the body's immune system and to prolong their circulation time in the body, as it was originally described by Abuchowski *et al*. (1977). There are several companies marketing different PEG–protein or PEG–drug conjugates for the treatment of cancer, hepatitis, etc.

D) Diffusion controlled release systems

Two types of diffusion-controlled systems have been developed; the first is a reservoir device in which the active agent forms a core surrounded by an inert diffusion barrier. These systems include membranes, capsules, microcapsules, liposomes, and hollow fibres. The second type is a monolithic device in which the active agent is dispersed or dissolved in an inert polymer. As in reservoir systems, drug diffusion through the polymer matrix is the rate-limiting step, and release rates are determined by the choice of polymer and its consequent effect on the diffusion and partition coefficient of the drug to be released. Alderborn and Aulton (2002) describe the release of an active agent from such a device in two steps:

- The liquid that surrounds the device penetrates the dosage form and dissolves the active agent, thus establishing a concentration gradient between the interior of the release device and the exterior liquid.

- The release of the active agent occurs as the dissolved drug diffuses in the pores of the release device or in the surrounding membrane.

To obtain a constant rate of drug release in reservoir devices, maintaining constant area of diffusion, path length, concentration and diffusion coefficient is necessary. This does not always happen in real practice as one or more terms change and sometime non-zero order release of drugs is possible. Common methods used to develop reservoir type devices are micro-encapsulation and press coating of tablets containing a drug core. Drug release from these types of systems is usually a combination of diffusion and dissolution (Figure 1.3). Materials, which are commonly used, include gelatin, methyl or ethyl cellulose and various waxes. In the matrix devices, solid drug is assumed to dissolve in the surface layer first. When this layer becomes exhausted, the next begins depleting.

Three major types of materials are generally used for the preparation of these devices: insoluble plastics, hydrophilic polymers and fatty compounds (Lee and Robinson, 2000).

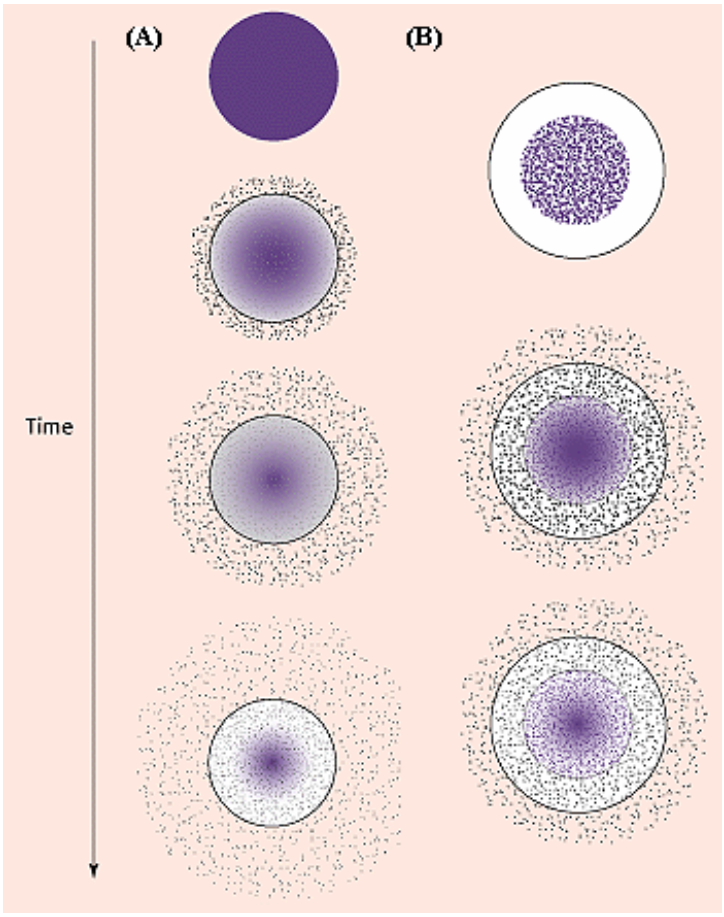

Figure 1.3 *Diagram showing drug release from (A) a typical matrix type device and (B) a typical reservoir type device.*

E) Dissolution controlled release

In dissolution controlled extended release devices, the rate at which the active agent dissolves in the gastrointestinal juices is the release controlling process. In dissolution systems, a drug with a slow dissolution rate can provide sustained drug levels. This makes possible preparation of good controlled release products by controlling the dissolution rate of drugs that are highly water-soluble. This can be done by preparing a suitable salt or by coating the drug with a slowly soluble material.

The dissolution system can be considered diffusion-layer controlled, where the rate of diffusion from the solid surface to the bulk solution through an un-stirred liquid film is the rate-determining step.

Two main types of systems exist in which dissolution determines the rate of release of the drug. These are encapsulated dissolution systems and matrix dissolution systems. Encapsulated systems can be prepared either by coating the particles or granules of drug with varying thicknesses of slowly soluble polymers or by micro encapsulation. Different natural and synthetic polymers are used as coating materials. The choice depends on the type of drug and release characteristics of drug and polymer. The most commonly used materials are ethyl cellulose, carnuba wax, shellacs, and gelatin (Linharat, 1989).

F) Erosion controlled extended release devices

In erosion controlled extended release devices the rate of drug release is controlled by the erosion of a matrix in which the active agent is dispersed. This may occur by one of the following two routes (Alderborn and Aulton, 2002):

1. In bulk erosion, the rate of water penetration into the solid device exceeds the rate at which the polymer transforms into water soluble materials. As the water enters the polymer, erosion transpires throughout the whole volume. Cracks and crevices form in the polymer, and it rapidly disintegrates. Meanwhile, the drug diffuses out of the polymer as more and more cracks are formed in the material. For bulk erosion, there are two stages in the release mechanism. The first stage is dictated by the hydrolysis of the drug or how much water is diffusing into the polymeric device. The second stage involves the diffusion of the drug through the polymeric matrix.

2. Surface erosion presents a different outlook. The rate at which water enters the polymer device is less than the rate of polymer transformation to water-soluble materials. The surface area of the polymer matrix limits the process. In time, the device becomes thinner while maintaining its structural integrity. To achieve this condition, the polymer needs to have a certain degree of hydrophobicity.

Scanning electron microscopy micrographs demonstrating both erosion mechanisms are presented in Figure 1.4.

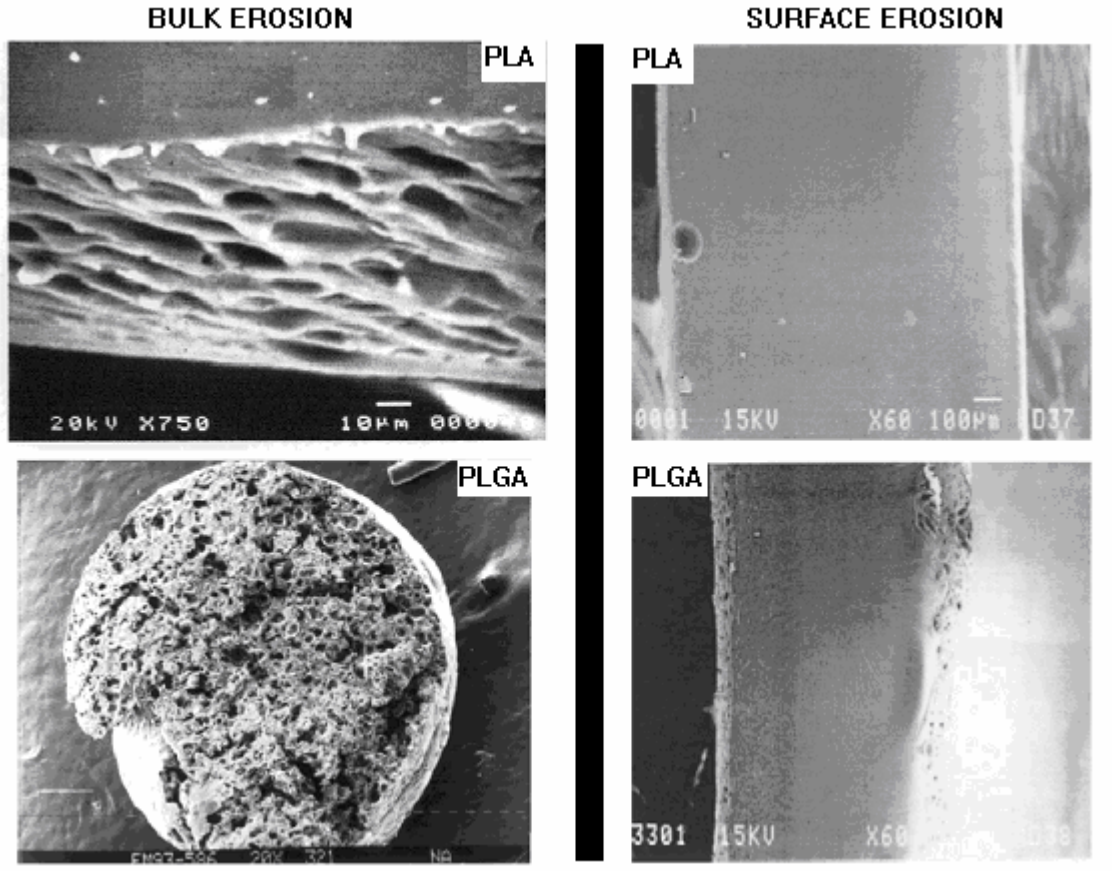

Figure 1.4 *Scanning electron micrographs of PLA and PLGA polymer samples undergoing bulk or surface erosion by altering degradation conditions (adapted from Agrawal and Athanasiou, 1997).*

1.5 Monolithic matrix devices

Monolithic devices or matrices represent a substantial part of available drug delivery systems. Matrix systems are prepared by dispersing the active agent in a slowly soluble polymer carrier. These devices are traditionally designed as single unit systems (monolithic systems). Matrices containing swellable polymers are referred to in the literature as hydrogel matrices (Bettini *et al*. 1994), polymeric matrices involving moving boundaries (Lee, 1981), swellable controlled release systems (Korsmeyer *et al.* 1983), hydrocolloid matrices or hydrophilic matrix tablets (Ranga Rao and Padmalatha Devi, 1988; Bettini *et al.* 1995; Colombo *et al.* 1995). They are generally made up of a blend of drug and one or more hydrophilic polymers. In general drug release from swellable matrix

tablets is based on glassy-rubbery transition of polymer as a result of water penetration into the matrix.

Whereas interactions between water, polymer and drug are the primary factors for release control, various formulation variables, such as polymer type, drug/polymer ratio, drug solubility, and drug and polymer particle size, can also influence drug release. The central element of the mechanism of drug release is the gel layer (rubbery polymer) which is formed around the matrix (Lee, 1981; Korsmeyer *et al*. 1983; Colombo *et al.* 1995). The gel layer is capable of preventing matrix disintegration and further rapid water penetration. Water penetration, polymer swelling, drug dissolution and diffusion and matrix erosion are the phenomena determining gel layer thickness. Drug release is also controlled by drug diffusion through the gel layer and/or by erosion of the gel layer. In order to follow gel layer dynamics during drug release in swellable matrices, the boundaries of such a layer have to be defined. It is well known that the gel layer is physically delimited by two sharp fronts that separate-different matrix states, i.e. the boundaries separating swollen matrix from solvent and glassy from rubbery polymer.

The possibility of the presence of a third front inside the gel layer has been described (Colombo *et al*. 1995). This additional front was termed the undissolved drug front or diffusion front and is a function of drug solubility and loading. Its presence can create conditions such that the release will be more controlled by drug dissolution than by polymer swelling. Thus in a swellable matrix tablet, three fronts can be expected:

- The swelling front, the boundary between the still glassy polymer and its rubbery state;
- The diffusion front, the boundary in the gel layer between the as yet undissolved solid drug, and the dissolved drug;
- The erosion front, the boundary between the matrix and the dissolution medium.

1.6 Hot melt extrusion technology

Methods of manufacturing solid dispersions are well documented in the literature; spray drying (Jung *et al*. 1999), co-milling (Nozawa *et al.* 1985; Nozawa *et al.* 1986), co-evaporation, co-precipitation (Sekikawa *et al.* 1978), freeze drying (Sekikawa *et al.* 1983)

and hot spin mixing (Dittgen *et al*. 1995) are just a few relevant examples. Hot melt extrusion represents an efficient manufacturing technology capable of dispersing drugs in a melt up to a true molecular solution of the active agent in a matrix.

Extrusion is the process of converting a raw material into a product of uniform shape and density by forcing it through a die under controlled conditions (Rauwendaal, 1986). Extrusion process technology can be divided into two categories; ram extrusion and screw extrusion. Ram extrusion consists of a positive displacement ram capable of generating high pressures forcing material through a shaping die while screw extrusion consists of a rotating screw or set of screws inside a barrel. Extrusion as a process is a well established manufacturing method. The first extruder is generally accepted to have been built when Joseph Bramah constructed a hand operated piston press for the manufacture of seamless lead pipes in England in 1797 (Lagassé, 2001).

In the following years this technology was adapted to process a range of other materials such as soap, pasta and building materials. Screw extrusion was first developed as a response to the inadequacy of ram extruders in cable covering operations. The first example of a screw extruder can be seen in the 1873 drawing owned by Phoenix Gummiwerke A.G. (Rauwnedaal, 1986). The first use of a twin screw extruder was in the manufacture of sausages by Follows and Bates in England in 1869. The first twin screw extruders for polymer processing were developed in Italy in the 1930s by Roberto Colombo and Carlo Pasquetti (Janssen, 1978; Rauwendaal, 1986). In 1939, Troester developed an extruder that incorporated air cooling, automatic temperature control (using a separate control cabinet), nitride-hardened barrel liner, a length/diameter ratio of 10 : 1, and a variable-speed drive. Figure 1.5 illustrates the relevant parts of a modern extruder screw.

In recent years twin screw extrusion has become a reliable process used in a range of applications particularly in polymer processing. Today, twin screw extruders are used in chemical plants for reactive processing including both polymerisation and grafting reactions. They are also used in post reactive processing steps such as coagulation and devolatilisation. However twin screw extruders find their main use in bulk processing of polymers. This includes compounding of particulates, blending and reactive processing as well as final shaping operations particularly in profile extrusion.

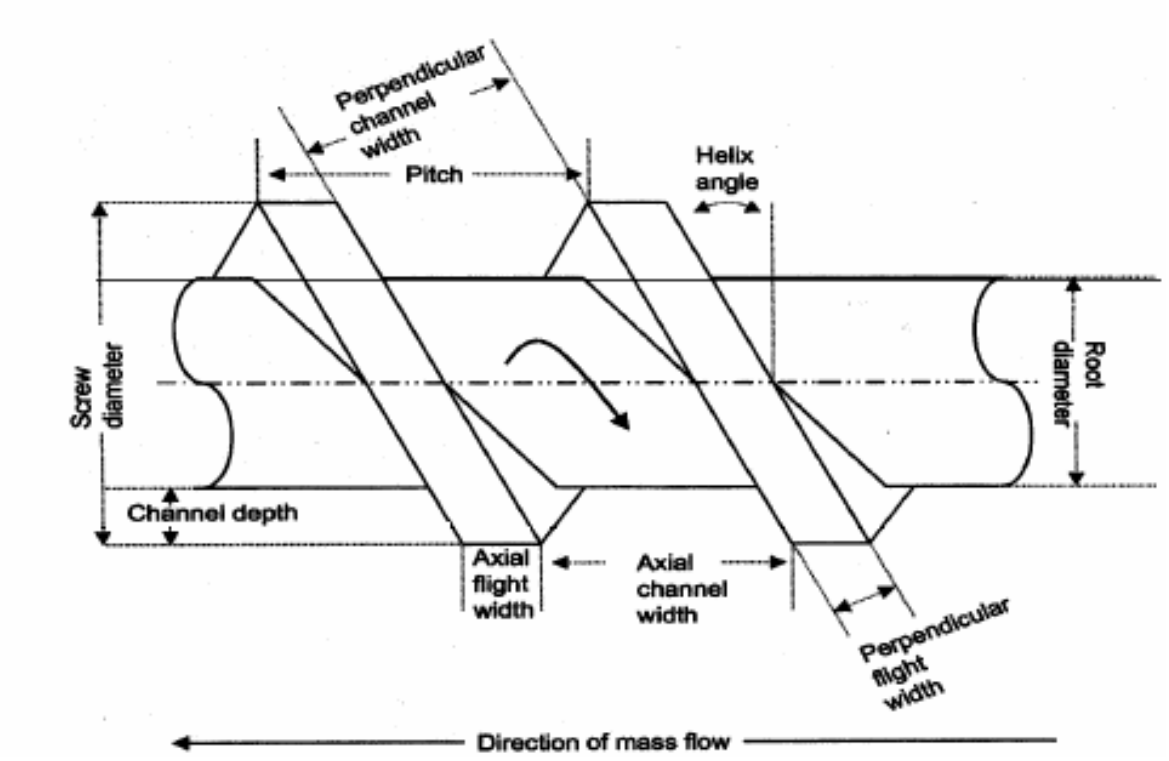

Figure 1.5 *Diagram detailing terms used in relation to screw dimensions (Fisher, 1976).*

Twin screw extruders represent not one technology but several. The screws may be co-rotating or counter-rotating, they may be intermeshing, non-intermeshing or tangential. Intermeshing screws may or may not be self wiping. In each case a separate historical and technological development may be discerned as well as specific advantages and disadvantages. As described by Martelli, twin-screw extruders were first categorised by Erdmenger who classified them in terms of the flow-path of the material within the screws both along and across the channel (1982). Erdmenger categorised multi-screw extruders as either lengthwise open or crosswise open, the former referring to extruders whose material moves on a path open from the inlet to the outlet and moving from the channels of one of the screws to that of the other screw. The latter (crosswise open) referring to extruders where there exists a path across the flights common to both the screws such that the material will move along the channel of one of the screws to two channels of the other screw. This may be logical in theory but in practice, it is difficult to categorise screws in such a manner due to the fact that the flow path of the materials does not depend solely on

the rotational direction of the screws but also on the geometry of the flights and the channel. Figure 1.6 shows the conventional view to classification of twin screw extruders.

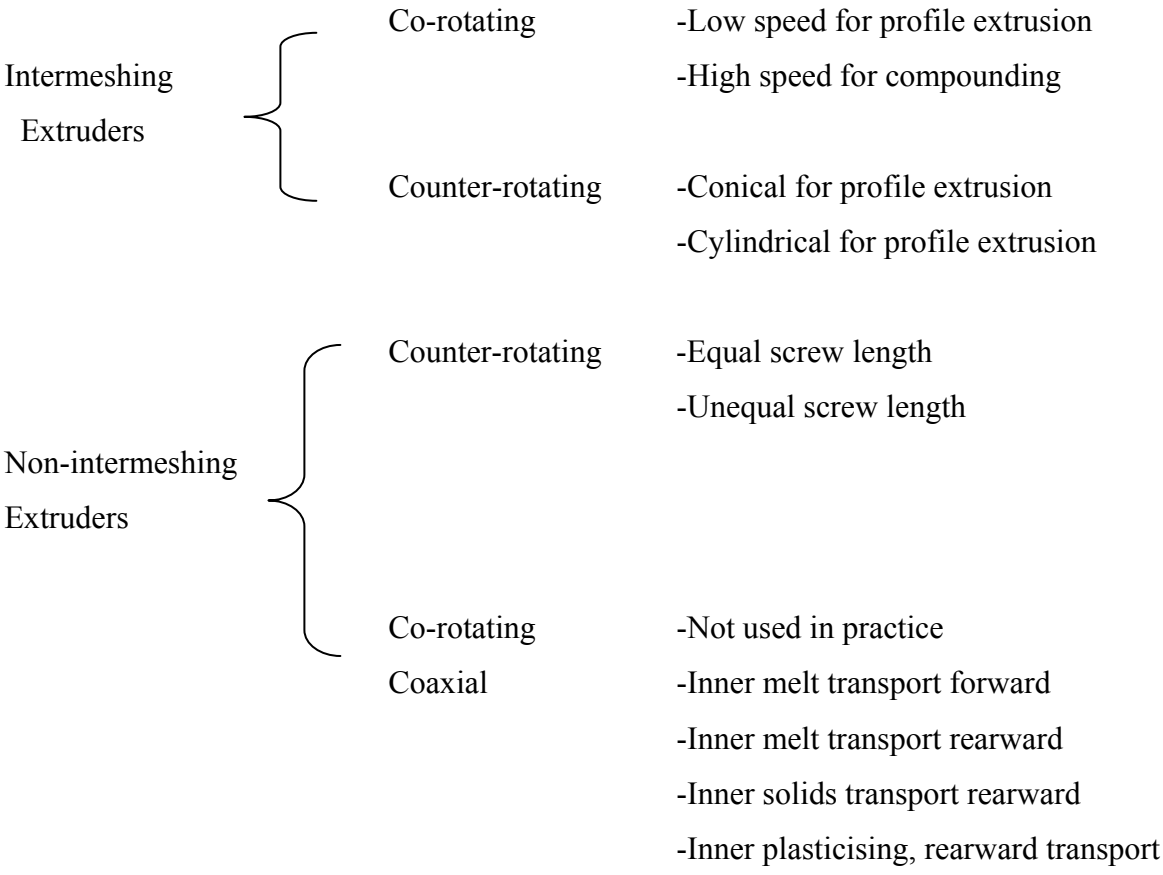

Figure 1.6 *Classification of twin screw extruders (adapted from Rauwendaal, 1986).*

When the two screws in a twin-screw extruder are intermeshing, the distance from the axis of the screws is less than the outer diameter of the screws and the surfaces of the screws are in 'near' contact. Positive conveying of the melt occurs in this configuration. Because of the intermeshing part of one screw not permitting material in the other screw to rotate freely implies that slip at the wall does not occur; this is one of the advantages of such a design. In the non-intermeshing configuration the distance from the axis of the screws is equal to or greater than the outer diameter of the screws and the surfaces of the screws do not have any contact (Janssen, 1987).

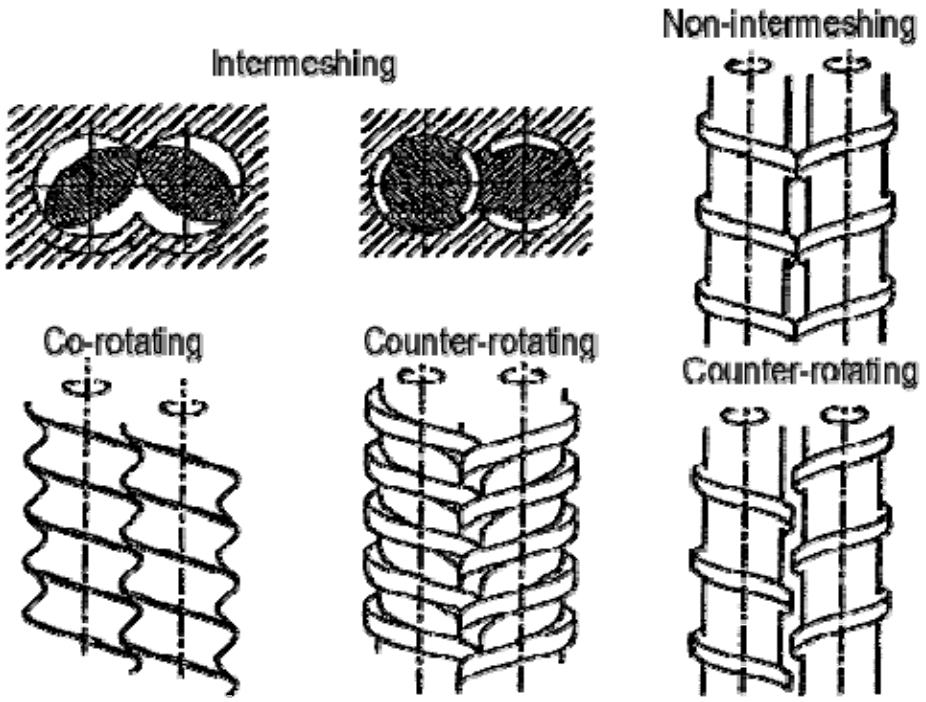

Figure 1.7 *Illustration of various extruder types.*

From the early 1920s to the 1950s patents were gained by Easton, Pease, Colombo, Meksat and Erdmenger which all expressed the mechanisms of operation of fully intermeshing co-rotating extruders (Schenkel, 1966). The surface velocities in the intermesh region for the co-rotating intermeshing twin screw extruder are in opposite directions. With this configuration, materials tend to be wiped from one screw to the other (self wiping), with a comparatively low percentage entering the intermesh gap. Materials tend to follow a figure-eight pattern in the flighted screw regions, and most of the shear is imparted by shear-inducing kneaders in localised regions.

Forward-flighted screw elements are used to convey materials, reverse-flighted screw elements are used to create pressure fields, while kneaders and shear elements are used to mix and melt.

Screws can be made shear intensive or less aggressive based on the number and type of shearing elements integrated into the screw design (Figure 1.8). As the self wiping design allows no material to travel through the nib between the two screws, the highest degree of mixing occurs in the transfer area between the screws with little mixing taking

place around the outside of the screws. Because the flight from one screw cannot clear the other, co-rotation is limited to bi-lobal mixing elements at standard flight depth (Coignet, 1869; Schenkel, 1966).

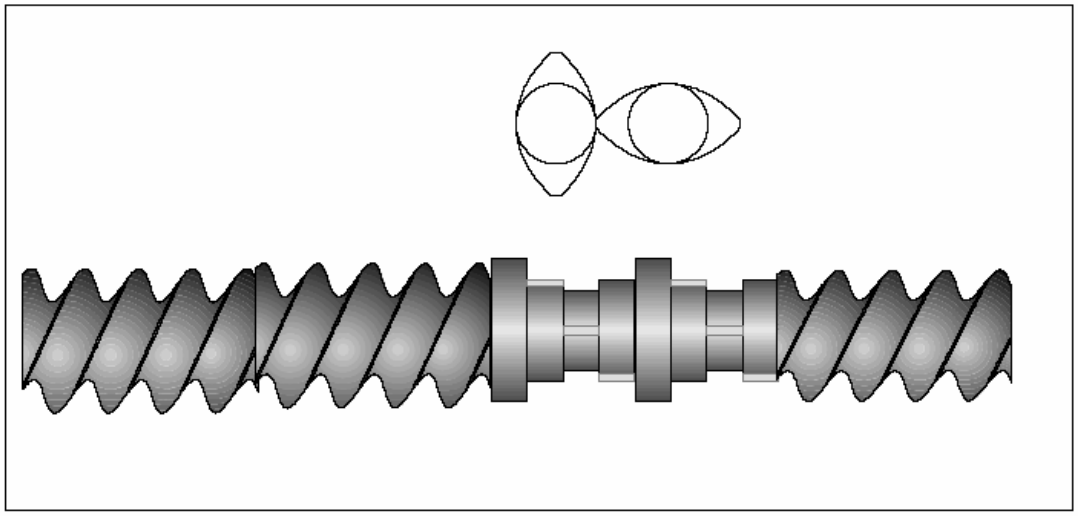

Figure 1.8 *Transporting and kneading elements in the co-rotating twin screw extruder, number of kneading elements: 8, upper image: front view, lower image: side view.*

Extrusion technology is extensively applied in the plastics and rubber industries, where it is one of the predominant fabrication processes. Examples of products fabricated from extruded polymers include piping, insulated wires, catheter components, and plastic and rubber sheeting. The drawbacks associated with extrusion technology generally relate to the high levels of power input required, mainly resulting from the need to produce elevated temperatures and large shear forces. Careful control of process parameters can reduce these drawbacks. The largest application of extrusion in the pharmaceutical industry is in the preparation of granules or pellets of uniform size, shape and density, containing one or more drug substance (Vervaet *et al*. 1995).

1.7 A review of recent literature on the preparation of drug dosage forms by hot melt extrusion.

Hot melt extrusion has not received much attention in the pharmaceutical literature until recently. Cellulose acetate phthalate pellets were prepared using a rudimentary ram

extruder in the late 1960s by Rippie and Johnson (1969) in order to facilitate study of dissolution rates based on pellet geometry. Mank *et al*. (1989, 1990) reported in two contributions on the extrusion of a number of thermoplastic polymers to produce sustained-release pellets.

Sprockel and co-workers (1991) reported a method for preparing a matrix drug delivery system based on melt extrusion method in which the molten materials were forced into a mould to form disks. The disks contained glyceryl fatty acid esters (Gelucire), poly(ethylene glycol) fatty acid esters, or a combination of the two with chlorpheniramine maleate as a model drug. The release of the drug into distilled water, pH 1.2 buffer, and pH 7.5 buffer exhibited square root of time dependence. An increase in the fatty acid ester hydrophilic-lipophilic balance (HLB) from 1 to 14 resulted in a 10-fold increase in the drug release rate. The maximum release rate was seen from the fatty acid ester with a melting point of 44°C. The pH of the dissolution medium had a minimal impact on the rate of drug release. The release rate was modified by blending gelucires of different melting points and HLB values.

Follonier *et al.* (1994) investigated the feasibility of using melt extrusion to produce sustained release pellets. The goal was to create a dosage form using a simple and continuous process. Diltiazem hydrochloride a relatively stable, freely soluble drug was incorporated into polymer based pellets. The polymers studied included ethyl cellulose, cellulose acetate butyrate (CAB), poly(ethyl acrylate / methyl methacrylate / trimethyl ammonio ethyl methacrylate chloride) (Eudragit® RSPM) and poly(ethylene-co-vinyl acetate) (EVAC) and the plasticisers utilised were triacetin and diethyl phthalate. It was found that the release rate of diltiazem hydrochloride was dibasic and that EVAC and CAB gave the slowest release rate. The researchers noted that the type and amount of plasticiser used, drying time of the polymers and extrusion times varied for each formulation. Thermal degradation was emphasised as a limitation of the hot melt extrusion process.

In a follow up study, again by Follonier and co-workers (1995) the authors examined different parameters influencing the release rate of dilitiazem hydrochloride from hot melt extruded pellets incorporated into hard gelatine capsules. Results of the follow on study indicated that release rate of drug was dependant on several critical factors including polymer type, drug/polymer ratio, addition of pore forming additives or hydrophilic

polymers and pellet size. The addition of hydrophilic polymers was used to avoid incomplete drug release due to encapsulated drug clusters trapped in the insoluble matrix. Swelling agents were utilised to reduce the initial burst release from the matrix and various excipients such as croscarmellose sodium (Ac-Di-Sol®) and sodium starch glycolate (Explotab®) were added to the matrix to vary the drug release rate. However the chemical stability of the drug was shown to be a function of processing temperature and residence time in the extruder.

Miyagawa, Sato and co-workers (1996, 1997) described a further application of hot melt extrusion as they studied the mechanism of release from a controlled release matrix containing the drug diclofenac. The authors used a twin-screw compounding extruder to prepare wax matrix granules composed of the model drug and other controlling agents. Their initial investigation showed that a wax matrix with high mechanical strength could be prepared even when processed at temperatures below the melting point of wax. Dissolution profiles of diclofenac from the wax matrix were strongly dependant on the formulation used. The rate controlling additives under investigation in their study were hydroxypropyl cellulose, methacrylic acid co-polymer (Eudragit L-100) and sodium chloride. The advantages of using the twin screw extruder for the processing of the wax matrix was emphasised by the authors due to the capacity for low processing temperatures, high kneading/dispersing ability and low residence time. The authors concluded in their second study (1997), that selection of rate-controlling agents based on physiochemical properties such as solubility and swelling characteristics had a significant impact on the release rate from the wax matrix.

McGinity and Koleng (1997) employed hot melt extrusion for the preparation of rapid release granules. The authors used the extrusion process to granulate acetaminophen and filler excipients with low molecular weight poly(ethylene glycol)s (PEG). The resultant granules were subsequently combined with additional additives such as disintegrants and lubricants and formed into tablets via a traditional compaction method. Drug release from bulk granules and tablets containing 15 to 25% PEG 6000 were compared, with the release from the bulk granules being superior to that of the tablets. Tablets containing 15% PEG released greater than 80% of the incorporated acetaminophen after 30 minutes as required under USP 23 for acetaminophen tablets.

Sprockel and co-workers (1997) continued their previous work utilising a melt extrusion method in which the molten materials were forced into a mould to form disks. The disks formed comprised poly(ethylene), poly(caprolactone), poly(vinyl acetate), and cellulose acetate butyrate with theophylline as a model drug at a 50% loading. The investigators found an 8 fold difference in the effective diffusion coefficient between the various polymers. The effective diffusion coefficient increased 10-fold when the theophylline load was increased from 50 to 70% in the poly(caprolactone) and poly(ethylene) disks. Disks with theophylline content greater than 70% by weight could not be made. Soluble additives such as sucrose, sodium chloride, Pluronic®, and PEG were used to modify the release rate.

The properties of poly(ethylene oxide) (PEO) as a drug carrier were investigated in 1999 (Zhang and McGinity) by studying the release rate of chloropheniramine maleate (CPM) from matrix tablets produced by hot melt extrusion. PEG 3350 was utilised as a processing aid and as a plasticiser. The loading of the drug as well as the molecular weight of the PEO and the inclusion of PEG were all found to contribute greatly to the processing conditions and the rate of release of the drug. In addition, the researchers showed that additional mixing of the components occurred in the barrel of the extruder, since the content uniformity of the extruded tablets was within 99.0% to 101.0% of the theoretical content. As the PEG 3350 concentration increased, the release of CPM from the extruded matrix tablets was found to increase. It was noted by the investigators that the hydration and dissolution rate of the system was accelerated due to the presence of the plasticiser. The rate of drug release was only slightly affected by changes in drug content until the drug loading reached 20%. This study by Zhang and McGinity serves to reinforce the reproducibility of dissolution results from tablets manufactured by hot melt extrusion.

In a further study by Zhang and McGinity (2000) the properties of poly(vinyl acetate) (PVAc) as a retardant polymer and the drug release mechanism of theophylline from matrix tablets formed using hot melt extrusion was investigated. The authors showed that the release rate of drug was dependant on granule size, drug loading and drug particle size which would seem to be consistent with the results discussed previously which were obtained by Follonier *et al*. (1995). As the size of hot-melt extruded theophylline/PVAc granules was increased, there was a significant decrease in the release rate of the drug.

Since the drug was released from the matrix by a diffusion mechanism, the decrease in the drug release rate from the tablets containing larger granules was concluded to be a result of a longer diffusion pathway. Higher drug loading in the matrix also showed higher release rates of drug. PEG 400 and lactose were also demonstrated to be efficient release rate modifiers for their system.

Liu *et al*. (2001) compared the properties of wax granules prepared by two different methods; high shear melt granulation and hot melt extrusion. Blends containing phenylpropanolamine hydrochloride, Precirol®, Sterotex®, and filler excipients; microcrystalline cellulose, lactose and Emcompress® were extruded using a single screw extruder with open end discharge with the extrudates subsequently being passed through a 14-mesh screen to form granules. Granules produced using hot melt extrusion were observed to be less spherical than high shear melt granules and had lower bulk density. Analysis of the hot-melt extruded granules showed better drug content uniformity among granules of different size ranges compared with high-shear melt granules, resulting in a more reproducible drug release from the corresponding tablets. At the same wax level, drug release from tablets decreased in the order of using microcrystalline cellulose, lactose and Emcompress® as the filler excipients. The observed differences in the dissolution properties of the tablets were attributed to the differences in the solubility, swellability and density of the various excipients used.

Hülsmann *et al*. (2000, 2001) used hot melt extrusion to increase the solubility of 17-Estradiol hemihydrate, a poorly water soluble drug. In extensive studies, PEG 6000 and a vinylpyrrolidone / vinylacetate copolymer were used as polymers with Sucroester® WE15 or Gelucire® 44/14 as functional excipients. The extrudate was cut into granules and compressed into tablets. The solid dispersions resulted in a significant increase in dissolution rate when compared with the pure drug or physical mixture.

In the first of two relevant studies Nakamichi and co-workers (2001) utilised nicardipine hydrochloride and hydroxypropylmethylcellulose acetate succinate, in a twin-screw extruder to prepare a floating sustained release dosage form. A puffy dosage form with regular small pores was obtained by adjusting the position of the high-pressure screw elements in the immediate vicinity of the die outlet and by controlling the barrel temperature. The study showed that the puffed dosage form prepared by twin-screw

extrusion, was very efficient as a floating dosage form that was retained for a period of up to 6 hours in the stomach. In the second study Nakamichi *et al*. (2002) also investigated the role of the kneading paddle and the effect of screw revolution on the preparation of a solid dispersion using a twin screw extruder. The investigators concluded that the kneading paddle elements of the screws are instrumental in altering the crystallinity and dissolution properties of a solid dispersion of nifedipine and hydroxypropylmethylcellulose phthalate.

Young and co-workers (2002) used hot melt extrusion to prepare spherical controlled release theophylline pellets. A powder blend of anhydrous theophylline, Eudragit® Preparation 4135 F, microcrystalline cellulose and poly(ethylene glycol) 8000 powder was sieved, blended and then melt-extruded in a Randcastle Microtruder®. The hot-melt extruded pellets were prepared by cutting the extrudate into symmetrical pellets and subsequently spheronizing them in a traditional spheronizer at elevated temperatures. The melt-extruded matrix pellets exhibited diffusion controlled drug release. Solubility of Eudragit® Preparation 4135 F, is pH dependent and as anticipated by the investigators, drug release from the acrylic matrix system was influenced by the pH of the dissolution medium.

In a study similar to the 1997 investigation by McGinity and Koleng; Perissutti and co-workers (2002) investigated the use of hot melt extrusion technology to improve dissolution of carbamazepine. The authors prepared a fast release dosage form containing a poorly water soluble model drug and PEG 4000 as a hydrophilic carrier and low melting binder. A ram type extruder was used by the authors to produce a dosage form with uniform shape and density. The researchers concluded that formulations of an equivalent composition formed using hot melt extrusion exhibited more rapid release than simple physical mixtures.

Crowley and McGinity (2002) studied the thermal stability of poly(ethylene oxide) (PEO) of various molecular weights in sustained release tablets prepared by hot-melt extrusion. Vitamin E, Vitamin E succinate and Vitamin E alpha-tocopheryl poly(ethylene glycol) succinate (Vitamin E TPGS) were used as plasticisers. The investigators concluded that the chemical stability of PEO was dependent on the storage and processing temperature, and the molecular weight of the polymer. Storage of the polymer above its melting point was found to significantly increase polymer degradation, and the degradation

process was also found to accelerate as the molecular weight of the polymer was reduced. The thermal stability of high molecular weight PEO (1,000,000 or PEO 1 million) in sustained release CPM tablets prepared by hot-melt extrusion was found to depend on the processing temperature and screw speed. Lower molecular weight PEO (PEO 100,000) was demonstrated to be a suitable processing aid for PEO 1 million.

Incorporation of PEO 100,000 reduced degradation of PEO 1 million and did not alter the release rate of CPM. The authors found that vitamin E, vitamin E succinate and Vitamin E TPGS were efficient stabilizers for PEO; ascorbic acid was shown to degrade the polymer in solution. The investigators demonstrated that vitamin E succinate and vitamin E TPGS were dispersed at the molecular level in hot-melt extruded tablets using thermal analysis. Solubilized vitamin E succinate and vitamin E TPGS were found to suppress the melting point of the poly(ethylene oxide). Drug release rates from hot-melt extruded tablets stabilized with antioxidants were found to be dependent on the hydrophilic nature of the antioxidant.

In a more recent study, the influence of xanthan gum parameters on the release of ibuprofen from hot melt extruded mini-matrices was investigated by Verhoeven *et al*. (2006). The researchers found that drug release, liquid uptake, swelling and erosion characteristics could easily be controlled by varying the xanthan gum concentration in the mini-matrices. *In vivo* investigations concluded that oral administration of the mini-matrices in 6 male mixed breed dogs was able to sustain plasma levels, and thus that mini matrices formulated using xanthan and prepared via hot melt extrusion were suitable for sustained release dosage forms. Fukuda and co-workers (2006) investigated the influence of pH, buffer species and ionic strength on the release rate of CPM from matrix tablets containing chitosan and xanthan gum prepared by hot melt extrusion. CPM release from matrices containing both chitosan and xanthan gum exhibited both pH and buffer species independent sustained release. The researchers attributed their results partially to the intra-molecular hydrogelation properties of chitosan below pH 6, and the intra-molecular hydrogelation properties of xanthan gum at pH 4, 6.8 and 7.4.

In addition to the descriptions of the *in vitro* testing of solid dispersions, details of human clinical trials carried out for hot melt extruded solid dispersions can be found in the patent literature. Vandecruys and Gerebern (1997) describe the preparation of antifungal

compositions of intraconazole as a solid dispersion using hot melt extrusion. In a limited number of volunteers the prepared solid dispersion gave an area under the curve (AUC) in the fasted state that was 2.3 times the AUC of the marketed reference capsules. Loviride, an antiretroviral agent, showed lower food effect from a melt extruded solid molecular dispersion when compared to capsules (Baert *et al*. 1997).

1.8 Drug administration

If an active agent is given intravenously, it is administered directly into the blood, and therefore, the entire drug reaches systemic circulation. In this case the drug is said to be 100% bioavailable. However, if the active agent is given by another route then there is no guarantee that the whole dose will reach systemic circulation intact. The relative amount of an administered dose of active drug that reaches the systemic circulation intact and the rate at which this occurs is known as bioavailability (Alderborn and Aulton, 2002).

For a drug which is administered orally to be 100% bioavailable, the entire dose must move from the dosage form to the systemic circulation. The drug must therefore be:

- Completely released from the dosage form;
- Fully dissolved in the gastrointestinal fluids;
- Stable in solution in the gastrointestinal fluids;
- Pass through the gastrointestinal barrier into the mesenteric circulation without being metabolised;
- Pass through the liver into the systemic circulation unchanged.

The possible routes of administration of drugs into the body can be divided into two classes; enteral and parenteral. In parenteral administration the gastrointestinal (GI) tract is bypassed. There are many parenteral routes. The most common of these routes are subcutaneous, intramuscular, and intravascular, but the drugs may also by injected intradermally or applied to the skin (transdermally). For local effect or to be absorbed transcutaneously, they may be introduced intra-nasally, or may be inhaled for direct action on the bronchial tree or to be absorbed into the blood at the alveoli. They may also be injected into or near the spinal column, introduced intra-vaginally or directly into other body cavities, or they may be injected directly into pathologic cavities such as abscesses

and tumour cavities. In enteral administration, the drug is placed directly into the GI tract either by placing under the tongue, by swallowing it, or by rectal administration.

Among all routes of administration, the oral route of administration has been the most popular and successful, in part due to higher levels of patient compliance. However, the oral route is constrained by the short and variable GI transit time, first pass metabolisim and varying pH levels along the length of the GI tract.

1.9 Active agents used in this study

A) Carvedilol is a non selective beta blocker and has been shown to be effective in treating symptoms and reducing morbidity and mortality in patients with left ventricular dysfunction (LVD), including those with no symptoms after an acute myocardial infarction (MI) and those with mild, moderate, or severe heart failure (Colucci *et al*. 1996; Packer *et al.* 1996, 2001).

The trials that demonstrated the benefits of carvedilol used an immediate release formulation, which, when given twice daily, produces plasma levels of the drug that fluctuate from peak to trough over a 4-fold range, while constantly maintaining plasma levels known to produce effective β-blockade over a 24-hour period (Packer, 2003). Rates of adherence to the prescribed carvedilol regimens in these clinical trials were high, generally exceeding 80%.

However, rates of adherence in clinical practice may differ from rates seen in clinical trials. All clinical trials place great emphasis on patient adherence to the prescribed study medication, and this message is repeated at every study visit. In contrast, in unstructured clinical or community settings adherence to prescribed regimens may falter, particularly when regimens require more than once-daily dosing (Claxton *et al.* 2001; Iskedjian *et al.* 2002; Wetzels *et al.* 2004). This leads to decreased efficacy in the treatment of heart failure. Hence, significant efforts have been made in recent years to develop once-daily sustained-release formulations of drugs whose immediate release formulations require twice-daily or thrice daily dosing to optimise adherence rates and maximise the benefits of treatment.

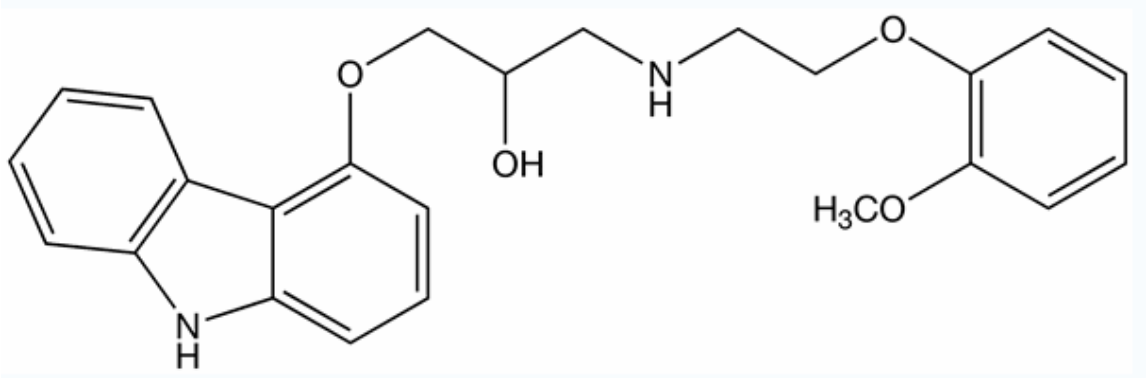

Figure 1.9 *Chemical structure of carvedilol.*

B) Diclofenac sodium is a potent nonsteroidal drug which has anti-inflammatory, analgesic and antipyretic properties. It is used for the treatment of degenerative joint diseases such as rheumatoid arthritis, osteoarteritis, and ankylosing spondilitis. It is characterised by rapid systemic clearance (Kendall *et al*. 1979; Willis *et al*. 1979) and thus necessitates repeated daily dosing when a course of treatment with this drug is required. Therefore, therapy with diclofenac sodium warrants the use of a sustained release formulation for prolonged action and to improve patient compliance (Willis *et al*. 1981).

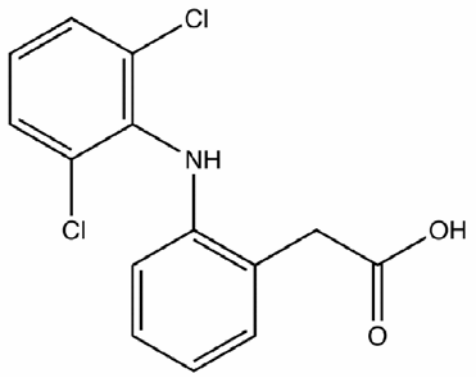

Figure 1.10 *Chemical structure of diclofenac (the sodium salt form was used in this work).*

1.10 The gastrointestinal (GI) tract

An important requisite for the successful design of a new drug delivery system is to understand the fate of such systems in the human body. Understanding the pathway a controlled delivery device must travel, including the related physiological systems and mechanisms, is vital for the development of a successful controlled delivery device.

The gastrointestinal tract is a muscular tube approximately 6m in length with varying diameters. It stretches from the mouth to the anus and consists of 4 main anatomical areas: the oesophagus, the stomach, the small intestine and the large intestine or colon (see Figure 1.11).

Once a controlled release device has been administered orally, the human digestion cycle begins. The mechanism for swallowing is co-ordinated by the swallowing centre in the medulla oblongata and pons. The swallowing reflex is initiated by touch receptors in the pharynx as the controlled release device is pushed to the back of the mouth by the tongue. The uvula is a small flap that hangs from the roof of the mouth. During swallowing it and the soft palate retract upward and to the rear to close the nasopharynx, which prevents the food from entering the nasal passages. When swallowed, the device enters the pharynx, which makes special adaptations to prevent choking or aspiration when swallowing occurs. The controlled delivery device is pushed down the oesophagus by the movement called peristalsis, which is an involuntary wave-like contraction of smooth muscle tissue, characteristic of the digestive system.

In general, most dosage forms when taken in the upright position, transit down the oesophagus in around 15 seconds. Drug delivery devices taken in the supine position, especially if taken without water, may lodge or adhere to the oesophageal wall. This may well cause a delay in the onset of action of the active agent incorporated in the delivery device or irritation of the oesophageal wall (e.g. potassium chloride tablets).

The drug delivery device enters the stomach upon passage through the cardiac sphincter. The two major functions of the stomach are:

1. To act as a temporary reservoir for ingested material and to deliver it to the duodenum at a controlled rate;
2. To reduce ingested solids to a uniform creamy consistency, known as chime, by the action of enzymatic and acid digestion.

The stomach has a capacity of approximately 1.5L, although under fasting conditions it generally contains no more than 50ml of fluid. In the fasted state the stomach contents include:

- Acid secreted by the parietal cells, which maintains the pH of the stomach between 1 and 3.5;
- The hormone gastrin;
- Pepsins, which break down proteins to peptides at low pH;
- Mucus for the protection of the stomach from autodigestion by the acid – pepsin combination.

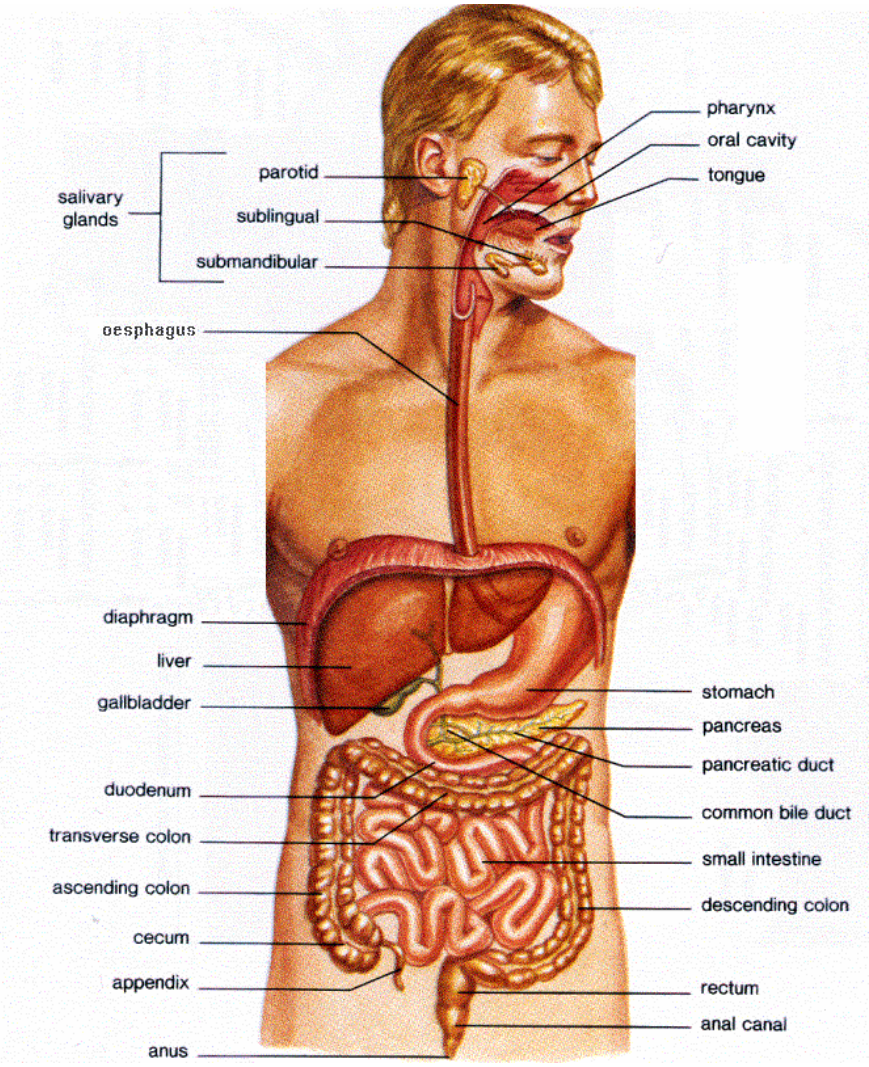

Figure 1.11 *Diagram showing the main anatomical features of the human digestive system (adapted from the national centre for technology in education).*

The distal region of the stomach (antrum) is the potential site of mixing and acts as a pump to facilitate the gastric emptying process. Gastric emptying occurs both during fasting and fed states, but the pattern varies. In the fasting state, interdigestive myoelectric or migrating myoelectric complex (MMC) cycles occur every 2 to 3 hours throughout the stomach and small intestine. The cycle is divided into four phases. The third phase is of short but intense and large peristaltic contractions called housekeeper waves, which last 4 to 6 minutes. This is responsible for sweeping out the undigested material from the stomach down to the intestine. This is also very critical to the integrity and movement of the dosage form, as it may be crushed before being transferred to the intestine (Moes, 1993). In the fed state, the gastric emptying rate is slowed because the onset of MMC is delayed, and this is responsible for the lag time prior to the onset of gastric emptying.

An example of how ingested substances spread out in the digestive tube rather than travel synchronously is shown in Figure 1.12. Camilleri *et al*. (1989) obtained this data from a human volunteer that ingested a meal containing ^{111}Indium-labeled pellets, the investigators measured the location of the radioactive signal over time by scintigraphy. It is clear that parts of the meal are entering the colon at the same time that other parts are still in the stomach. Apart from the presence of food, many factors can have an influence on gastric emptying: these include the postural position, the composition of the food, the effect of drugs, reproductive state and the disease state. The size of the dosage form also plays an important role in the process. Sometimes a dosage form swells to a considerable size and volume in the stomach (especially controlled-release systems). Such systems are often referred to as plug-type systems and exhibit a tendency to remain lodged at the pyloric sphincter for a longer time before transit to the intestine.

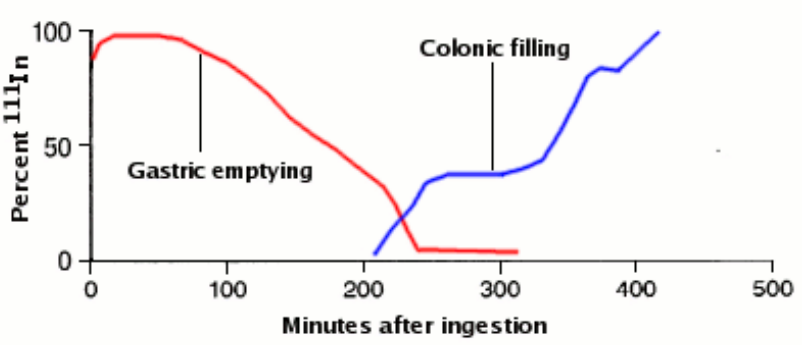

Figure 1.12 *Diagram outlining the gastric emptying and colonic filling timescales after food ingestion (adapted from Camilleri et al. 1989).*

After being processed in the stomach, the drug delivery device is passed to the small intestine via the pyloric sphincter. The small intestine is the longest (~4-5m) portion of the GI tract. Its main functions are:

- Digestion: the process of enzymatic digestion, which began in the stomach, is completed in the small intestine.
- Absorption: the small intestine is the region where most nutrients and other materials are absorbed.

The small intestine is divided into the duodenum (~200-300mm), the jejunum (~2m) and the ileum (~3m). The small intestine is an excellent absorption site due to folds and projections unique to this part of the digestive system. The submucosal folds of Kerckring are several millimeters in depth and are particularly prevalent in the duodenum and jejunum These allow for large increases in the surface area of the intestinal wall. Finger like projections into the lumen called villi, each covered my brush like microvilli, are supported by an intricate network of blood and lymphatic vessels allowing for rapid absorption of fats and nutrients. The blood, which has absorbed nutrients, is carried away from the small intestine via the hepatic portal vein and goes to the liver for filtering, removal of toxins, and nutrient processing. The primary activity here is regulation of blood glucose levels through a process of temporary storage of excess glucose that is converted in the liver to glycogen in direct response to the hormone insulin. Between meals, when blood glucose levels begin to drop, the glycogen is converted back to glucose in response to the hormone glucagon.

The pH of the small intestine is between 6 and 7.5. Brunners glands secrete bicarbonate in order to neutalise the acid emptied from the stomach. As chyme enters the first 200mm of the small intestine it is further mixed with 3 different liquids:

1. bile (to promote absorption of dietary fats),
2. pancreatic secretions (sodium bicarbonate and enzymes),
3. intestinal enzymes of the alkaline mucosal membranes (including maltase, lactase, sucrase, trypsin and chymotrypsin).

Small intestine transit time is relatively constant, at around 3 hours. The small intestine does not discriminate between solids and liquids or between the fed and fasted state. Small intestine transit time is particularly important for controlled release dosage forms as the small intestine is the main site of absorption for most active agents

After moving through the small intestine, the drug delivery device passes to the large intestine. The large intestine has several parts: the caecum (~85mm), the ascending colon (~200mm), the transverse colon (~400mm), the descending colon (~300mm) the stigmoid colon (~400mm) and the rectum. The pH of the caecum is around 6-6.5 increasing to about 7-7.5 towards the distal end of the colon. In the large intestine, water is reabsorbed, and the foods that cannot pass through the villi in the small intestine, such as dietary fiber, can be stored. The colon is permanently colonized by a large population and variety of bacteria capable of several metabolic reactions, including the reduction of inactive conjugated drugs to their active form. The material that cannot be broken down is called faeces. This material is stored and compacted in the rectum until it is expelled through the anus. The transport of active agents in the large intestine is variable and depends on the design of the drug delivery device. It is typically characterised by short bursts of activity followed by prolonged periods of inactivity. In most humans, mouth to anus transit times typically exceeds 24 hours.

1.11 Tablets

As mentioned in the previous sections, the oral route is the most common and convenient method for the administration of drug substances. Among the methods of drug delivery to the GI tract, tablets, of various types, remain the most popular and convenient dosage form. A tablet consists of one or more active pharmaceutical ingredients as well as a number of excipients (such as binders, stabilisers and disintegrants) used in the formulation of a complete preparation. Tablets are formed by compressing a therapeutic agent(s) that has previously been mixed / granulated with the other necessary excipients. A typical flow chart for the production of a tablet type dosage form is shown in Figure 1.13.

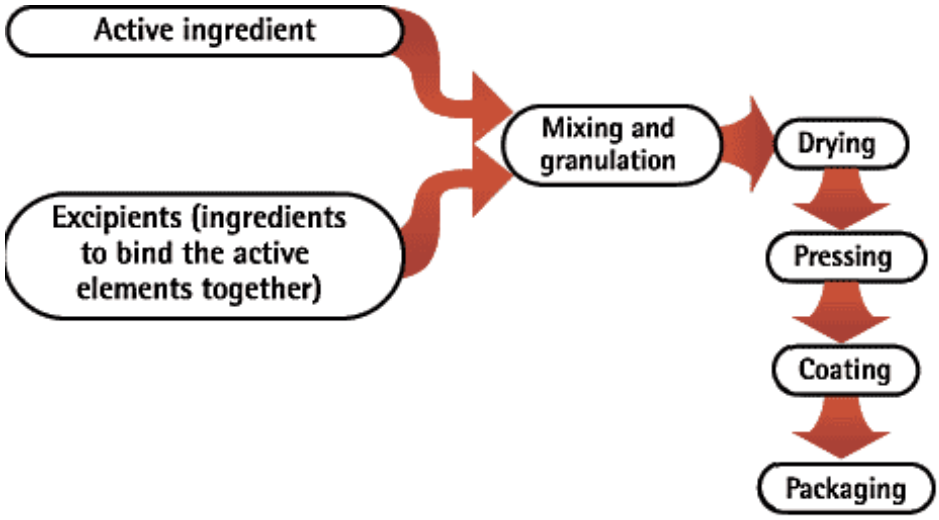

Figure 1.13 *A typical tablet manufacturing process.*

A number of technical problems can arise during the tabletting procedure, the most frequent are:

- High weight and dose variation of the tablets
- Low mechanical strength of the tablets
- Capping and lamination of the tablets
- Adhesion or sticking of powder material to punch tips
- High friction during tablet ejection

1.12 Capsules

Capsules are dosage forms, generally produced from gelatin, within which the active agent is encapsulated. Two forms of capsule exist: soft (one-piece) and hard (two piece). Soft capsules are generally made of gelatin plasticised by the addition of glycerin or sorbitol. This type of capsule is used primarily to hermetically seal and encapsulate liquids, suspensions or dry powders. A hard capsule consists of two pieces in the form of cylinders closed one end: the shorter piece, called the ‘cap’, fits over the open end of the longer piece, called the ‘body’.

The original rationale for developing the capsule as a dosage form was based on the capsule's ability to mask the taste and/or odour of specific medicinal compounds. It gained

further popularity based on: ease-of-swallowing, attractive appearance, ability to hold a color, neutral taste, as well as its ability to be filled and processed easily.

Figure 1.14 *A picture of a commercially available hard gelatin capsule.*

1.13 Micro-injection moulding

Micro-injection moulding is a viable alternative to compaction for the production of dosage forms for oral drug delivery. Kukla *et al.* (1998) defined micro-injection molded parts as:

1) Parts with micro-weight,
2) Parts with micro-structured regions, and
3) Parts with micro-precision dimensions.

Parts with micro-weight are parts with masses of a few milligrams, but their dimensions are not necessarily on the μm scale (Figure 1.15). Parts with micro-structured regions are characterised by local micro-features of the μm order, such as micro-holes and slots. Parts with micro-precision are parts of any dimension that they have tolerances in the μm range. In addition to the possibility of producing micro-injected tablets, micro-moulding offers the ability to mould micro dosage forms which could then be loaded into hard gelatin capsules for site specific drug delivery.

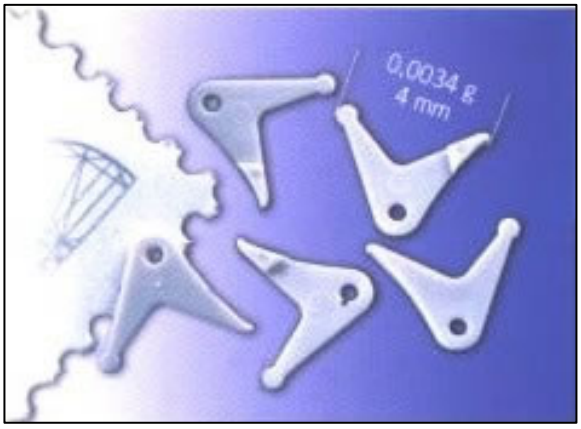

Figure 1.15 *Diagram showing an example of a micro-injection moulded part.*

Up until recently the injection moulding of very small components usually involved the adaptation of conventional injection moulding equipment. Unfortunately there are two main reasons why these machines are unsuitable for manufacture of parts below a certain shot weight.

- The plasticising screws are unsuitable for the production of micro-parts because the shot to screw volume ratio is so low that residence time of material in the screw can become a problem and may result in injection of degraded material.

- The positional control of the machines does not have the resolution to accurately deliver the small melt dose required during the moulding of micro-parts.

The advent of micro-moulding technology has brought improvements in sophistication, reliability, and efficiency compared to conventional moulding techniques. This has lead to new applications in various fields, such as communications, environmental analytics, transport, medicine, and safety (Michaeli *et al.* 1999; Hill, 2001). Recent years have seen an exponential rise in interest in the technology, particularly in the medical and micro electro-mechanical systems sectors, as industry becomes aware of the ability of the process to manufacture highly complex, 3-dimensional micro-scale devices in high

volumes at a fraction of the cost of current techniques. Some of the attractive benefits of using a micro-injection moulding process include:

- *Process tailored for miniature parts*. Micro-injection molding machines have very small capacities (3-6 gram barrels and clamps of 2-5 tons). The plastic has a very short heat history and therefore less chance of degrading in the barrel.

- *Reduced tool sizes*. The tools used for micro-moulding are significantly smaller than those used for standard injection moulding, for example a 3 or 4 cavity micro-moulding tool can compete with a 16 cavity standard injection moulding tool. This means that manufacturing costs for these tools is much lower and also helps to keep time required for a tool change to a minimum. This means that both set up costs and running costs can be kept to a minimum.

- *Reduced part cost.* Due to their small size micro-moulding machines require considerably less energy than their standard sized counterparts. This combined with the reduced cost of manufacturing tooling means that the cost of a product can be kept down and ensure prices can be kept competitive against standard injection moulding.

- *Increased part accuracy*. Due to the increased accuracy required for micro-moulding parts accuracy will be significantly better than that associated with conventional injection moulding. The reliability of this accuracy is also improved over conventional moulding giving a greater level of consistency. This combination of improvements means far fewer quality issues and less rejected mouldings leading to further cost reductions.

- *Improved cycle times*. Due to the low shot weights associated with micro-moulding cycle times are much shorter than with conventional injection moulding. The reduced movement associated with micro-moulding machines also means they are able to carry out moulding processes more quickly than a standard injection moulding machine.

The micro-moulding process uses the same procedure as conventional moulding. Polymers in solid form (granulate, powder) are melted in the plasticising unit of an injection molding machine at a specific temperature. The polymer melt is then injected under pressure into the mould cavity of an injection moulding tool. After solidification of the moulded article, the tool is opened and the component ejected. A number of pure plastics such as, poly(carbonate), poly(styrene), poly(propylene), and poly(oxymethylene) have been successfully used in the micro-molding process (Bourdon and Schneider, 1998; Despa *et al*. 1999; Fasset, 1995; Palmskog 1997), and the technique is well suited for most materials from high temperature engineering plastics to commodity resins.

1.14 Aims of this study

This work focuses on the development of monolithic matrices for controlled oral drug delivery. Conventional polymer processing techniques were utilized as a means of producing the drug loaded matrices as these processes can both be scaled up for production at a substantial cost saving when compared with standard tabletting operations. The filler systems outlined in this work had not been reported on in the literature and have never been used for this application before. In addition to the novel filler systems utilised in this study, the supercritical fluid assisted extrusion process described here had never been used to produce the type of matrices discussed herein. Micro-thermal analysis was applied in the investigation of the matrices produced using the supercritical fluid assisted extrusion process This test technique had not been used in the analysis of such materials before this work. The micro-moulding technology, and the uniquely designed micro-moulding tool, have thus far not been reported in the literature and have not, prior to this work, been applied to the moulding of controlled release polymer matrices for oral drug delivery.

Chapter 2

Experimental Details

2.1 Materials

The active agents incorporated in this work were carvedilol (Mw 406.48, T_m 114.5°C), and dicofenac sodium (Mw 318.14, T_m 284°C), obtained from Pharmaplaz Ltd. Pre-blended matrix material containing poly(ethylene oxide) (PEO), Mw 200,000 as the matrix forming material and 14% by weight carvedilol, was also donated by Pharmaplaz Ltd. PEO (Mw 200,000, 900,000 & 5 million) were sourced from Polysciences Ltd and PEO (Mw 180,000 and 900,000) were sourced from Meisei Chemical Works Ltd. Tone P-767 poly(e-caprolactone) (Mw 50,000) was obtained from Dow Ltd. Eudragit EPO, Eudragit L100 and the experimental carrier material Eudragit preparation 4155F were donated by Degussa Ltd. Microcrystalline cellulose (Avicel PH101) was purchased from FMC Ltd, Ireland. The organically modified layered silicate (OMLS) used in this study was Cloisite® 93A, a natural montmorillonite modified with a ternary ammonium salt obtained from Southern Clay Products Inc. The cells used for *in vitro* studies were the Caco-2 and the HepG2 cell lines. Both cell lines were taken from the European Cell and Culture Collection (ECACC). The Caco-2 cell line, established from a human intestinal adenocarcinoma of a 72 year old Caucasian male, was obtained at passage 41. The HepG2 cell line was derived from a human hepatocyte carcinoma of a 15 year old caucasian male and was obtained at passage 38. The lactate dehydrogenase cytotoxicity assay-kit was purchased from Sigma-Aldrich Ltd and the 5-bromo-2-deoxy-uridine labelling and detection kit I was sourced from Roche Ltd.

2.2 Hot melt extrusion conditions

Unless otherwise indicated, all the melt compounding detailed herein was carried out on a bench-top Prism™ twin screw extruder (Figure 2.1) with 16mm diameter screws and a 25/1 length to diameter ratio. Prism™ co-rotating extruder screws are designed and manufactured in a modular construction. The screws are made up of individual sections that slide onto a keyed or splined shaft. Therefore, different screw configurations using narrow disk bi-lobal kneading elements can be arranged at any location along the shaft to generate controlled shear or mixing effects. The design of the screw assemblies has a significant impact on the degradation of drugs or excipients (Breitenbach, 2002). In the case of the

compounding detailed in this work, the screws were assembled in the co-rotating intermeshing mode.

Figure 2.1 *The Prism™ twin screw extruder used in this work.*

The screw configurations were assembled from the following segments:

- extrusion screw sections
- feed screw sections
- half feed screw sections
- half reverse feed screw sections
- mixing elements (paddles) 30^{o} offset
- mixing elements (paddles) 60^{o} offset
- mixing elements (paddles) 90^{o} offset

Thus, in addition to the screw speed and temperature profile, the screw and mixing configurations were varied to optimise the processing of the matrix used for each individual section. The required compounding temperature profile was established on the Prism™ extruder by means of four temperature controllers placed along the length of the barrel. A fifth temperature controller was used to regulate the temperature at the die.

The material to be compounded was fed at a constant speed into the hopper of the Prism™ twin screw extruder by means of a screw feed system. In all cases the speed of the delivery screws was maintained at such a rate as to ensure that the materials were starve fed into the mixing screws. This ensured that in all cases output was independent of screw speed. The resultant homogeneous melt was extruded through a cylindrical die to form a strand. Extrudate was cooled via two cool air knifes and was subsequently granulated using a Prism™ granulator.

2.2.1 Compounding of materials to investigate the effect of polymer molecular weight on the matrix forming properties of PEO

The screws were assembled with a long continuous mixing section made up of 30°, 60° and 90° bi-lobal kneading elements that ensured that the transition from conveying to high shear mixing was very gradual. The mixing section was positioned towards the die end of the extruder. The positions of the heating zones and mixing section are visible on the schematic diagram of the barrel of the Prism™ twin screw extruder in Figure 2.2. The batches of polymer matrices described in Table 2.1 were compounded using the extrusion profile outlined in Table 2.2.

Table 2.1 *Batch composition used to investigate the effect of varying PEO molecular weight on the properties of a PEO based monolithic matrix.*

Batch No.	PEO Mw 200,000 (% by Weight)	PEO Mw 1 million (% by Weight)	PEO Mw 5 Million (% by Weight)	Carvedilol (% by Weight)
1	20	50	30	0
2	30	50	20	0
3	30	40	30	0
4	17	42.5	25.5	15
5	25.5	42.5	17	15
6	25.5	34	25.5	15
7	14	35	21	30
8	21	35	14	30
9	21	28	21	30

Table 2.2 *Extrusion conditions used to compound materials for trials to investigate the effect of varying PEO molecular weight on the properties of a PEO based monolithic matrix.*

Screw Speed (RPM)	Temperature (°C)				
	Die	Zone 4	Zone 3	Zone 2	Zone 1
15	115	110	110	100	60

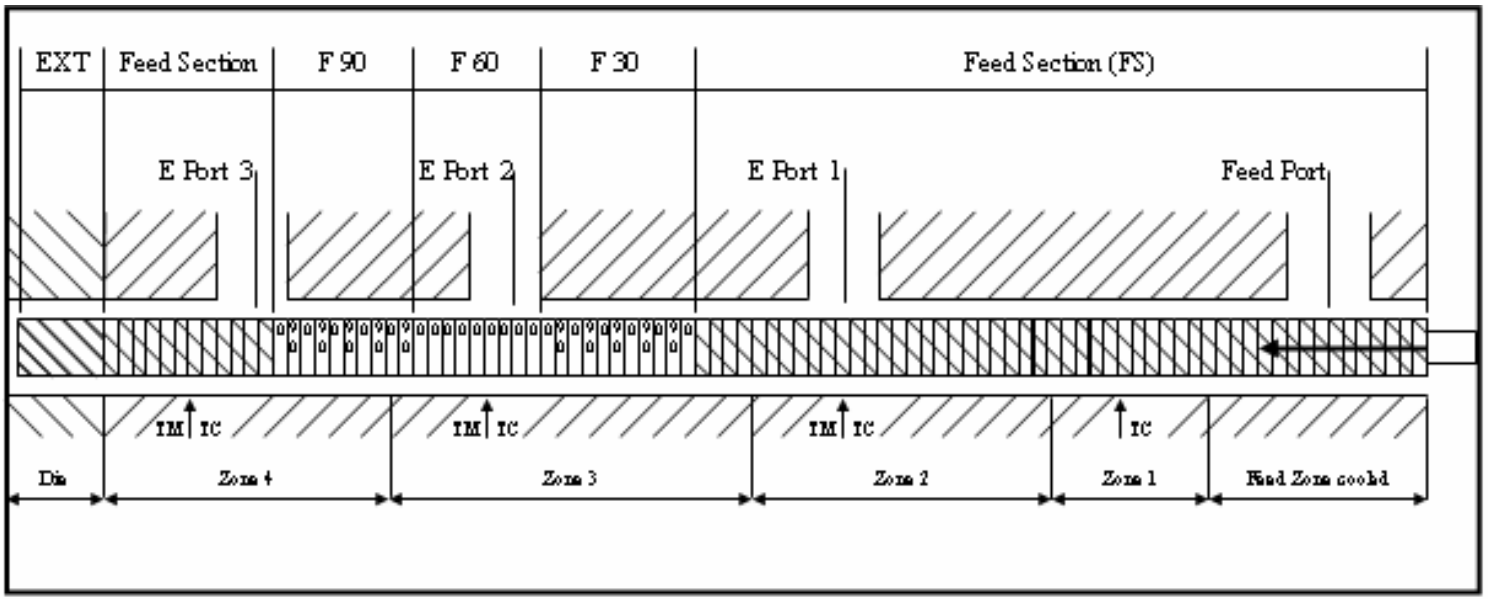

Figure 2.2 *Schematic representation of Prism™ twin screw extruder barrel and screw configuration used to compound materials for trials to investigate the effect of varying PEO molecular weight on the properties of a PEO based monolithic matrix.*

2.2.2 Examination of the processing stability of PEO

Pre-blended matrix material containing PEO (Mw 200,000) and 14% by weight carvedilol was compounded separately using an extruder screw configuration identical to that illustrated in Figure 2.2. The extrusion conditions used are outlined in Table 2.3. After the initial processing step, extrudate was then reprocessed four times with samples removed after each processing run for testing.

Table 2.3 *Extrusion conditions used to examine the processing stability of PEO.*

Screw Speed (RPM)	Temperature (°C)				
	Die	Zone 4	Zone 3	Zone 2	Zone 1
60	85	80	80	75	60

2.2.3 Compounding of matrices to investigate the effect of storage conditions on PEO

The processing conditions and temperatures outlined in Table 2.3 were used to prepare batches of pure PEO of molecular weight 180,000 and 900,000. The resultant extrudate was then subjected to a range of storage conditions and testing.

2.2.4 Effect of the variation of processing conditions on novel PCL/PEO based matrix

The compounding of materials in this section was carried out on a Leistritz Micro 27 labscale twinscrew extruder with a 27mm screw diameter and a 38/1 length to diameter ratio. An image of the extruder is displayed in Figure 2.3 with a schematic diagram of the barrel of the Leistritz Micro 27 labscale extruder presented in Figure 2.4. In the case of the work carried out in this section, the extended length of the screws in the Leistritz Micro 27 labscale extruder when compared with the Prism™ twin screw extruder allowed for longer residence time and better mixing. Thus, the screw configuration used contained no mixing sections and was made up completely of feed sections. The required compounding temperature profile was established on the Leistritz Micro 27 labscale extruder by means of nine temperature controllers placed along the length of the barrel. A tenth temperature controller was used to regulate the temperature at the die.

Figure 2.3 *Leistritz Micro 27 labscale extruder used in this study.*

The material to be compounded was fed at a constant speed into the hopper of the Leistritz Micro 27 labscale extruder by means of a screw feed system. In all cases the speed of the delivery screws was maintained at such a rate as to ensure that the materials were starve fed into the mixing screws. This ensured that in all cases output was independent of screw speed. The resultant homogeneous melt was extruded into a strand through a cylindrical die. Extrudate was cooled via two cool air fans and was subsequently granulated using a Scheer™ granulator.

Table 2.4 *Batch compositions used to determine the effect of processing conditions on PCL/PEO blends.*

Batch No.	PCL (% by weight)	PEO Mw 1 million (% by weight)	Carvedilol (% by weight)
1	49	49	2
2	73.5	24.5	2
3	24.5	73.5	2
4	40	40	20
5	60	20	20
6	20	60	20

The batches of polymer matrices described in Table 2.4 were compounded using two different temperature profiles and three different screw speeds as outlined in Table 2.5. The active agent incorporated in this work was diclofenac sodium.

2.2.5 Preparation of monolithic matrices for oral drug delivery using a supercritical fluid assisted hot melt extrusion process

For the compounding detailed in this work, the screws were assembled in the co-rotating intermeshing mode with a long continuous mixing section made up of 30°, 60° and 90° bi-lobal kneading elements that ensured that the transition from conveying to high shear mixing was very gradual. The mixing section was positioned towards the die end of the extruder downstream from the supercritical CO_2 injection port.

Batches of material were prepared with and without the assistance of supercritical CO_2: a full list of the batches prepared can be seen in Table 2.6. The extrusion conditions used are outlined in Table 2.7. The positions of the heating zones, mixing sections and injection port are visible on the schematic diagram of the barrel of the Prism™ twin screw extruder in Figure 2.5. For the batches prepared using the assistance of supercritical CO_2, a P50 reciprocal high pressure pump from Thar™ Technologies Ltd was used. The pump was connected via a high pressure line to the extruder at E port 2, and was controlled using a hand held display.

2.2.6 Agar as a novel constituent in hot melt extruded dosage forms

The extruder screw configuration used in this work was identical to that described in Figure 2.2. The temperature profile used for this section is detailed in Table 2.8 and the full list of batch compositions can be seen in Table 2.9.

Table 2.5 *Extrusion conditions used to examine the effect of variations in processing conditions on PCL/PEO blends.*

	Screw Speed (RPM)	Temperature (°C)			
		Feed	Metering 1	Metering 2- 8	Die
Temperature profile 1	25	50	75	85	95
	50	50	75	85	95
	100	50	75	85	95
Temperature profile 2	25	50	95	110	120
	50	50	95	110	120
	100	50	95	110	120

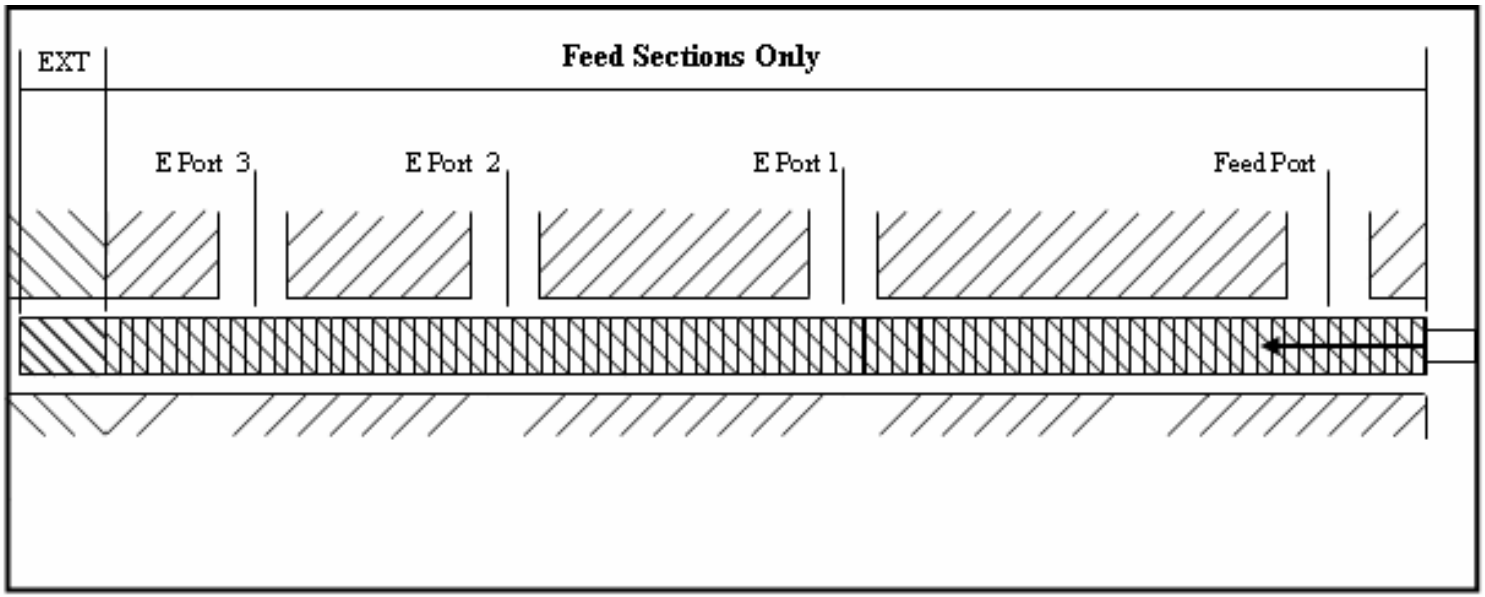

Figure 2.4 *Schematic representation of Leistritz Micro 27 extruder barrel.*

Table 2.6 *Batch composition used to examine the effect of a supercritical fluid assisted extrusion process on the preparation of monolithic matrices.*

Batch No.	PEO Mw 200,000 (% Weight)	Eudragit EPO (% Weight)	Carvedilol (% Weight)	Supercritical CO_2 assisted (1200 Psi)
1	86	0	14	No
2	64.5	21.4	14	No
3	43	43	14	No
4	89.5	0	10.5	No
5	67.125	22.375	10.5	No
6	44.75	44.75	10.5	No
7	92.5	0	7.5	No
8	69.375	23.125	7.5	No
9	46.25	46.25	7.5	No
10	86	0	14	Yes
11	64.5	21.4	14	Yes
12	43	43	14	Yes
13	89.5	0	10.5	Yes
14	67.125	22.375	10.5	Yes
15	44.75	44.75	10.5	Yes
16	92.5	0	7.5	Yes
17	69.375	23.125	7.5	Yes
18	46.25	46.25	7.5	Yes

Table 2.7 *Extrusion conditions used to compound matrices using agar as a novel filler system.*

Screw Speed (RPM)	Temperature (°C)				
	Die	Zone 4	Zone 3	Zone 2	Zone 1
30	140	130	130	130	70

Table 2.8 *Extrusion conditions used to examine the effect of a supercritical fluid assisted extrusion process on the preparation of monolithic matrices.*

Screw Speed (RPM)	Temperature (°C)				
	Die	Zone 4	Zone 3	Zone 2	Zone 1
35	140	130	130	130	50

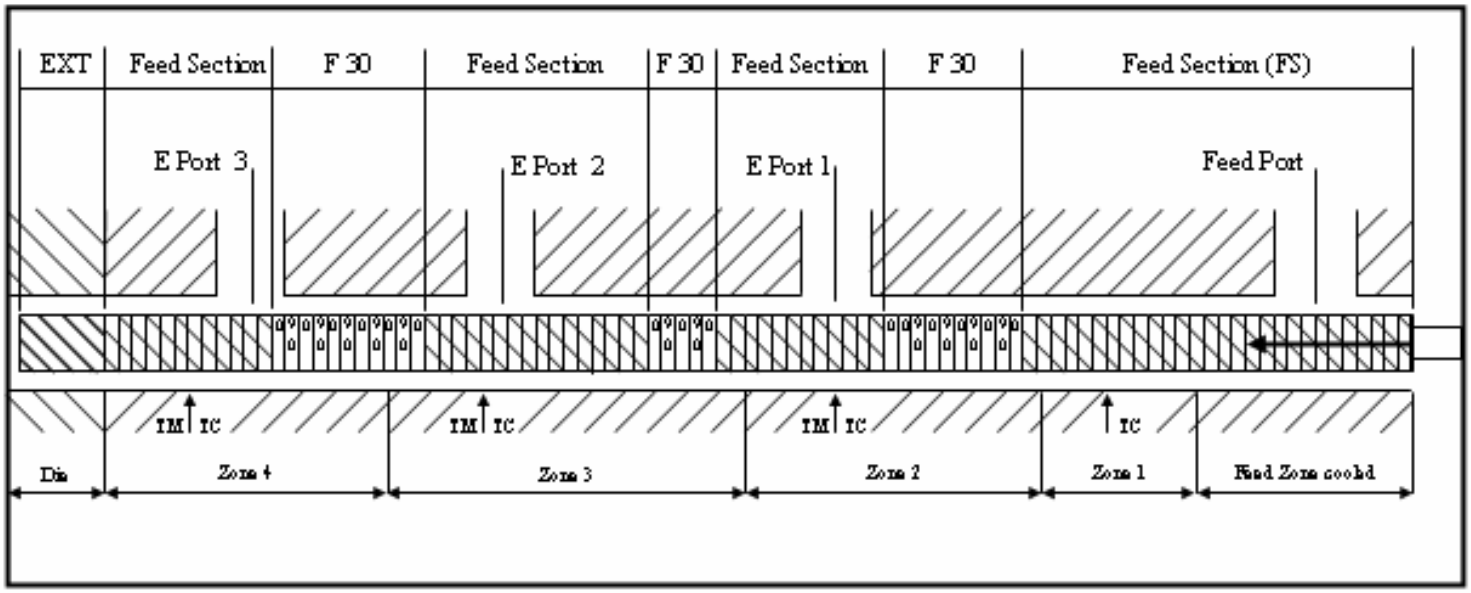

Figure 2.5 *Schematic representation of Prism™ twin screw extruder barrel and screw configuration used to examine the effect of a supercritical fluid assisted extrusion process on the preparation of monolithic matrices.*

Table 2.9 *Batch composition used for the compounding of matrices for the development of a novel filler system containing agar (all values are in grams).*

Batch name	PEO (MW 1 Million)	PEO (MW 200,000)	Eudragit L 100	Diclofenac sodium	Agar	MCC
1	20	20	0	0	0	0
2	32.5	32.5	0	15	0	0
3	27.5	27.5	0	15	10	0
4	22.5	22.5	0	15	20	0
5	17.5	17.5	0	15	30	0
6	27.5	27.5	0	15	0	10
7	22.5	22.5	0	15	0	20
8	17.5	17.5	0	15	0	30
9	0	20	20	0	0	0
10	0	32.5	32.5	15	0	0
11	0	27.5	27.5	15	10	0
12	0	22.5	22.5	15	20	0
13	0	17.5	17.5	15	30	0
14	0	27.5	27.5	15	0	10
15	0	22.5	22.5	15	0	20
16	0	17.5	17.5	15	0	30

2.2.7 The incorporation of an organically modified layered silicate in monolithic matrices produced using hot melt extrusion

The process of delamination and dispersion of the nanoclay particles requires extended mean residence time, not high shear intensity. Increased mean residence time increases delamination and dispersion, but increased shear intensity can decrease delamination and dispersion. Thus for the work outlined herein a low screw speed of 30 RPM as used in previous work was maintained. The extrusion conditions used were identical to those outlined in Table 2.7.

For ease of processing and to ensure accurate measurement of percentage nanoclay inclusion, the polymer and nanoclay were master-batched together at a 40:60 nanoclay to polymer ratio. This master-batch was then added to virgin polymer in order to produce the desired percentage nanoclay incorporation. The batches prepared are outlined in Table 2.10.

Table 2.10 *Batch composition used to produce monolithic matrices incorporating an organically modified layered silicate.*

Batch name	Polymer	API (% by Weight)	OMLS (% by Weight)
Batch 1	PEO (5 Million)	Carvedilol (14%)	-
Batch 2	PEO (5 Million)	Carvedilol (14%)	Cloisite® 93A (2%)
Batch 3	PEO (5 Million)	Carvedilol (14%)	Cloisite® 93A (4%)
Batch 4	PEO (5 Million)	Carvedilol (14%)	Cloisite® 93A (6%)

2.2.8 Extrusion of monolithic matrices for comparison with matrices produced in a novel micro-moulding process

The extruder screw configuration used in this work was identical to that illustrated in Figure 2.2. The temperature profile used for this section is detailed in Table 2.11 and the batches prepared are outlined in Table 2.12.

Table 2.11 *Extrusion conditions used to prepare matrices.*

Screw Speed (RPM)	Temperature (°C)				
	Die	Zone 4	Zone 3	Zone 2	Zone 1
35	125	125	120	115	50

Table 2.12 *Batch composition of the monolithic matrices produced.*

Batch No.	Polymer	Diclofenac sodium (%wt)
1	80%*wt EPO*	20
2	80%*wt* 4155F	20
3	*80%wt* PEO (40%*wt* Mw 1 million + 30%*wt* Mw 900,000 + 30%*wt* Mw 100,000)	20
4	40%*wt* PEO(comprising 40%*wt* Mw 1 million + 30%*wt* Mw 900,000 + 30%*wt* Mw 100,000) + 40%*wt* PCL	20

2.3 Injection moulding conditions

The injection moulding in this work was carried out on an Arburg™ Allrounder 221 K, as displayed in Figure 2.6. The Allrounder injection moulding machine has a maximum clamping force of 350kN with a screw diameter of 25mm and the theoretical stroke volume for this machine is 49 cm^3 with a maximum injected part weight of 41g. The required temperature profile was established on the Arburg™ Allrounder 221 K injection moulder by means of four temperature controllers placed along the length of the barrel. A fifth temperature controller was used to regulate the temperature at the nozzle (Tables 2.13 and 2.14). The mould used was maintained at 25°C my means of a separate mould temperature controller unit. The mould used was a family type mould producing type 'A' test specimens to ISO 294-1 and ISO 6239 international standard. Settings for injection pressure, holding pressure, back pressure, holding time and cooling time were optimised for the batches under consideration prior to sample acquisition.

Table 2.13 *Injection moulding profile used to mould test specimens to examine the effect of varying the molecular weight of polymer in PEO based matrices.*

	Zone1	Zone 2	Zone 3	Zone 4	Nozzle	Mould
Temperature (^oC)	65	80	85	85	95	25
Holding Time: 6.5 sec.		Back Pressure: 10 bar				
Cooling Time: 20 sec.		Injection Pressure: 450 bar				
		Holding Pressure: 400 bar				

Figure 2.6 *The Arburg™ Allrounder 221 K employed in this study.*

Table 2.14 *Injection moulding profile used to investigate the incorporation of an organically modified layered silicate on the properties of monolithic matrices.*

	Zone 1	Zone 2	Zone 3	Zone 4	Nozzle	Mould
Temperature (^{o}C)	110	120	130	130	140	25
Holding Time: 6.5 sec.		Back Pressure: 10 bar				
Cooling Time: 15 sec.		Injection Pressure: 400 bar				
		Holding Pressure: 300 bar				

2.3.1 Micro-moulding conditions

The micro-injection moulding was carried out on a BOY™ 22 D with diptronic controls, as presented in Figure 2.7. The injection moulding machine has a maximum clamping force of 220kN with a screw diameter of 14mm and the theoretical stroke volume for this machine is 6.1 cm^3 with a maximum injected part weight of 5.6g. The required temperature profile was established on the Boy™ 22 D injection moulder by means of three temperature controllers placed along the length of the barrel. A fourth temperature controller was used to regulate the temperature at the nozzle. The mould used was maintained at 25°C by means of a separate mould temperature controller unit.

The injection moulding profile used for all of the batches in this study is detailed in Table 2.15. Settings for injection pressure, holding pressure, back pressure, holding time and cooling time were optimised for the batches under consideration prior to sample acquisition.

Figure 2.7 *The BOY™ 22 D used in this work.*

Table 2.15 *Micro-injection moulding profile used to prepare samples for comparison with samples produced using hot melt extrusion alone.*

	Zone 1	Zone 2	Nozzle	Mould
Temperature (^{o}C)	130	130	130	25
Holding Time: 6.5 sec.		Back Pressure: 10 bar		
Cooling Time: 15 sec.		Injection Pressure: 300 bar		
		Holding Pressure: 200 bar		

An experimental test mould was designed specifically for this work. The mould was developed to produce micro-moulded parts capable of fitting into standard gelatin capsules for oral drug delivery. The mould cooling system and ejection system were designed to be compatible both with standard injection moulding and micro-moulding equipment. The test mould was capable of producing two types of basic tablet shapes. Both tablet types were cylindrical with a diameter of 6.5mm. The larger tablet type had a length of 5mm with the smaller tablet type having a length of 3mm. Both tablet types were designed to fit into commercially available gelatin capsules and their cylindrical shape was chosen to allow

reproducible erosion rates, which is strongly dependant on tablet surface area. The sprue and runner system were designed so as to allow selective filling of the cavities if desired. An abridged schematic of the mould is shown in Figure 2.8.

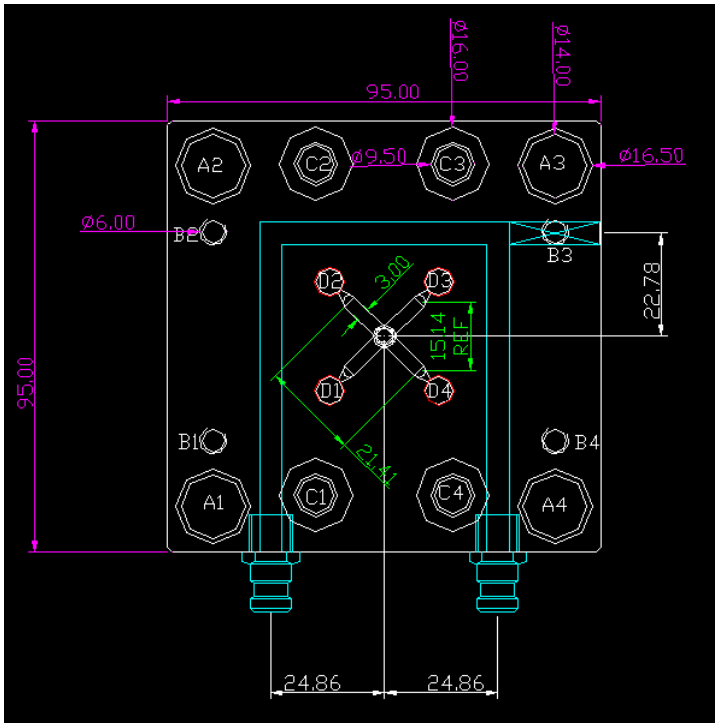

Figure 2.8 *Abridged schematic of the experimental test mould.*

2.3.2 Ram injection moulding

The ram injection moulding was carried out on a Ray-Ran model 2 test sample injection moulding apparatus which is shown in Figure 2.9. The injection moulding machine has a maximum ram pressure of 430 bar and a maximum shot size of 48cm^3. The required temperature profile of 130^{o}C was established on the test sample injection moulding apparatus by means of a single temperature controller placed along the length of the barrel. The mould being used was maintained at ambient temperature by means of a separate tool temperature controller unit. The cam operated tool block is designed to accommodate tool inserts. A simple tool insert was designed for this work and is also presented in Figure 2.8. The tool insert was designed to produce moulded matrices with a height of 9mm and a radius of 3.55mm.

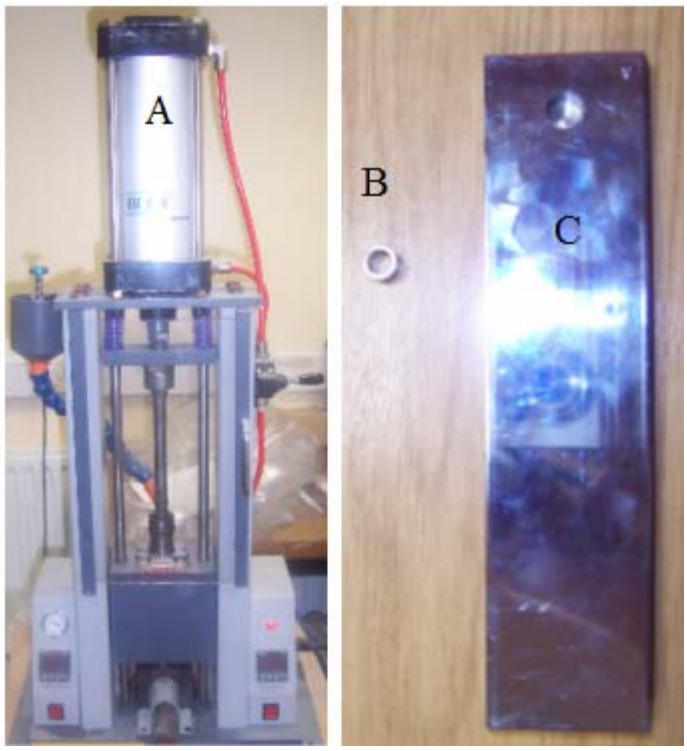

Figure 2.9 *Ray-Ran model 2 test sample injection moulding apparatus (A), the insert (B) and the tool (C) used for the ram injection moulding carried out in this work. The insert and tool are not shown to scale.*

2.4 Stability Testing

2.4.1 Effect of storage temperature on PEO

Extruded PEO material (Mw 180,000) was subjected to two storage temperatures over a 60 day period. Samples of extruded material were stored in two thermostated Gallenkamp ovens at 20 and 40°C. A relative humidity of 22% was achieved using saturated solutions of potassium acetate and potassium fluoride in each oven respectively. Each day a sample from each oven was removed for testing and the levels of the saturated solutions were replenished. The removed polymer samples were dissolved in 100ml of chloroform solvent. Polymer / chloroform solution was placed into a Type 'A' Ostwald viscometer. The viscometers were suspended in a thermostated bath at 37°C. The polymer solution was allowed ten minutes to reach thermal equilibrium in the viscometer before relative viscosity tests were carried out. Five tests were carried out on each sample and the representative averages were calculated.

2.4.2 Effect of storage conditions on PEO of varying molecular weight

Extruded PEO material (Mw 180,000 and 900,000) was subjected to storage at 20°C over a 60 day period. Relative humidity of 22% was maintained in the oven using a saturated solution of potassium acetate. Each day a sample of each molecular weight material was removed from the oven for further testing and the level of the saturated solution were replenished. Viscometry testing was carried out on the removed samples in the manner outlined in section 2.4.1.

2.4.3 Effect of UV exposure on PEO

PEO material (Mw 180,000) was subjected to two storage conditions over a 60 day period. One batch of material was stored at ambient temperature and humidity. A second batch was exposed to two UVA 340 ultra violet (UV) lamps (Q-panel lab products) in an enclosed chamber over a 60 day period at ambient temperature and humidity. Each day a sample from each was removed and subjected to viscometry testing as described in section 2.4.1 and thermal analysis as outlined in section 2.5.

2.5 Differential scanning calorimetry (DSC)

A TA instruments 2010 DSC and a Perkin Elmer Pyris 6 DSC were used throughout the course of this work for thermal characterisation of materials (Figure 2.9). Samples of between 9.0 and 9.8 mg were weighed out using a Sartorius scales having a resolution of 1 x 10^{-5}g. Samples were then placed in non-perforated aluminium pans which were crimped before testing, with an empty crimped aluminium pan being used as the reference cell. Volatiles were removed from the purging head with nitrogen at a rate of 30ml/min. Calorimetry scans were carried out over varying temperature ranges between -50 and 250°C. Calibration of the instrument was preformed using indium as standard. Sub-ambient DSC was carried out exclusively on the TA instrument 2010 DSC with the test cell brought to low temperature with the aid of liquid Nitrogen. After each scan was completed the melting points were analysed to determine heats of fusion (ΔH) and melting point (T_m) of each batch.

Figure 2.10 *A TA instruments 2010 DSC.*

2.5.1 Modulated differential scanning calorimetry (MDSC)

Samples tested using MDSC were subjected to the same sample preparation technique as outlined in section 2.5. The thermal characterisation was preformed using a DSC 2920 Modulated DSC (TA Instruments) coupled with a refrigerated cooling system, which is shown in Figure 2.11. Calorimetry scans were carried out over a temperature range of 20 to 190°C. All MDSC measurements were carried out at a scanning rate of 1°C/min. Volatiles were removed from the purging head with nitrogen at a rate of 30ml/min. Calibration of the instrument was preformed using indium as standard. After each scan was completed the melting points were analysed to determine heats of fusion and T_m of each batch.

Figure 2.11 *The DSC 2920 Modulated DSC (TA Instruments) coupled with a refrigerated cooling system.*

2.6 Mechanical Testing

Tensile tests on injection moulded specimens were carried out using both an Instron 3360 series tensile testing apparatus and a Lloyd Lr 10K tensile testing apparatus (Figure 2.12). In all cases, the tensile tests were carried out in adherence to ISO 6239 at ambient temperature and pressure, with 5 test specimens tested from each batch, and a test speed of 5 mm/min.

The second mode of mechanical testing employed was the determination of indentation hardness under ISO 868. A type D shore durometer was used to test 5 specimens of equal thickness on a flat anti-vibration bench. A 5kg weight was centred on the axis of the indenter to acquire reproducible results.

Figure 2.12 *The Lloyd Lr 10K tensile testing apparatus.*

2.7 Steady state rheometry

The method used to study the rheological properties of all of the materials detailed in this study was steady state parallel plate viscometry, utilising an AR1000™ rheometer from TA instruments (Figure 2.13). It is fitted with an environmental test chamber (ETC), for use as the temperature control environment in the analysis of polymer melts using parallel plate or cone / plate measurement geometries with provision for nitrogen purging.

Figure 2.13 *The AR1000 and ETC used for rheological testing.*

The air bearing guard was removed prior to use. The instrument was calibrated for inertia and the geometry was set for the 25mm steel parallel plates used in this study. The instrument was mapped and with the ETC closed the rheometer was brought to the test temperature of 140°C.

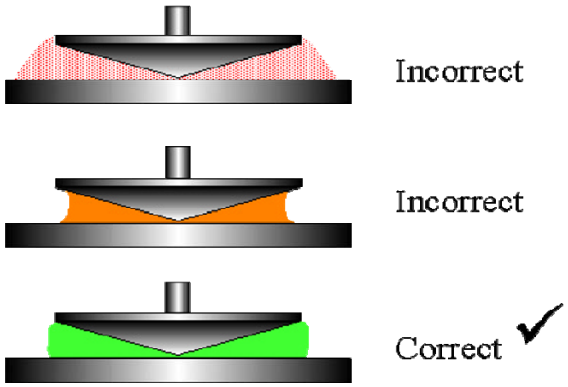

Figure 2.14 *Correct sample loading for the AR 1000 rheometer.*

The gap between the plates was zeroed, the doors were opened and the sample was loaded. The amount of sample loaded has an effect on the accuracy of the results, and so extreme care was taken during sample loading to ensure the correct fill (Figure 2.14). The head was brought down onto the sample in incremental steps to avoid wasting material or inducing stress in the sample; as shown in Figure 2.15. Data was recorded at a rate of 10 points per decade with 5% tolerance. After each test a bronze scraper was used to remove the sample from the plates, before the machine was brought back to temperature for the next sample.

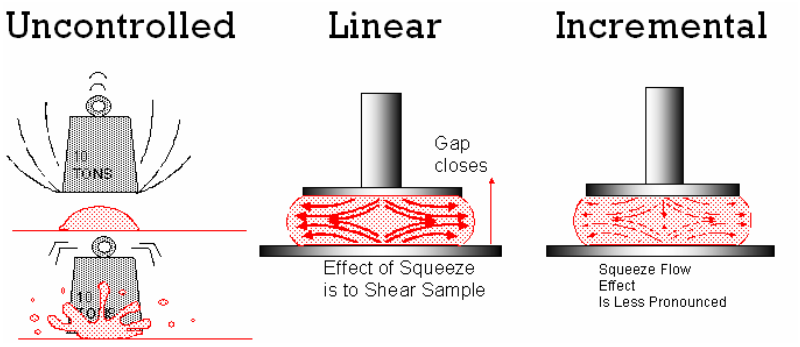

Figure 2.15 *Methods of lowering rheometer head.*

2.8 Surface Analysis

2.8.1 AFM studies of polymer matrices comprising PEO of varying molecular weights

AFM studies were carried out on 50µm and 1µm samples in co-operation with Intertek ASG and the university of Stellenbosch, South Africa, respectively. In both cases scans were obtained using a Topometrix Explorer SPM. The parameters for each test remained constant, with the exception of sample scan size and the mode of scan. The scans carried out at Intertek ASG were carried out in non-contact mode while the scans carried out at the university of Stellenbausch were carried out in tapping mode. Samples were mounted onto a metal stub using double-sided adhesive tape, such that the cross-section of each sample was face up to be analysed. Topography and phase imaging were obtained on sample regions in non-contact mode, using standard SPM probe tips.

The conditions used were as follows:

- Range = 20-650kHz
- **Amplitude = 1V**
- **Freq. = 327.859 kHz**
- **Input gain =1**
- **Set Point = 40% (non-contact)**
- **Set Point = 5 (contact)**
- **Proportional gain = 1**
- **Integral gain = 0.6**
- Derivative gain = 0
- Resolution = 300

Note: the values used in the parameters highlighted in bold varied slightly for several samples. These were altered to ensure optimum conditions were achieved for image acquisition of each sample.

2.8.2 Surface analysis of matrices incorporating an organically modified layered silicate

A Topometrix explorer AFM was utilised to study the effect of the nanoclay incorporation on the surface of the polymer / API matrix (Figure 2.16). The data acquired from the AFM was the forward and reverse topography and the forward and reverse lateral force in contact mode. Scans were acquired on the surface of the injection moulded test specimens. The PID settings were optimised for each scan in order to ensure accurate data acquisition. The scan range was set to 100 μm with a scan rate of 200 μm/s, and the set point used was 8 nA.

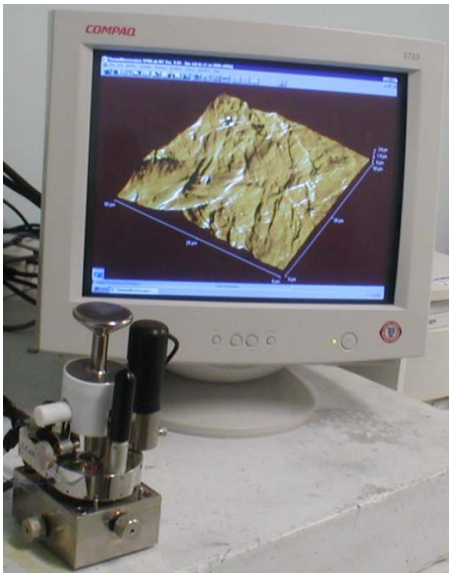

Figure 2.16 *The Topometrix explorer AFM unit and sample mounting base.*

2.8.3 Micro-thermal analysis

Micro-thermal analysis (μTA) is a materials characterisation technique combining the visualisation power of atomic force microscopy (AFM) with the characterisation capabilities of thermal analysis. A 2990 micro–thermal analyser incorporated into a Topometrix explorer AFM was used to characterise all of the blends in this study. Figure 2.17 shows a thermal tip typical of those used in this study.

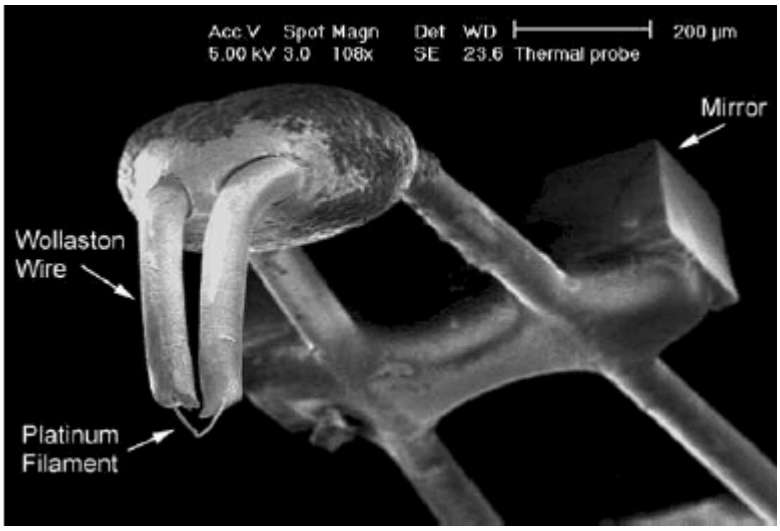

Figure 2.17 *Pictomicrograph of a standard probe used for µTA.*

Characterisation of materials was carried out in two modes: micro-modulated thermal analysis (µMDTA) in which thermal transitions are measured in a way analogous to MDSC and micro-thermomechanical analysis (µTMA), which can be used for the measurement of expansion, softening, melting and glass transitions.

Surface visualisation scans were acquired on a cross-section of the extruded granules with a constant probe temperature of 40°C. Samples were mounted onto a metal stub using double-sided adhesive tape, such that the cross-section of each sample was face up to be analysed. The PID settings were optimised for each scan in order to ensure accurate data acquisition. The scan range was set to 100 µm with a scan rate of 200 µm/s, and the set point used was 10 nA. µMDTA and µTMA measurements were taken at various surface points at a rate of 20°C per minute from ambient temperature to 350°C. A frequency of 2.2 KHz and heating amplitude of 3°C was used to record 150 points per second.

2.9 Dissolution testing

Dissolution testing was carried out using a Sotax AT7 smart dissolution system from Carl Stuart Ltd, displayed in Figure 2.18. Tests were carried out in triplicate using the Basket method (USP XXV). The dissolution media used in these tests consisted of 0.2M hydrochloric acid (pH 1.2), and manually prepared phosphate buffer solutions (pH 7.2). All tests was carried

out at 37°C ± 0.5°C. The stir rate was set to 100 rpm with 600 ml of dissolution media used per vessel. The wavelength and absorption of a 100% drug concentration for the API was determined using a Perkin Elmer Lambda 40 UV/Vis spectrometer. These values were entered into software calculations prior to commencement of testing. In the case of extruded samples, test specimens of constant size and surface area were produced by cutting the extrudate strands manually to give granules of length 0.5 cm, for moulded samples the moulded article was added to the dissolution media without further sample preparation. Samples were automatically taken every 15 minutes, filtered and passed through a Perkin Elmer Lambda 20 UV/Vis spectrometer, before being returned to the dissolution chamber. The dissolution profile was observed from a plot of time versus absorbance.

Figure 2.18 *The Sotax AT7 smart dissolution system.*

2.10 Optical Microscopy

Optical microscopy of samples was carried out on a Wild M3Z stereo-zoom microscope using an optical ring illuminator system at ten times magnification. The microscope is displayed in Figure 2.19.

Figure 2.19 *The Wild M3Z microscope.*

2.11 Thermal imaging

An IRI 4010 thermal imager was used to obtain thermal images of extrusion equipment during this work and is presented in Figure 2.20. The IRI 4010 has a temperature range from -10°C to 250°C with a sensitivity of 0.15°C. All thermal images were collected at a distance of 3 feet from the processing equipment.

Figure 2.20 *The IRI4010 thermal imager.*

2.12 Toxicological assessment

Both continuous cell lines were grown from frozen ampoules and routinely subcultured according to standard procedures, as summarised in Table 2.16 (Freshney, 1987).

Table 2.16 *HepG2 and Caco-2 cell culture medium constituents, storage temperature, and volume.*

Medium component	Storage temperature [°C]	HepG2 consituents Volume [ml]	Caco-2 consituents Volume [ml]
Foetal calf serum (FCS)	- 20	10	10
L-Glutamine	- 20	1	1
Penicillin/Streptomycin	- 20	0.5	0.5
Amphotercin	- 20	0.5	0.5
DMEM (Hepes modification)	+ 4	44	87
HAMS F-12 (Hepes modification)	+ 4	44	-
Non essential amino acids	+4	-	1

In order to maintain a sterile working environment all culture manipulation of cells was carried out in a class II laminar flow cabinet in a dedicated cell culture laboratory. In order to achieve a satisfactory level of sterility, aseptic technique was strictly adhered to according to standard procedures. At regular intervals the CO_2 incubator was cleaned out using 70% ethanol.

2.12.1 Harvesting and subculture

Once the cells reached 80 % confluency, the culture flask was removed from the 37°C incubator and the medium was aspirated off prior to rinsing with sterile PBS (0.01 M phosphate buffer, containing 0.0027 M KCl and 0.137 M NaCl at pH 7.4). Subsequently, 2 to 5 ml of 0.25 % trypsin EDTA (ethylenediaminetetracetic acid) was added and the flask swirled prior to removal of all but 0.5 ml of trypsin EDTA and the flask incubated at 37^{o}C for 5-10 minutes, or until complete detachment had occurred. The cells were then collected in 5 ml of complete media, transferred to a sterile universal and centrifuged at 2000 rpm for 5 minutes. The supernatant was discarded and the pellet re-suspended in 4 ml of culture medium which were incubated at the appropriate temperature of 37^{o}C at 5 % relative humidity (Freshney, 1987).

2.12.2 Preparation of matrices

To minimise the risk of contamination, the matrices were UV sterilised under a UV-light radiating lamp (263 nm) for 8 min. The material was then diced into small fragments

to enhance solubilisation. In order to obtain appropriate test solutions for toxicity testing, the polymers were dissolved in PBS at pH 7.4. A 5 % [w/v] solution of each test matrix was prepared by placing 2.5 g of test material into a 50 ml volumetric flask which was filled with PBS and stirred constantly until the polymers were fully dissolved. Due to their high viscosity, the samples had to be further diluted with PBS and cell culture medium to be applicable for chosen *in vitro* toxicity tests.

2.12.3 The 3-(4, 5-dimethylthiazol-2yl)-2, 5-diphenyl-2H-tetrazoliumbromid (MTT) assay

A 5mg/ml MTT concentration was prepared by adding 50 mg MTT to 10 ml PBS in a sterile container and the solution was stored in the dark at +4^{o}C. Prior to use, this mixture was incubated at 37^{o}C for 1 hour and filter sterilised, using a 0.2 µm pore sized syringe filter to remove crystal formation.

Cytotoxic effects on the growth and viability of HepG2 and Caco-2 cells were determined by using 96 microwell plates seeded at 1-5 x 10^4 cells in 100 µl culture media containing 10 % FCS. The 96 microwell plates were then incubated overnight at 37^{o}C until the desired percentage of confluency (40-60 %) was observed. From the 5 % (w/v) polymer stock solution, a concentration range of between 1.25 – 0.25 % was prepared. The percentage of culture media in the final solutions was 75 % to ensure that cell death was not a result of adverse culture conditions. To remove bulk material from the test solutions, samples were filtered with a 0.45 µm pore sized syringe filter. The cell medium was replaced with 100 µl of prepared matrix solutions and further incubated for up to 24 hours at 37^{o}C.

After incubation the medium containing test chemicals was discarded and the wells were washed twice with warmed PBS. After the washing step 100 µl of fresh media followed by 10 µl of prepared MTT solution was added to each well to obtain a final MTT concentration of 0.5 mg/ml. After 4 hours incubation at 37°C, the MTT containing medium was carefully aspirated of the cells and the formation of blue formazan crystals was solubilised by the addition of 100 µl of dimethyl sulfoxide (DMSO) to each well. To support solubilisation the plates were shaken gently and the absorbance was determined using a multiwell plate reader (Titerek Multiscan plus) at a test wavelength of 540 nm.

2.12.4 The lactate dehydrogenase (LDH) assay

LDH leakage resulting from exposure of Caco-2 and HepG2 cells to test material was monitored using the lactate dehydrogenase Cytotoxicity Assay-Kit (Sigma).

Table 2.17 *Contents of LDH Cytotoxicity Assay-Kit.*

Content	***Quantity***
LDH Assay Substrate Solution	25 ml
LDH Assay Cofactor	25 ml
LDH Assay Dye Solution	25 ml
LDH Assay Lysis Solution	10 ml

The LDH assay cofactor solution was prepared by adding 25 ml tissue culture grade water to the bottle of lyophilised cofactors. At the time of use Lactate Dehydrogenase Assay mixture was prepared by mixing equal amounts of LDH assay substrate, Cofactor and Dye solution.

Caco-2 and HepG2 cells were harvested and seeded in 96-well cell culture dishes at a concentration of 5 x 10^4 cells in 200 µl volumes per well. Following incubating at 37^{o}C for 24-48 hours, depending on the cell line, the desired degree of confluence was obtained (80 – 90 %). From the 5 % (w/v) matrix stock solution a concentration range of between 1.25 – 0.25 % was prepared. Subsequently culture medium was replaced with 200 µl of prepared polymer solutions and further incubated for 12 or 24 hours at 37^{o}C. Maximum LDH release (set as 100 % LDH release) was facilitated by incubating 20 µl of LDH assay lysis solution with cell medium for 45 minutes.

Following incubation, 150 µl of the polymer-containing culture medium was carefully removed from the wells, transferred into individual microtubes and centrifuged at 250 g for 4 minutes to pellet cells. After transferring 100 µl of each supernatant into separate wells of a new multi-well plate, 200 µl of assay mixture was added to each well to initiate the enzymatic reaction. The plates were covered with an opaque material to protect from light and incubated at room temperature for 30 minutes. The absorbance of each well was simultaneously determined using a multiwell plate reader (Titerek Multiscan plus) at a

test wavelength of 490 nm. To eliminate background the absorbance of culture medium and matrix solutions used in the assay were also determined in the absence of the enzymatic reaction and subtracted from each individual result. The untreated control was set as spontaneous release and also subtracted from results obtained for relative and maximum release. Percentage LDH release of the sample was calculated as follows:

$$\text{LDH release [\%]} = \frac{(A_{\text{sample}} - A_{\text{spontaneous}}) \times 100}{(A_{\text{maximum}} - A_{\text{spontaneous}})}$$

Where:

A_{sample} = Absorbance values for the cells treated with polymers
$A_{\text{spontaneous}}$ = Absorbance value for spontaneous LDH release
A_{maximum} = Absorbance value for maximum LDH release in lysed cells

2.12.5 The single cell gel electrophoresis (SCGE) or 'Comet' assay

The following solutions and reagents were prepared as listed in Table 2.18 and made up to their final volume using double distilled water (ddH_2O). HepG2 cells were suspended at a density of 3 x 10^4 cells per ml and 2 ml aliquots of cell suspension was added to individual wells of a 24 well plate and incubated over night at 37°C. From the 5 % (w/v) matrix stock solution a concentration range from 1.25 – 0.25 % was prepared. Culture medium was replaced with 2 ml of prepared matrix containing medium and further incubated for 24 hours at 37°C. A 100 mM working stock of hydrogen peroxide (H_2O_2) was prepared and diluted in complete culture medium to give the following concentrations: 50, 5 and 0.5 mM and 20 µl of each H_2O_2 concentration was then added to duplicate wells to give final concentrations of H_2O_2 of 500, 50 and 5 µM prior to incubation for 1 h at 37°C. Subsequently, the medium was removed and the wells rinsed twice with 1 ml PBS. The cells were harvested by adding 300 µl of 0.25 % trypsin EDTA to each well for 5 minutes at 37°C followed by a further 700 µl of culture medium and centrifugation at 10,000 rpm for 5 minutes. Cells were then re-suspended in 200 µl of ice-cold PBS and stored on ice.

A 1 % low melting point (LMP) agarose in PBS solution was prepared by dissolving 0.2g agrose in 20 ml PBS and kept at 45°C to prevent solidifiction. Next, 200 µl aliqouts of cells were mixed with 400 µl of LMP agarose and 100 µl were pipetted onto

individual gel bond strips (Gel Bond Electrophoresis Film; Sigma), coverslipped and stored at 4°C for 5-10 min or until the gel had set. After removing the coverslips, the strips were placed in Quadriperm plates (Sartorious) and the cells were subjected to lysis by immersion in ice cold lysis buffer pH 10 for 5 min at 4°C followed by rinsing 5 times in TAE buffer pH 8 to remove residual salt.

Alkaline electrophoresis was preceded by a 20 min unwinding step in 0.3 M NaOH. Electrophoresis was performed at 28 V and 350 mA for 5 min in a 2 liter capacity 35 cm tank and Power Pac 300 (Bio-Rad), with gel bond strips placed horizontally side by side avoiding gaps. Prior to analysis DNA was stained by pipetting 40 µl ethidium bromide (10 µg/ml) onto each gel bond strip, the gels coverslipped and observation made at 40x oil magnification using Leica fluorescent microscope equipped with an excitation filter of 515 – 560 nm and a 590 nm barrier filter. Images of 40 randomly selected cells (20 images/replicate slide) were analysed for 'tail moment' using computerised image analysis software (Comet Assay IV, Perceptive Instruments, UK) and DNA damage expressed as a function of the measured 'tail moment' parameter.

2.12.6 The unscheduled DNA synthesis (UDS) assay

HepG2 cells were harvested and seeded at a density of 8 x 10^4 cells per ml on sterilised coverslips in 6 well plates and were incubated for 1 hour at 37°C to allow cells to adhere. Subsequently the coverslips were examined for cell attachment and 3 ml of complete culture medium was carefully pipetted into each well and cells were cultured overnight at 37°C.

The culture medium was replaced with 3 ml low serum medium containing 0.5 % foetal calf serum (FCS) and the cells were cultured for 65 h before replacing the low serum medium (0.5 %) with high serum medium (10 % FCS) for a further 6 h incubation at 37°C. Cells were arrested in early S phase by 14 hours incubation in complete medium containing 2.5 mM hydroxyurea.

Table 2.18 *Preparation of buffer solutions for the SCGE.*

Solution / Reagent	Ingredient	Concentration	Amount added	pH	Final volume
Lysis solution	EDTA	100 mM	37.22 g	10 (using 5 M NaOH)	1 L
	Tris	10 mM	1.21 g		
	NaCl	2.5 M	146.1 g		
	Triton X-100	1 %	10.0 ml		
TAE buffer	Tris-acetate	40 mM	4.84 g	8 (using 1 M acetic acid)	1 L
	EDTA	1 mM	0.372 g		
NaOH solution	NaOH	0.3 M	12.0 g		1 L
Electrophoresis Buffer (x 10)	NaCl NaOH EDTA	2.7 M 0.3 M 10 mM	157.79 g 12 g 0.744 g		1L
Electrophoresis buffer (x 1)	200 ml of 10 x electrophoresis buffer, made to final volume with ddH_2O				2L

The detection of UDS in HepG2 cells was maintained by using the 5-bromo-2-deoxy-uridine labelling and detection Kit I (Roche). During DNA synthesis bromodeoxyuridine (BrdU) is incorporated into DNA in place of thymidine, with the incorporated BrdU detected via a monoclonal antibody against BrdU and a fluorochrome-conjugated second antibody.

All solutions used for the labelling and detection method were prepared shortly before use and stored appropriately. The Brdu labelling medium was prepared by diluting

0.1 ml of BrdU labelling reagent with 100 ml of complete culture medium (final concentration 10μM).

Table 2.19 *Contents of the BrdU Labeling and Detection Kit I.*

Label	*Content*
BrdU labelling reagent	1 x 10 ml BrdU stock solution (1000 x conc.) in 10 mM sterile PBS
Washing buffer concentrate	1 x 100 ml PBS (10 x conc)
Incubation buffer	1× 100 ml [66 mM Trisbuffer, 0.66 mM MgCl, 1 mM 2-mercaptoethanol]
Anti-BrdU	1× 1 ml anti-BrdU, mouse monoclonal antibody (clone BMG 6H8 IgG 1) containing nucleases for DNA denaturation, in PBS/glycerin
Anti-mouse Ig- fluorescein	from sheep; immunosorptively purified, lyophilised, stabilised

An anti-BrdU working solution was prepared by diluting 1 ml of anti-BrdU (mouse monoclonal antibody containing nucleases for DNA denaturing) with 9 ml of incubation buffer. In addition, the anti-mouse lgG-fluorescein working solution was prepared by resuspending the lyophilised anti-mouse lgG-fluorescein in 1 ml double distilled water prior to diluting in 9 ml of PBS. The washing buffer was prepared by diluting 30 ml of washing buffer concentrate with 270 ml double distilled water. A solution, containing 50 mM glycine in 95% ethanol was used as a fixative.

Using the 5% (w/v) matrix stock solutions a final concentration range from 1.25-0.25% was prepared by diluting the stock in culture media containing 10 % FCS and 2.5mM hydroxyurea. To obtain comparable results, the percentage of culture medium in the final solution of each polymer was 75 %. Synchronisation culture medium was replaced with 3 ml of prepared polymer containing medium and further incubated for 3 hours at 37 °C.

A 100mM working stock of hydrogen peroxide (H_2O_2) was also prepared in complete culture medium containing 2.5mM hydroxyurea and various dilutions were performed to give the following concentrations: 50, 5 and 0.5mM, of which 30µl of each was added to duplicate control wells for 1 hour at 37°C to give final concentrations of H_2O_2 of 500, 50 and 5µM.

The test media was replaced with 3 ml of BrdU labelling medium for a further 60 min incubation at 37°C after which the BrdU labelling medium was removed and the cells washed three times with sufficient amount of washing buffer. The cells were then fixed with the ethanol fixative for 30 min at –20°C followed by another wash step. Binding of the anti- BrdU monoclonal antibody was performed by incubating the cells at 37°C for 30 min in 350 µl of anti-BrdU working solution (added carefully to cover all cells).

Before performing a similar incubation step in 350µl of anti-mouse lg-fluorescein working solution, cells were washed three times with washing buffer. Finally, after an additional washing step the coverslips were mounted with Citofluor (glycerol; PBS; 1:1) on glass slides and analysed via fluorescence microscope.

Chapter 3

Results and Discussion

3.1 Evaluation of PEO for suitability as a matrix forming polymer

3.1.1 Effect of polymer molecular weight on the matrix forming properties of PEO

3.1.1.1 Introduction

In hot melt extruded monolithic matrices for drug delivery, the active agent is embedded in a carrier formulation comprising one or more melt processable substances as well as other functional excipients such as antioxidants, plasticisers, thermal stabilisers, etc. The selection of an appropriate carrier material is vital to the final matrix formulation. The properties of the carrier material dictate not only the processing conditions used in the hot melt extrusion of the matrix but also influence the release rate of the active agent from the matrix. Polyethylene oxide (PEO) is a non-ionic, highly hydrophilic water soluble polymer. The structure of PEO is presented in Figure 3.1. Pharmaceutical PEO grades hold official status in USP 23-NF 18. All commercially available grades of PEO are white to off-white powder with a mild ammonical odour. Due to their chemical structure, PEO materials are among various hydrophilic polymers that, in the presence of water, control the release of an active moiety either by swelling (Mw > 2,000,000) or by eroding and swelling (Mw < 900,000) (Pinto *et al*. 2004). Due to its ability to control the release of an active agent, its regulatory acceptability and its non-toxicity, PEO has gained much interest as a pharmaceutical excipient.

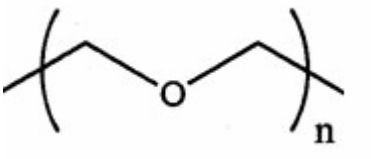

Figure 3.1 *Chemical structure of PEO, with 'n' indicating the number of repeat units.*

PEO materials have found use in swellable and erodible implants (Witt *et al*. 2000), scaffolds for tissue engineering (Washburn *et al.* 2002) and hydrogels (Savas and Guven, 2001). However, most attention has recently been focused on PEO as a material for producing controlled release solid dosage forms such as matrices (Zhang and McGinity, 1999; Crowley and McGinity, 2002) or coated cores (Efentakis *et al*. 2000; Lim *et al*. 2000, Repka and McGinity, 2000). PEO has been used for controlled-release matrix systems of water-insoluble as well as water-soluble drugs. The drug-release mechanism is controlled by several variables in a dynamic process. The release kinetics of the drug from the tablet are dependent upon the relative magnitude of the rate of polymer swelling at the moving rubbery-glassy front and the rate of polymer erosion at the swollen polymer-dissolution medium front. It is preferable to attain the synchronisation of the velocities of the swelling front and the erosion front to achieve zero-order release kinetics from PEO matrices. Water-soluble drugs are released by diffusion of the drug through the swollen gel layer, and insoluble drugs are released by erosion of the polymer layer. The molecular weight of PEO, concentration of polymer, solubility of the drug and the amount of the drug, affect the release of the drug from the matrices.

Table 3.1 *Batch composition used to investigate the effect of varying PEO molecular weight on the properties of a PEO based monolithic matrix.*

Batch No.	PEO Mw 200,000 (*%wt*)	PEO Mw 1 million (*%wt*)	PEO Mw 5 Million (*%wt*)	Carvedilol(*%wt*)
1	20	50	30	0
2	30	50	20	0
3	30	40	30	0
4	17	42.5	25.5	15
5	25.5	42.5	17	15
6	25.5	34	25.5	15
7	14	35	21	30
8	21	35	14	30
9	21	28	21	30

In this section the use of PEO as a matrix forming material in hot melt extruded monolithic matrices is examined. The effect of drug loading on the matrix, in addition to the effect of the molecular weight of the matrix material on the processability, strength and drug release characteristics of an oral dosage form is also considered. The batches prepared for testing in this section are outlined in Table 3.1.

3.1.1.2 Processing observations

Extruder torque is a measure of the resistance that the drive motor experiences as a consequence of the melt viscosity of the polymer inside the barrel. Verreck *et al.* (2006) discussed the use of the extruder torque values as a method of measuring relative viscosities of polymer melts at set values of processing temperature, feed rate and screw speed. In this study, the extruder torque reading was supplemented with measurement of die head pressure during processing. Die head pressure is a measurement obtained by a pressure transducer which records the pressure exerted by the polymer melt at the shaping die. Higher viscosity melts will exert more pressure than melts with lower viscosities. In this work, changes in the measured extruder torque and die head pressure were used as a method of measuring changes in the viscosity of the formulation being processed and thus gauging the relative processability of the matrices when the ratio of the different molecular weights of PEO material making up the matrix is altered (Figure 3.2).

The measurements obtained during the processing of the formulations indicate that PEO matrices containing larger proportions of higher molecular weight material (Mw 1 million and Mw 5 million) are more difficult to extrude as they exhibit higher values of torque and die head pressure during processing. The melt behaviour of PEO has been reported to be pseudoplastic in nature (Bicerano, 1996) and incorporation of active pharmaceutical ingredient (API) is seen to plasticise the polymer matrix with reduction in the motor load and die head pressure occurring with increasing API loading. This behaviour has previously been reported by Ozeki *et al*. (1997). It was noted during the moulding of the test specimens that matrices containing high ratios of high molecular weight PEO were very difficult to mould. In all cases control over the moulding process was very limited with moulding defects such as short shots resulting in a small proportion of the parts produced being discarded.

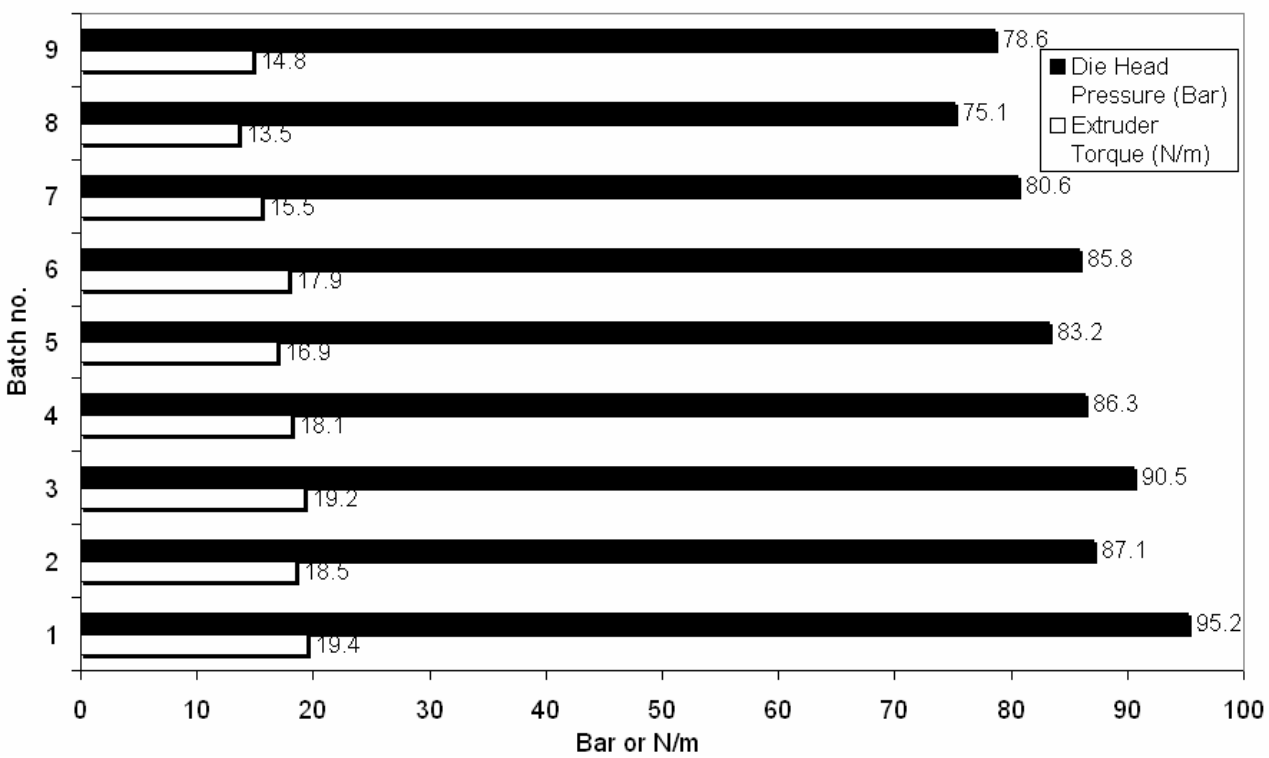

Figure 3.2 *Torque and die head pressure measurements taken during the hot melt extrusion process.*

3.1.1.3 Thermal analysis

Thermal analysis of the polymer samples was carried out in order to determine if variations in the ratios of different molecular weight species of PEO present in the matrix had an effect on the thermal properties of the polymer. Figure 3.3 shows thermograms typical of those obtained in this study.

The presence of an intense peak indicates the semicrystalline nature of the polymer. As stated in previous work by Ozeki *et al*. (1997) and in agreement with values observed in the torque and die head pressure readings obtained in the processing of the polymer matrices, the API is shown to have a plasticising effect on the polymer matrices examined. The plasticising effect is manifested by a depression in the melting point of the polymer matrices, the magnitude of which increases with increasing API inclusion: the PEO matrix comprising 20%wt Mw 200,000, 50%wt Mw 1 million and 30%wt 5 million exhibited a melting peak at 70.69°C. This melting peak was depressed to 67.01°C upon addition of 15%wt active agent. The melting peak was further depressed to 62.69°C with addition of 30%wt active agent.

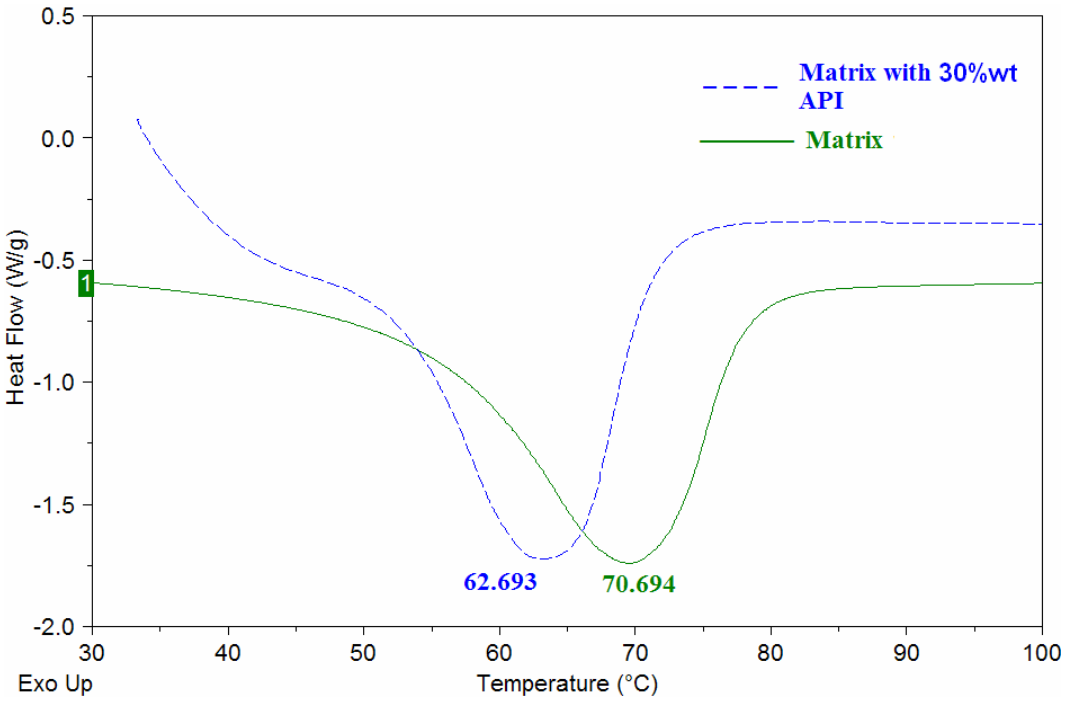

Figure 3.3 *DSC thermogram obtained for the PEO matrix comprising 20%wt Mw 200,000, 50%wt Mw 1 million and 30%wt 5 million, also depicted is the thermogram for the same matrix loaded with 30%wt API.*

As the molecular weight of PEO increases so to does the melting point. Herman *et al.* (1986) proposed that the melting point remains constant at 65°C over a range of molecular weights from about 6,000 to 2 million. Table 3.2 illustrates the changes in the melting point up to a molecular weight of 2,000,000.

Table 3.2 *Changes in the melting point of PEO (adapted from Herman et al. 1986).*

Approximate Molecular Weight	Melting Point (°C)
200	Supercools
300	-15 to -8
400	4 to 8
600	20 to 25
1,000	37 to 40
1,500	43 to 46
4,000	53 to 56
6,000	60 to 63
300,000	62 to 65
2,000,000	62 to 65

Ozeki and co-workers (1999) noted that the onset of melting and the melting point of PEO increased as the molecular weight increased. The results obtained by Ozeki *et al.* showed good agreement with a recent study by Crowley and investigators (2002) where DSC thermograms of PEO with a molecular weight of 1 million showed a melting range from 55°C to 80°C. Thermograms obtained in this work support the findings of Ozeki *et al.* (1999) and Crowley *et al*. (2002). In this case, increases in the loading of PEO Mw 5 million in the matrix is seen to result in increases in the observed melting point of the matrix.

3.1.1.4 Steady state rheometry.

As previously discussed, the die head pressure and torque readings obtained during the extrusion process allowed changes in melt viscosity to be monitored during processing. Steady state parallel plate rheometry was used to augment these measurements and more quantitatively investigate the rheological properties of the matrices.

The rheological data presented in Figure 3.4 shows the change in the viscosities for matrices containing different loadings of active agent. The viscosity of the matrix decreases with increased loading of active agent over a range of shear rates. These results are in agreement with the observed changes in torque and die head pressure during the extrusion of the matrices and with the plasticising effect noted in the thermal analysis.

Figure 3.5 illustrates differences in viscosity as the ratios of the PEO constituents in the matrices under investigation are altered. The data presented shows that matrices with higher proportions of higher molecular weight PEO (Mw 1 million and Mw 5 million) are more viscous than matrices made up of higher proportions of PEO Mw 200,000. This is consistent with the data obtained during processing and thermal analysis of the batches in question. These results would also indicate that moulding of matrices containing high molecular weight PEO would require equipment capable of very high injection pressures.

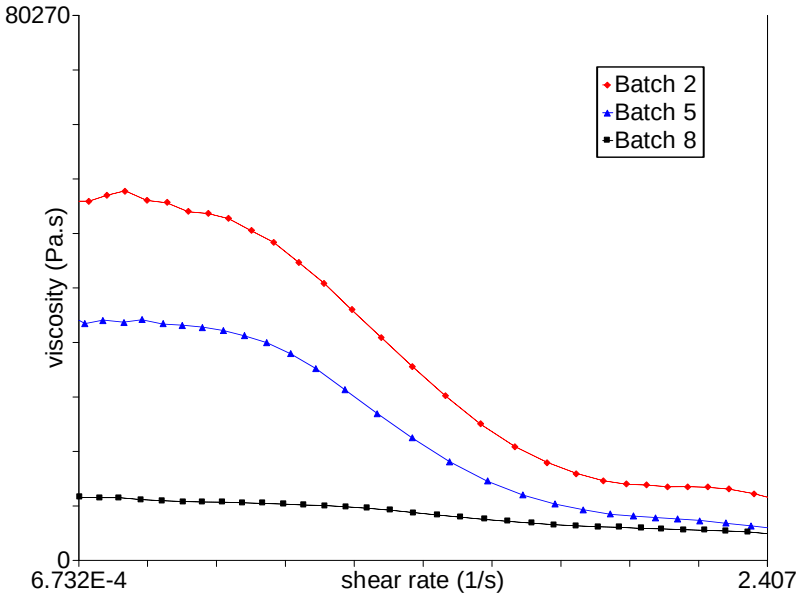

Batch number	*PEO Mw 200,000 (%wt)*	*PEO Mw 1 million (%wt)*	*PEO Mw 5 million (%wt)*	*API (%wt)*
2	*30*	*50*	*20*	*0*
5	*25.5*	*42.5*	*17*	*15*
8	*21*	*35*	*14*	*30*

Figure 3.4 *Steady state viscosity data recorded for batches 2, 5 and 8.*

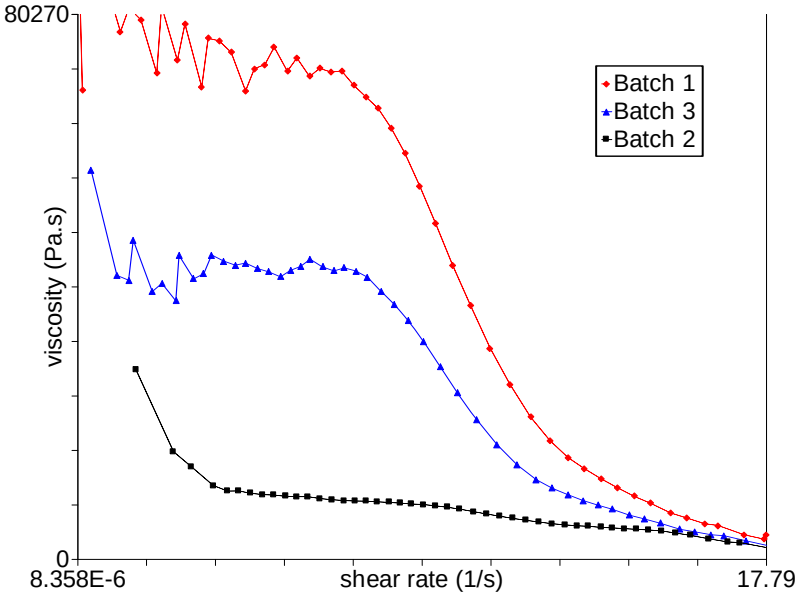

Batch number	*PEO Mw 200,000 (%wt)*	*PEO Mw 1 million (%wt)*	*PEO Mw 5 million (%wt)*	*API (%wt)*
1	*20*	*50*	*30*	*0*
2	*30*	*50*	*20*	*0*
3	*30*	*40*	*30*	*0*

Figure 3.5 *Steady state viscosity data recorded for batches 1, 2 and 3.*

Viscosity change in PEO is a direct result of chain entanglements in the polymer melt and not as a result of changes in the density of PEO. Figure 3.6 shows the molecular weight of the commonly used commercial polymer poly(styrene) with the corresponding density values, compared with those of PEO. It can be seen that there is a negligible difference in the density of PEO on increasing molecular weight, remaining constant from approximately 200 upwards, whereas poly(styrene) (PS) has a steep climb up to about 20,000 where it evens out.

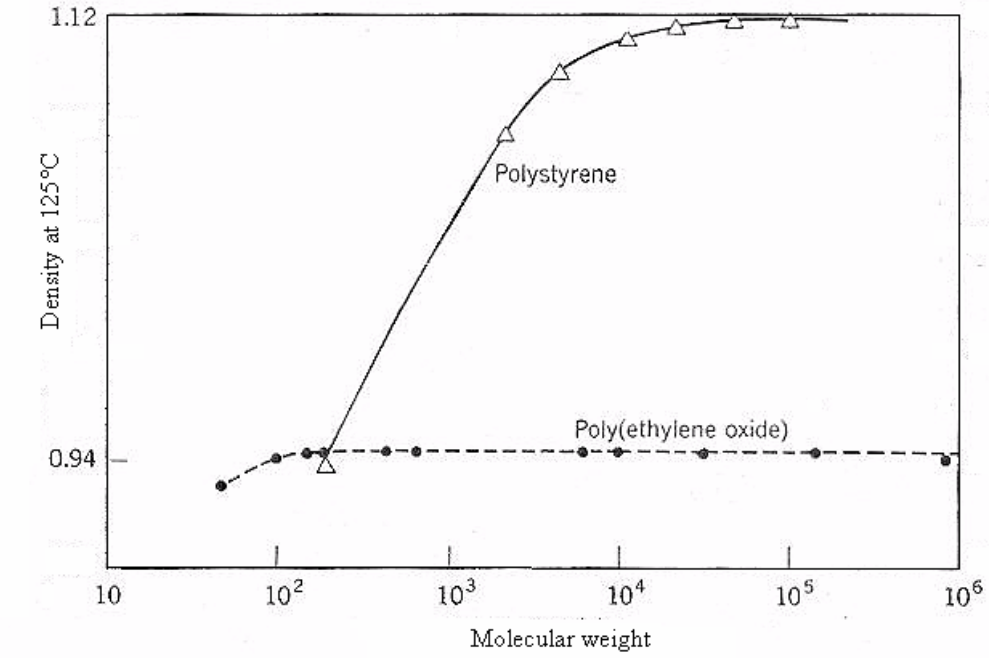

Figure 3.6 *Molecular weight of PEO and PS plotted as a function of melt density (Adapted from Herman et al. 1986).*

3.1.1.5 Mechanical analysis

Extruded material from each batch was injection moulded into test specimens in order to allow the mechanical properties of the matrices under investigation to be analysed. Figure 3.7 illustrates the average maximum tensile stress and extension at break for each of the batches tested. Matrices containing higher proportions of PEO materials with higher molecular weights exhibit higher tensile stress at break and better overall mechanical properties than those with higher proportions of PEO, Mw 200,000, in the matrix. The effect of the inclusion of the active agent has an obvious effect on the mechanical properties of the matrices. Increased loading of active agent leads to increased extension at break and decreased tensile strength. This behaviour is typical of a polymer with increased

plasticiser loading, further reinforcing the observation that the active agent acts as a plasticiser in the polymer matrix

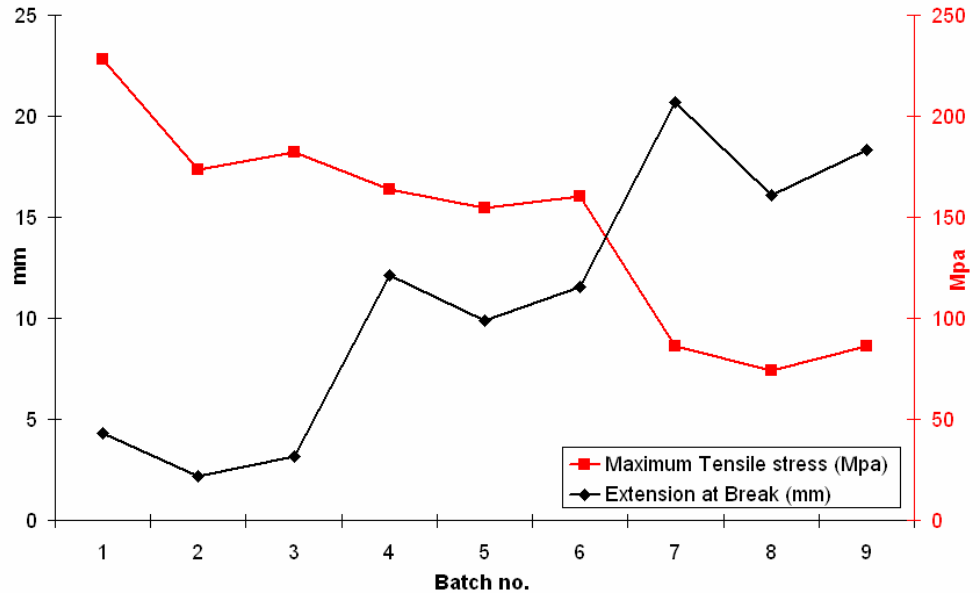

Figure 3.7 *Selected mechanical properties of the batches under investigation.*

3.1.1.6 Surface analysis using Atomic Force Microscopy (AFM)

Surface analysis of the batches under investigation was carried out using AFM. Each batch was scanned in non-contact mode in three distinct regions, with both phase and topography information being recorded. Figures 3.8, 3.9, and 3.10 show the scans obtained for batches 3, 6 and 9 respectively.

The images obtained show that inclusion of the active agent tends to break up the spherulitic crystalline structure observed in PEO without active agent incorporation. Spherulites are clearly visible in the phase images of batch 3, comprising 30%wt Mw 200,000, 40%wt Mw 1 million and 30%wt Mw 5 million and does not contain any active agent loading. Batches 6 and 9 are matrices of the same composition as batch 3 but are loaded with 15%wt and 30%wt API respectively. Phase imaging of batch 6 reveals a small amount of partially formed spherulites. However, in batch 9 at 30%wt active agent loading, no evidence of spherulitic structures remain. The topography of the PEO matrices remains similar, regardless of their composition or API loading.

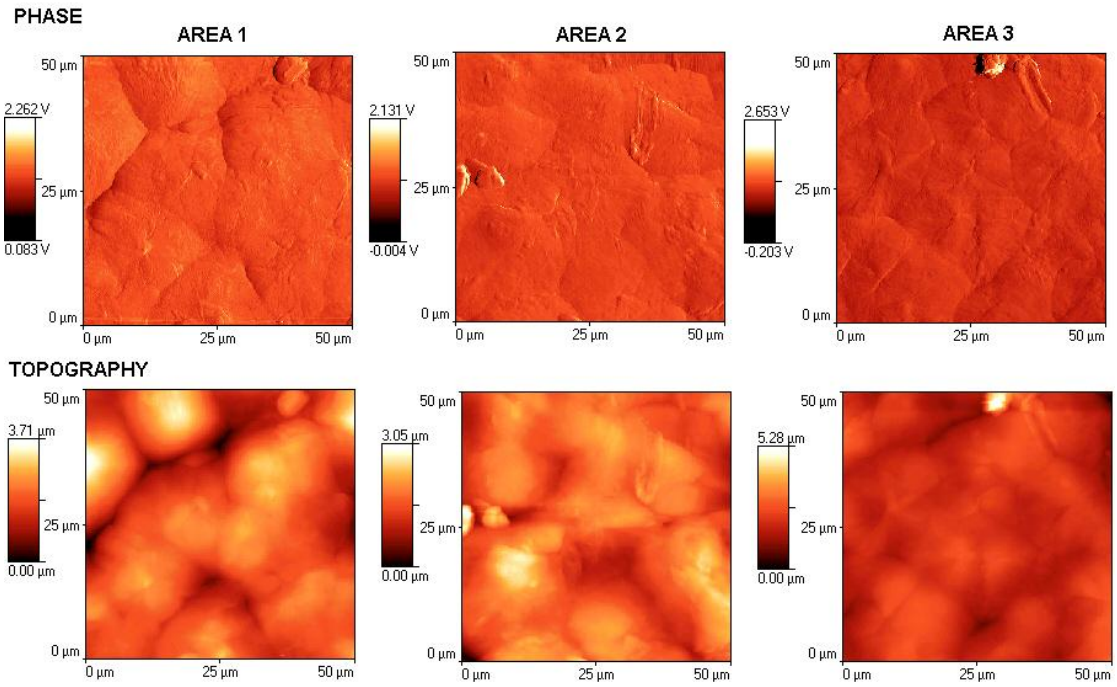

Figure 3.8 *Phase and topography images obtained from 3 distinct regions on batch 3 comprising 30%wt Mw 200,000, 40%wt Mw 1 million and 30%wt Mw 5 million.*

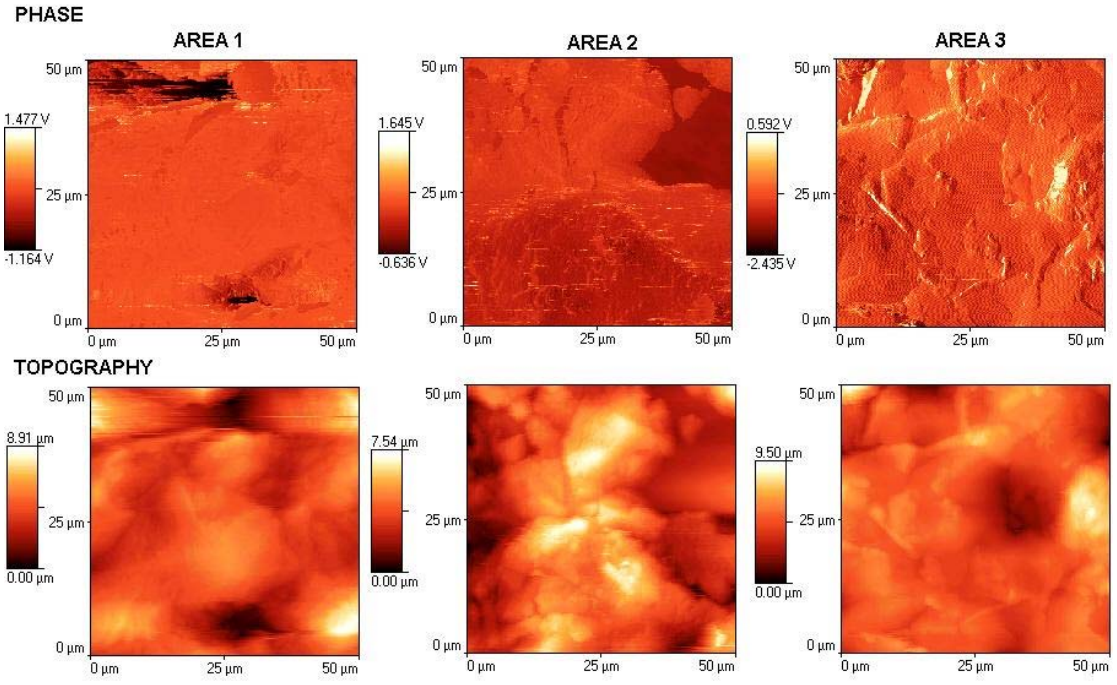

Figure 3.9 *Phase and topography images obtained from 3 distinct regions on batch 6. The composition of batch 6 is identical to that of batch 3 but with 15%wt API loading.*

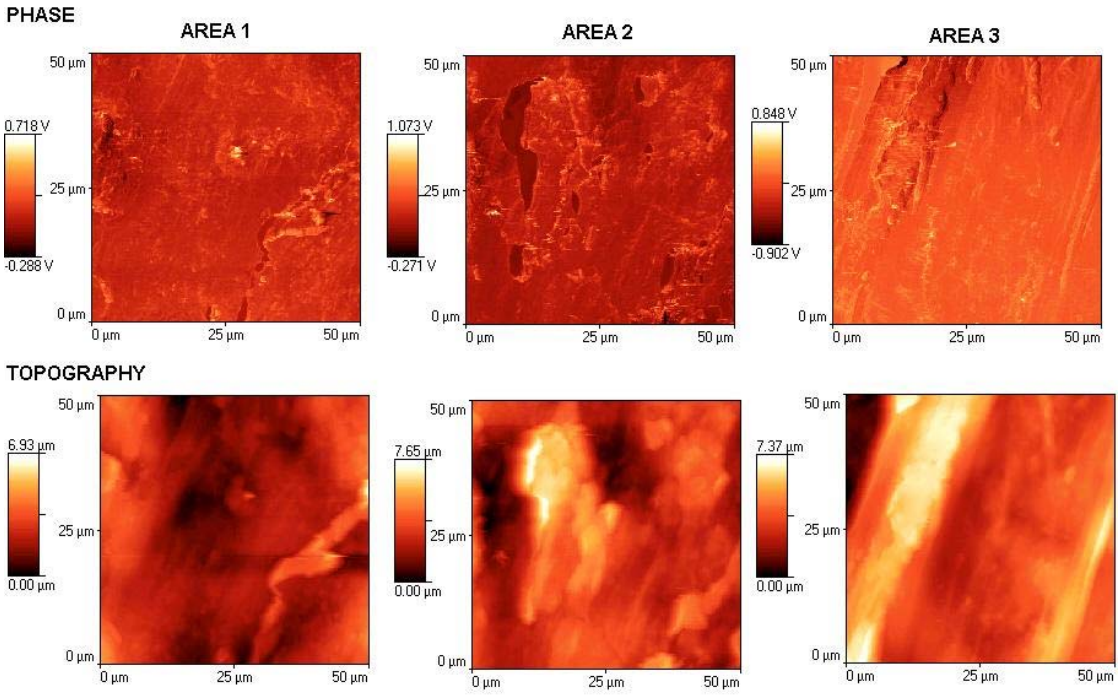

Figure 3.10 *Phase and topography images obtained from 3 distinct regions on batch 9. The composition of batch 9 is identical to that of batch 3 but with 30%wt API loading.*

3.1.1.7 Drug release

Drug release studies were carried out for all the batches with an active agent incorporated in the matrix. The results of these studies are presented in Figures 3.11, 3.12, 3.13 and 3.14. The drug release profiles of the polymer matrices are not observed to be substantially altered by the pH of the dissolution medium. This is consistent with findings in the literature (Kim *et al*. 1998). This result suggests that PEO is a good candidate for oral drug delivery systems as oral dosage forms must travel along the gastrointestinal tract and be subjected to the fluctuating pH values typical of that environment.

The matrices containing higher proportions of PEO Mw 5 million in the matrix form gels that take longer to release the active agent. In addition, after the period of dissolution some gel remains in the test vessel. Maggi *et al*. (2002) evaluated the relative influence of drug diffusion and polymer erosion mechanisms of PEO in the drug delivery process.

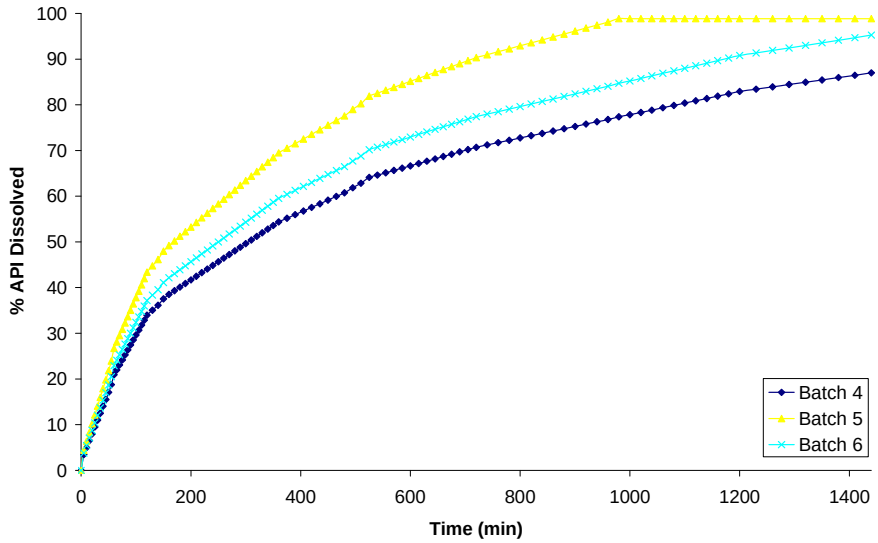

Batch number	*PEO Mw 200,000 (%wt)*	*PEO Mw 1 million (%wt)*	*PEO Mw 5 million (%wt)*	*API (%wt)*
4	*17*	*42.5*	*25.5*	*15*
5	*25.5*	*42.5*	*17*	*15*
6	*25.5*	*34*	*25.5*	*15*

Figure 3.11 *Drug release data for matrices loaded with 15%wt API in pH 7.2 buffer solution.*

Results obtained by Maggi and co-workers showed that the PEO with the higher molecular weight swelled to a greater extent and formed, upon hydration, a stronger gel, which is therefore less liable to erosion than the PEO of lower molecular weight. Apicella and co-workers (1993) observed that the drug release from high molecular weight PEO was strictly related to polymer swelling rather than dissolution and drug release from the low molecular weight PEO was strictly dependent upon the polymer dissolution mechanism.

An added benefit of using PEO as a rate controlling matrix is that due to the non-ionic nature of the polymer, no interaction between the drug and polymer is expected. Batches 7, 8 and 9 exhibited faster dissolution times than batches 4, 5, and 6. This is simply believed to be due to higher loading of the active agent and therefore less rate controlling polymer being present in the polymer matrix.

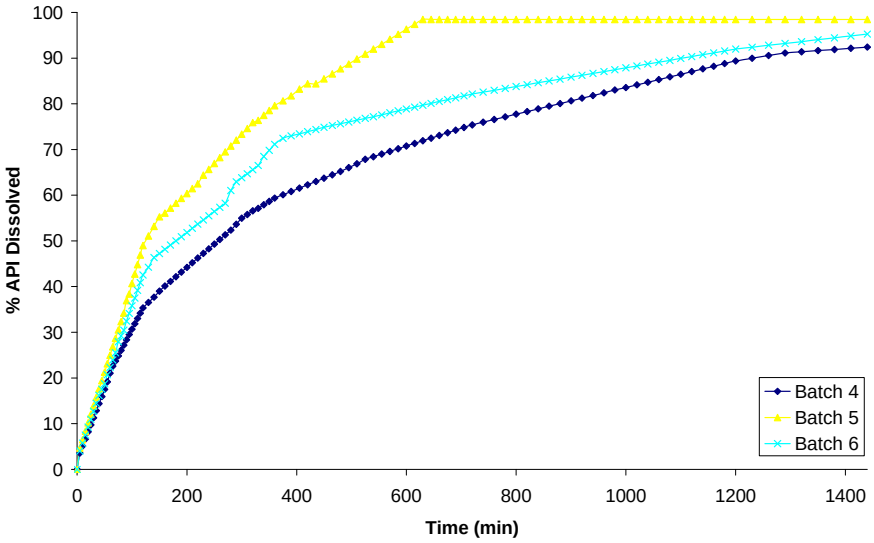

Batch number	PEO Mw 200,000 (%wt)	PEO Mw 1 million (%wt)	PEO Mw 5 million (%wt)	API (%wt)
4	17	42.5	25.5	15
5	25.5	42.5	17	15
6	25.5	34	25.5	15

Figure 3.12 *Drug release data matrices loaded with 15%wt API in 0.2M HCl (pH 1.2).*

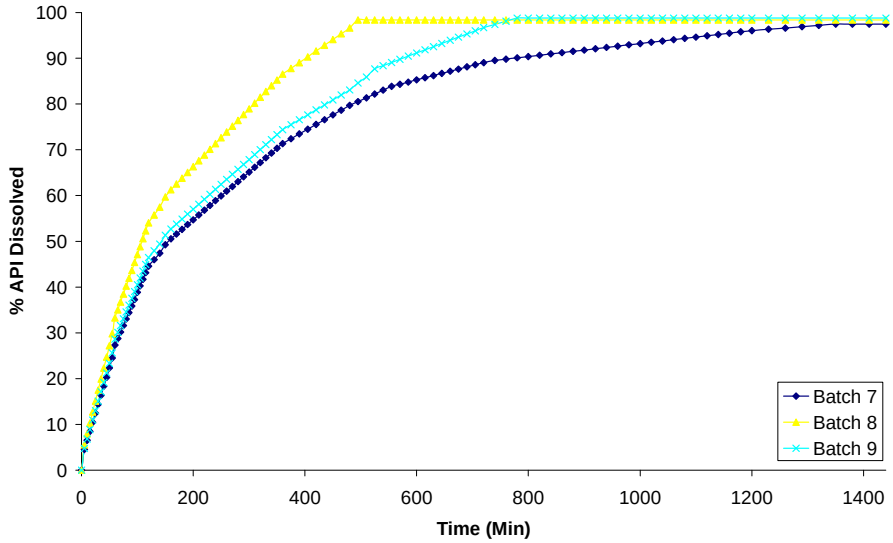

Batch number	PEO Mw 200,000 (%wt)	PEO Mw 1 million (%wt)	PEO Mw 5 million (%wt)	API (%wt)
7	14	35	21	30
8	21	35	14	30
9	21	28	21	30

Figure 3.13 *Drug release data for matrices loaded with 30%wt API in pH 7.2 buffer solution.*

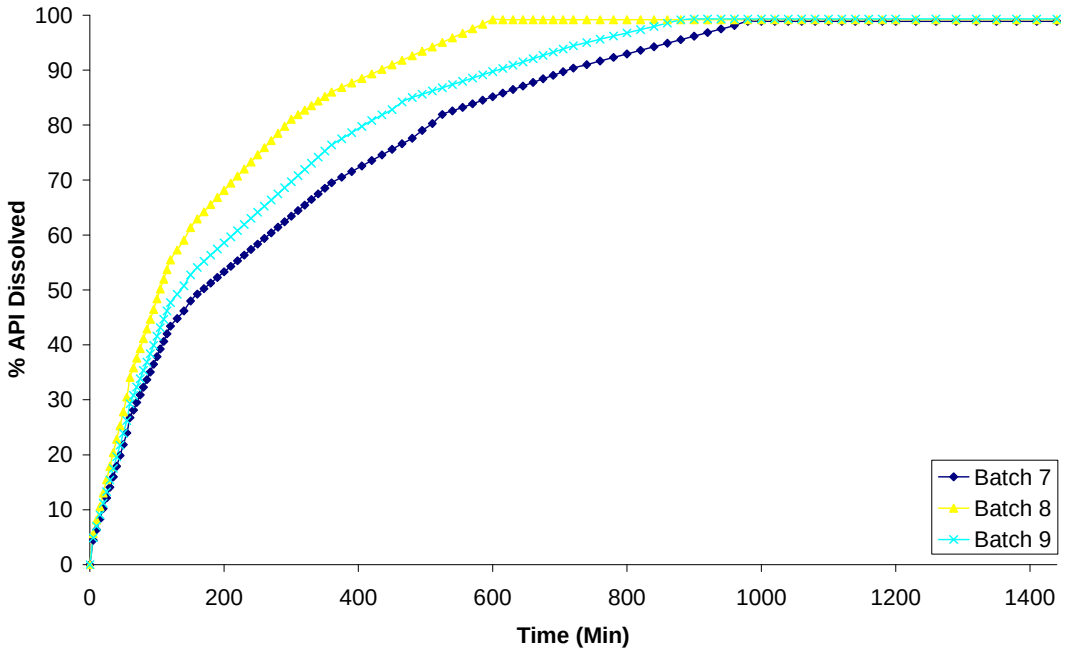

Batch number	PEO Mw 200,000 (%wt)	PEO Mw 1 million (%wt)	PEO Mw 5 million (%wt)	API (%wt)
7	14	35	21	30
8	21	35	14	30
9	21	28	21	30

Figure 3.14 *Drug release data matrices loaded with 30%wt API in 0.2M HCl (pH 1.2).*

3.1.1.8 Summary

The work presented in this section describes the use of PEO polymer matrices for controlled drug delivery. The molecular weight of the PEO polymers forming the matrix was varied in order to investigate the effect of PEO molecular weight on the processability and drug release characteristics of the matrix. In addition, batches of material were prepared with varying levels of API inclusion to investigate the effect of drug loading on the characteristics of the matrix. Torque and die head pressure measurements taken during the processing of the matrices indicate that a high percentage inclusion of PEO Mw 5 million in the matrix renders it more difficult to process due to the high viscosity of the Mw 5 million material. This was confirmed by steady state rheometry. Incorporation of PEO Mw 5 million also imparted more strength to the matrix and resulted in longer dissolution times for the active agent.

PEO matrices released the API at a rate independent of the pH of the test media. The active agent was observed by thermal analysis and rheometry to have a plasticising

effect on the polymer matrix. This was consistent with observations made during processing of the matrix. Higher loading of API was seen by AFM to disrupt the PEO crystallisation process. As the proportion of API inclusion increased the speed of drug release from the polymer matrix increased. It was postulated that this was due to less rate controlling polymer being present in the matrix at higher API loading. PEO has been demonstrated to be a viable carrier material for active agents in monolithic dosage forms. It was deemed necessary to study the stability of the PEO dosage form, in order to determine if degradation during processing, or post processing, would reduce the materials effectiveness.

3.1.2 Processing stability of PEO

3.1.2.1 Introduction

Polymer degradation is a problem that frequently occurs when a polymer is subjected to an extrusion process. Degradation usually appears as discoloration, loss of volatile components (smoking) or loss of mechanical properties. According to the mode of initiation, the following types of degradation can be distinguished: thermal, chemical, mechanical and biological. Improper drying or overheating of the material (i.e., processing the polymer at too high a temperature) may cause degradation. Overshearing the material (i.e., processing the polymer at too high a screw speed or using the wrong screw design) or keeping the polymer in the molten state too long (i.e., long residence time) may also lead to degradation. Figure 3.15 outlines the various interactions that take place during the extrusion process. A combination of these interactions can result in material degradation. Property changes occur primarily because these factors affect the polymers chemical composition. Some polymers, such as poly(ethylene terephthalate) (PET), are very sensitive to process parameters and can degrade easily, while other polymers, such as poly(ethylene), are very forgiving. Degradation processes are generally quite complex; often more than one type of degradation is operational, e.g. thermo-oxidative degradation, thermo-mechanical degradation, etc.

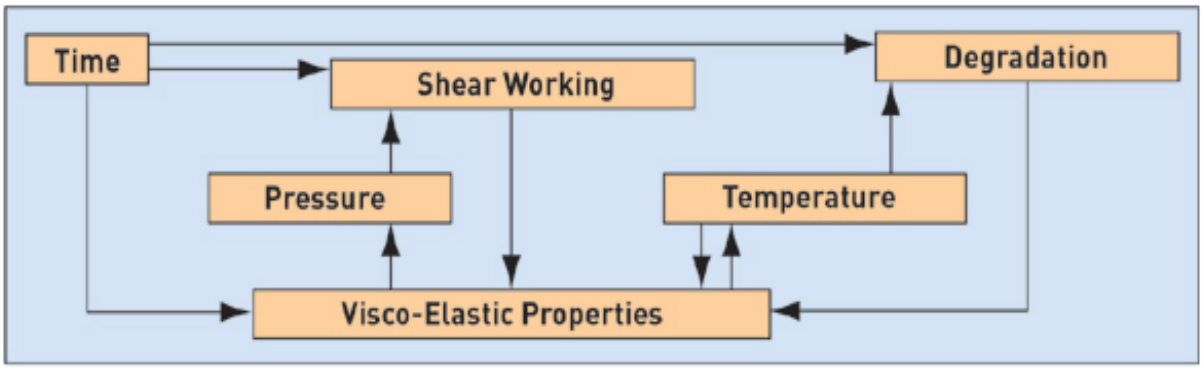

Figure 3.15 *Various interactions taking place during the extrusion process.*

Another cause of degradation in extrusion is multiple melting process steps. Multiple process steps results in heat and shear histories, in addition to the heat and shear histories that will be created in the final processing operation. As the ultimate goal of this project is to use the compounded matrices as the feedstock in a moulding process that will shape the drug delivery device, this section examines the resistance of PEO to multiple processing steps.

3.1.2.2 Processing observations

As previously discussed in section 3.1.1.2, extruder torque is a measure of the resistance that the motor experiences as a consequence of the melt viscosity inside the barrel and die head pressure is a measurement of the pressure exerted by the polymer melt at the shaping die. Measurement of these factors during processing yields useful information about the viscosity of the polymer. PEO (Mw 200,000) and PEO (Mw 200,000) containing 14% API, were reprocessed 5 times to examine the effect of multiple process steps on the materials.

As can be seen in Figure 3.16, a decrease in the viscosity of the polymer after the third processing run was observed. This decrease in viscosity is likely an effect of chain scission, leading to a reduction in the molecular weight of the polymer. A similar trend is noted in Figure 3.17, for pure PEO.

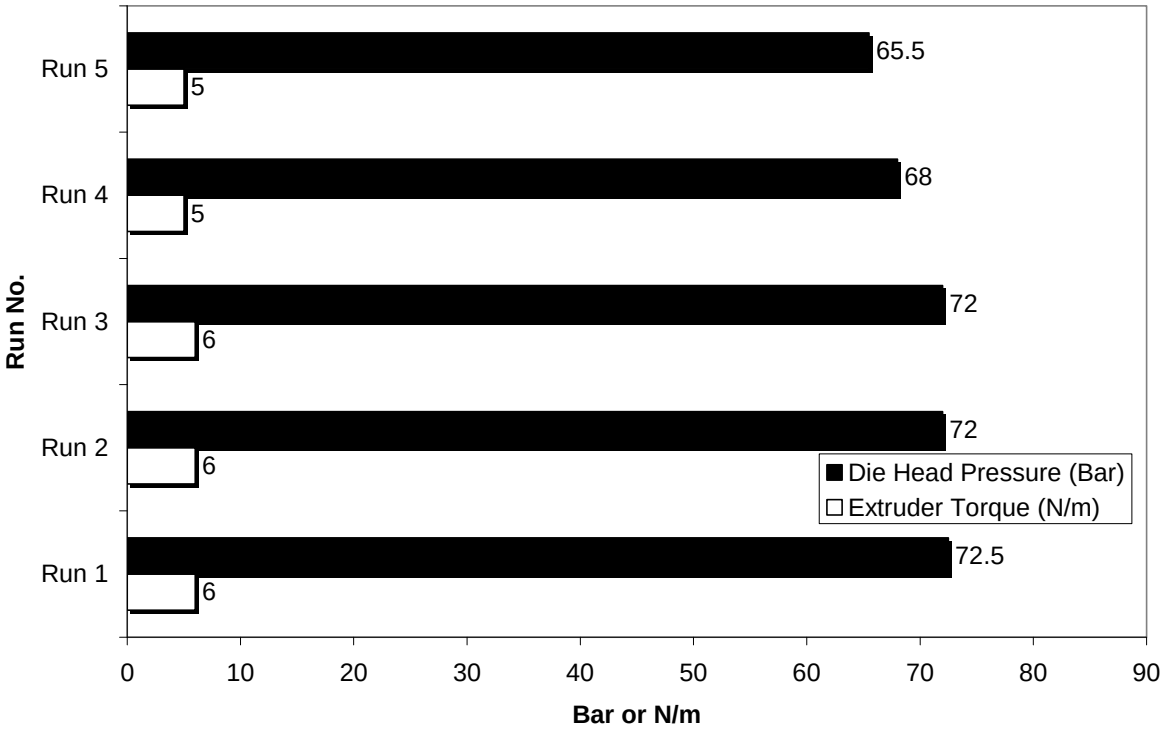

Figure 3.16 *Extruder torque and die head pressure readings observed during processing of PEO (Mw 200,000) loaded with 14% carvedilol.*

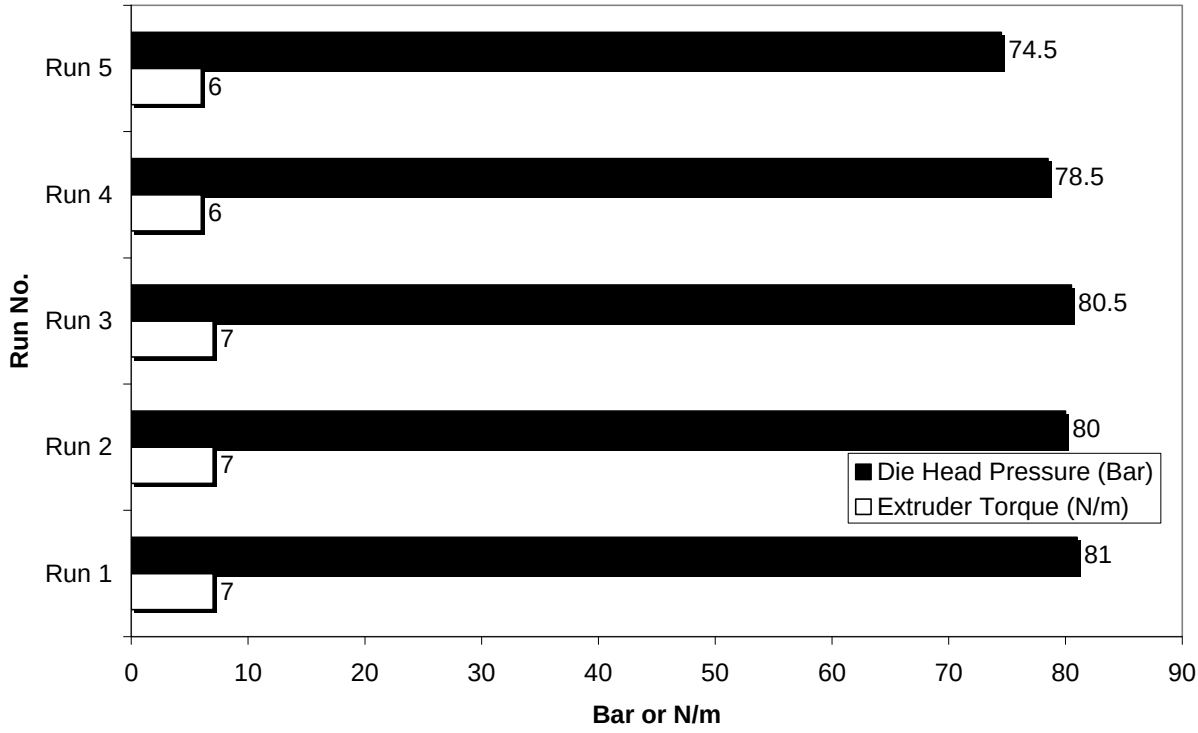

Figure 3.17 *Extruder torque and die head pressure readings observed during processing of PEO (Mw 200,000).*

3.1.2.3 Thermal analysis

Pre-blended matrix material containing 14% by weight carvedilol and PEO (Mw 200,000) was reprocessed 5 times with samples removed after each processing run for DSC analysis. The thermogram displayed in Figure 3.18 shows the collated results. Very little change in the melting point is detected after the multiple processing steps. However, a variation in the area under the curve between the samples taken after the first processing run and after the last processing run is noted. Polymer crystallinity can be determined with DSC by quantifying the heat associated with melting (fusion) of the polymer; these values are determined by the area under the curve. It is apparent that there is a marginal increase in the degree of crystallinity in samples reprocessed five times.

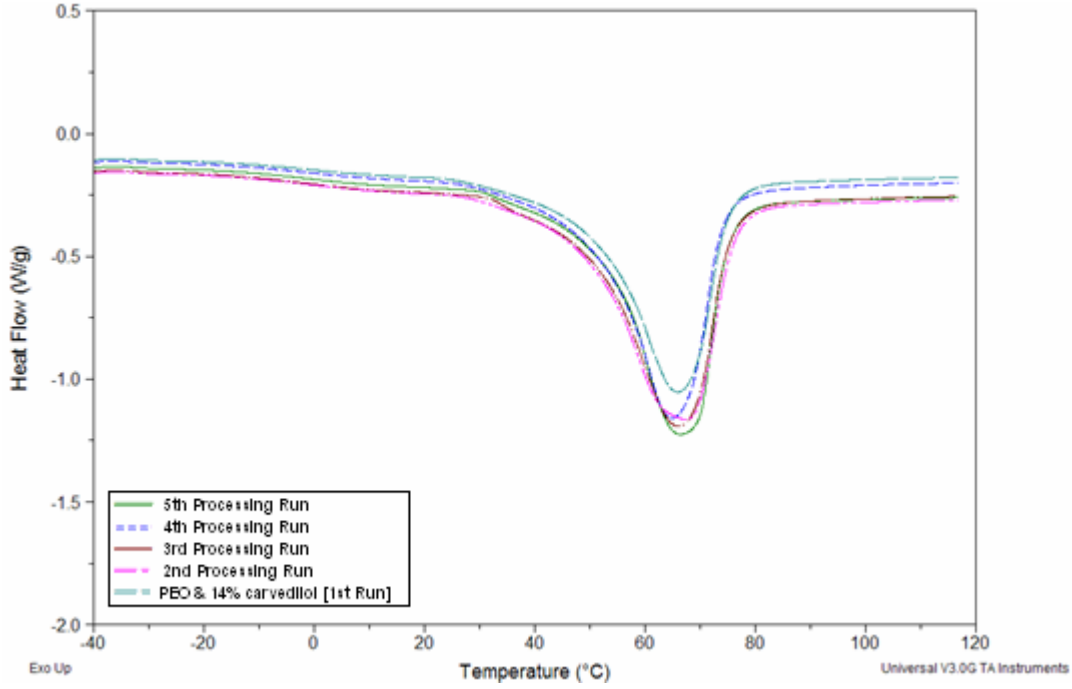

Figure 3.18 *Collated thermograms of PEO (Mw 200,000) matrices incorporating 14% carvedilol after multiple processing steps.*

Costa *et al*. (2005) found that factors that are important in determining the rate of degradation are: residence time and residence time distribution, which is determined by the velocity profiles in the machine; melt temperature and distribution of melt temperatures; deformation rate and deformation rate distribution and the presence of degradation agents. In a study on PEO (Crowley *et al*. 2002), the researchers suggest that thermal degradation

rather than mechanical degradation was the dominant mechanism. Processing temperature and the transit time through the extruder were the parameters that were identified as significantly influencing the extent of PEO degradation. It is possible that the observed increase in crystallinity in this study occurred as a result of the shearing of large polymer chains and subsequent creation of smaller polymer chains with higher mobility with which to crystallise. A similar trend was observed in the case of pure PEO as depicted in Figure 3.19.

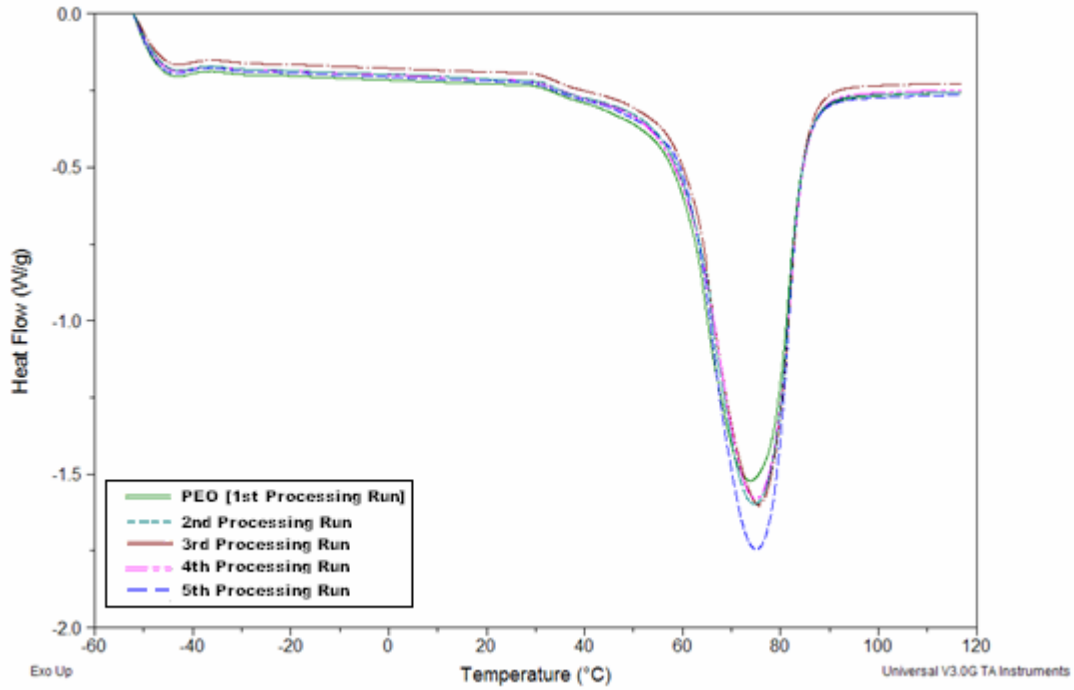

Figure 3.19 *Collated thermograms for PEO (Mw 200,000) matrices after multiple processing steps.*

3.1.2.4 Summary

The stability of PEO (Mw 200,000) when subjected to multiple extrusion operations, both with and without an incorporated active agent, was investigated. A significant decrease in the viscosity and by inference, a decrease in the molecular weight of the material, in addition to changes in the morphology of the polymer was noted after the third processing step. The results obtained indicate that careful processing of PEO matrices is necessary in order to ensure that extruded material produced is suitable for use as a monolithic matrix for oral drug delivery.

3.1.3 Effect of storage conditions on PEO based monolithic matrices

3.1.3.1 Introduction

There is little information available in the literature concerning the stability of polymers in sustained release matrix tablets prepared by hot-melt extrusion. PEO is sensitive to UV-irradiation or treatment with oxidising agents. Oxidative degradation is the result of a chemical reaction between oxygen molecules and the polymer. The incorporation of oxygen into the backbone of an aliphatic chain polymer results in thermal instability since the C–O bond is less stable than a C–C bond (Mandorsky and Straus, 1959). When exposed to air or oxygen, PEO has been reported to oxidatively degrade in both bulk (Scheirs *et al*. 1991) and in solution (McGary, 1960). Degradation of PEO has been reported to accelerate at elevated temperatures and upon exposure to ultraviolet light; thermal, radiation and photochemical degradation of pure PEO has also been investigated (Rabek, 1987; Scheirs *et al*. 1991; Rabek, 1995).

3.1.3.2 Effect of storage temperature

Extruded PEO (Mw 180,000) prepared using the processing conditions and temperatures outlined in 2.1.1, was subjected to two storage temperatures over a 60 day period. Aliphatic ethers can react with oxidising agents such as oxygen and hydrogen peroxide to form hydroperoxides. These peroxides can further decompose in a variety of ways resulting in chain scission. Poly(ethylene oxide)s are susceptible to degradation through similar oxidising agents. Chain scission leads to a reduction in molecular weight. As molecular weight of a polymer decreases so too does the viscosity of the polymer thus, solution viscometry was used as a convenient method of examining the effects of storage environment on the molecular weight of the polymer carrier. Figure 3.20 shows the results of the solution viscometry analysis carried out each day during the test period.

At 20°C PEO (Mw 180,000) demonstrates good stability with less than a 1.20 percent viscosity loss after 60 days. At 40°C the same material shows a 2.40% viscosity loss over the same time period, indicating that an increase in storage temperature does lead to a small decrease in the molecular weight of the polymer. The results obtained are consistent with those obtained in a similar investigation by Crowley *et al*. (2002).

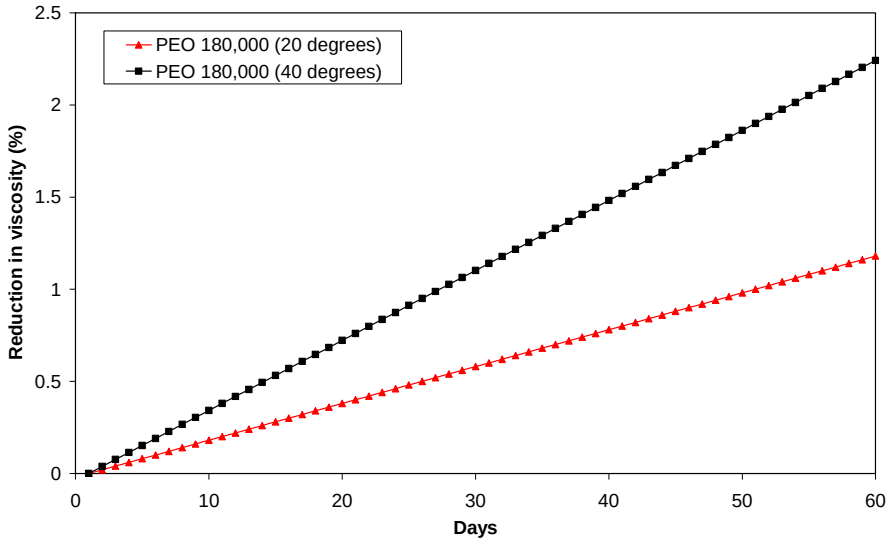

Figure 3.20 *Solution viscometry graph showing the effect of storage temperature on PEO (Mw 180,000).*

3.1.3.3 Effect of storage conditions on PEO of varying molecular weight

Polymer molecular weight also affects the viscosity loss as a function of storage time. The number of chain cleavages taking place per unit time is independent of polymer molecular weight. However, each chain cleavage has a larger impact on the measured viscosity for a high molecular weight polymer than found for a low molecular weight grade, since it leads to a wider polydispersity. This can be seen in Figure 3.21, which compares the viscosity change for high and low molecular weight grades of PEO stored at 20°C for 60 days.

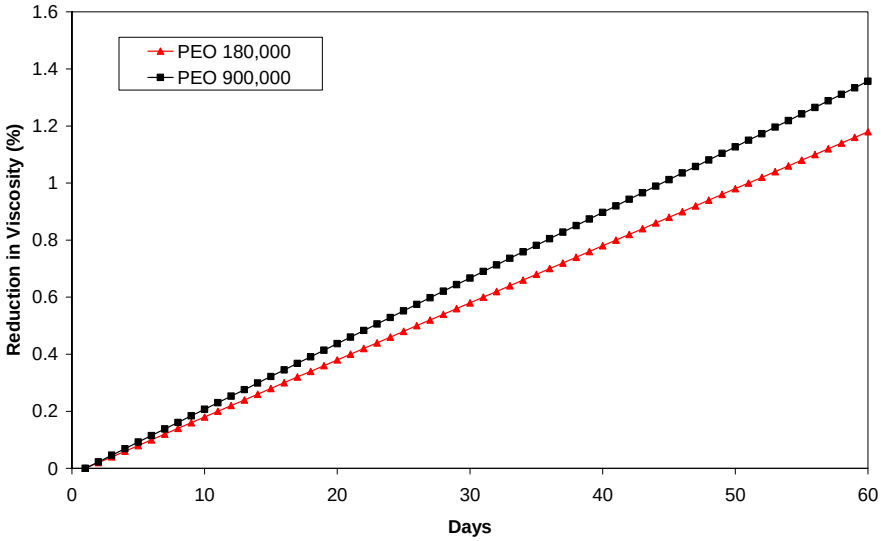

Figure 3.21 *Solution viscometry graph showing the effect of storage time on PEO (Mw 180,000 and 900,000).*

3.1.4 Effect of UV exposure on PEO

3.1.4.1 Introduction

PEO is a semicrystalline polymer, consisting of spherulitic crystals embedded in an amorphous matrix. The crystallinity of PEO with a molecular weight 1,000,000 has been reported to be in the range of 45–55% using dilatometry (Maclaine and Booth, 1975). Since oxygen permeability of a polymer in the solid state increases with polymer chain mobility, the oxygen diffusion rate is significantly lower in the crystalline region than in the amorphous region, due to the highly ordered structure of the crystalline spherulites (Ozeki *et al*. 1999). The degree of crystallinity in UV-irradiated PEO samples has been reported to increase due to the fast decay of the amorphous phase (Kaczmarek *et al*. 2001). Any increase in the crystallinity or decrease in the molecular weight of PEO matrices during storage would alter the drug release from the monolithic matrices and would therefore reduce the effectiveness of the drug delivery device.

3.1.4.2 Solution viscometry

Solution viscometry tests carried out (Figure 3.22) show a significant decrease in the viscosity of PEO (Mw 900,000) upon prolonged exposure to UV light.

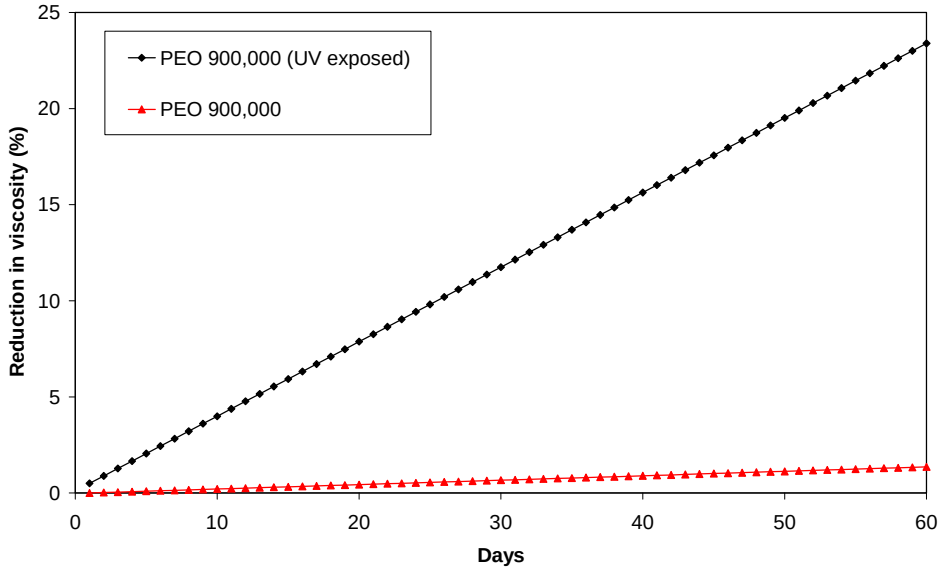

Figure 3.22 *Solution viscometry graph showing the effect of UV exposure on PEO (Mw 900,000).*

The photodegradation processes in PEO has been previously investigated using IR spectra by Kaczmarek *et al*. (2001). In that study, the decrease in the intensity of the peaks characteristic of ether groups (at 1145, 1115 and 1061 cm^{-1}) when PEO was exposed to UV radiation was postulated by those authors to confirm the occurrence of chain scission. In this work, samples subjected to UV were visibly different to those stored over the same period at ambient temperature and pressure without exposure to UV radiation. Figure 3.23 shows a sample of PEO (Mw 900,000) subjected to UV for 60 days and a sample of the same material stored over the same period at ambient temperature and pressure.

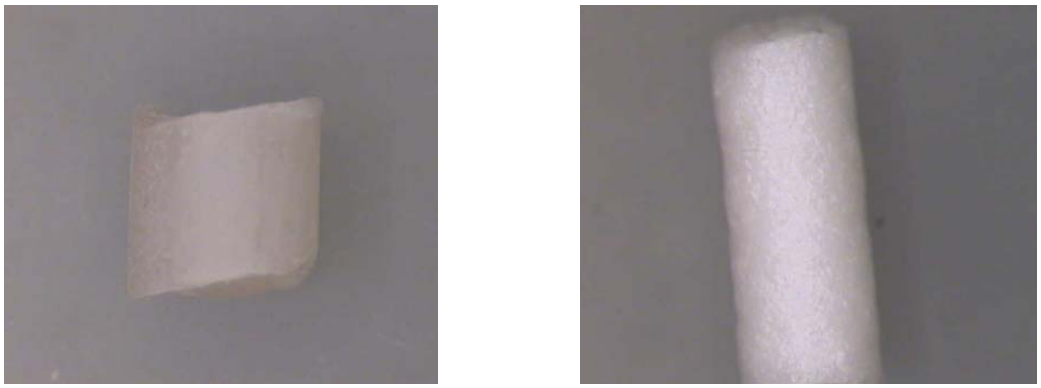

Figure 3.23 *Images of PEO (Mw 900,000) after 60 days storage. The image on the left was stored at ambient temperature and pressure. The image on the right was subjected to UV radiation under the same conditions.*

3.1.4.3 Thermal analysis

DSC was used to ascertain if the UV exposure altered the crystallinity in the PEO sample, thus altering its appearance. As described in section 3.1.2.3, polymer crystallinity can be determined using DSC by quantifying the heat associated with melting (fusion) of the polymer. Figure 3.24 and Figure 3.25 show the thermograms of the non-UV exposed and UV exposed PEO samples, respectively. The results from the scans are presented in tabular form in Table 3.3

Table 3.3 *Summary of findings from thermal analysis of stored samples.*

Sample	Melt Onset (Temperature °C)	Melt Peak (Temperature °C)	Enthalpy (J/g)
PEO 900,000 (UV exposed)	55.76	66	97.98
PEO 900,000	55.95	67.15	75.41

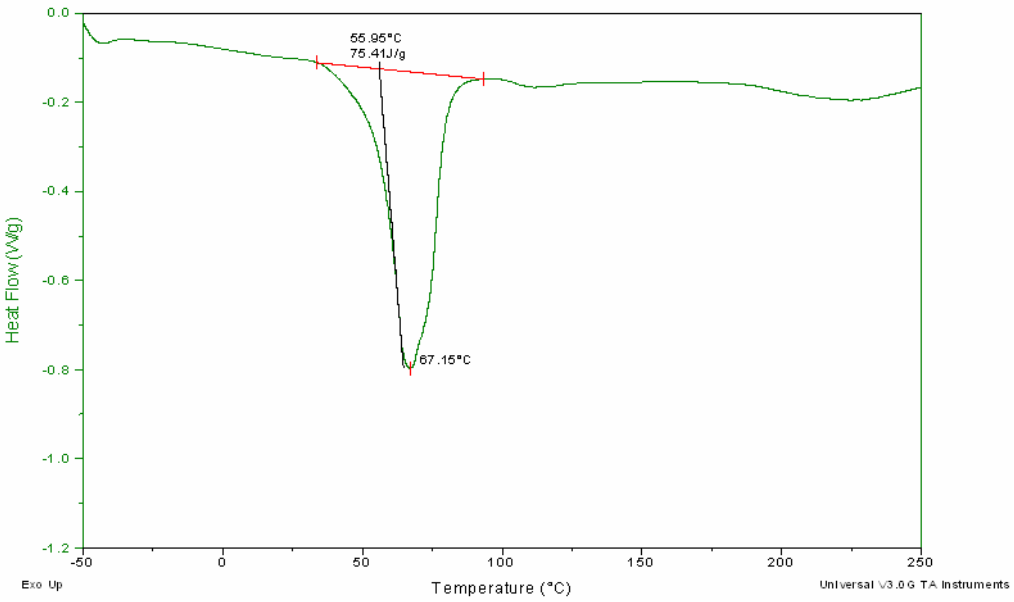

Figure 3.24 *Thermogram of PEO (Mw 900,000) after 60 days storage at ambient temperature and pressure.*

Interpretation of the DSC data reveals that the sample subjected to UV radiation is indeed more crystalline than the sample stored at ambient temperature and pressure. Enthalpy is considered to be directly proportional to the percentage crystallinity. The UV exposed sample has a much higher enthalpy and therefore a higher degree of crystallinity than the sample not subjected to UV radiation. The melting peak is also slightly broader for the sample stored at ambient temperature and pressure, indicating there are more amorphous regions in this sample than in the UV exposed sample.

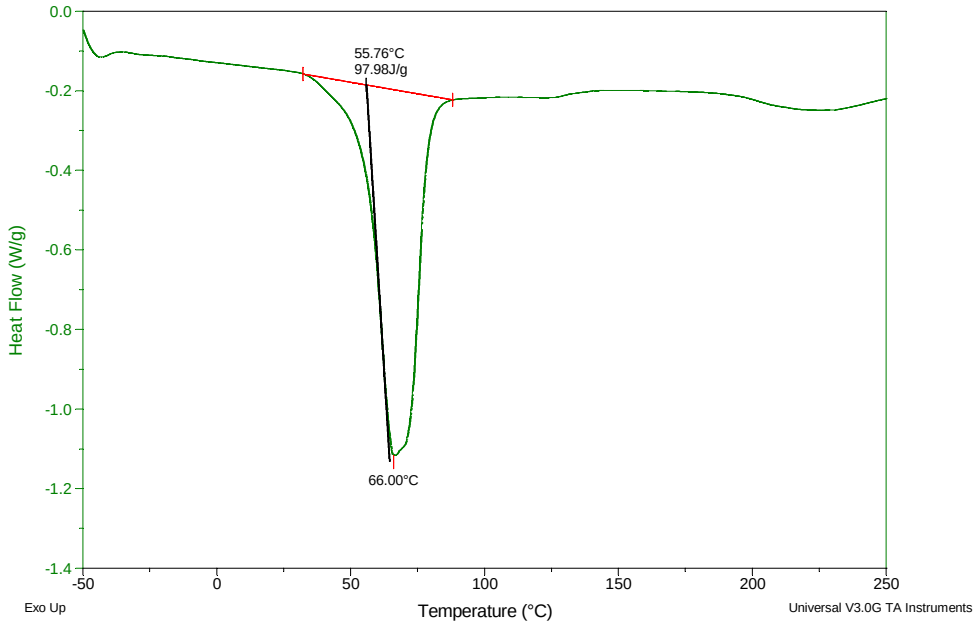

Figure 3.25 *Thermogram of PEO (Mw 900,000) after 60 days storage exposed to UV radiation at ambient temperature and pressure.*

Kaminska *et al.* (1999) have postulated several reasons for the increase in the degree of crystallinity during UV-irradiation. Those investigators reason that in semicrystalline polymers such as PEO, photo-oxidative degradation starts in the amorphous phase because of easy diffusion of oxygen to the unordered macrochains. The access of oxygen to tightly packed, rigid crystalline regions is restricted and this phase remains unchanged for longer periods during UV-irradiation. Additionally, Kaminska and co-workers considered the possibility of delocalisation of excitation energy through the crystal lattice. The fast degradation of the amorphous phase leads to the formation of low molecular weight products which can diffuse out decreasing the mass of the amorphous polymer and hence, the ratio of crystalline to amorphous fraction. Such degraded macromolecules have higher mobility facilitating the formation of well-ordered structures. Thus, it can be postulated that in this case during UV exposure, very small crystallites are reordered and replaced by slowly growing larger crystallites.

3.1.4.4 Summary

Storage conditions have an affect on the molecular weight and crystallinity of PEO. Higher storage temperatures were shown to reduce the molecular weight of PEO matrices

quicker than lower storage temperatures. Higher molecular weight PEO matrices were shown to be more vulnerable to decreases in molecular weight during storage than matrices made up of lower molecular weight material. PEO matrices exposed to UV radiation were shown to have undergone a substantial decrease in molecular weight. An increase in the degree of crystallinity of PEO matrices subjected to UV radiation was also observed. Careful consideration of the storage conditions to which the polymer will be subjected must take place if the polymer is to be useful as a monolithic matrix for oral drug delivery. The stability of PEO post processing has been determined, however, the effects of altering the processing conditions on the viability of PEO matrices is not fully understood. Therefore further investigations were carried out to determine the effects of variations in the processing conditions on PEO matrices.

3.2 The effect of compounding conditions on monolithic matrices for oral drug delivery

3.2.1 Significance of variation in extrusion speeds and temperatures on a novel PEO / PCL blend based matrix

3.2.1.1 Introduction

After the discovery of the major commodity and engineering plastics materials in the early to mid part of the 20th century, the cost of bringing a new polymer material to market began to rise dramatically. As a result, both the polymer industry and academia began to focus on developing polymer blends with novel and valuable properties, in order to enlarge the spectrum of available polymers. Various polymeric materials are known for specific or unique characteristics and melt blending of polymers during extrusion is a useful method combining the desired properties of different polymers. A polymer blend can be defined as a combination of two polymers without any chemical bonding between them (Paul, 1978). However, in practice, some blends involve copolymers and there are cases where some chemical interaction occurs between components. Processing of polymer blends requires that the compounding equipment quickly melts each polymer (concurrently or sequentially), and then rapidly and efficiently affect distributive and dispersive mixing of

the melt components. Co-rotating twin screw extruders are capable of easily satisfying these elementary steps in blending operations.

Twin screw extruders are commonly used to mix together two or more materials into a homogeneous mass in a continuous process. A conceptual representation of the twin screw compounding process is shown in Figure 3.26. In distributive mixing, the components are uniformly distributed in space, in a uniform ratio without being broken down. Dispersive mixing on the other hand involves the breaking down of agglomerates.

The work described in this section investigates the production of monolithic matrices by melt blending PEO with a biodegradable poly(ester) in varying ratios, in order to 'tune' the degradability of the resultant matrices. Poly(e-caprolactone) (PCL) is widely used in drug delivery applications (Chasin and Langer, 1990). PCL is much more resistant to chemical hydrolysis and is achiral, a feature that limits the possibility of property modulation through the configurational structure of polymer chains. High permeability to many drugs and a lack of toxicity has made PCL well suited to controlled drug delivery. It is a highly hydrophobic crystalline polymer that degrades very slowly *in vitro* and *in vivo*. The structure of PCL is shown in Figure 3.27.

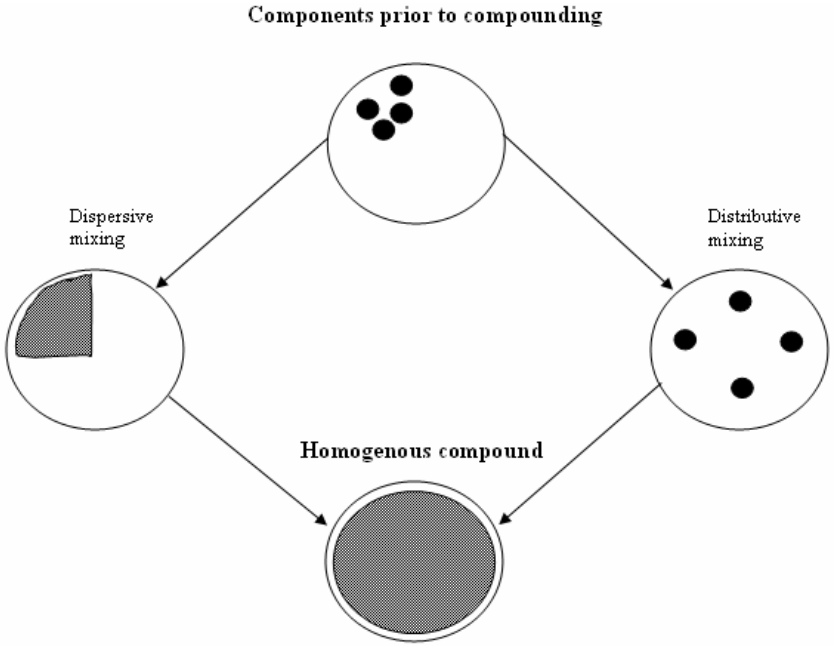

Figure 3.26 *Conceptual representation of the compounding process.*

Variables such as processing temperature and screw speed could potentially have an effect on the properties of the blends produced via hot melt extrusion. In order to investigate the effect of process variables on the properties of monolithic matrices, PEO / PCL blends (Table 3.4) were compounded over a range of processing temperatures and screw speeds.

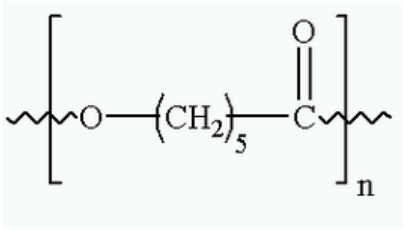

Figure 3.27 *Chemical structure of PCL, with 'n' indicating the number of repeat units.*

Table 3.4 *Batch compositions used to determine the effect of processing conditions on PCL/PEO blends.*

Batch No.	PCL (% by weight)	PEO Mw 1 million (% by weight)	Carvedilol (% by weight)
1	49	49	2
2	73.5	24.5	2
3	24.5	73.5	2
4	40	40	20
5	60	20	20
6	20	60	20

3.2.1.2 Processing observations

As previously described, changes in the measured extruder torque and die head pressure during the hot melt extrusion process may be used as a method of measuring changes in the viscosity of the formulation being processed and thus gauging the relative processability of the matrices under investigation. Figure 3.28 shows the torque and die head pressure readings recorded during processing of the PEO / PCL blends over a range of temperatures and screw speeds.

Several trends are apparent in the presented torque and die head pressure data. Inclusion of higher percentages of API results in lower viscosity of the polymer melt and higher processability of the extrudate. Incorporation of PCL to the polymer matrix also results in lower melt viscosity during extrusion, as the percentage inclusion of PCL increases, the observed values for torque and die head pressure show an incremental proportional decrease. In all cases, higher screw speeds result in higher values of torque and die head pressure as would be expected due to the higher volumes of material being processed per unit time. At the higher processing temperature, lower values for die head pressure and torque are noted as a result of the temperature dependency of polymer melts. Melt viscosity is inversely related to the fractional free volume in the polymer melt, which increases from a small value at the glass transition temperature (T_g) linearly with increasing temperature.

Figure 3.29 shows thermal images of the barrel recorded during processing over the range of temperatures and screw speeds employed. The barrel is observed to be much cooler during processing at the lower temperature profile and no material hotspots or dead zones are observed as a result of higher shear intensity at the higher screw speeds. Hot spots in the extrusion process can detrimentally affect energetic materials (such as API's), which decompose at or above a critical temperature. Dead zones are stagnant regions where the molten material accumulates and deteriorates. The material in dead zones changes the shape of the flow domain. This material eventually fractures and then re-enters the stream of material being processed, affecting the overall quality of the material.

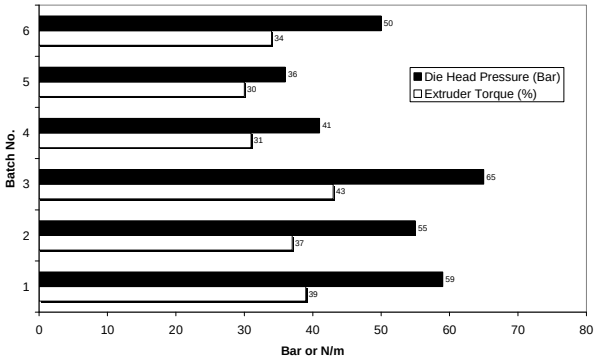

(a) Torque and die head measurements obtained at 25RPM, temperature profile 1.

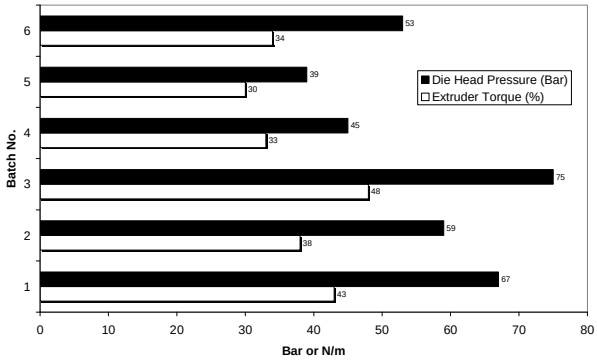

(b) Torque and die head measurements obtained at 50RPM, temperature profile 1.

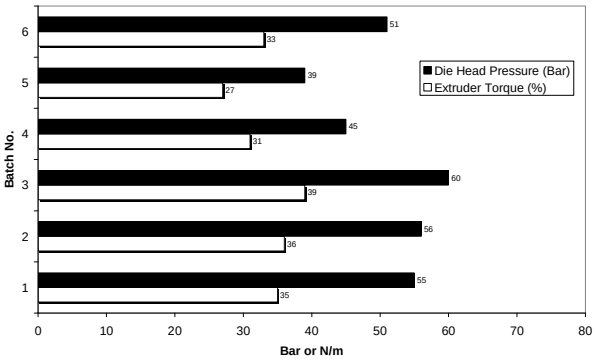

(c) Torque and die head measurements obtained at 100RPM, temperature profile 1.

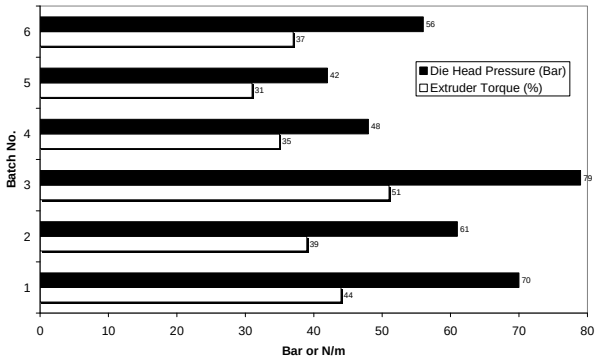

(d) Torque and die head measurements obtained at 25RPM, temperature profile 2.

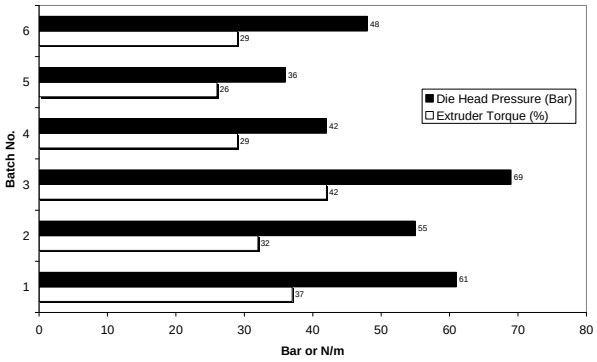

(e) Torque and die head measurements obtained at 50RPM, temperature profile 2.

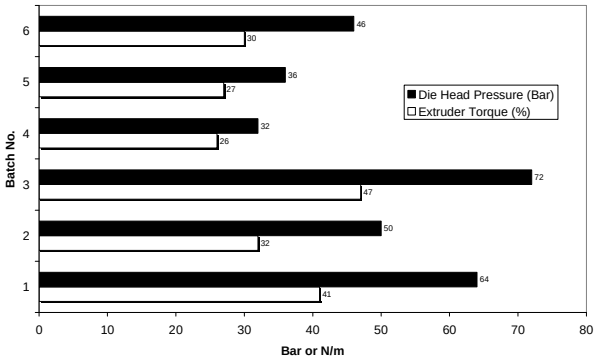

(f) Torque and die head measurements obtained at 100RPM, temperature profile 2.

Figure 3.28 *Torque and die head measurements obtained during the compounding of PEO / PCL blends.*

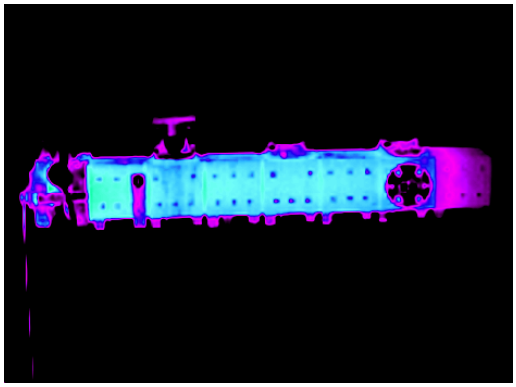

(a) Thermal image obtained at 25RPM, temperature profile 1.

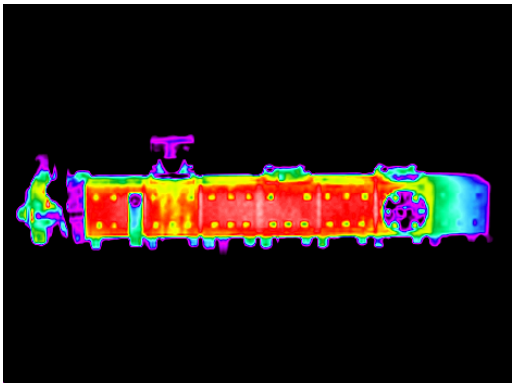

(b) Thermal image obtained at 25RPM, temperature profile 2.

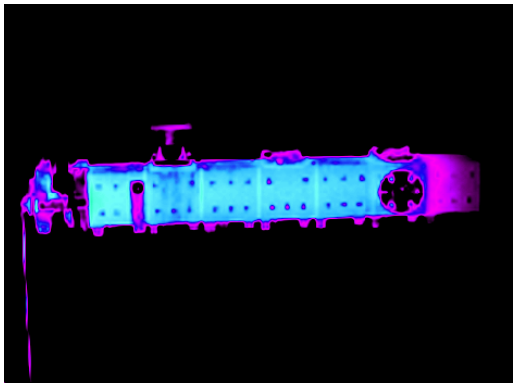

(c) Thermal image obtained at 50RPM, temperature profile 1.

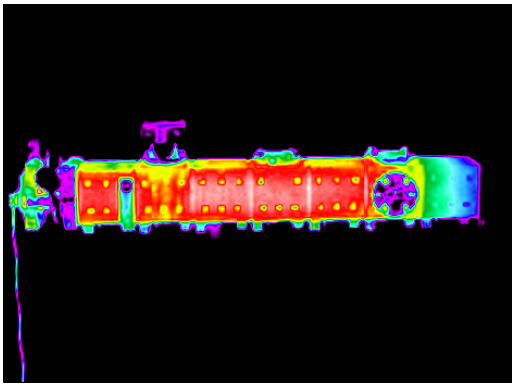

(d) Thermal images obtained at 50RPM, temperature profile 2.

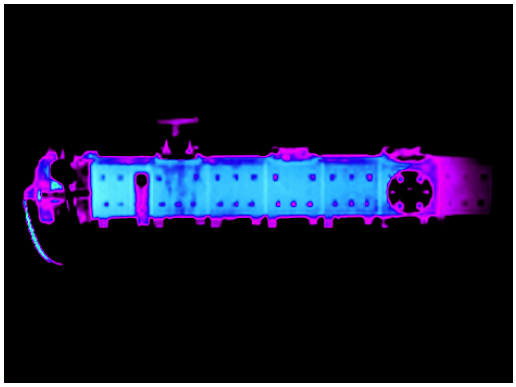

(e) Thermal image obtained at 100RPM,temperature profile 1.

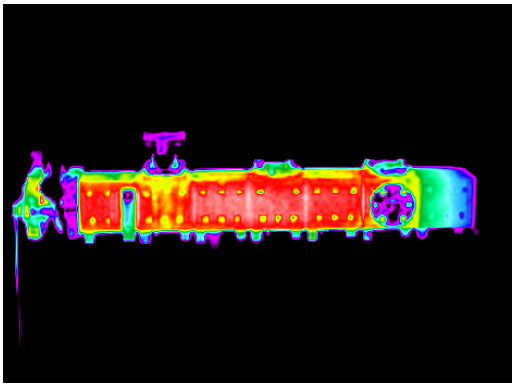

(f) Thermal image obtained at 100RPM, temperature profile 2.

Figure 3.29 *Thermal images of the extruder during processing.*

3.2.1.3 Thermal analysis

Thermal analysis of the batches was carried out to investigate the effects of melt blending PCL and PEO on the thermal properties of the resultant monolithic matrices. Figure 3.30 shows the thermograms of batch 1, 2 and 3 processed using temperature profile 1 at 50 RPM.

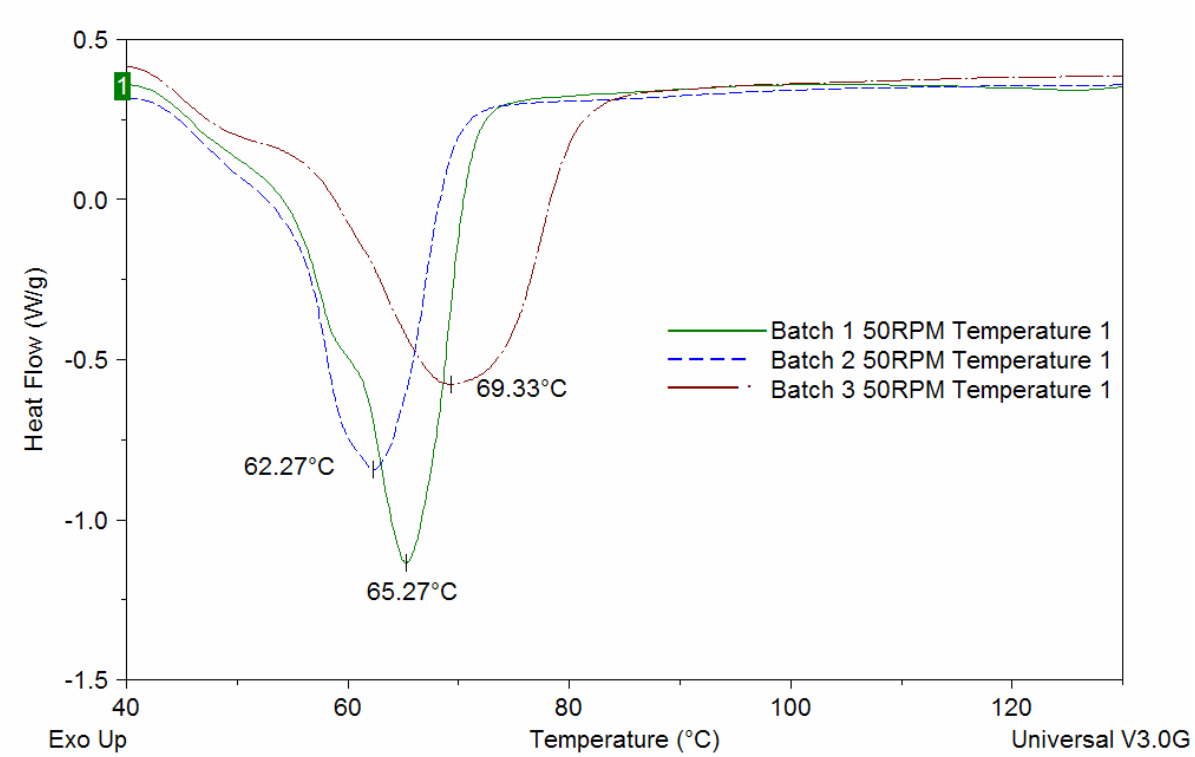

Batch number	*PCL (%wt)*	*PEO Mw 1 million (%wt)*	*API (%wt)*
1	*49*	*49*	*2*
2	*73.5*	*24.5*	*2*
3	*24.5*	*73.5*	*2*

Figure 3.30 *Overlaid thermograms of batches 1, 2 and 3.*

Both virgin PEO and virgin PCL exhibit the T_m as a well defined exothermic peak. The PCL polymer used in this section melts at 60°C, compared with a melting point of 69°C for the PEO material used in this work. However in the blended materials, there is one melting peak and one shoulder corresponding to the T_m of the two components, with the shape of the melting peak changing with blend composition. The inclusion of PCL is seen to result in a depression of the melting point of the matrix. The depression in the

melting point becomes more substantial with increasing percentage inclusion of PCL. This behaviour has been noted in the literature (Qiu *et al.* 2003).

Processing variables are not seen to have any discernable impact on the melting points of the resultant matrices. The melting points for all the matrices under investigation in this section are presented in Table 3.5. Batches 4, 5 and 6 comprise the same polymer ratios as batches 1, 2 and 3; however batches 4, 5 and 6 are loaded with 20%*wt* API. The batches containing higher percentages of API were seen to exhibit depressed melting points compared to matrices with lower drug loadings. This phenomenon is due to the API acting as a plasticiser in the matrix. This has been noted in the literature in previous work by Ozeki *et al*. (1997). This is also in agreement with values observed in the torque and die head pressure readings obtained in the processing of the polymer matrices.

Table 3.5 *Melting temperatures of the PCL / PEO blends compounded at a range of temperatures and screw speeds.*

Processed using temperature profile 1						
Screw speed (RPM)	Batch 1 (°C)	Batch 2 (°C)	Batch 3 (°C)	Batch 4 (°C)	Batch 5 (°C)	Batch 6 (°C)
25	65.215	63.685	68.475	64.61	63.485	66.18
50	65.105	63.635	67.675	64.47	63.85	66.985
100	66.325	64.215	67.535	64.04	62.195	65.625
Processed using temperature profile 2						
Screw speed (RPM)	Batch 1 (°C)	Batch 2 (°C)	Batch 3 (°C)	Batch 4 (°C)	Batch 5 (°C)	Batch 6 (°C)
25	63.91	61.465	67.465	63.69	61.39	66.615
50	64.445	62.98	66.545	63.6	61.58	65.18
100	65.015	64.425	66.795	62.685	60.255	63.365

Miscibility of polymer blends is generally studied using DSC. A single glass transition temperature is the most widely and conventionally used criterion for determining the miscibility of a polymer blend. A single composition dependant T_g indicates full miscibility conversely, an immiscible polymer blend exhibits more than one T_g. However, because the melting and glass transition temperatures of PEO and PCL are relatively close, determination of miscibility by conventional DSC is not possible in this case. Kuo *et al.*

(2002) reports that PEO and PCL are miscible by studying the crystallisation temperatures of the blends, compared with those of the homopolymers. A recent study (Qiu *et al*. 2003) showed that PEO / PCL blends are immiscible. In that work the investigators questioned the validity of the findings of Kuo *et al*. In the case of the matrices in this work, miscibility of PCL and PEO is not a requisite for the matrices to function as drug delivery vehicles and was therefore not investigated further.

3.2.1.4 Steady state rheometry

Steady state rheometry was carried out on all the matrices under investigation in order to ascertain the rheological effects of incorporation of PCL into the polymer matrix. The effect of altering the process parameters on the flow behaviour of the matrices was also investigated in this manner. Figure 3.31 shows the data obtained from steady state testing of batches 1, 2 and 3 processed at 50 RPM using temperature profile 1. The data presented shows a trend typical of that obtained in all the batches under investigation. The batches containing higher proportions of PEO are seen to be more viscous than the batches containing higher loadings of PCL. This is in agreement with observations made during processing of the blends, which showed that the blends containing PCL were easier to process.

The effect of processing at different temperatures was not seen to have any discernable effect on the rheological properties of the resultant matrices. However, the effect of processing at different screw speeds is seen to have a slight effect on the flow behaviour of the matrices. Figure 3.32 displays the rheological data for batch 1 processed at different screw speeds. It can be seen from the data presented that processing at 100 RPM results in a slight drop in the viscosity of the matrix. This is likely to be as a result of the mechanical shearing of polymer chains at the higher screw speed. This slight drop in viscosity is not seen to be significant enough to adversely affect the matrices as no corresponding drop in the melting point of the matrices processed at 100 RPM was noted during thermal analysis. The percentage inclusion of API was seen to have an effect on the viscosity of the matrices. Higher loadings of API resulted in reduced viscosity of the matrices consistent with the API acting as a plasticiser, as suggested during analysis of the thermal behaviour of the matrices.

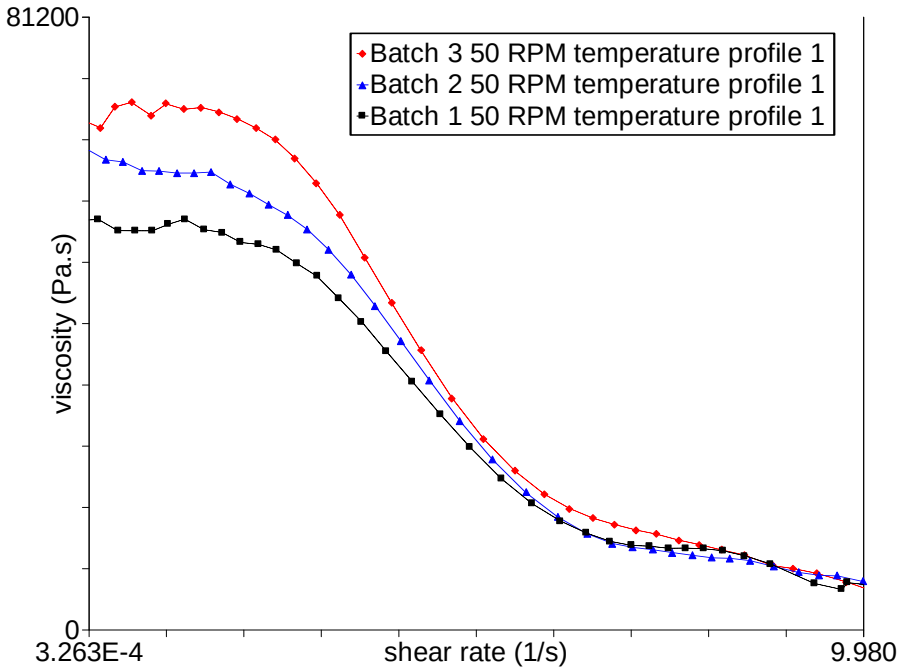

Batch number	*PCL (%wt)*	*PEO Mw 1 million (%wt)*	*API (%wt)*
1	*49*	*49*	*2*
2	*73.5*	*24.5*	*2*
3	*24.5*	*73.5*	*2*

Figure 3.31 *Steady state data for batches 1, 2 and 3.*

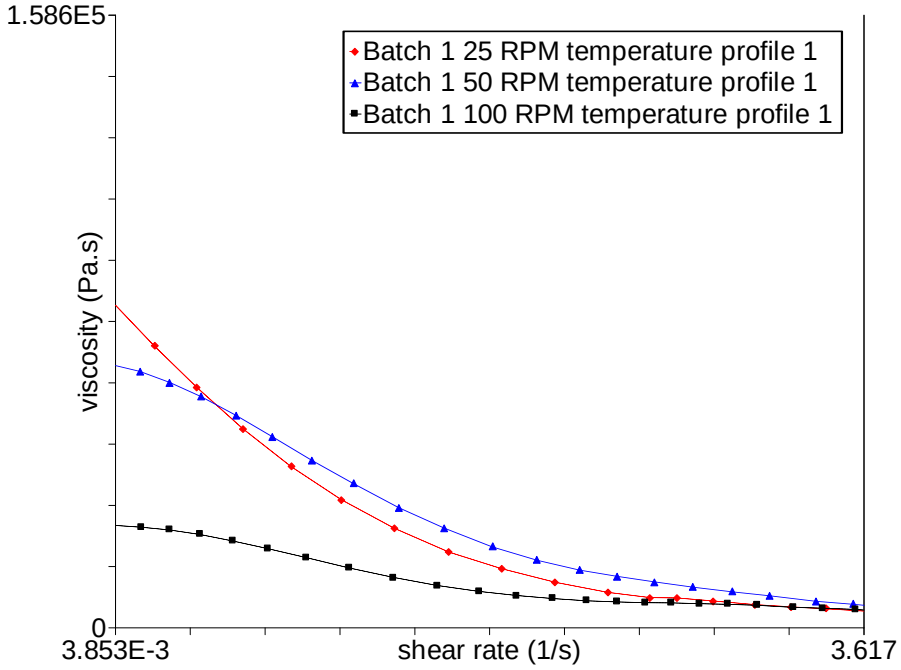

Figure 3.32 *Steady state data for batch 1 (a 49%wt:49%wt PEO/PCL blend, loaded with 2%wt API) after processing at varying screw speeds.*

3.2.1.5 Drug release

PCL – PEO block copolymer micelles have been reported as efficient drug carriers (Allen *et al*. 2000; Aliabadi *et al.* 2005; Geng and Discher; 2006). In addition PCL / PEO blends have been used as microspheres for drug delivery (Lin *et al.* 1999; Park *et al.* 2005) and as drug loaded biodegradable nerve guides (Verreck *et al*. 2005). In this section the drug release profiles from the prepared monolithic matrices were examined, in 0.2M HCl (pH 1.2). Figures 3.33 and 3.34 show dissolution profiles typical of those obtained.

Drug release from the monolithic matrices was found to vary substantially as the amount of PCL in the matrices was altered. The incorporation of PCL in the matrices was seen to retard the drug release from the polymer matrices, with the degree of retardation being proportional to the amount of PCL in the matrix. This is to be expected as PCL is a highly hydrophobic polymer.

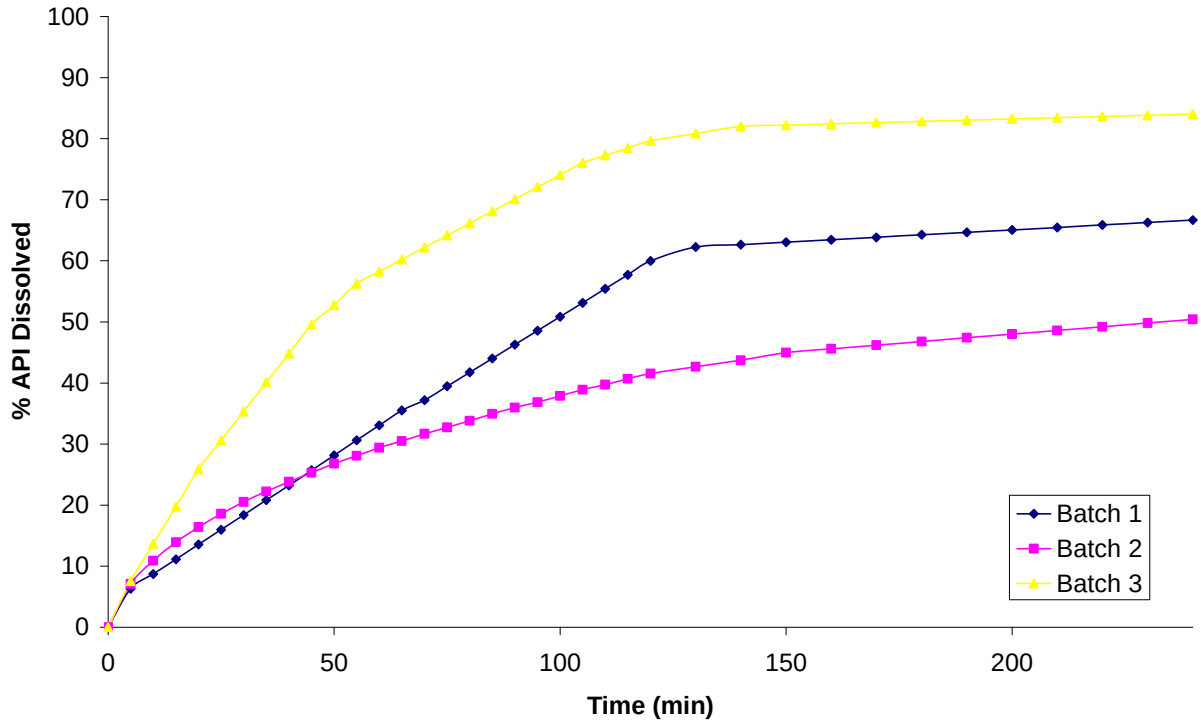

Batch number	*PCL (%wt)*	*PEO Mw 1 million (%wt)*	*API (%wt)*
1	*49*	*49*	*2*
2	*73.5*	*24.5*	*2*
3	*24.5*	*73.5*	*2*

Figure 3.33 *Dissolution results obtained from batches 1, 2, and 3 processed at 25RPM using temperature profile 1.*

The matrices prepared in this work show that the rate of drug release in a PCL / PEO monolithic matrix can easily be tailored by simply altering the composition of the binary blend.

Matrices with higher loading of API were seen to release the active agent at a slightly quicker rate than those with lower loadings. This is thought to be due to less rate controlling polymer being present in the matrices with higher drug loading. This behaviour was also noted in section 3.1.1.7.

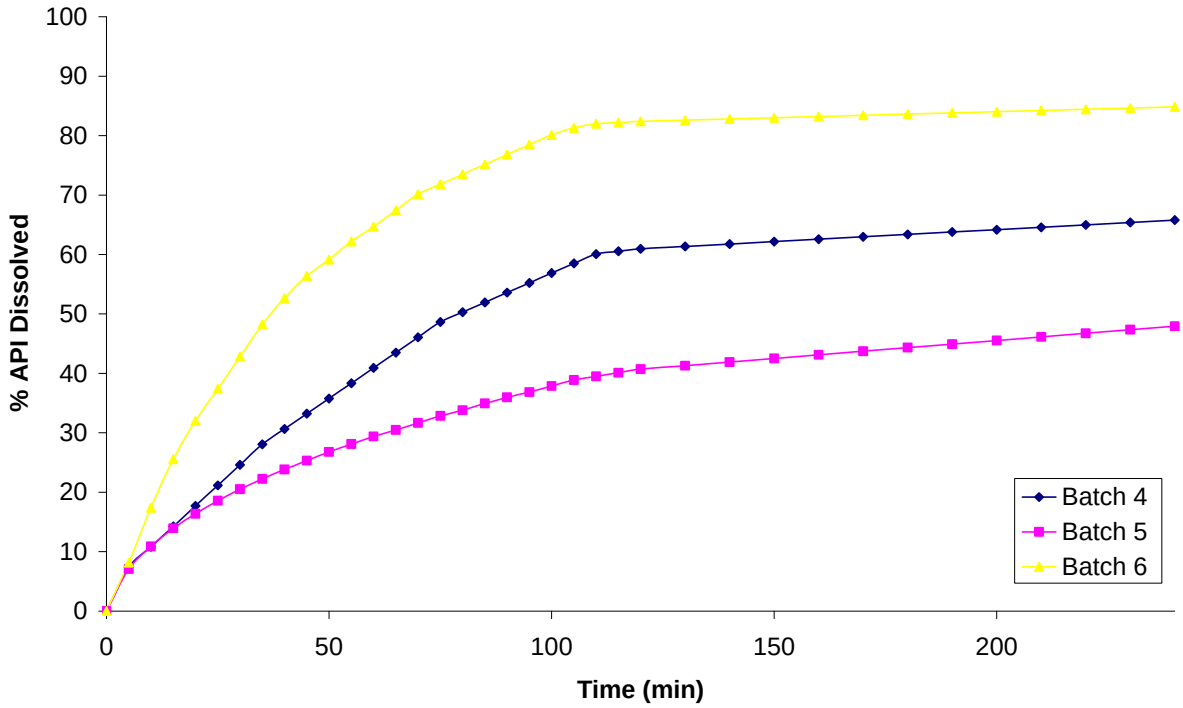

Batch number	*PCL (%wt)*	*PEO Mw 1 million (%wt)*	*API (%wt)*
4	*40*	*40*	*20*
5	*60*	*20*	*20*
6	*20*	*60*	*20*

Figure 3.34 *Dissolution results obtained from batches 4, 5 and 6 processed at 25RPM using temperature profile 1.*

Tables 3.6 and 3.7 show summarised data for the dissolution tests carried out in this work. Neither the screw speed nor the temperature profiles employed in the compounding of the matrices were seen to have a significant effect on the drug release profiles from the matrices.

Table 3.6 *Summarised drug release data obtained from dissolution testing of the batches outlined in Table 2.4 processed using temperature profile 1, where t25%, t50% and t75% represent the time taken in minutes for 25%, 50% and 75% of the total API contained in the matrix to become dissolved in the test medium respectively.*

	Temperature (°C)			
	Feed	*Metering 1*	*Metering 2- 8*	*Die*
Temperature profile 2	*50*	*95*	*110*	*120*

	Batch 1	**Batch 2**	**Batch 3**	**Batch 4**	**Batch 5**	**Batch 6**
Processed at 25 RPM using temperature profile 1						
t25% (min)	45	45	20	35	45	15
t50% (min)	100	240	50	80	-	40
t75% (min)	-	-	105	-	-	85
% API released after 240 min	66.68%	50.42%	84.04%	65.79%	47.95%	84.83%
Processed at 50 RPM using temperature profile 1						
t25% (min)	50	45	20	30	40	15
t50% (min)	110	235	45	85	235	40
t75% (min)	-	-	115	-	-	90
% API released after 240 min	64.35%	51.01%	79.32%	63.84%	50.56%	85.37%
Processed at 100 RPM using temperature profile 1						
t25% (min)	45	45	20	30	45	15
t50% (min)	95	-	50	90	-	35
t75% (min)	-	-	110	-	-	85
% API released after 240 min	68.16%	48.09%	81.93%	67.54%	49.63%	81.36%

Table 3.7 *Summarised drug release data obtained from dissolution testing of the batches outlined in Table 2.4 processed using temperature profile 2, where t25%, t50% and t75% represent the time taken in minutes for 25%, 50% and 75% of the total API contained in the matrix to become dissolved in the test medium respectively.*

	Temperature (°C)			
	Feed	*Metering 1*	*Metering 2- 8*	*Die*
Temperature profile 1	*50*	*75*	*85*	*95*

	Batch 1	**Batch 2**	**Batch 3**	**Batch 4**	**Batch 5**	**Batch 6**
Processed at 25 RPM using temperature profile 2						
t25% (min)	40	50	25	35	40	15
t50% (min)	95	-	50	80	235	45
t75% (min)	-	-	110	-	-	85
% API released after 240 min	68.50%	46.31%	81.69%	64.39%	50.61%	85.69%
Processed at 50 RPM using temperature profile 2						
t25% (min)	45	45	20	35	50	20
t50% (min)	100	-	50	80	-	40
t75% (min)	-	-	105	-	-	95
% API released after 240 min	66.31%	48.37%	85.13%	65.06%	45.32%	81.51%
Processed at 100 RPM using temperature profile 2						
t25% (min)	40	45	20	35	45	15
t50% (min)	105	235	45	75	240	40
t75% (min)	-	-	95	-	-	85
% API released after 240 min	63.23%	50.96%	87.07%	66.37%	50.19%	86.38%

3.2.1.6 Summary

The work presented in this section describes both the use of PCL / PEO blends as monolithic dosage forms and also the effect of extrusion process variables on the properties of the resultant matrices. The percentage inclusion of PCL in the matrices was altered in order to investigate the effect of PCL on the properties of the matrix. Both processing temperature and screw speed were varied during the production of the matrices described in this section to ascertain if the process parameters used could affect the end properties of the matrices. Torque and die head pressure measurements taken during processing, indicate that inclusion of PCL renders the matrices more easily processable. Higher processing temperatures also resulted in easier processing of the matrices due to lower polymer melt viscosity. Higher screw speeds resulted in higher observed values of torque and die head pressure due to the higher shear being generated during the extrusion process, yet no material hotspots were observed as a result of the higher shear rates. Thermal analysis of the blends indicated that as the blend composition varied, so too did the melting behaviour. No adverse thermal effects were associated with varying the processing conditions. Steady state rheometry of the matrices indicated that the blends incorporating higher levels of PCL were less viscous than those consisting of higher levels of PEO. Higher screw speed was observed to result in slightly lower matrix melt viscosity when compared with matrices compounded using lower screw speeds. Dissolution testing showed that the incorporation of hydrophobic PCL polymer into a PEO matrix results in a retarded drug release profile. The greater the amount of PCL, the slower the drug release.

The work outlined in this section demonstrated that modulation of drug release from PEO / PCL melt blended matrices was achievable by altering the ratio of PCL to PEO in the matrix. In addition, it was seen that the processing parameters used during the compounding had no substantial effect on the end properties of the matrices. The high viscosity of PEO matrices remains however, a drawback to the use of PEO as a carrier material. It was postulated that the use of supercritical CO_2 in the extrusion process may allow easier processing of PEO matrices.

3.2.2 Preparation of monolithic matrices for oral drug delivery using a supercritical fluid assisted hot melt extrusion process

3.2.2.1 Introduction

The use of supercritical CO_2 as a solvent in the processing of various biodegradable / biocompatible polymers for pharmaceutical and medical applications in the forms of particles and microcellular foam has gained much attention in the last decade. A supercritical fluid is defined as a substance for which both pressure and temperature are above the critical values (Kazarian, 2000).

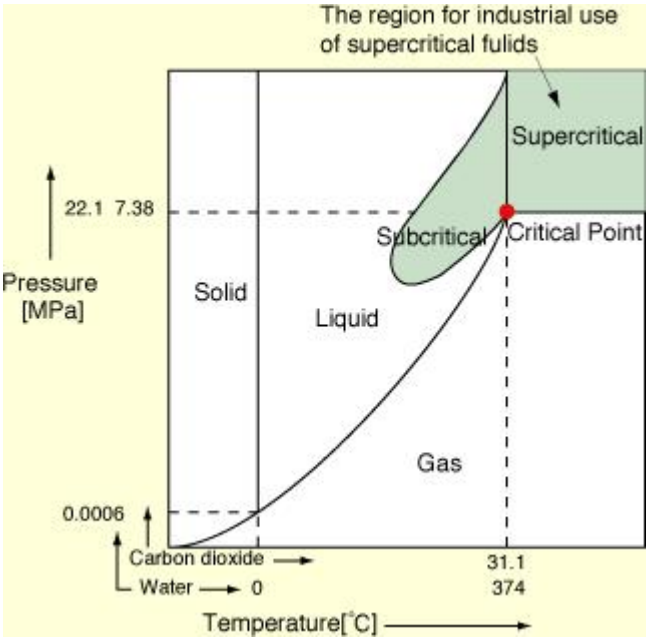

Figure 3.35 *Phase diagram illustrating the supercritical region.*

CO_2 is a promising alternative to noxious organic solvents and chlorofluorocarbons. It has shown versatility as a supercritical fluid in the synthesis as well as processing areas for polymers owing to its attractive physical properties. It is non-toxic, non-flammable, chemically inert and inexpensive. Its supercritical conditions are easily attained (T_c = 304.15 K, P_c = 7.38 MPa) and it can be removed from a system by simple depressurisation (Nalawade *et al*. 2006).

The processing of polymers is highly influenced by the viscosity of the bulk materials. Raising the processing temperature or the addition of volatile or harmful processing aids is often seen as a solution in overcoming the inherent difficulties encountered when processing high molecular weight polymers. However, higher temperatures during processing can lead to thermal degradation. Also, added processing aids remain in the product and thus alter its properties and performance. The low thermal stability of high molecular weight biodegradable polymers has led to the emergence of supercritical CO_2 as a useful processing aid. There are many examples in the literature of the use of pressurised gases to lower the melt viscosity of numerous amorphous and semicrystalline polymers. Poly(ethylene glycol) (Daneshvar *et al*. 1990; Weidner *et al*. 1997; Gourgouillion *et al*. 1998; Gourgouillion *et al*, 1999; Lopez *et al.* 2000), poly(styrene) (Kiran *et al.* 1993; Kwag *et al.* 1999; Lee *et al.* 1999) and poly(dimethylsiloxane) (Mertsch and Wolf, 1994; Xiong and Kiran, 1995; Bae and Gulari, 1997; Gerhardt *et al*. 1997) are examples of polymers where a viscosity reduction has been demonstrated upon the incorporation of supercritical CO_2. Biomaterials such as methyl oleate and anhydrous milk fat (Tuan *et al*. 1999), as well as poly(ethylene) / poly(styrene) blends (Lee *et al*. 1998) have exhibited similar behaviour. Verreck *et al*. (2006) noted in a recent publication that although numerous examples describing the effect of supercritical CO_2 as a plasticiser for polymers can be found in the literature, there are relatively few publications dealing with pharmaceutically acceptable polymers.

This section of work reports on the use of supercritical CO_2 as a plasticiser during the processing of a hot melt extruded dosage form based on poly(ethylene oxide). The impact on the production of hot melt prepared matrices (Table 3.8), in addition to the release rate of an active pharmaceutical ingredient from the prepared matrices both with and without the utilisation of supercritical CO_2 during compounding was investigated.

Table 3.8 *Batch composition used to examine the effect of a supercritical fluid assisted extrusion process on the preparation of monolithic matrices.*

Batch No.	PEO Mw 200,000 (% Weight)	Eudragit EPO (% Weight)	Carvedilol (% Weight)	Supercritical CO_2 assisted (1200 Psi)
1	86	0	14	No
2	64.50	21.50	14	No
3	43	43	14	No
4	89.5	0	10.5	No
5	67.125	22.375	10.5	No
6	44.75	44.75	10.5	No
7	92.5	0	7.5	No
8	69.375	23.125	7.5	No
9	46.25	46.25	7.5	No
10	86	0	14	Yes
11	64.50	21.50	14	Yes
12	43	43	14	Yes
13	89.50	0	10.5	Yes
14	67.125	22.375	10.5	Yes
15	44.75	44.75	10.5	Yes
16	92.50	0	7.5	Yes
17	69.375	23.125	7.5	Yes
18	46.25	46.25	7.5	Yes

3.2.2.2 Processing observations

Supercritical fluid assisted extrusion / compounding requires the injection of high pressure gas into the barrel of the extruder. Injecting CO_2 into the extruder barrel may cause leakage of the gas resulting in a limited building up of pressure during processing. Therefore, the screw configuration was carefully considered in order to be able to mix the CO_2 with the polymer melt at appropriate pressures. Lee *et al*. (1998) suggested a number of different aspects which must be taken into account when designing the extruder set up

and screw configuration for supercritical CO_2 assisted compounding: (a) at the injection port of the carbon dioxide, the pressure fluctuations should be minimised to obtain a stable injection. Therefore, transport elements instead of kneading elements should be used at the site of injection, (b) injected CO_2 should not be allowed to leak from upstream orifices, requiring the use of a melt seal using reversed elements, (c) the pressure downstream should be maintained at a sufficiently high level to ensure that the supercritical CO_2 remains dissolved in the polymer. This can be obtained by providing high die resistance, and (d) complete dissolution of CO_2 can be assured by using kneading elements to improve mixing downstream of the supercritical fluid introduction. The compounding process was optimised for supercritical CO_2 assisted extrusion prior to the compounding of the batches used in this trial. It was concluded during the optimisation process that the use of a melt seal generated by reverse mixing elements as suggested by Lee *et al*. (1998) and Verreck *et al*. (2006) was unnecessary in this instance due to the flow behaviour of the materials used, which precluded leakage of CO_2 upstream through the barrel. In addition, the design of the strand die used in this work was found to produce sufficiently high resistance so as to ensure that the supercritical CO_2 remained dissolved in the polymer during compounding.

As the residence time of the supercritical CO_2 / matrix mixture in the extruder is relatively short, an estimate of the time required to form a single-phase solution is important prior to continuous processing. Diffusion theory has been used in the literature as a method of making such an estimate (Park and Suh, 1996 a; Park and Suh, 1996 b), for a typical polymer viscosity of 200 Pa-s, this method suggests that single-phase solution formation can be achieved sufficiently quickly so as to allow for industrial scale up (Park and Suh, 1996 b). Shear action in the extruder causes the break-up of larger CO_2 bubbles into smaller ones and hence, enhanced mass transfer that shortens the time for formation of a single-phase solution. The recorded values of torque and die head pressure displayed in Figures 3.36 and 3.37 indicate that at constant temperature and screw speed, a drop in the melt viscosity of the polymer melt occurs upon addition of supercritical CO_2 to the hot melt extrusion process.

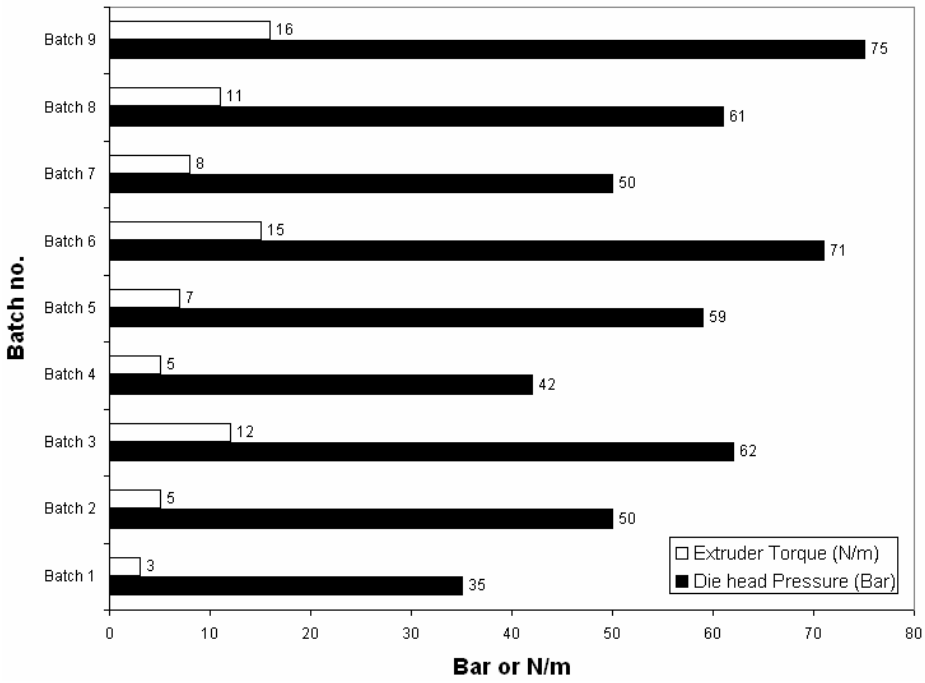

Figure 3.36 *Torque and die head pressure data for samples processed without the assistance of supercritical CO_2.*

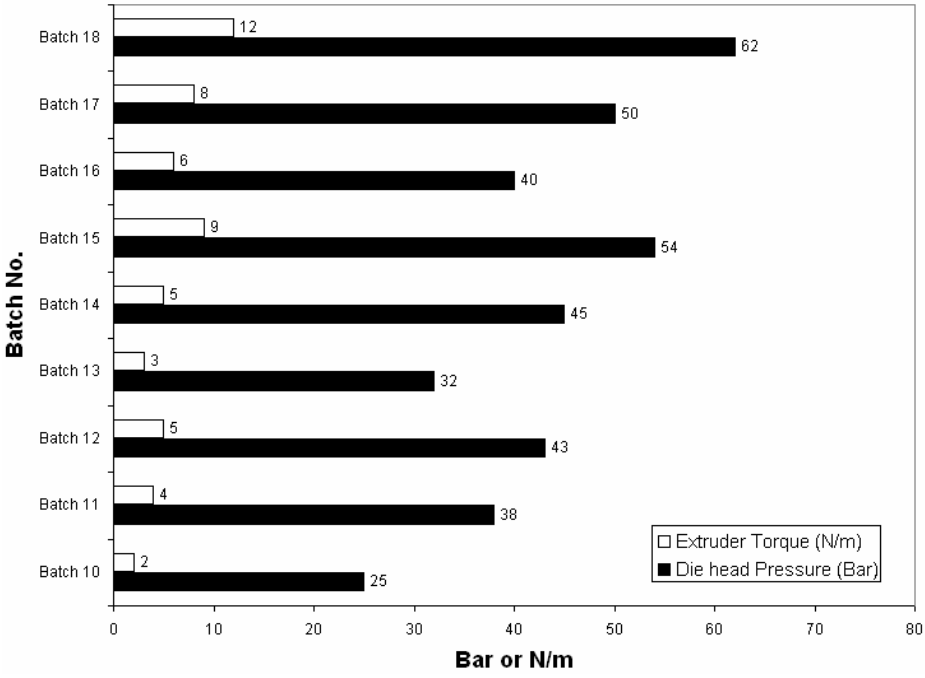

Figure 3.37 *Torque and die head pressure data for samples processed with the assistance of supercritical CO_2.*

The observed values for torque and die head pressure were reduced for each polymer matrix processed using the assistance of supercritical CO_2. Chiou *et al*. (1985) describes the primary methods by which supercritical fluid effects plasticisation in the barrel of the extruder. Firstly, carbon dioxide is absorbed between the polymer chains causing an increase of free volume and a decrease in chain entanglements. Secondly, carbon dioxide acts as a molecular lubricant that reduces melt viscosity. Supercritical CO_2 induced plasticisation of polymers has been widely studied in the literature using a wide range of methods including: positron annihilation lifetime spectroscopy (Yuan *et al*. 1998), chromatography (Edwards *et al*. 1998), dynamic mechanical response (Fried *et al*. 1989), high pressure DSC (Chiou *et al*. 1985), FTIR (Kazarian *et al*. 1996), and X-ray diffraction (Houde *et al*. 1992). The reduction in motor load and head pressure observed with the addition of supercritical CO_2 are akin to what would be expected to occur when melt processing temperatures are increased. This possible improvement in throughput without the risk of thermal degradation is one of the most favourable properties of supercritical fluid assisted hot melt extrusion. As previously described, incorporation of the API is seen to plasticise the polymer matrix with reduction in the motor load and die head pressure occurring with increasing API loading.

3.2.2.3 Thermal analysis

MDSC analysis was carried out on all the batches of extrudate produced, in order to ascertain if the use of supercritical CO_2 during the processing of the polymer matrices had any lingering effect on their thermal properties.

Figure 3.38 shows two thermograms typical of those obtained in this work. The results obtained indicate no significant change in the melting behaviour of the extrudate produced using the supercritical CO_2 assisted process occurs when compared to extrudate of the same composition produced via a conventional hot melt extrusion process. As noted previously and in agreement with the literature (Ozeki *et al*. 1997) the API is observed to have a plasticising effect on the polymer matrices tested.

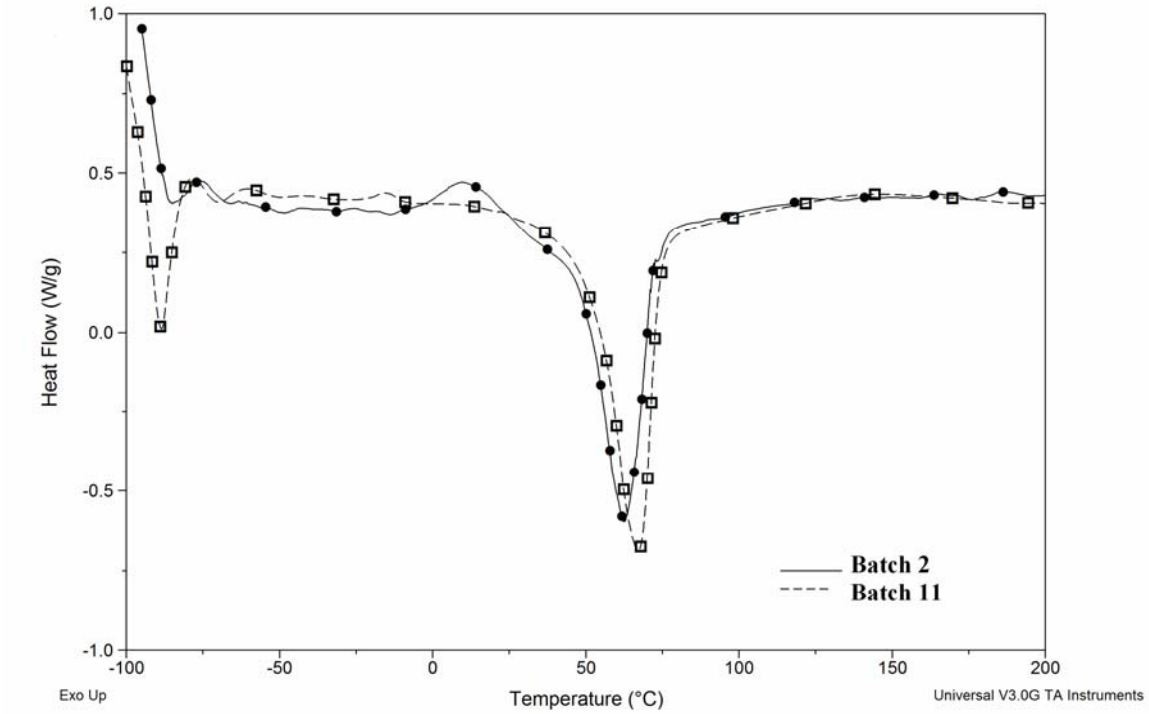

Figure 3.38 *MDSC thermograms obtained for extruded batches 2 and 11. Both matrices consist of 32.5%wt PEO 1 million and 32.5%wt PEO 200,000 with an API loading of 15%wt. Batch 2 was processed conventionally while batch 11 was processed using the assistance of supercritical CO_2.*

In this case, the plasticising effect is manifested by a depression in the melting point of the polymer matrices, the magnitude of which increases with increasing API inclusion: at 14% by weight, the average observed depression in matrix melting point was 3.43°C.

3.2.2.4 Steady state rheometry

The melt viscosity during processing was monitored using torque and die head pressure data. Steady state parallel plate rheometry was carried out to ascertain if the viscosity reduction occurred only in the barrel during supercritical CO_2 assisted processing or if the mobility of the polymer blends remained elevated after processing.

The data obtained indicated that the viscosity reducing effect of supercritical CO_2 occurs only in the barrel of the extruder during supercritical CO_2 assisted processing. Figure 3.39 illustrates the viscosity curves obtained for four of the batches produced in this study. These results are typical of those obtained. Batches 4 and 13 have identical composition (89.5%*wt* PEO Mw 200,000 and 10.5%*wt* API); similarly batches 9 and 18 have identical composition (46.25%*wt* PEO Mw 200,000, 46.25%*wt* EPO and 7.5%*wt* API). Batches 13 and

18 were produced using supercritical CO_2 assisted processing while batches 4 and 9 were produced using conventional processing. Negligible difference in the viscosities of the extrudates is observed when comparing those produced via a supercritical CO_2 assisted process and those produced using conventional processing.

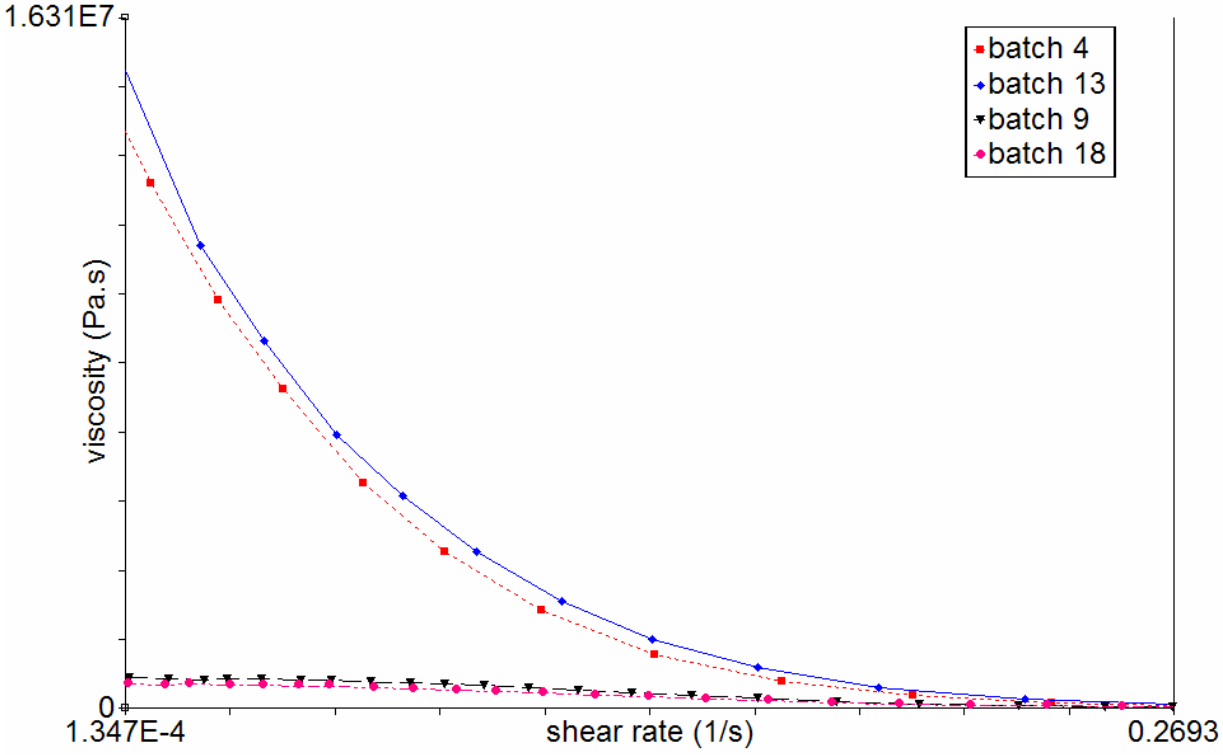

Batch No.	*PEO Mw 200,000 (% Weight)*	*Eudragit EPO (% Weight)*	*Carvedilol (% Weight)*	*Supercritical CO_2 assisted (1200 Psi)*
4	*89.5*	*0*	*10.5*	*No*
13	*89.5*	*0*	*10.5*	*Yes*
9	*46.25*	*46.25*	*7.5*	*No*
18	*46.25*	*46.25*	*7.5*	*Yes*

Figure 3.39 *Steady state viscosity data recorded for batches 4, 9, 13 and 18.*

3.2.2.5 Surface analysis (AFM & µTA)

Micro thermal analysis (µTA) was used to characterise the surface of the polymer matrices produced. Thermal conductivity images for batches 8 and 17 are shown in Figure 3.40. Both batches have identical composition (69.375%wt PEO Mw 200,000, 23.125%wt EPO and 7.5%*wt* API), batch 8 was processed conventionally and batch 17 was processed with the assistance of supercritical CO_2. Although the conductivity image is dominated by

surface topography in the image presented, PEO spherulites are clearly visible in batch 17. µMDTA and µTMA measurements were taken at the positions indicated in Figure 3.40. Figure 3.41 shows the µMDTA and µTMA trace obtained on the surface of batch 8.

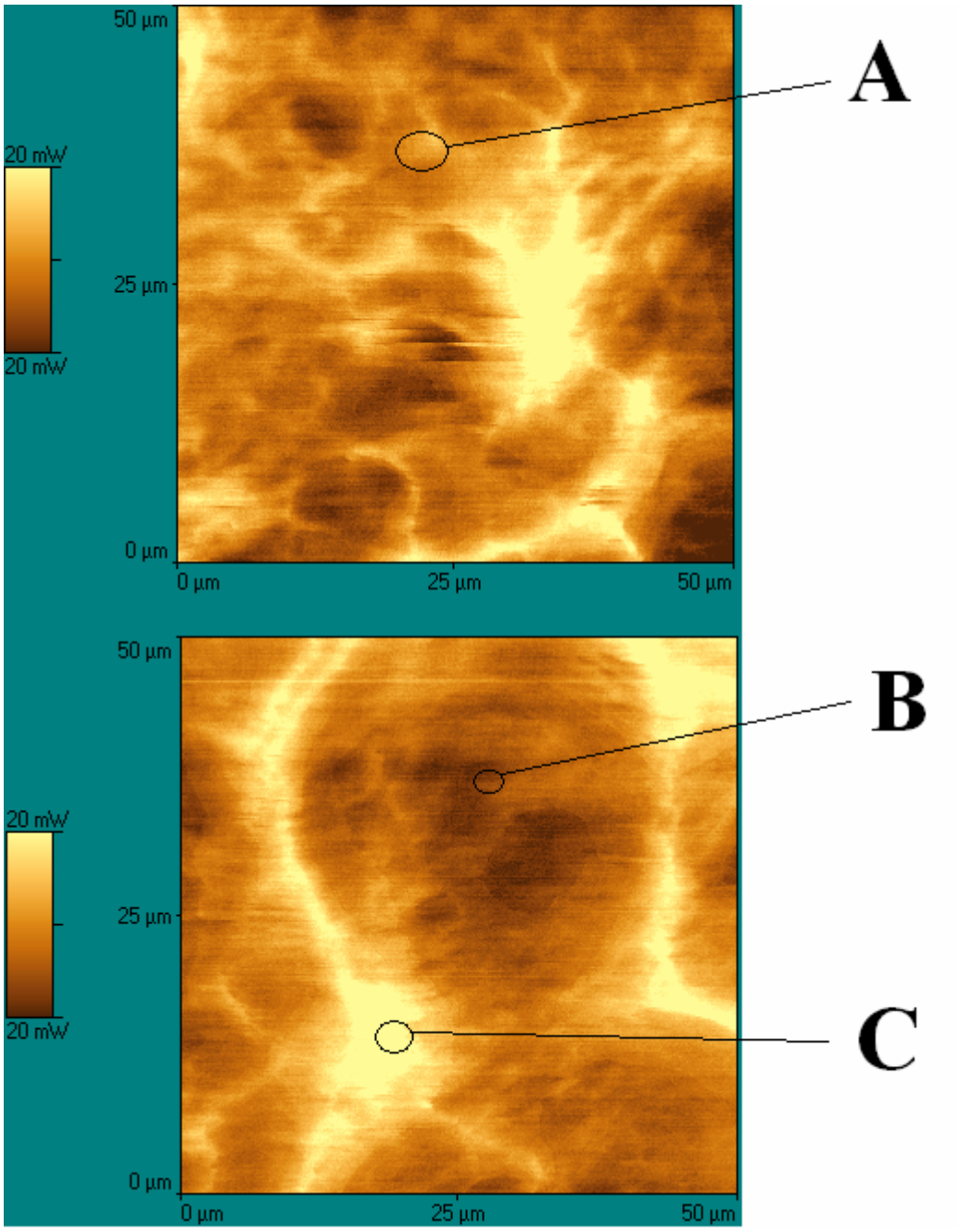

Figure 3.40 *Surface conductivity images for sample 8 (upper image) and sample 17 (lower image). Both batches consist of 69.375%wt PEO Mw 200,000, 23.125%wt EPO and 7.5%wt API. Batch 8 was processed conventionally; batch 17 was processed using a supercritical fluid assisted process.*

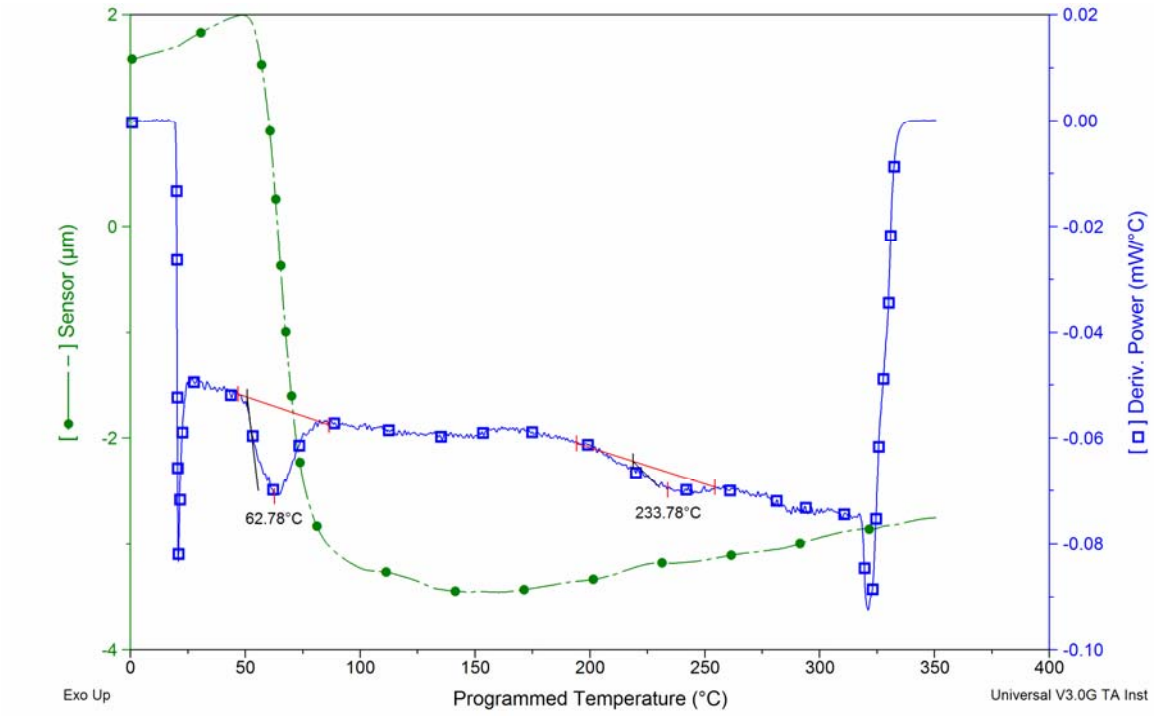

Figure 3.41 *µMDTA and µTMA scans obtained for area 'A' indicated in Figure 3.40.*

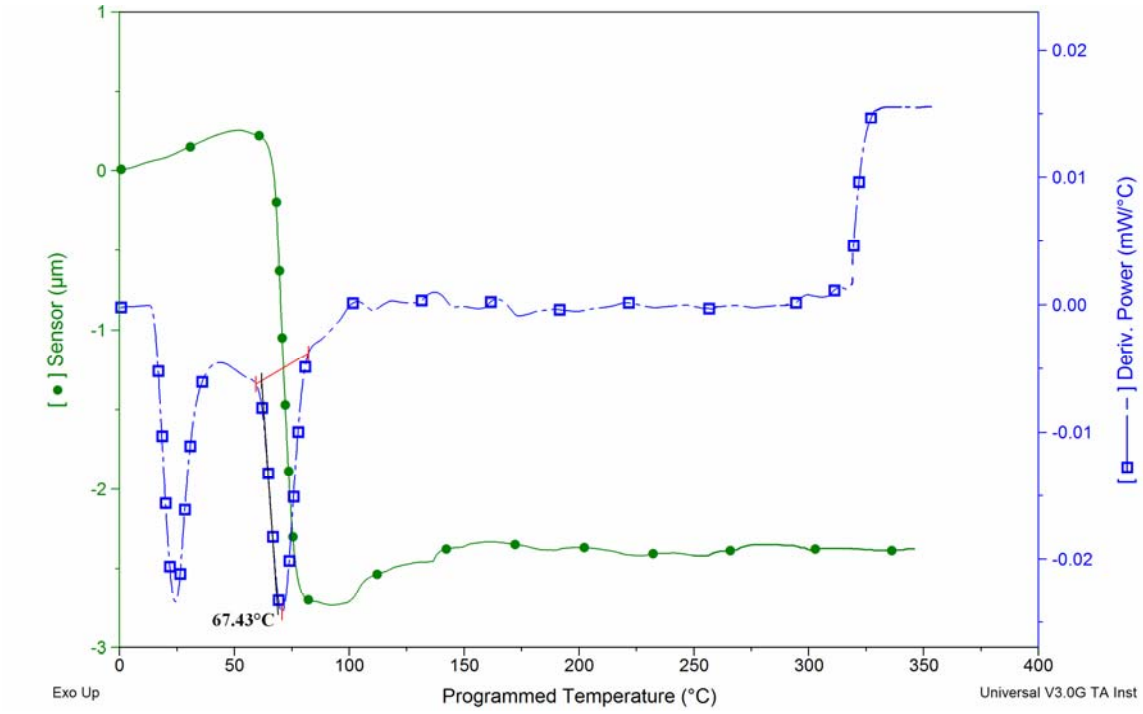

Figure 3.42 *µMDTA and µTMA scans obtained for area 'B' indicated in Figure 3.40.*

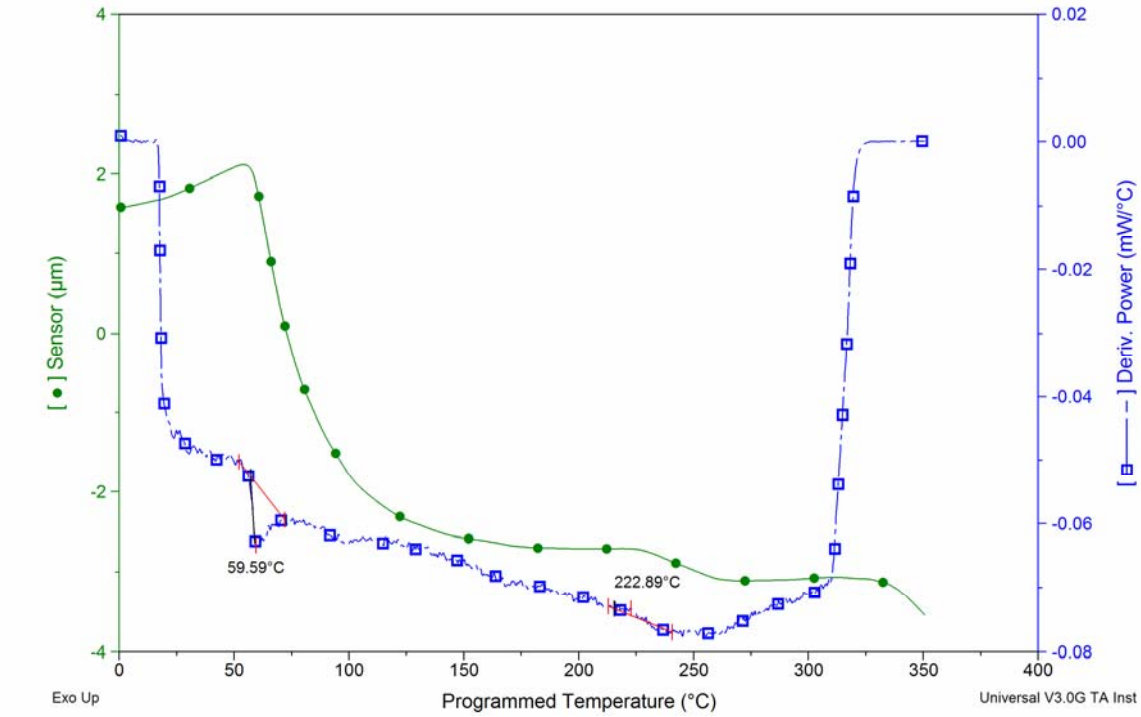

Figure 3.43 *µMDTA and µTMA scans obtained for area 'C' indicated in Figure 3.40.*

In Figure 3.41, a melting point at 62°C is visible, as is a transition at 233°C which is typical of depolymerisation and functional group instability in EPO. A melting point at 67°C, typical of PEO, is observed when µMDTA and µTMA scans are obtained on the spherulite (B) as can be seen in Figure 3.42. In both Figures 3.41 and 3.42 rapid softening of the polymer occurs at the melting point as can be clearly seen in the µTMA sensor trace. Figure 3.43 is taken from the interspherulitic region of batch 17 (C) and shows transitions at 59°C and 222°C which are typical of EPO, thus indicating that the incorporation of the supercritical CO_2 results in a higher crystallinity of PEO than non- supercritical CO_2 assisted extrusion, with the EPO material in the matrix being restricted to the interspherulitic regions of the matrix. The increased crystallinity of the PEO occurs due to the supercritical CO_2 induced mobility of the PEO chains, allowing them to rearrange into kinetically favoured configurations. These effects were also noted for PET (Zhong *et al*. 1999) and PC (Gross *et al*. 2000).

3.2.2.6 Drug release

In vitro dissolution testing was carried out in two media; 0.2M HCl (pH 1.2) and pH 7.2 buffer. The results obtained are displayed in Figures 3.44, 3.45 and 3.46.

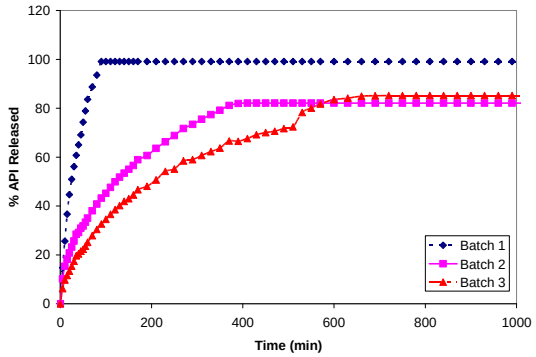

(a) Drug release from batches 1,2 and 3 in pH 7.2

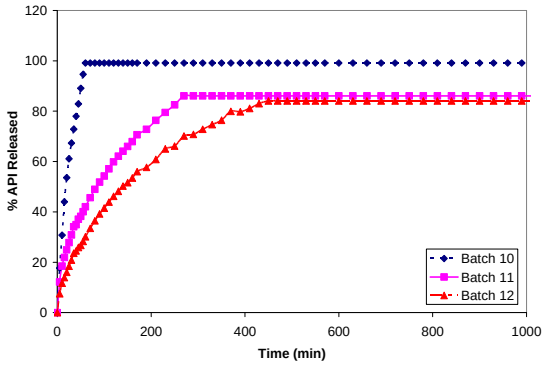

(b) Drug release from batches 10,11 and 12 in pH 7.2

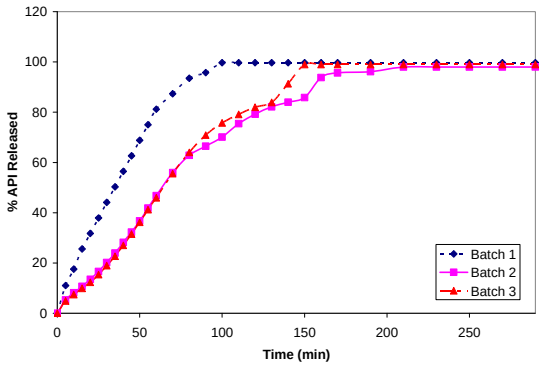

(c) Drug release from batches 1,2 and 3 in 0.2M HCl(pH 1.2)

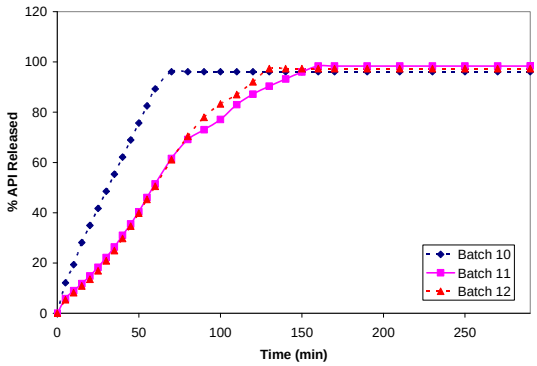

(d) Drug release from batches 10,11 and 12 in 0.2M HCl(pH 1.2)

Batch No.	*PEO Mw 200,000 (% Weight)*	*Eudragit EPO (% Weight)*	*Carvedilol (% Weight)*	*Supercritical CO_2 assisted (1200 Psi)*
1	*86*	*0*	*14*	*No*
2	*64.5*	*21.4*	*14*	*No*
3	*43*	*43*	*14*	*No*
10	*86*	*0*	*14*	*Yes*
11	*64.5*	*21.4*	*14*	*Yes*
12	*43*	*43*	*14*	*Yes*

Figure 3.44 *Drug release data for batches of polymer matrix containing 14%wt API.*

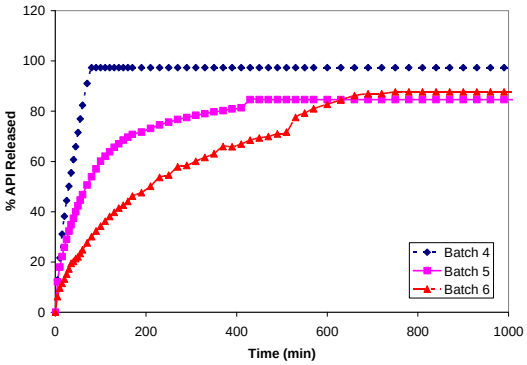

(a) Drug release from batches 4,5 and 6 in pH 7.2

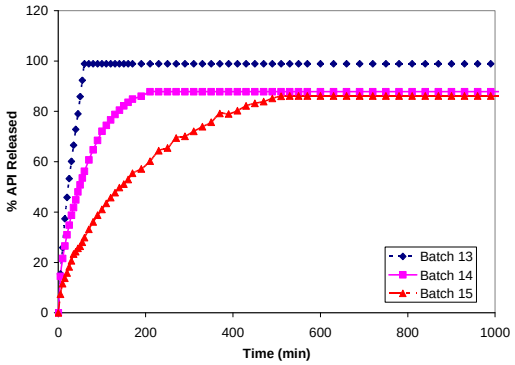

(b) Drug release from batches 13,14 and 15 in pH 7.2

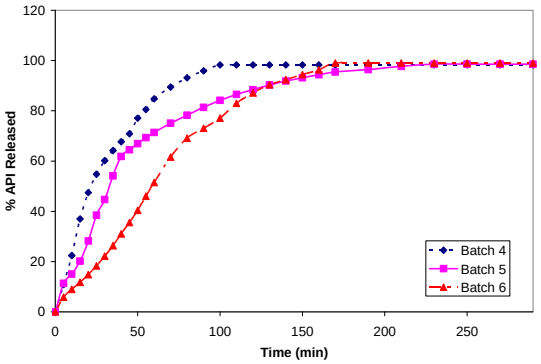

(b) Drug release from batches 4,5 and 6 in 0.2M HCl(pH 1.2)

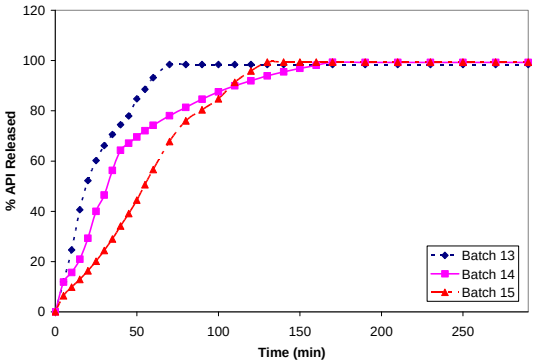

(d) Drug release from batches 13,14 and 15 in 0.2M HCl (pH 1.2)

Batch No.	*PEO Mw 200,000 (% Weight)*	*Eudragit EPO (% Weight)*	*Carvedilol (% Weight)*	*Supercritical CO_2 assisted (1200 Psi)*
4	*89.5*	*0*	*10.5*	*No*
5	*67.125*	*22.375*	*10.5*	*No*
6	*44.75*	*44.75*	*10.5*	*No*
13	*89.5*	*0*	*10.5*	*Yes*
14	*67.125*	*22.375*	*10.5*	*Yes*
15	*44.75*	*44.75*	*10.5*	*Yes*

Figure 3.45 *Drug release data for batches of polymer matrix containing 10.5%wt API.*

For ease of comparison the t25%, t50% and t75% dissolution values obtained are displayed in Tables 3.9 and 3.10. Dissolution of the polymer matrix proceeds at a slightly faster rate as the percentage of drug contained in the polymer matrix is increased. This is thought to be as a direct result of less rate controlling polymer being present in the matrix at higher drug loadings. This is consistent with findings throughout this work.

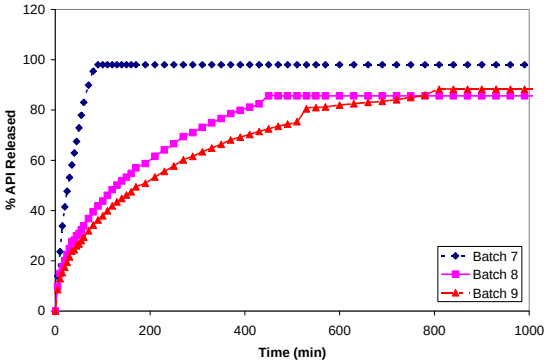

(a) Drug release from batches 7,8 and 9 in pH 7.2

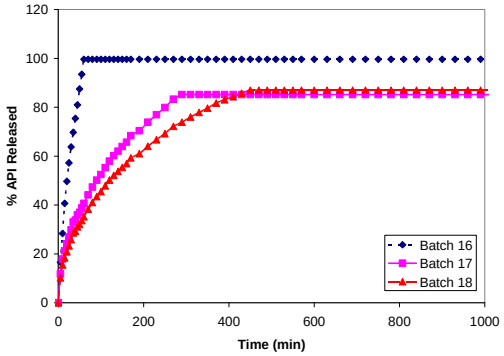

(b) Drug release from batches 16,17 and 18 in pH 7.2

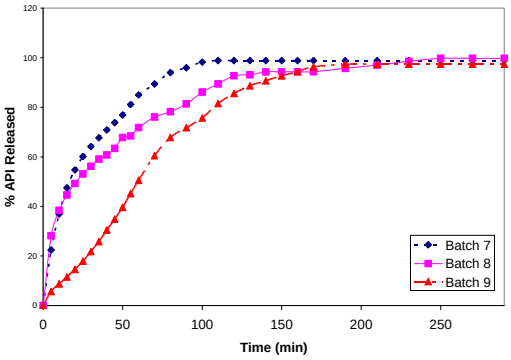

(c) Drug release from batches 7, 8 and 9 in 0.2M HCl (pH 1.2)

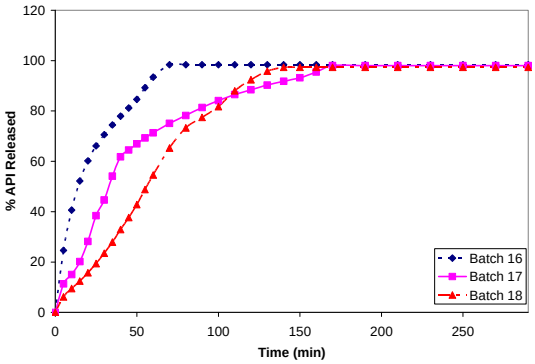

(d) Drug release from batches 16,17 and 18 in 0.2M HCl (pH 1.2)

Batch No.	*PEO Mw 200,000 (% Weight)*	*Eudragit EPO (% Weight)*	*Carvedilol (% Weight)*	*Supercritical CO_2 assisted (1200 Psi)*
7	*92.5*	*0*	*7.5*	*No*
8	*69.375*	*23.125*	*7.5*	*No*
9	*46.25*	*46.25*	*7.5*	*No*
16	*92.5*	*0*	*7.5*	*Yes*
17	*69.375*	*23.125*	*7.5*	*Yes*
18	*46.25*	*46.25*	*7.5*	*Yes*

Figure 3.46 *Drug release data for batches of polymer matrix containing 7.5%wt API.*

The drug release occurs at a much quicker rate in pH 1.2 than in the pH 7.2 buffer solution. In all cases studied, samples prepared via supercritical CO_2 assisted processing reached 75% dissolution quicker than those prepared by conventional extrusion. It is proposed that the quicker dissolution is due to higher internal surface area in the supercritical CO_2 produced samples as these matrices were observed visually to have a more foam like structure. Eudragit EPO does not dissolve above pH 5.5, but swells. This

resulted in slower release of API from batches containing EPO in the buffer solution. Samples containing EPO did not release 100% drug in the buffered solution over the length of the experiment. This is most likely a result of active agent remaining entrapped in un-dissolved EPO regions.

Table 3.9 *Dissolution times in 0.2M HCl (pH 1.2) of the batches under investigation.*

	0.2M HCl (pH 1.2)								
	Matrices prepared using conventional extrusion								
	Batch 1	*Batch 2*	*Batch 3*	*Batch 4*	*Batch 5*	*Batch 6*	*Batch 7*	*Batch 8*	*Batch 9*
t25% (min)	15	35	35	10	20	35	5	5	35
t50% (min)	35	65	65	20	30	60	15	25	60
t75% (min)	55	110	100	50	70	90	45	70	100
	Matrices prepared by supercritical fluid assisted extrusion								
	Batch 10	*Batch 11*	*Batch 12*	*Batch 13*	*Batch 14*	*Batch 15*	*Batch 16*	*Batch 17*	*Batch 18*
t25% (min)	15	35	35	10	20	30	5	20	30
t50% (min)	30	60	60	20	30	55	15	30	55
t75% (min)	50	100	90	40	60	80	35	70	80

Table 3.10 *Dissolution times in pH 7.2buffer of the batches under investigation.*

	pH 7.2 buffer								
	Matrices prepared using conventional extrusion								
	Batch 1	*Batch 2*	*Batch 3*	*Batch 4*	*Batch 5*	*Batch 6*	*Batch 7*	*Batch 8*	*Batch 9*
t25% (min)	10	30	60	10	20	60	10	30	45
t50% (min)	25	130	210	30	70	210	30	130	190
t75% (min)	50	310	510	55	250	530	50	330	510
	Matrices prepared by supercritical fluid assisted extrusion								
	Batch 10	*Batch 11*	*Batch 12*	*Batch 13*	*Batch 14*	*Batch 15*	*Batch 16*	*Batch 17*	*Batch 18*
t25% (min)	10	20	45	10	15	45	10	20	30
t50% (min)	20	90	140	25	50	150	20	90	120
t75% (min)	40	210	330	40	110	350	40	210	310

3.2.2.7 Summary

The work presented described the use of supercritical CO_2 as a plasticiser in the hot melt production of a range of polymer matrices for sustained oral drug delivery. Several batches of matrix material were prepared incorporating an active pharmaceutical ingredient and

processed both with and without supercritical CO_2 incorporation. Torque and die head pressure readings taken from the extruder during processing indicate that supercritical CO_2 acts as a plasticiser during the extrusion process, thus allowing for higher extrusion speeds to be achieved. Characterisation of the resultant matrices revealed that the plasticising effect occurs only in the barrel of the extruder and no viscosity reduction is observed after processing. The matrices were seen to be thermally stable with the incorporation of supercritical CO_2 having no effect on the thermal properties of the matrix when measured post processing. μTA revealed that the incorporation of supercritical CO_2 leads to a higher propensity for crystallisation in PEO. Dissolution analysis showed that the use of supercritical CO_2 during the extrusion process resulted in a faster dissolution of API when compared with unassisted extrusion. The results detailed within this section indicate that supercritical fluid assisted hot melt extrusion is a viable enhancement to conventional hot melt extrusion for the production of monolithic dosage forms.

However, from a production point of view, PEO carrier materials are relatively expensive and may cause the overall cost of the matrix to be prohibitively high. In order to decrease the cost of manufacture of the drug delivery device, it was deemed necessary to investigate the use of cheaper filler materials in the matrix.

3.3 Evaluation of novel filler systems for monolithic dosage forms produced via hot melt extrusion

3.3.1 Agar as a novel constituent in hot melt extruded dosage forms

3.3.1.1 Introduction

Hydrogels from agar (polysaccharide) have received particular attention, due to their natural origin, low cost and good biocompatibility (Brown and Johnson, 1981; Gehrke, 1993; Tabatha and Ikada, 1998). Furthermore, their resemblance to human tissues is of value for these polymers to be used to study or mimic solute transport through biological media (Favre and Girand, 2001). They have been widely used in drug delivery systems (Sumathi and Ray, 2002; Lead *et al*. 2003). However studies on the use of agar as a filler material in hot melt prepared dosage forms have thus far not been carried out.

In this work the use of agar as a novel filler material in hot melt extruded dosage forms was investigated. Two hot melt prepared matrices were used to test the release rate of an active pharmaceutical ingredient when agar was incorporated as a filler material. These matrices were compared with matrices incorporating the common pharmaceutical excipient microcrystalline cellulose (Table 3.11).

Table 3.11 *Batch composition used for the compounding of matrices for the development of a novel filler system containing agar (all values are in grams).*

Batch number	PEO (MW 1 Million)	PEO (MW 200,000)	Eudragit L 100	API	Agar	MCC
1	20	20	0	0	0	0
2	32.5	32.5	0	15	0	0
3	27.5	27.5	0	15	10	0
4	22.5	22.5	0	15	20	0
5	17.5	17.5	0	15	30	0
6	27.5	27.5	0	15	0	10
7	22.5	22.5	0	15	0	20
8	17.5	17.5	0	15	0	30
9	0	20	20	0	0	0
10	0	32.5	32.5	15	0	0
11	0	27.5	27.5	15	10	0
12	0	22.5	22.5	15	20	0
13	0	17.5	17.5	15	30	0
14	0	27.5	27.5	15	0	10
15	0	22.5	22.5	15	0	20
16	0	17.5	17.5	15	0	30

3.3.1.2 Processing observations

During the hot melt extrusion processing of the batches outlined in Table 3.10, the values for die head pressure and extruder torque were recorded. The trends observed showed increases in the die head pressure and the torque values obtained for batches containing filler materials. The increase in the torque and die head pressure observed was more pronounced for the batches containing agar filler than for the batches containing microcrystalline cellulose (MCC) filler, indicating that the blends containing the agar filler were more viscous than those containing the MCC filler. The values obtained also indicated that the incorporation of the active agent led to a plasticising effect in the hot melt extrusion process as the values for torque and die head pressure observed were lower than for batches containing matrix material alone. The values for the torque and die head pressure observed during the hot melt processing step can be seen in Figures 3.47 and 3.48.

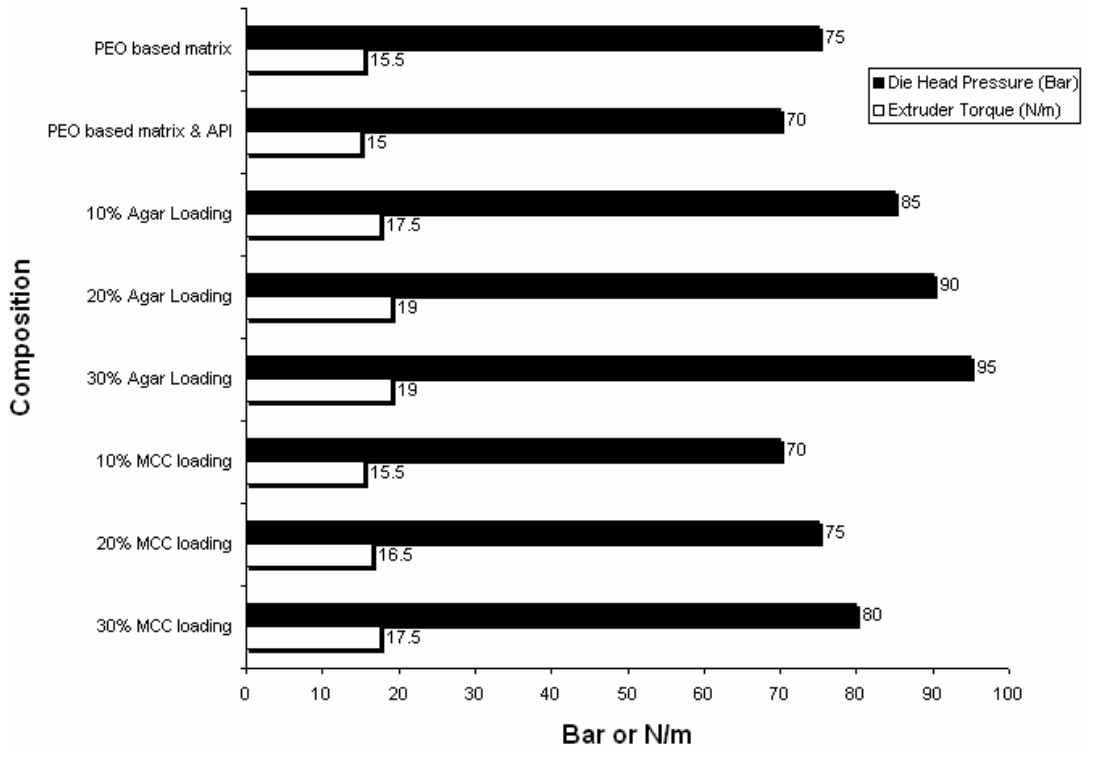

Figure 3.47 *Extruder torque and die head pressure values observed during hot melt processing of PEO based matrices.*

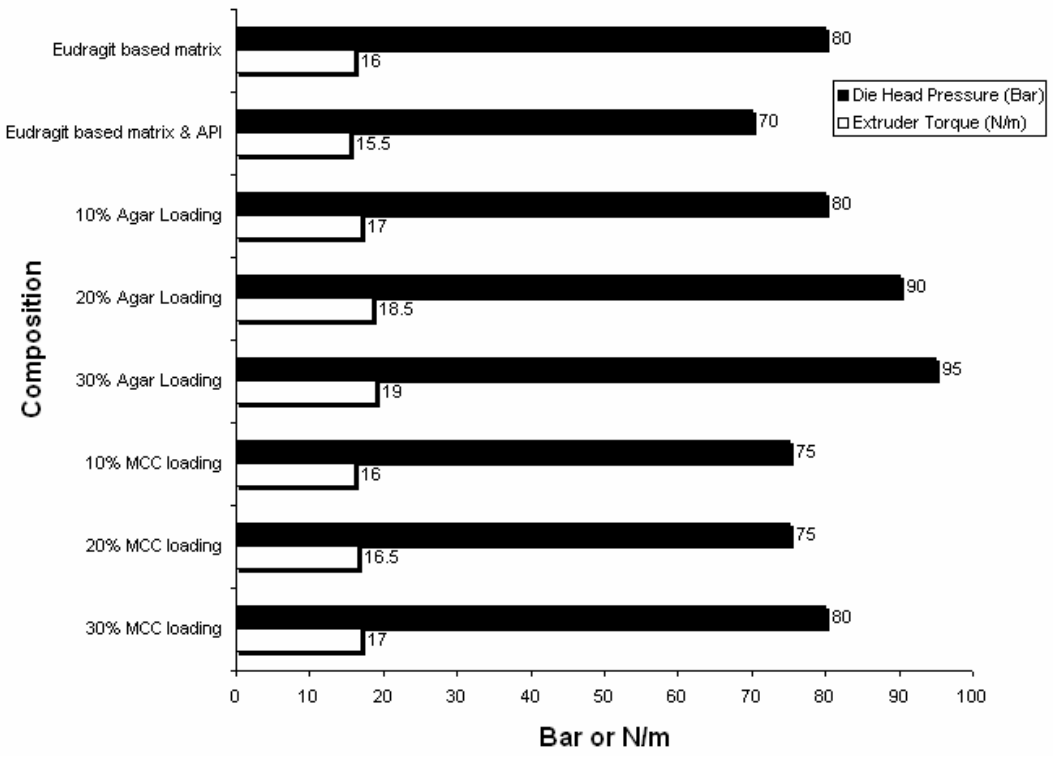

Figure 3.48 *Extruder torque and die head pressure values observed during hot melt processing of Eudragit based matrices.*

3.3.1.3 Thermal analysis

Differential scanning calorimetry was used to ascertain if the inclusion of the diclofenac sodium (API) or the filler materials had any effect on the thermal characteristics of the matrix material. Figure 3.49 shows an MDSC thermogram of batch 1 which was typical of the MDSC scans obtained. The MDSC scans obtained showed a drop of approximately 3°C in the T_m of both the PEO based and Eudragit based matrices; with the melting point of the PEO based matrix dropping from 57.23°C to 54.43°C and the melting point of the Eudragit based matrix dropping from 62.76°C to 59.96°C. These results indicate that the diclofenac sodium acts as a plasticiser in the polymer matrix, confirming the observations made during the hot melt processing of the samples. The plasticisation effects of API molecules on the polymer melt during processing have been reported in the literature (Ozeki *et al*. 1997) and have been observed extensively throughout this body of work.

Endotherms associated with hydration of the diclofenac sodium are visible in the vicinity of 100°C. These endotherms disappear when the matrix containing the active agent has been heated to above 100°C and reappear slowly when the dried active agent containing matrix

has been stored in a humid environment. This effect was previously reported in the literature (Fini *et al.* 2005) and would not prove to be an obstacle to the use of diclofenac sodium in hot melt prepared dosage forms as long as the diclofenac sodium was sufficiently dried prior to the extrusion process and the resultant extrudates were stored in a dry environment prior to packaging. The inclusion of both the filler materials had a negligible effect on the melting behaviour of the matrix indicating that the agar would be a viable alternative excipient for hot melt processing.

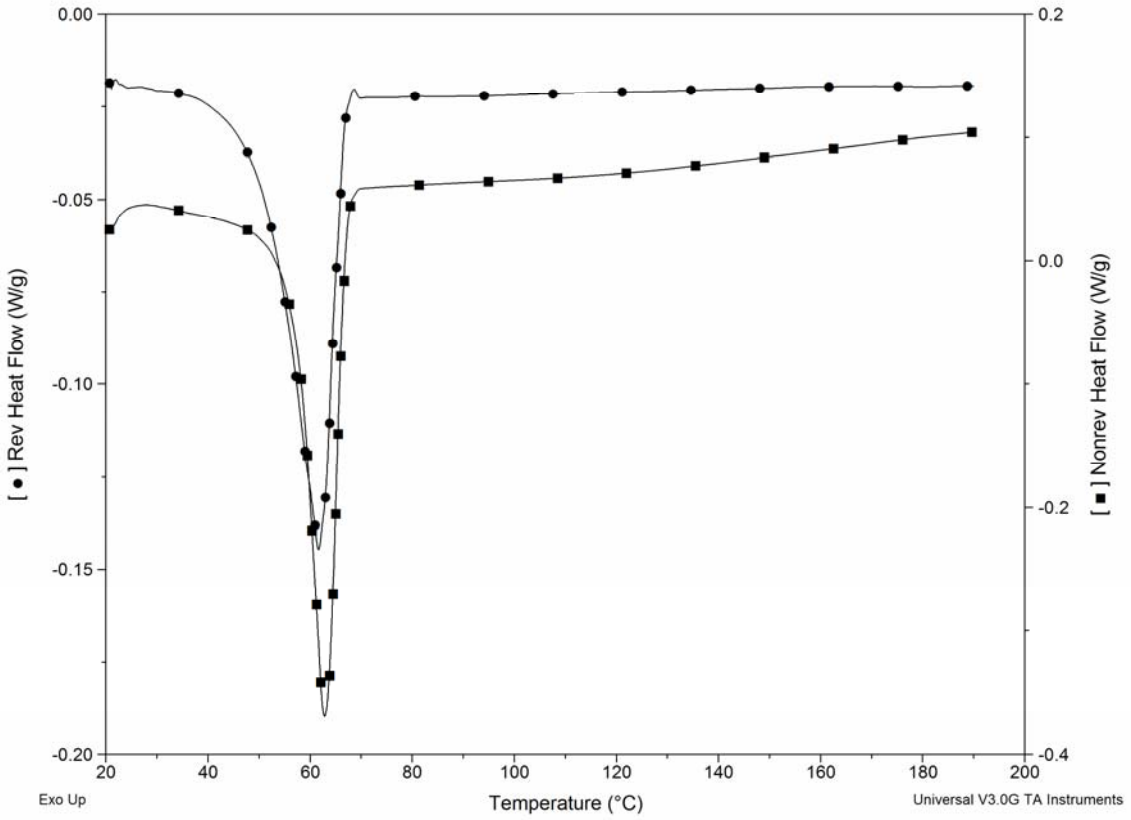

Figure 3.49 *Modulated DSC thermogram of the PEO based matrix (batch 1), showing both the reversing heat flow and non-reversing heat flow signals.*

3.3.1.4 Steady state rheometry

The effect of filler on both matrices is to increase the viscosity of the matrix. The increase of viscosity of the matrix becomes more pronounced as the percentage of filler is increased. Figures 3.50 & 3.51 show steady state rheometry results for both matrices, with viscosity displayed as a function of shear rate.

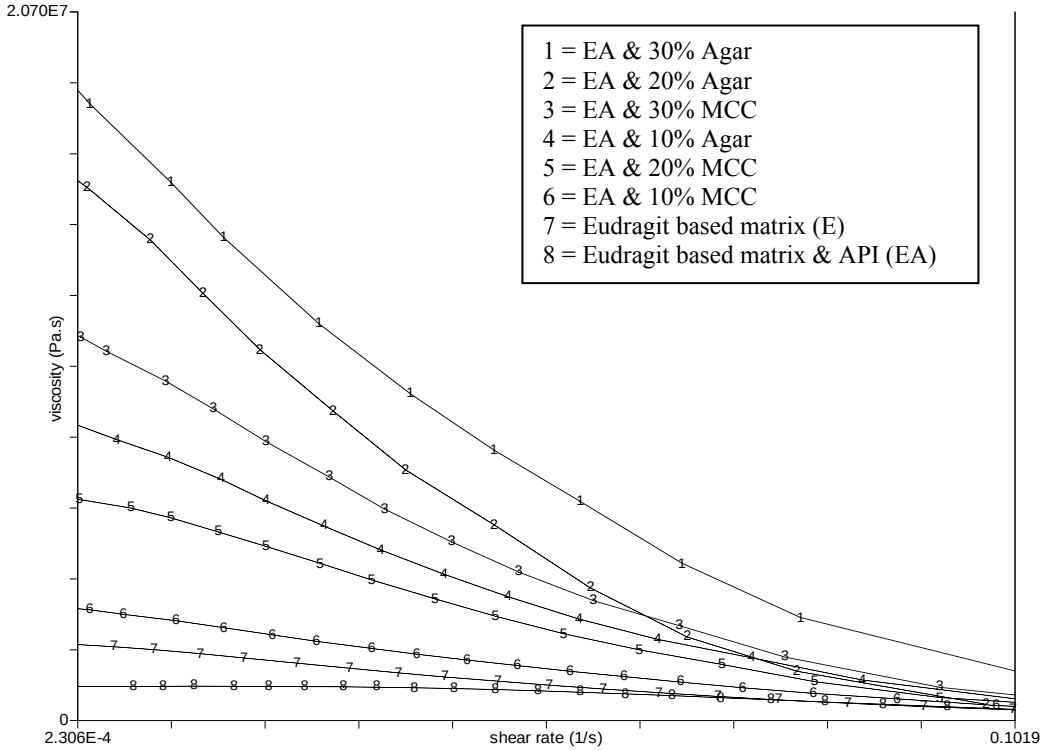

Figure 3.50 *Viscosity curves for Eudragit based matrix and filled Eudragit based matrices.*

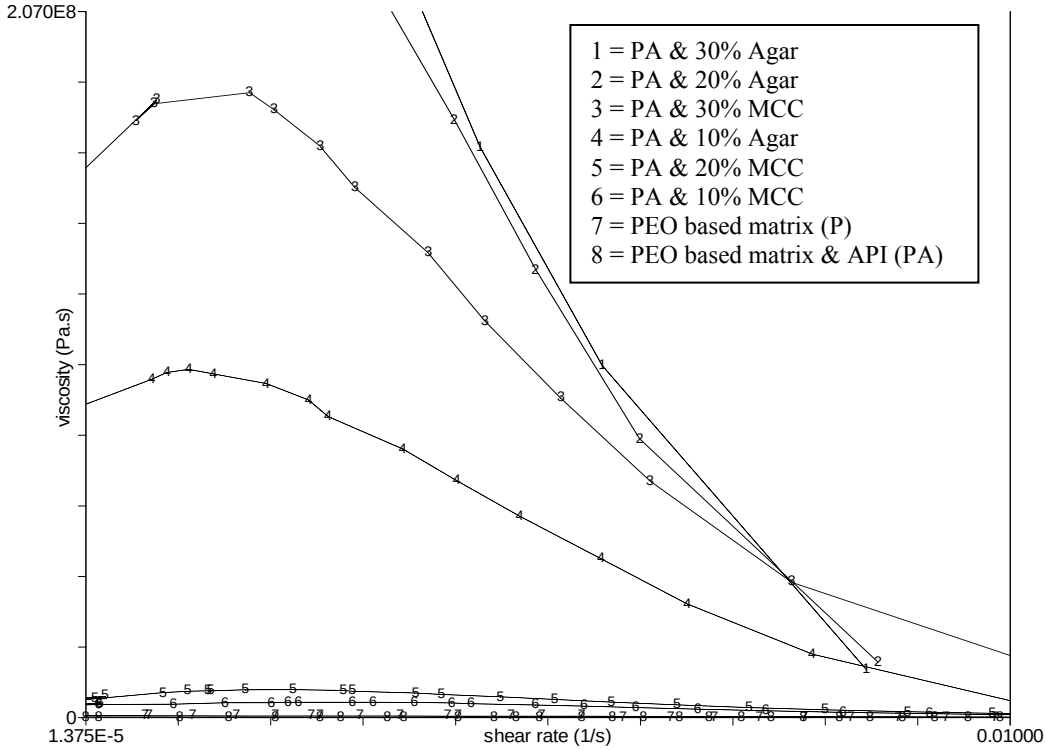

Figure 3.51 *Viscosity curves for PEO based matrix and filled PEO based matrices based matrices.*

A more substantial increase in viscosity is obtained with the inclusion of agar as a filler material when compared to the inclusion of microcrystalline cellulose. This can be explained by the fibrous nature of the microcrystalline cellulose compared to the stronger gel forming capabilities of agar.

3.3.1.5 Drug release

It has been reported in the literature (Zhang and McGinity, 1998) that Eudragit L100 and different molecular weight blends of PEO have proved useful for modulating the release of active agents in monolithic devices for drug release. The dissolution profile shown in Figure 3.52 is that of Eudragit L100 and PEO based matrices without fillers other than the API. It can be clearly seen from this plot that the PEO based matrix releases the active agent quicker than Eudragit based matrix.

The addition of the microcrystalline cellulose filler to both matrices has a marked effect on the dissolution rate. As can be seen from both Figures 3.53 and 3.54, the incorporation of microcrystalline cellulose is seen to decrease the release rate. This effect becomes more pronounced as the percentage of microcrystalline cellulose in the matrix increases, correlating with findings in the literature by Thommes and Kleinebudde (2006).

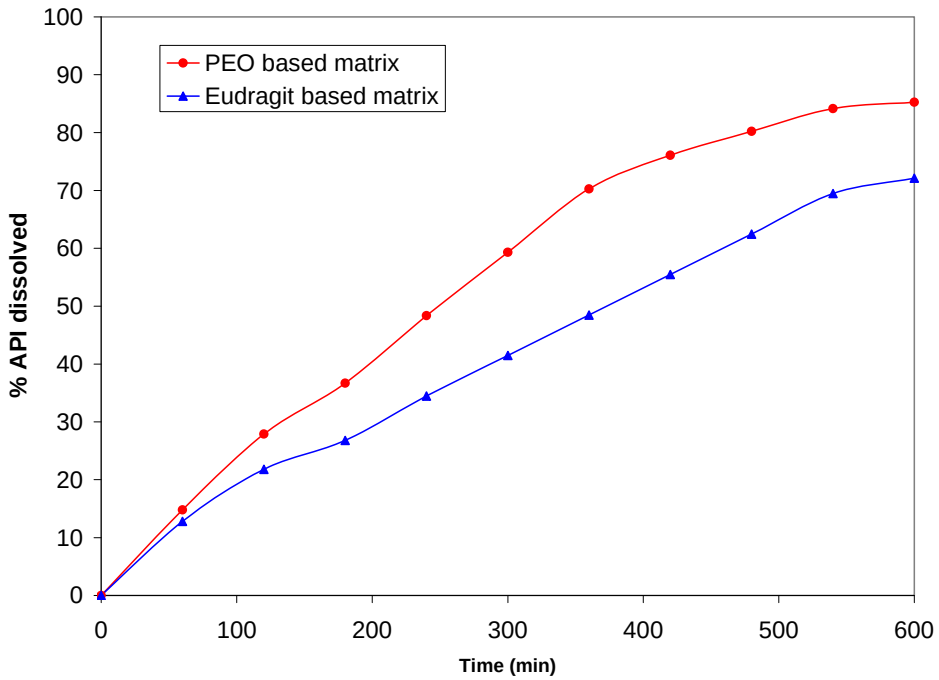

Figure 3.52 *Drug release from PEO based matrix and Eudragit based matrix.*

The main characteristics of the use of microcrystalline cellulose as a filler material is the lack of disintegration (Schroeder and Kleinebudde, 1995) which results in a prolonged matrix type drug release (Zimm *et al*. 1996). For drugs with low solubility, the time for complete release might be slower than the gastrointestinal passage time, resulting in decreased bioavailability and excretion of active pharmaceutical ingredient. However, the use of microcrystalline cellulose as a filler material in extended release devices has a major disadvantage in the reported adsorption of some drugs on to MCC (Okada *et al*. 1987; Rivera and Ghodbane, 1994; AlNimry *et al*. 1997) which could affect the drug release. Also, a decomposition of some drugs in the presence of MCC could be observed (Basit *et al*. 1999).

As can be seen in Figure 3.55 and Figure 3.56 the matrix blends containing agar show a similar trend as those containing microcrystalline cellulose. The incorporation of the agar into the polymer matrix leads to a reduction in the release rate of the active pharmaceutical ingredient, prolonging the release time of the matrix.

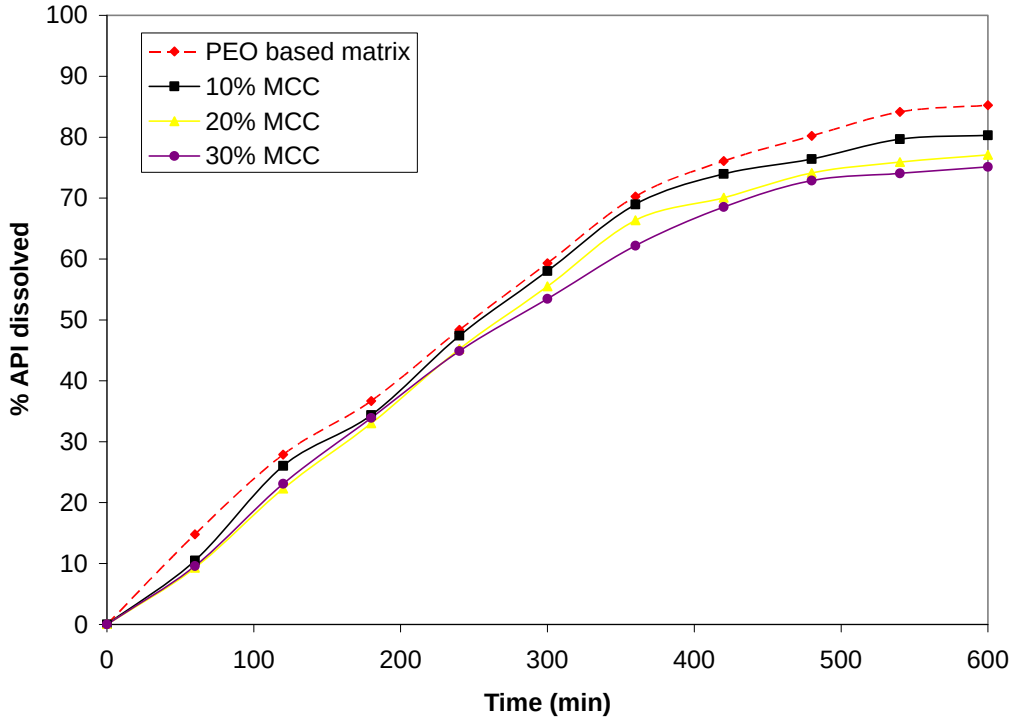

Figure 3.53 *Drug release from PEO based matrix and MCC filled PEO based matrices.*

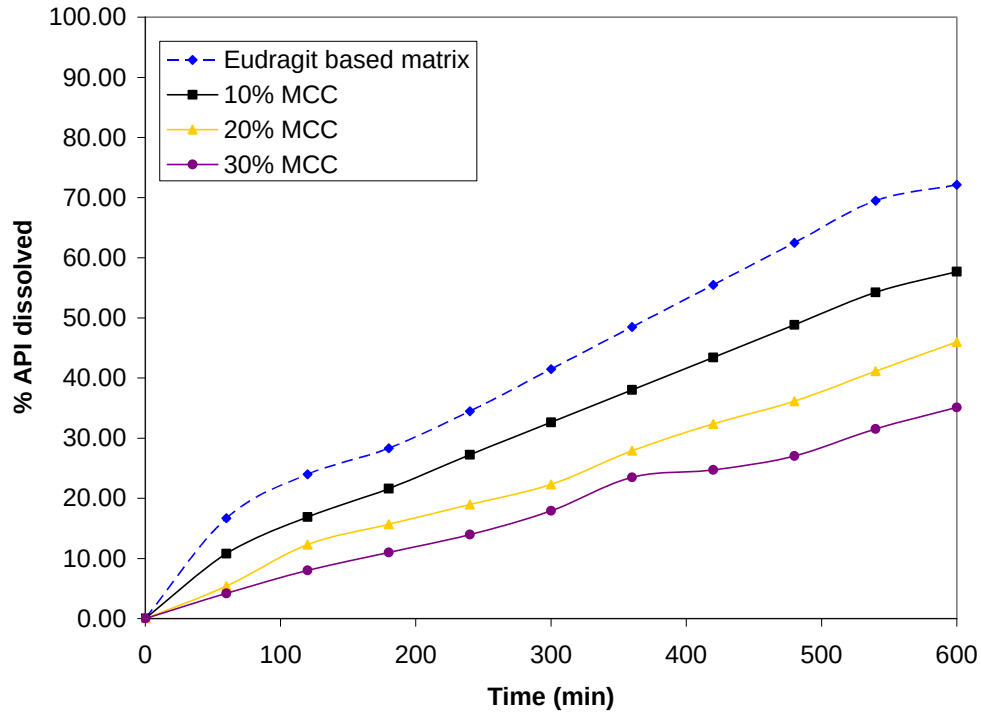

Figure 3.54 *Drug release from Eudragit based matrix and MCC filled Eudragit based matrices.*

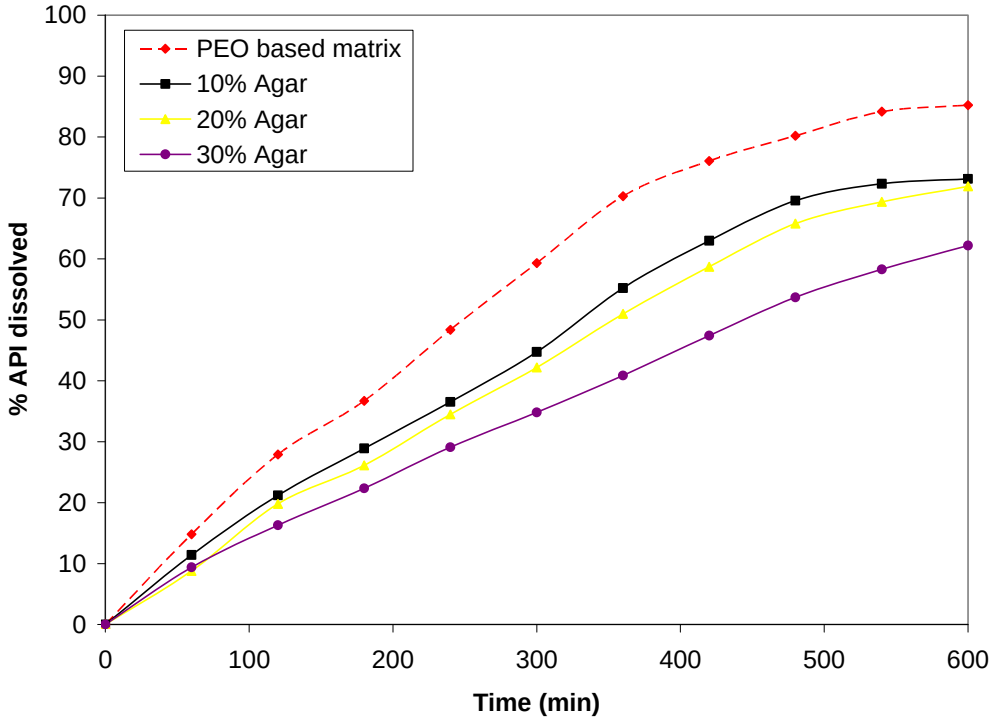

Figure 3.55 *Drug release from PEO based matrix and Agar filled PEO based matrices.*

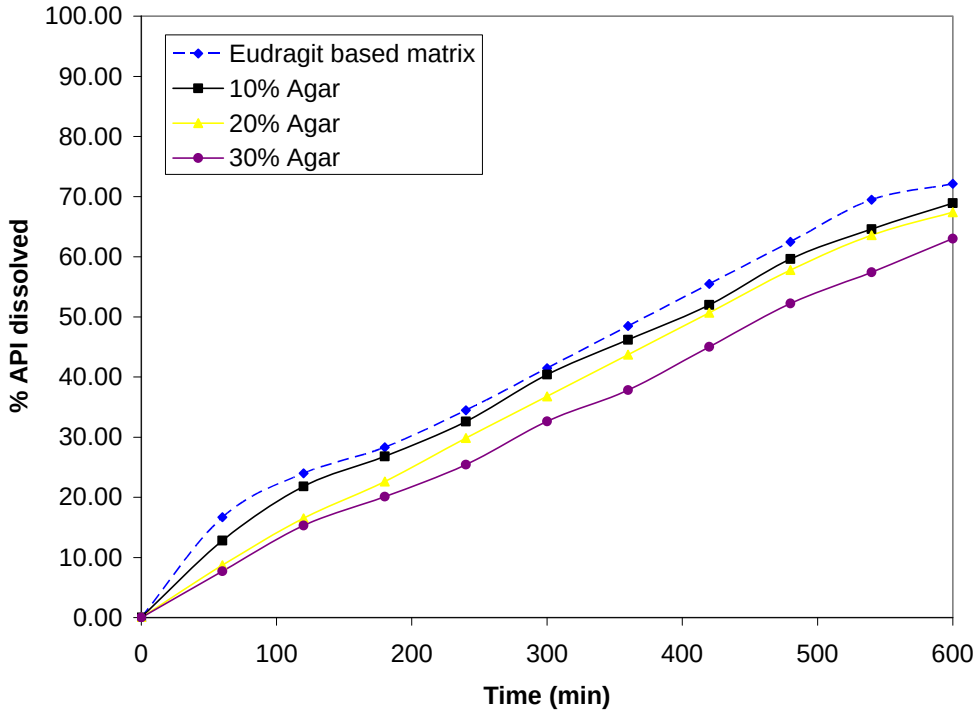

Figure 3.56 *Drug release from Eudragit based matrix and Agar filled Eudragit based matrices.*

3.3.1.6 *In vitro* biocompatibility evaluation

Adverse effects from drug delivery devices have been well documented (Recum, 1998). In some of these cases it is unclear as to the cause of the patient's problems, with medical staff unable to identify if the complications were due to the underlying disease, the active ingredient, or the drug delivery component itself. Consequently, any toxic potential of such devices should be determined and appropriate steps taken to minimise any adverse effect to the patient. Thus, when considering benefits versus risk from delivery devices, it is not adequate simply to consider them in terms of whether the risk to the patient are greater if the device is used or not used, but rather in terms of whether or not, within the context of current knowledge and technology the device produces the maximum benefit to the patient with a minimum of risk. Toxicological evaluation of the materials investigated in this section is necessary to ensure that the formulation and manufacturing process have not significantly altered the properties of the material and that no toxic additives were introduced.

The purpose of the chosen assay systems was to obtain a broad spectrum of knowledge of the cytotoxic and genotoxic potential of the polymers. The *in vitro*

cytotoxicity and genotoxicity assays performed during the course of this study utilised continuous cell lines that were approximate models of potential toxicity sites *in vivo* (i.e. liver and GIT). The Caco-2 cell line has been found to share characteristics of the gastro intestinal tract (Baker and Baker, 1993), the site where polymeric matrices used for oral drug delivery have a prolonged contact time *in vivo*. After absorption from the intestinal tract, the first organ exposed to orally ingested materials is normally the liver, the organ responsible for a considerable level of detoxification. Therefore, HepG2 cells, a liver carcinoma derived cell line, were used to determine the target organ toxicity and to detect possible bioactivated metabolites since HepG2 cells are metabolically competent (Dierickx, 1998).

3.3.1.6.1 *In vitro* assessment of cytotoxicity

Tissue specific cytotoxicity involves undesirable effects on particular types of differentiated cells, therefore comparative studies on the HepG2 and Caco-2 cell line were performed. The Caco-2 cell line, isolated from a human intestinal adenocarcinoma, shares characteristics and functions of the epithelial lining of the gastro intestinal tract. This is the first area of exposure to the polymers *in vivo* (Baker and Baker, 1993), as they are being used in oral drug delivery. The HepG2 cells were chosen because of their metabolic activity and ability to detect bioactivated metabolites, due to the fact that they retain many specialised functions and drug metabolising enzyme activities comparable with human *in vivo* hepatocytes (Dierickx, 1998).

The chosen *in vitro* cytotoxicity assays detect the amount of toxicity the test chemical exerts by assessing the mitochondrial activity (MTT assay) and the integrity of the plasma membrane (LDH assay). In order to conduct a comparative study and to assess target cell toxicity both cell lines used in this study were treated the same with respect to test chemical concentration, cell density and time of incubation.

3.3.1.6.2 The 3-(4, 5-dimethylthiazol-2yl)-2, 5-diphenyl-2H-tetrazoliumbromid (MTT) assay

The ability of the mitochondria to convert the yellow tetrazolium salt (MTT) to a blue formazan product (Mosmann, 1983) can only occur in viable cells. Short exposure (6

hours) of both HepG2 and Caco-2 cell lines to the polymer matrices at a concentration range of 1.25-0.25 % (w/v) caused only slight decreases in cell viability. Incubation with different polymer solutions in both cell types lead to similar results whereby the decrease in viability did not exceed a maximum of 10 %. However, the amount of formazan produced decreased with prolonged exposure time (12-24 hours) and increasing concentration of matrix in both cell types with the Caco-2 cell line appearing slightly more susceptible than HepG2 at concentration ≥ 1.0 % (w/v).

Figure 3.57 shows the viability of HepG2 and Caco-2 cells at 12 and 24 hours exposure to each of the matrices. Cells incubated for 24 hours with polymer samples containing eudragit had a somewhat decreased viability when compared with samples containing only PEO. However, the maximum cytotoxicity observed still did not exceed 15 %. Short incubation (10 min) with the cytotoxic reference chemical SDS led to an expected dose dependent decrease in viability, indicating that the chosen assay conditions were appropriate.

3.3.1.6.3 The lactate dehydrogenase (LDH) assay

The effect of the polymers on cell membrane integrity was studied using the LDH assay, which quantifies the released LDH protein content from damaged cells into the cell medium. Exposure of both cell lines to the polymer samples did not cause fatal damage to the cells plasma membrane. The level of LDH leakage from cells was very low compared to the maximum release control. Even after incubation for 24 hours with the highest matrix concentration of 1.25 % the majority of cells from both cell lines remained intact and only minimal LDH leakage was observed. Figure 3.58 shows results typical of those obtained including the standard error of mean (SEM).

The matrices containing eudragit were observed to provoke a slightly higher LDH release in both HepG2 and Caco-2 cell lines at concentrations ≥ 1.0 % (w/v) for both 12 and 24 h exposures. Overall, the Caco-2 cells appear slightly more susceptible to the exposure to the polymeric matrices.

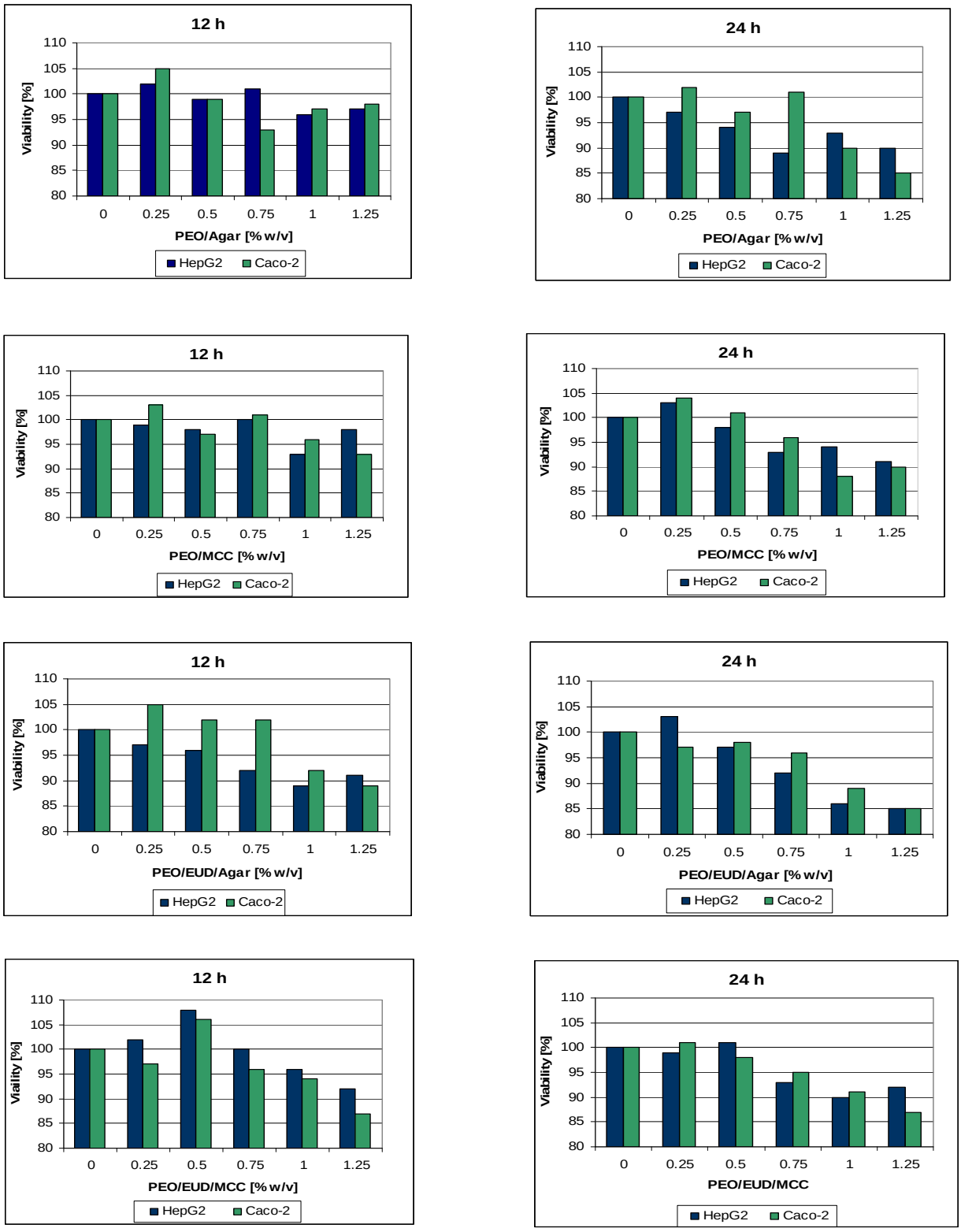

Figure 3.57 *Comparison of the effect of each polymer sample on the viability of HepG2 and Caco-2 cells at 12 and 24 hours exposure.*

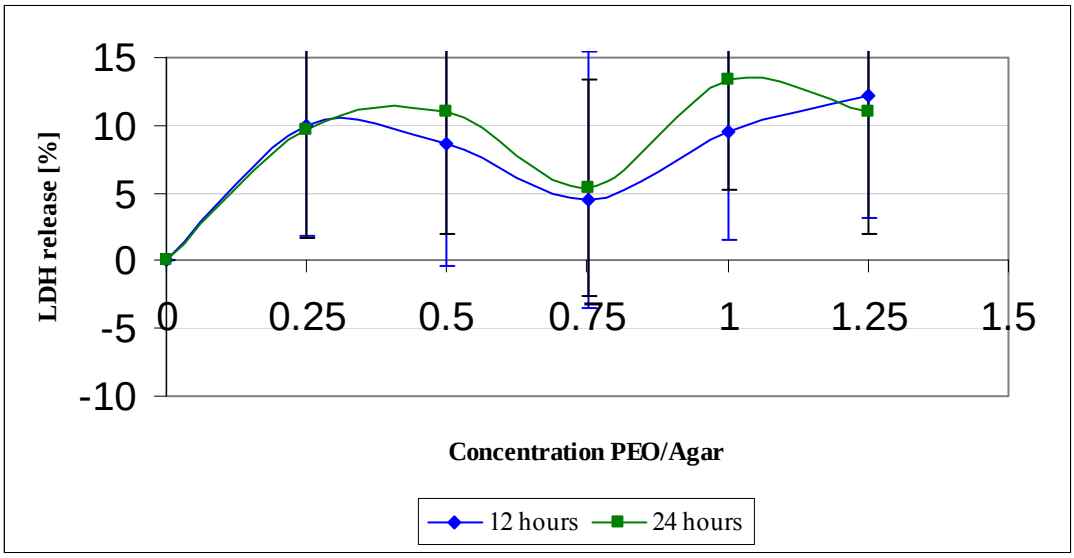

Figure 3.58 *LDH release [%] from CaCo2 cells after exposure to increasing concentrations of PEO/Agar for varying exposure times (± SEM).*

3.3.1.6.4 *In vitro* assessment of genotoxicity

Genetic toxicology test systems measure the outcome of damage or alteration to DNA, which is the basic blueprint for the transmission of hereditary information to daughter cells. The comet assay and the UDS assay were chosen because they measure different genotoxic endpoints, allowing for a broader assessment of the genotoxic potential of test samples to induce DNA strand breakage and DNA repair respectively as an index of damage. Due to its metabolic capabilities, which are an absolute requirement for *in vitro* genotoxicity testing, the HepG2 cell line was utilised in this study (Dierickx, 1989).

3.3.1.6.5 The single cell gel electrophoresis (SCGE) or 'Comet' assay

Comet tail moment is defined as the product of the tail length and fraction of total DNA in the tail. This parameter is considered to be one of the best indices of DNA damage as it takes in to consideration both the extent and amount of DNA migration from damaged cells (Fairbairn *et al*. 1995). The mean value of the tail moment of two independent experiments was used as an index to express cell damage.

Images of 40 randomly selected cells were analysed for tail moment for each concentration of matrix, using image analysis software and fluorescence microscopy as shown in Figure 3.59.

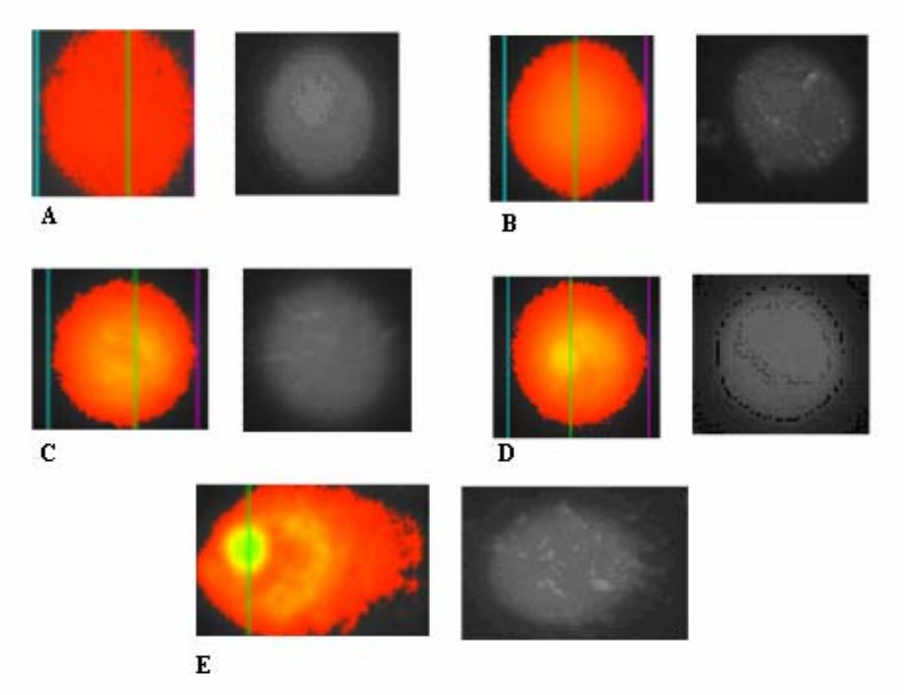

Figure 3.59 *Pseudo/non-pseudo coloured images of HepG2 cells captured via a fluorescence microscope attached to CCD camera and the Comet IV image analysis system. Visualised cells were exposed to highest concentration [1.25 % w/w] of (A) PEO/Agar (B) PEO/MCC (C) PEO/EUD/Agar (D) PEO/EUD/MCC and (E) H_2O_2 [50 µM].*

Over the concentration ranges tested in this study (1.25–0.25 % w/v) none of the formulations appeared to have caused a significant degree of damage at the genetic level as indicated by the extent of DNA migration in the comet assay. The mean tail moment of each matrix at the observed concentration range was in the same range as the untreated control in the interval ≤1. In order to establish that the comet assay conditions were optimum for detection of DNA damage (strand breaks), a dose range of the positive control chemical hydrogen peroxide (H_2O_2) was used.

The purpose of the positive control was to assure that the assay conditions were correct and accurate. The distribution of percentage tail moment parameters for the highest concentration of tested polymers, the untreated and the positive control are shown in Figure 3.60.

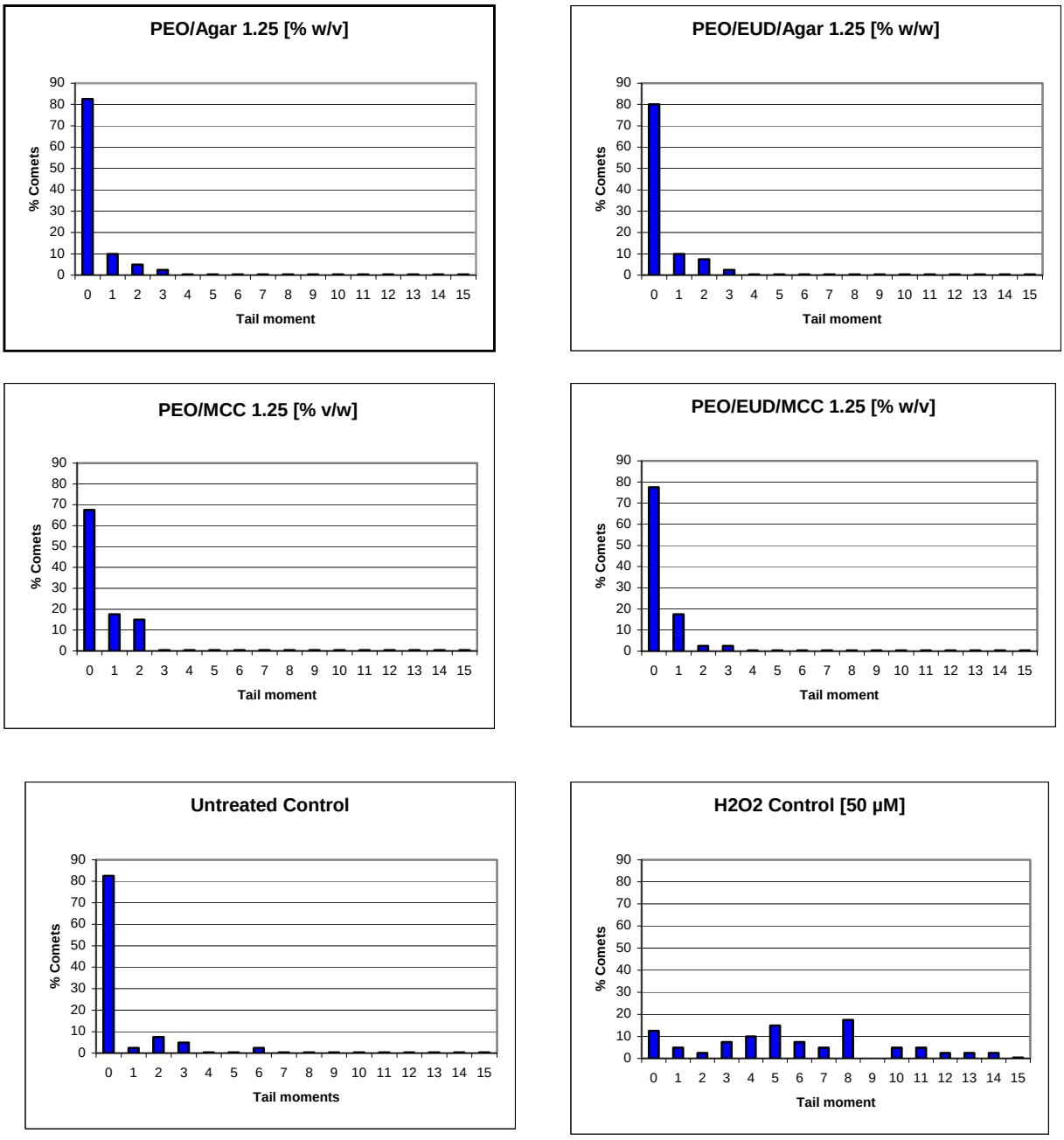

Figure 3.60 *The distribution of percentage tail moments after treatment with the highest concentration of polymer solutions (1.25 % v/w), untreated control, and positive control (H_2O_2 50 µM). Each histogram represents data analysed for 40 cells over 2 independent experiments.*

High percentage comets remain within the undamaged cell tail moment categories for both untreated and polymer exposed cells. Conversely, higher percentage comets distributed to higher tail moment categories were obtained for H_2O_2 treated cells.

3.3.1.6.6 The Unscheduled DNA Synthesis (UDS) assay

The UDS assay was performed to measure DNA repair as an index of DNA damage after exposure to the various matrices via the incorporation of BrdU into cellular DNA which was visualised qualitatively by an immunofluorescence assay.

Figure 3.61 shows images of fluorescence emitting cells as observed in the UDS assay. Cells emitting a low degree of fluorescence due to a smaller number of labelled DNA bases present throughout the cell body, were considered to have undergone UDS as a result of spontaneously induced DNA damage.

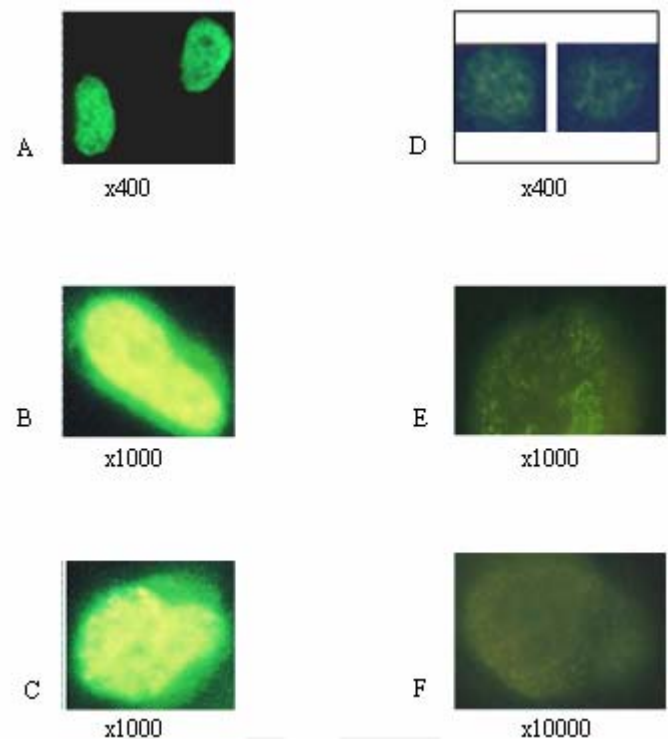

Figure 3.61 *Typical HepG2 cell images obtained with the BrdU labelling and detection kit at two different magnifications (x400 and x1000). Heavy labelled cells (A-C) were considered to have undergone normal DNA replication. Cell images (D-E) express low immunofluorescence labelling which may be a result of operating UDS.*

Cells emitting a high degree of fluorescence were considered to have undergone semi-conservative DNA replication due to passing the S-phase of the cell cycle. The cell synchronisation method appeared to be effective, although loss of viability was observed as a side effect from the prolonged serum deprivation. As observed via microscopy the main part of the pre-treated (Hydroxyurea and serum deprivation) cell populations was arrested

in early S-phase and only a small number of cells emitting high levels of fluorescence were observed.

Cell populations treated with increasing concentrations of polymeric solutions did not lead to an increase in the amount of weak labelled cells compared to control samples thus not indicating the presence of induced UDS. An elevated level of cells emitting low fluorescence was only observed via the exposure to the highest concentration [500 μM] of the positive control H_2O_2 which may be an indicator for the presence of induced UDS.

The observed fluorescence intensity of the cells treated with matrix solutions appeared to be similar for each individual concentration to the synchronised control cells. Therefore, the very small amount of cells undergoing UDS was considered negligible.

3.3.1.6.7 Summary

The use of agar as a novel filler substance for hot melt extruded dosage forms was investigated and compared to the commonly used pharmaceutical excipient microcrystalline cellulose. It was found that the presence of the agar filler in the matrix material led to an increase in the viscosity of the matrix material, thus affecting the hot melt extrusion process. This viscosity increase was confirmed by steady state rheometry analysis. The rheometry analysis also confirmed that the increase in matrix viscosity was a direct result of percentage inclusion of filler. However, the increase in viscosity was not so substantial as to rule out the use of agar as a filler material in hot melt produced dosage forms. It would, however, limit the amount of agar filler that could be used in the dosage form under normal processing conditions. Dissolution studies carried out on the dosage forms produced showed that the agar filler slowed down the release of the pharmaceutical agent in an acidic environment. The extent of the increase in dissolution time increased in proportion to the amount of filler present in the matrix. This effect could be of use for extended release dosage forms. The cytotoxic and genotoxic tests showed that cells treated with each of the matrices showed high viability rates with little DNA damage indicating, that the matrices maybe safe for use in the body. The agar filler system explored in this section proved to be a viable alternative to microcrystalline cellulose as a filler system in hot melt extruded dosage forms.

Since the agar and MCC filler systems investigated in this system were only effective at high loading levels, it was deemed prudent to investigate filler systems that may be viable at lower loading levels.

3.3.2 The incorporation of an organically modified layered silicate in monolithic matrices produced using hot melt extrusion

3.3.2.1 Introduction

In recent years, the use of inorganic nanoparticles as additives to enhance the performance of polymers in many applications has been investigated (Alexandre and Dubois, 2000; Oya *et al*. 2000; Mohanty *et al*. 2001; Pandey *et al*. 2005). Various nanoreinforcements currently being developed include layered silicates [nanoclays] (Giannelis, 1996; Giannelis *et al*. 1999; LeBaron *et al*. 1999; Sinha and Biswas, 2001; Sinha and Okamoto, 2003) ultra fine layered titanate (Hiroi *et al*. 2004), cellulose nanowhiskers (Mohanty *et al*. 2003), and carbon nanotubes (Mitchell *et al*. 2002; Potschke *et al*. 2003; Andrews and Wisenberger; 2004). Nanocomposites of polymer and organically modified layered silicate (OMLS) are of particular interest. This combination has exhibited remarkably improved properties when compared to pure polymers or conventional composites (Okamoto, 2004). These improvements can include increased mechanical properties (Gianneilis, 1998; Alexandre and Dubois, 2000), decreased gas permeability (Yano *et al*. 1993), decreased flammability (Gilman, 1999) and decreased biodegradability of biodegradable polymers (Sinha *et al.* 2002). The main reason for these improved properties in polymer/layered silicate nanocomposites is the strong interfacial interactions between matrix and OMLS as opposed to conventional composites (Chen *et al.* 2002).

Layered silicates generally have layer thickness in the order of 1 nm and very high aspect ratios (e.g. 10–1000). A few weight percent of OMLS that are properly dispersed throughout the matrix create a much higher surface area for polymer filler interactions than conventional composites. Early attempts at preparing polymer / clay composites are described in the patent literature (National Lead C o., 1950; Union Oil Co., 1963). These attempts at clay incorporation proved unsuccessful due to the failure to achieve sufficient dispersion of clay particles in the polymer matrix.

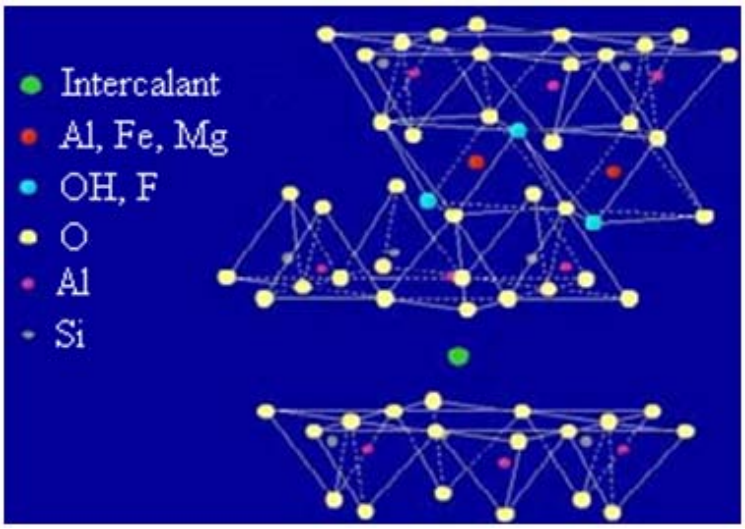

Figure 3.62 *Representation of the structure of montmorillonite. The basic structural unit is a layer consisting of two inward-pointing tetrahedral sheets with a central alumina octahedral sheet.*

The melt intercalation method has become a commonly used technique for preparation of polymer / OMLS nanocomposites in order to optimise interaction and dispersion. One of earliest systems studied by this method has been poly(ethylene oxide) with layered silicates, such as montmorillonite (MMT) (Kraweic *et al*. 1995; Vaia *et al.* 1995). This method involves the blending of OMLS and molten polymer statically or under shear. During the melt intercalation process, the polymer chains diffuse from the bulk polymer melt into the galleries between the silicate layers (Vaia and Giannelis, 1997). The major advantage of the melt intercalation process is that it is fully compatible with current industrial plastics processing techniques such as hot melt extrusion.

In this work, the use of an organically modified layered silicate as a novel filler material in hot melt extruded dosage forms was investigated. Hot melt prepared matrices were used to examine the release rate of an active pharmaceutical ingredient when a natural montmorillonite modified with a ternary ammonium salt was incorporated as a filler material.

3.3.2.2 Processing observations

During the hot melt extrusion process, the values for the die head pressure and the extruder torque were recorded, in order to ascertain if the addition of the nanoclay to the

polymer had any effect on the polymer and API matrix during the extrusion process. The nanoclays used in this work were organically modified using onium ion modification. This forms a clay-chemical complex using an intercalant (surface treatment) containing an ammonium functional group. The groups modify the nanoclay surface by ionically bonding to it, converting the surface from a hydrophilic to an organophilic species (favouring the attraction of hydrocarbons or materials which are miscible in hydrocarbons).

During the twin screw extrusion process it is believed that the delamination and the dispersion of the nanoclay particles occurs via the following steps; the MMT particles shear apart giving tactoids or polymer intercalated MMT. Subsequently, intercalated MMT in stacks about 100-150nm high disperse when polymer enters the galleries of the clay pushing platelets apart which eventually allows the platelets to peel off the intercalated MMT stack. As can be seen in Figure 3.63, the addition of the nanoclay to the polymer / API matrix has little effect on the observed pressure at the extruder die or on the torque recorded on the extruder motor.

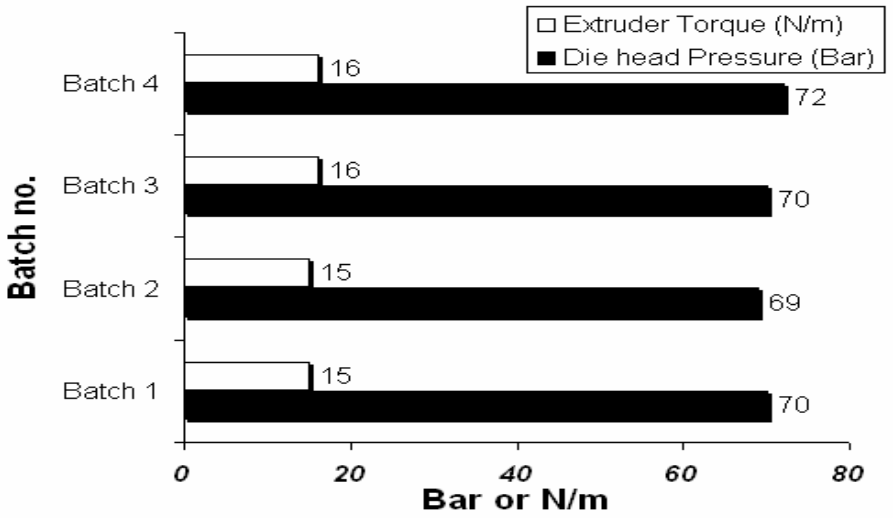

Batch name	*Polymer*	*OMLS (% by Weight)*	*API (% by Weight)*
Batch 1	*PEO (5 Million)*	-	*Carvedilol (14%)*
Batch 2	*PEO (5 Million)*	*Cloisite® 93A (2%)*	*Carvedilol (14%)*
Batch 3	*PEO (5 Million)*	*Cloisite® 93A (4%)*	*Carvedilol (14%)*
Batch 4	*PEO (5 Million)*	*Cloisite® 93A (6%)*	*Carvedilol (14%)*

Figure 3.63 *Die head pressure and extruder torque recorded during melt compounding.*

The minimal impact of the nanoclay particles on the extrusion process is to be expected due to the relatively low amount of nanoclay being incorporated into the polymer / API matrix. The results do indicate that should the inclusion of nanoclays prove beneficial to

the drug delivery matrix, their addition will have little effect on the throughput of the matrix for this process.

3.3.2.3 Thermal analysis

Modulated differential scanning calorimetry was used to ascertain if the inclusion of the API (carvedilol) or the nanoclay particles had any effect on the thermal characteristics of the matrix material. Figure 3.64 shows a typical MDSC scan obtained. The MDSC scans obtained showed a small drop (63.06°C to 59.98°C) in the T_m of the PEO based matrix upon inclusion of the API, indicating that the carvedilol is acting as a plasticiser in the polymer matrix. Thus confirming the observations made during the hot melt processing of the samples. The plasticisation effects of API molecules on the polymer melt during processing have been reported in the literature (Ozeki *et al*. 1997) and have been described extensively throughout this body of work.

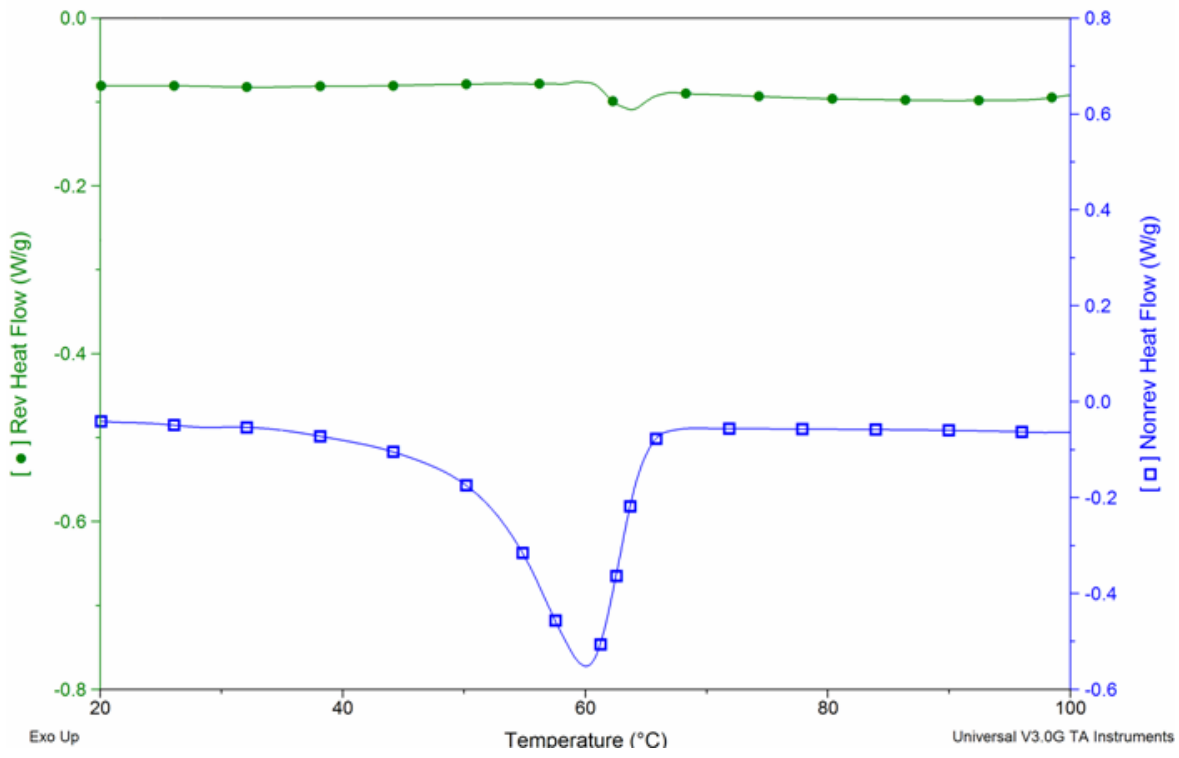

Figure 3.64 *Modulated differential calorimetry scan for batch 2 (PEO Mw 5 million with 2%wt OMLS and 14% API) showing both the reversing heat flow and non-reversing heat flow signals.*

The inclusion of the nanoclay filler material at these low loading levels has a negligible effect on the melting behaviour of the matrix. Despite the minimal impact of the nanoclay particles on the T_m of the matrix, reports from the literature suggest that nanoclay incorporation increases both the heat distortion temperature (HDT) (Sinha *et al.* 2003) and the thermal stability (Chang *et al*. 2003) of polymer matrices.

3.3.2.4 Steady state rheometry

Steady state rheometry was carried out on the batches outlined in Table 2.10. The results are shown in Figure 3.65 in the form of a graph of viscosity versus shear rate. The incorporation of nanoclay particles does not result in a pronounced effect on the melt viscosity of the polymer. However it can be seen that as the shear rate is increased, batch 4 which contains the maximum amount of nanoclay incorporated in this trial (6%) shows more pronounced shear-thinning behaviour than the virgin polymer. This is consistent with findings by Sinha Ray and Bousmina (2005), who observed that with increasing shear rate, nanocomposites exhibit higher degrees of shear-thinning behaviour compared to the pure polymer.

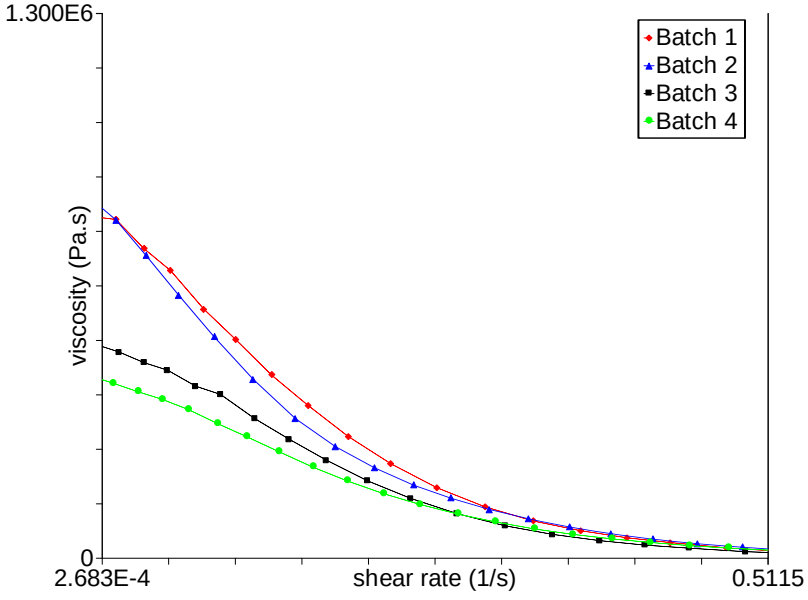

Batch name	*Polymer*	*OMLS (% by Weight)*	*API (% by Weight)*
Batch 1	*PEO (5 Million)*	-	*Carvedilol (14%)*
Batch 2	*PEO (5 Million)*	*Cloisite® 93A (2%)*	*Carvedilol (14%)*
Batch 3	*PEO (5 Million)*	*Cloisite® 93A (4%)*	*Carvedilol (14%)*
Batch 4	*PEO (5 Million)*	*Cloisite® 93A (6%)*	*Carvedilol (14%)*

Figure 3.65 *Steady state rheometry results for the batches under investigation.*

Similar behaviour was also observed by Krishnamoorti and Giannelis (1997) in the case of exfoliated PCL-based nanocomposites with several silicate loadings. In further work Krishnamoorti *et al*. (2001) observed that the steady shear viscosities for the nanocomposites exhibited enhanced shear-thinning behaviour at low shear rates. Although the exact mechanism which causes the shear-thinning behaviour remains unclear, it is believed that the orientation of the silicate layers under shear is the main cause (Sinha Ray and Bousmina, 2005). With increasing shear rate, the intercalated polymer chain conformations change as the coils align parallel to the flow (Krishnamoorti *et al*. 1996). However the shear thinning behaviour is not pronounced at the loadings examined herein, and the effect of the nanoclay inclusion on the polymer matrix would appear to be minimal, an observation verified by the readings for torque and die head pressure recorded during the hot melt extrusion process step.

3.3.2.5 Mechanical analysis

As can be seen from Figures 3.66 and 3.67 there is an increase in all of the mechanical properties of the polymer / API matrix upon addition of the nanoclay particles.

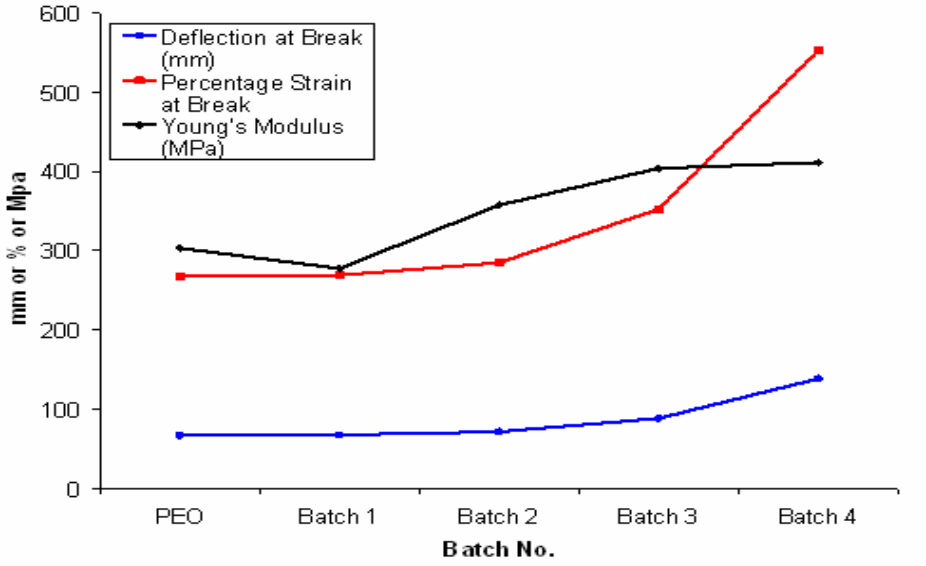

Batch name	*Polymer*	*OMLS (% by Weight)*	*API (% by Weight)*
PEO	*PEO (5 Million)*	-	-
Batch 1	*PEO (5 Million)*	-	*Carvedilol (14%)*
Batch 2	*PEO (5 Million)*	*Cloisite® 93A (2%)*	*Carvedilol (14%)*
Batch 3	*PEO (5 Million)*	*Cloisite® 93A (4%)*	*Carvedilol (14%)*
Batch 4	*PEO (5 Million)*	*Cloisite® 93A (6%)*	*Carvedilol (14%)*

Figure 3.66 *Selected mechanical data for the batches under investigation.*

The increase is observed to become more pronounced as the percentage inclusion of nanoclay increases. These observations appear to be in line with several reports throughout the literature (Lee *et al*. 2003; Sinha Ray and Okamoto, 2003; Chang *et al.* 2006). The enhancement of the Young's modulus for such extremely low clay concentrations cannot be attributed simply to the introduction of the high modulus inorganic filler layers. A theoretical explanation is to assume the existence of a layer of affected polymer on the filler surface, with a much higher modulus than the bulk polymer (Shia *et al*. 1998). This affected polymer can be thought of as the region of the polymer matrix that is physabsorbed on the silicate surface and is thus stiffened through its affinity for and adhesion to the filler surfaces. Thus, for high aspect ratio fillers such as those used in this work, the surface area exposed to the polymer is very large and the significant increases in the modulus with very low filler content are unsurprising.

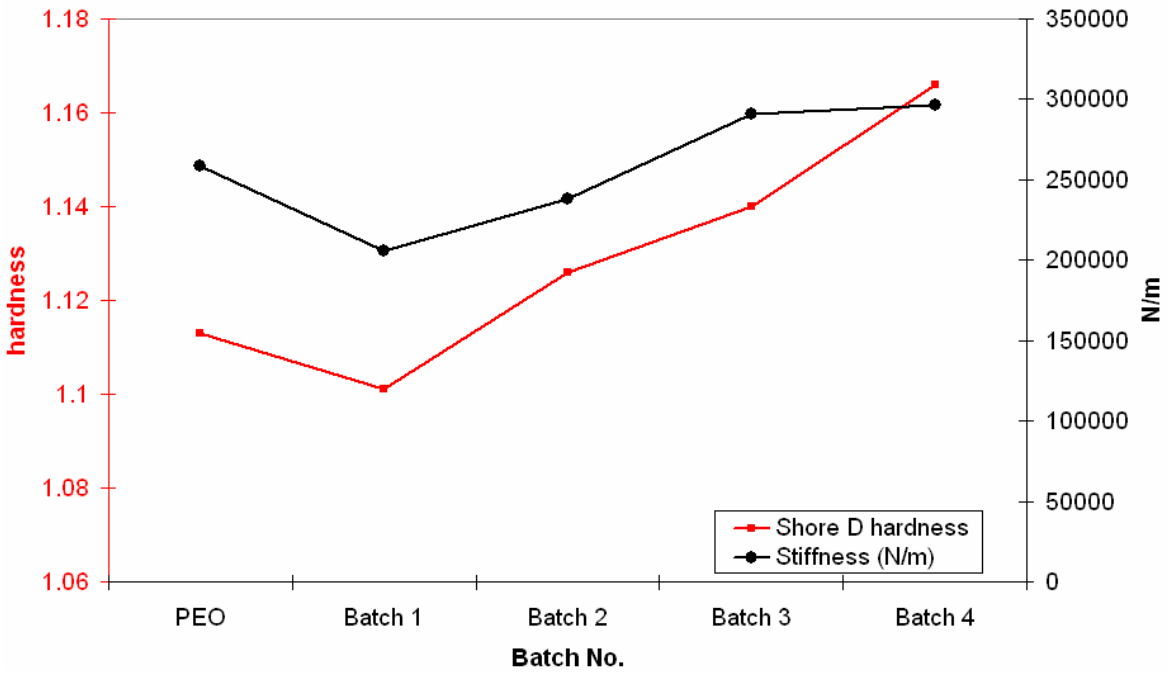

Batch name	*Polymer*	*OMLS (% by Weight)*	*API (% by Weight)*
PEO	*PEO (5 Million)*	-	-
Batch 1	*PEO (5 Million)*	-	*Carvedilol (14%)*
Batch 2	*PEO (5 Million)*	*Cloisite® 93A (2%)*	*Carvedilol (14%)*
Batch 3	*PEO (5 Million)*	*Cloisite® 93A (4%)*	*Carvedilol (14%)*
Batch 4	*PEO (5 Million)*	*Cloisite® 93A (6%)*	*Carvedilol (14%)*

Figure 3.67 *Further mechanical data for the batches under investigation.*

3.3.2.6 Surface analysis (AFM)

Topographic images of batches 1 and 4 are displayed in Figures 3.68 & 3.69 respectively. As can be seen from the images, the nanoclay incorporation has a negligible effect on the surface of the polymer / API matrix.

In order to ascertain the dispersion of the nanoclay particles in the matrix, lateral force microscopy was also carried out. Lateral force microscopy (LFM), also sometimes referred to as "frictional force microscopy," is essentially a derivative of standard contact mode AFM scanning. As the probe tip is scanned across the sample surface, the friction between tip and sample causes the cantilever to flex laterally. This flexing, or torsion, can be detected by a quadrant of the standard photodetector.

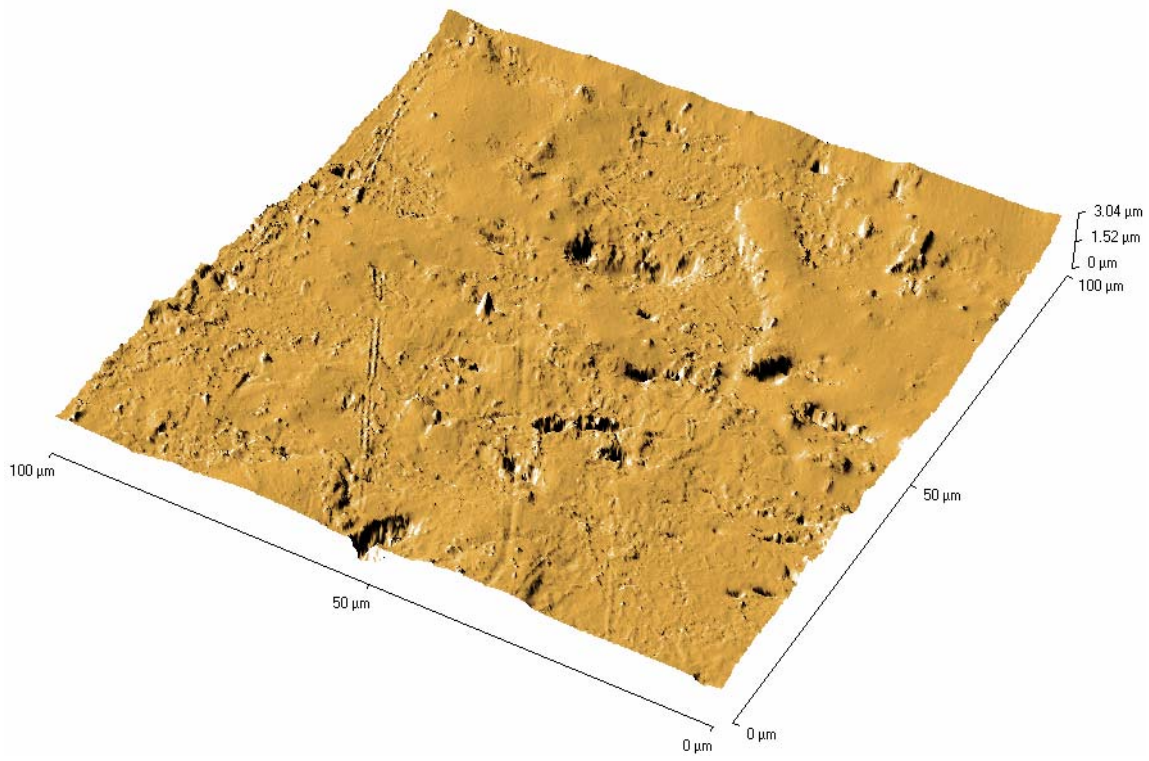

Figure 3.68 *Topographic image of batch 1(PEO Mw 5 million and 14%wt carvedilol).*

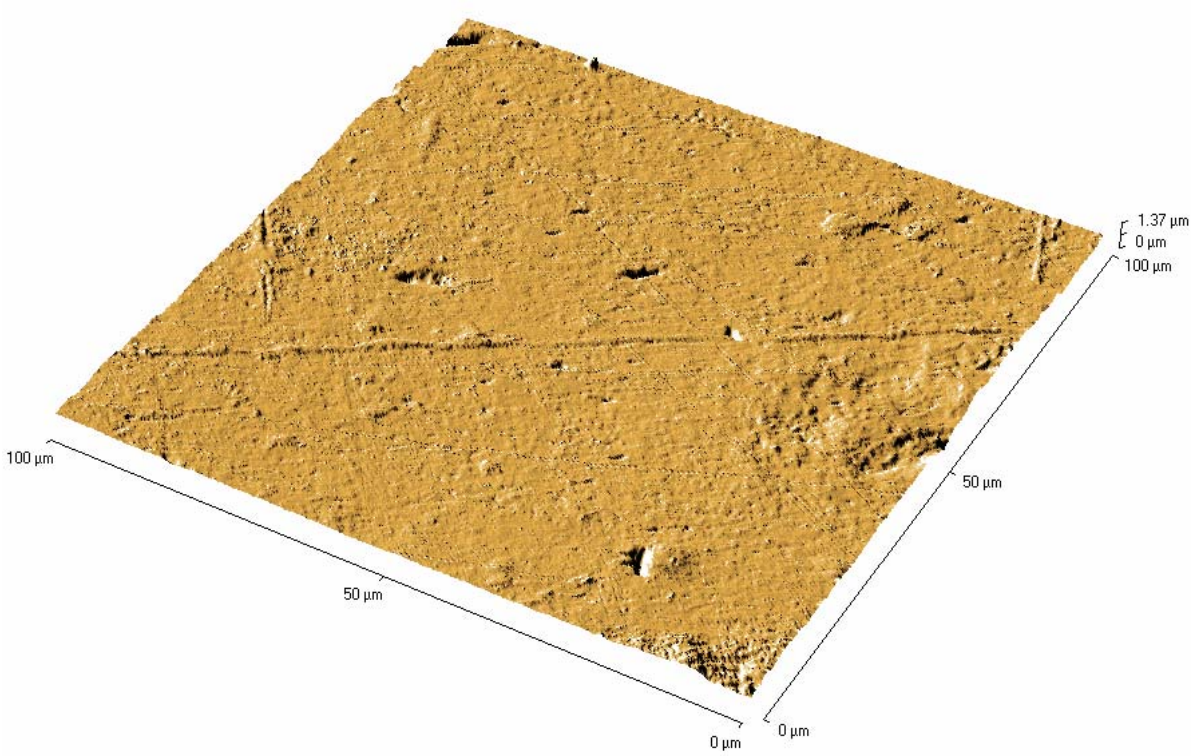

Figure 3.69 *Topographic image of batch 4 (PEO Mw 5 million, 6%wt Cloisite 93 A and 14%wt carvedilol)*

Lateral force scanning can accurately detect the boundaries between different materials where the topographic change between the materials is minimal. Lateral force data reveals little topography when compared with standard SPM modes, but because the tip does sense lateral forces due to friction caused by features, some topography is contained in the lateral force signal.

The amount of topographic information in the lateral force images obtained during this work was minimised by summing the lateral force image acquired when scanning in the forward direction, with the lateral force image acquired in the reverse scan. The direct output of the photodetector corresponding to the torsional movement of the cantilever, in units of nA, is the photo-induced current which was directly used to construct the lateral force image. Lateral force images for batches 1 and 4 are shown in Figures 3.70 & 3.71 respectively.

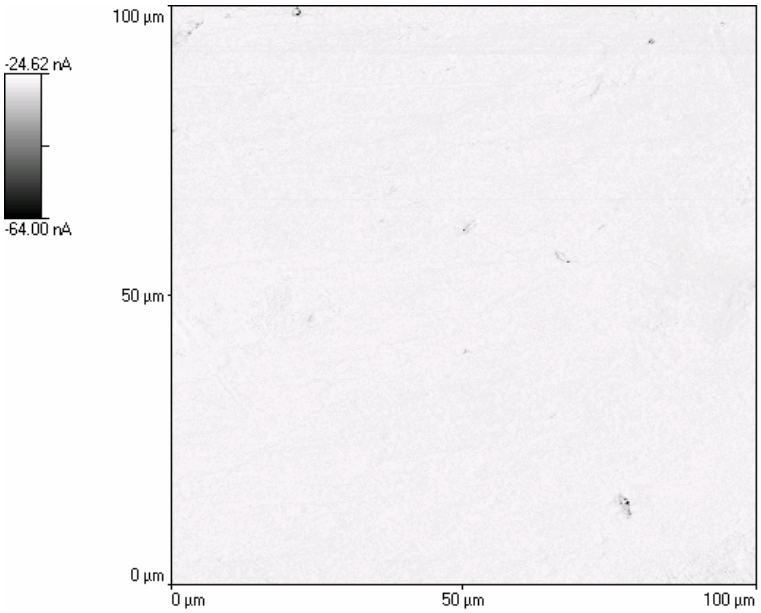

Figure 3.70 *Lateral force image of batch 1(PEO Mw 5 million and 14%wt carvedilol).*

As can be seen from the lateral force images of batches 1 & 4, the inclusion of the nanoclay particles can be clearly seen. The nanoclay particles are displayed as the darker regions (regions with lower torsional forces) in the lateral force image displayed in Figure 3.71.

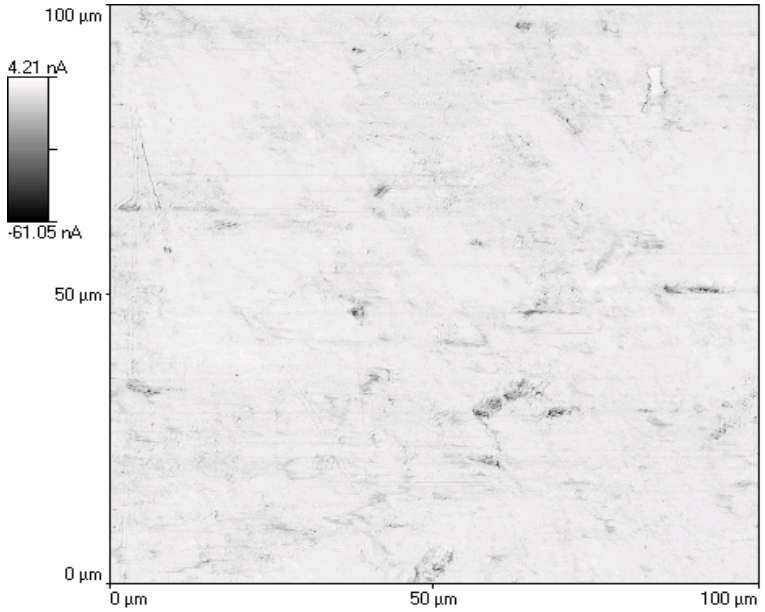

Figure 3.71 *Lateral force image of batch 4 (PEO Mw 5 million, 6%wt Cloisite 93 A and 14%wt carvedilol).*

The image obtained for batch 4 suggests that the melt extrusion has not fully exfoliated the nanoclay particles. The size of the darker regions in Figure 3.70 would appear to be too large for fully exfoliated nanoclay particles. However, the size of the darker images would appear to suggest the melt extrusion has had the effect of intercalating the nanoclay particles with polymer chains. This would seem to agree with the other results obtained in this work, which show an improvement in the mechanical properties of the polymer matrix once the nanoclay particles have been included. As full exfoliation of the nanoclay particles requires extended residence time in the extruder to occur, it is probable that the reduced screw speed employed in this work was only sufficient to allow intercalation to occur. As the Prism™ twin screw extruder employed in this work is of relatively small L/D, it is possible that use of an extruder with a larger L/D would allow full exfoliation to occur.

3.3.2.7 Drug release

PEO has been shown to be useful for modulating the release of active agents in monolithic devices for sustained drug delivery. The release profile depicted in Figure 3.72 was observed for the batches under investigation in this work. The release rate of the active agent, in pH 1.2, decreases as the percentage inclusion of nanoclay increases. It is probable that the mechanism responsible for the decrease in the release rate of the active agent from nanoclay containing matrices is similar to the mechanism by which nanoclays increase the gas barrier properties in conventional nanocomposites. Given the observed trend, it is likely that the nanoclay particles are creating a maze or "tortuous path" as illustrated in Figure 3.73, retarding the ingress of buffer molecules through the matrix material.

It is also likely that the reduction in the release rate of the API in the batches containing nanoclay is related to changes in the local permeability due to the molecular level of transformation in the polymer matrix in the presence of silicate layers. This factor is directly related to the molecular level interaction of polymer matrix with the silicate layers.

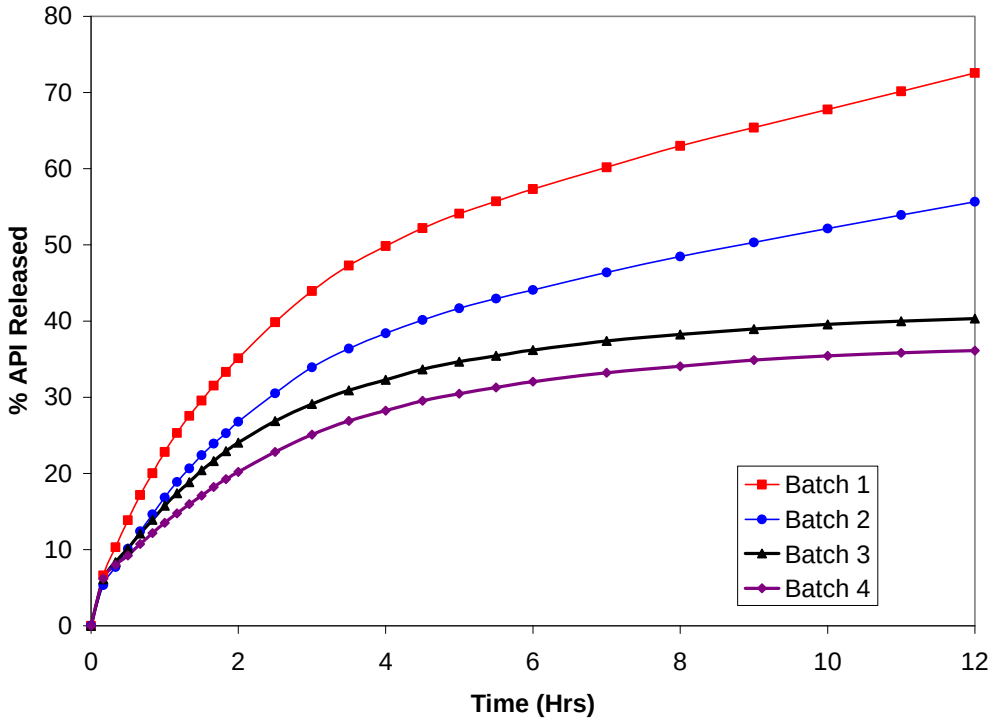

Batch name	*Polymer*	*OMLS (% by Weight)*	*API (% by Weight)*
Batch 1	*PEO (5 Million)*	-	*Carvedilol (14%)*
Batch 2	*PEO (5 Million)*	*Cloisite® 93A (2%)*	*Carvedilol (14%)*
Batch 3	*PEO (5 Million)*	*Cloisite® 93A (4%)*	*Carvedilol (14%)*
Batch 4	*PEO (5 Million)*	*Cloisite® 93A (6%)*	*Carvedilol (14%)*

Figure 3.72 *Dissolution results for the batches under investigation.*

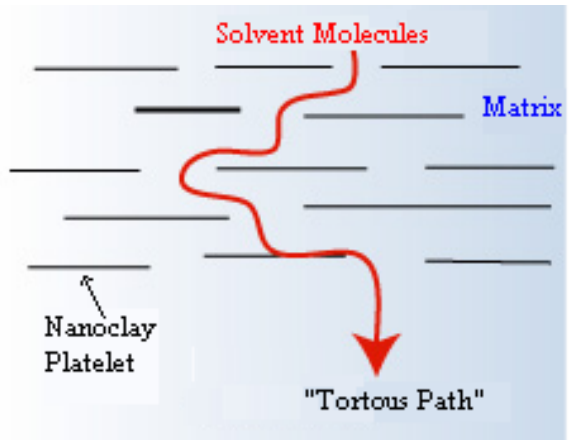

Figure 3.73 *Illustration of the "tortuous path" created by nanoclays in the polymer matrix.*

However it is also possible that some interaction between the API molecule and the nanoclay filler is occurring in the matrix. There are numerous mechanisms that may be involved in the interaction between clay minerals and organic molecules. The predominant mechanism depends largely on the specific clay mineral involved (Browne *et al*. 1980), in this case montmorillonite, as well as on the functional groups (Lagaly, 2001) and the physical chemical properties (Tolls, 2001) of the API. Early studies by Carstensen and Kenneth, (1971) and Kenneth and Carstensen, (1972) investigated bonding via adsorption and ion–dipole interactions between acidic and non-ionised molecules and montmorillonite. A study on the interaction between montmorillonite and four alkaloids carried out by Wai and Banker (1966) found differences in the bonding mechanisms depending on molecule size and basicity. In some cases drug molecules were quantitatively bound to the clay mineral via cation exchange. Other mechanisms were believed to be responsible for the adsorption of larger molecules and the fourth alkaloid, niacinamide, was not bound to the clay, because it mainly occurred in the neutral form. An investigation by McGinity and Lach (1976) confirmed that basic molecules bonded strongly to montmorillonite. However, complexes with anionic and non-ionic drugs were found to have much weaker bonds to the montmorillonite and more rapid desorption kinetics.

3.3.2.8 Summary

The work described in this section outlines the use of an organically modified layered silicate as a novel filler material in a hot melt extruded dosage form for oral drug delivery. It was confirmed by both steady state rheometry and by direct measurement of the torque on the extruder motor and pressure at the extruder die, that the level of inclusion of nanoclay examined herein did not have sufficient effect on the melt flow properties of the polymer / API matrix to negatively impact the hot melt preparation of the monolithic matrix. These results were in good agreement with MDSC measurements carried out on the matrices prepared using the nanoclay material at different levels of inclusion, which indicated that the presence of the nanoclay material did not have an effect on the melting behaviour of the polymer / API matrix. The mechanical properties of the polymer / API matrix were seen to improve upon addition of the nanoclay filler, the degree of the improvement in the mechanical properties was directly proportional to the percentage inclusion of nanoclay particles.

The presence of the nanoclay filler was shown to retard the release of the API from the monolithic matrix in an acidic buffer. It was proposed that the mechanism of retardation was similar to the mechanism by which nanoclay incorporation improves the gas barrier properties in conventional nanocomposites. The degree of retardation of the API release from the monolithic matrix was also observed to increase in direct proportion to the percentage inclusion of nanoclay. Lateral force AFM images indicate that the nanoclays were not fully exfoliated in the polymer / API matrix. It is believed that a twin screw extruder with a larger L/D ratio to the equipment used in this trial would more fully exfoliate the nanoclay particles in the polymer / API matrix. The work described herein indicates that nanoclay materials may be of use in the modulation of drug release from sustained release monolithic matrices produced using hot melt extrusion.

3.4 Moulding of monolithic matrices using conventional polymer processing technologies

3.4.1 Introduction

The ultimate goal of this project is to create a range of polymer based matrices capable of delivering an active agent in a controlled manner to sites along the GI tract. The compounding of carrier materials and API's within a conventional twin screw extruder has been previously discussed throughout this work and shown to be a viable method of creating drug delivery matrices. However, the strands of material used thus far in the drug release studies would be unsuitable for human consumption due to their size and shape distribution. A common problem with oral controlled delivery devices is making them easy to swallow. Capsules are a good shape for swallowing because the tongue automatically aligns them with the long axis pointing down the throat. For this section, experimental moulds were designed to allow monolithic matrices to be injection moulded using both a novel micro-moulding process and a bench-top vertical ram-type injection moulding process, into cylindrical shapes which could subsequently be loaded into capsules for oral drug delivery. In using capsules to deliver the dosage form to the stomach, no taste masking of the matrices was necessary. The use of capsules also affords the possibility of using two or more matrices in one dosage form, thus accommodating different release profiles of the

same API to be used in one dose (i.e. one burst release matrix and one sustained release matrix) or the use of matrices containing different active agents which need to be administered in tandem.

3.4.2 Processing observations

The four matrices used in this trial (Table 3.12) were compounded using twin screw extrusion. The four matrices were subsequently subjected to two separate moulding operations.

Table 3.12 *Batch composition of the monolithic matrices produced.*

Batch No.	Polymer	API (Diclofenac sodium)
1	80%wt EPO	20 (%wt)
2	80%wt 4155F	20 (%wt)
3	80%wt PEO (comprising 40%wt Mw 1 million + 30%wt Mw 900,000 + 30%wt Mw 100,000)	20 (%wt)
4	40%wt PEO(comprising 40%wt Mw 1 million + 30%wt Mw 900,000 + 30%wt Mw 100,000) + 40%wt PCL	20 (%wt)

3.4.2.1 Micro-moulding.

In the case of the Eudragit materials (EPO and preparation 4155) used to form pH sensitive matrices, no micro-moulding was possible. The materials exhibited extreme 'slip' behaviour (material not conveying properly along the screw) in the injection moulding equipment. Plasticising of the materials was difficult to achieve without the self wiping profile of the twin screw extruder. However, the main difficulty with the materials was when injection into the mould cavity was attempted. The material was observed to move back over the flights of the screw as the screw moved forward for injection. Material was also seen to adhere to the root diameter of the screw along the length of the barrel, as a result of this behaviour no injection phase was achieved. Various processing additives were used to counteract this behaviour such as silica (an anti-slip agent due to its thixotropic

properties) and talc, however no improvement in processability of the materials was observed. It is possible that the API, which has been noted throughout this work to act as a plasticiser during the extrusion process, is acting as a slip agent during the plasticising step. This would have a more profound effect on the Eudragit materials as they are of a lower molecular weight than the PEO matrix or the PEO / PCL blend matrix. It was postulated that a ram-type injection moulding approach may succeed where the screw-type injection moulding technique failed.

The PEO matrix was also difficult to process using the micro-moulding technology. The material was observed to have too high a viscosity for the moulding equipment used in this trial to be capable of plasticising and injecting the material into the mould. When using the highest possible motor and injection pressure settings, inconsistent injection into the mould was achieved. The material when moulded was seen to be tacky and 'gum' like, clogging the sprue and runner channels in the mould and solidifying before moulding of the desired parts was achieved. Furthermore, removal of the frozen sprue and runner system proved extremely difficult, with the moulded material tending to stick to the interior of the sprue and stretch when removal was attempted. Alteration of the process parameters was not seen to result in any improvement in the moulding operation and had the mould been moved to larger moulding equipment, with sufficient motor power with which to plasticise and inject the material, the dimensional accuracy of such equipment would not be high enough to produce suitable parts. No viable PEO matrices were formed from the micro-moulding process.

The PEO / PCL matrix blend was marginally easier to mould. The PCL present in the blend appeared to alter the viscosity of the material enough to allow the injection moulding equipment to process the matrix. However, the consistency of the material remained problematic in the mould. Removal of the sprue and runner system was difficult and labour intensive. PEO / PCL blend matrices were moulded successfully using the micro-moulding process, nonetheless, this technique would be extremely difficult to scale up to a production level. The micro moulded parts are displayed in Figure 3.74.

The micro-moulding process setup used to attempt to mould the matrices discussed herein was also used to mould traditional thermoplastic engineering materials, PE and HIPS, in order to ascertain if the moulding difficulties encountered were related to the

materials used or the process. In the case of these materials, PE and HIPS micro-moulded parts were successfully obtained, indicating that the process difficulties were purely material related.

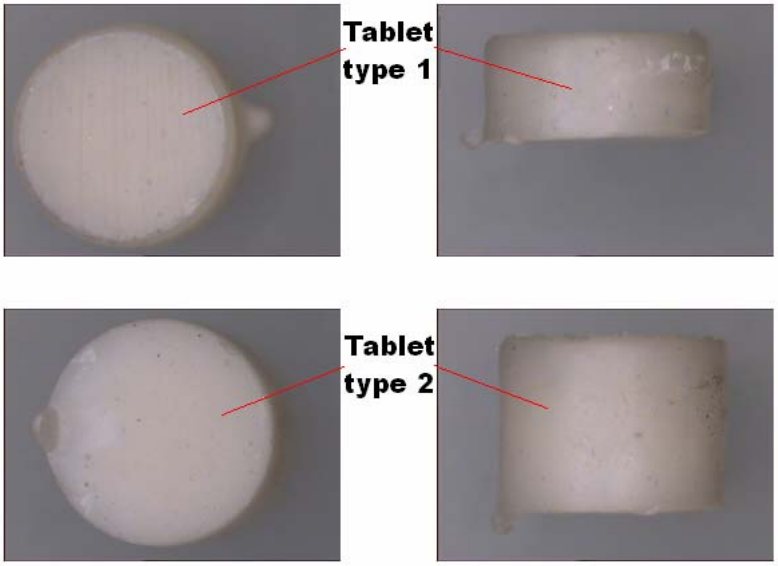

Figure 3.74 *Images of PEO / PCL blend micro-moulded matrices. The images on the top are a front and side view of tablet type 1 (height = 3mm, width =6.5mm) and the images on the bottom are a front and side view of tablet type 2 (height = 5mm, width = 6.5mm).*

3.4.2.2 Vertical ram-type injection moulding

All four matrices were moulded successfully using the bench-top vertical ram-type injection moulding equipment. The ram injection equipment proved far superior for the processing of both of the Eudragit materials with no plasticising phenomena noted when compared with observations made during the screw plasticising step in the micro-moulding process. However, both the PEO matrix and the PEO / PCL matrices were again observed to cause blockage of the sprue and runner system in this mould, despite both components being considerably shorter than their counterparts in the micro-mould. Matrices obtained using the vertical ram-type injection moulding technique did not have the same high degree of dimensional accuracy and reproducibility as matrices moulded using the micro-moulding system. Moulded matrices typical of those obtained using this technique are displayed in Figure 3.75.

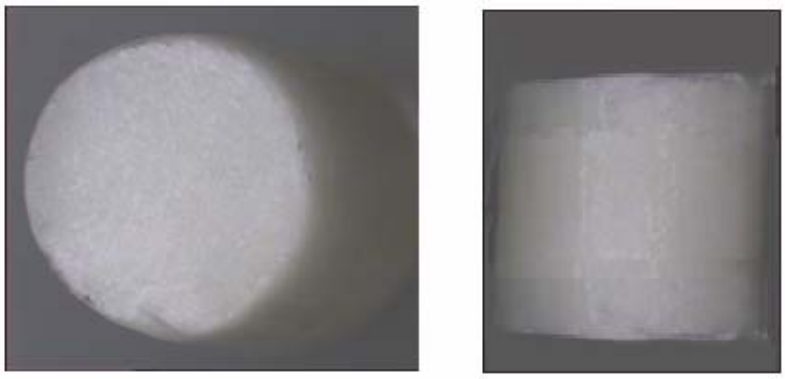

Figure 3.75 *Images of PEO / PCL blend matrices. The images are a front and side view of a matrix produced using the vertical ram-type injection moulding system (height = 9mm, width = 3.55mm).*

3.4.3 Steady state rheometry

Rheological analysis of the compounded batches confirms the observations made during the micro-moulding of the matrices. The viscosity curves presented in Figure 3.76 show that the PEO matrix is much more viscous than either of the Eudragit materials.

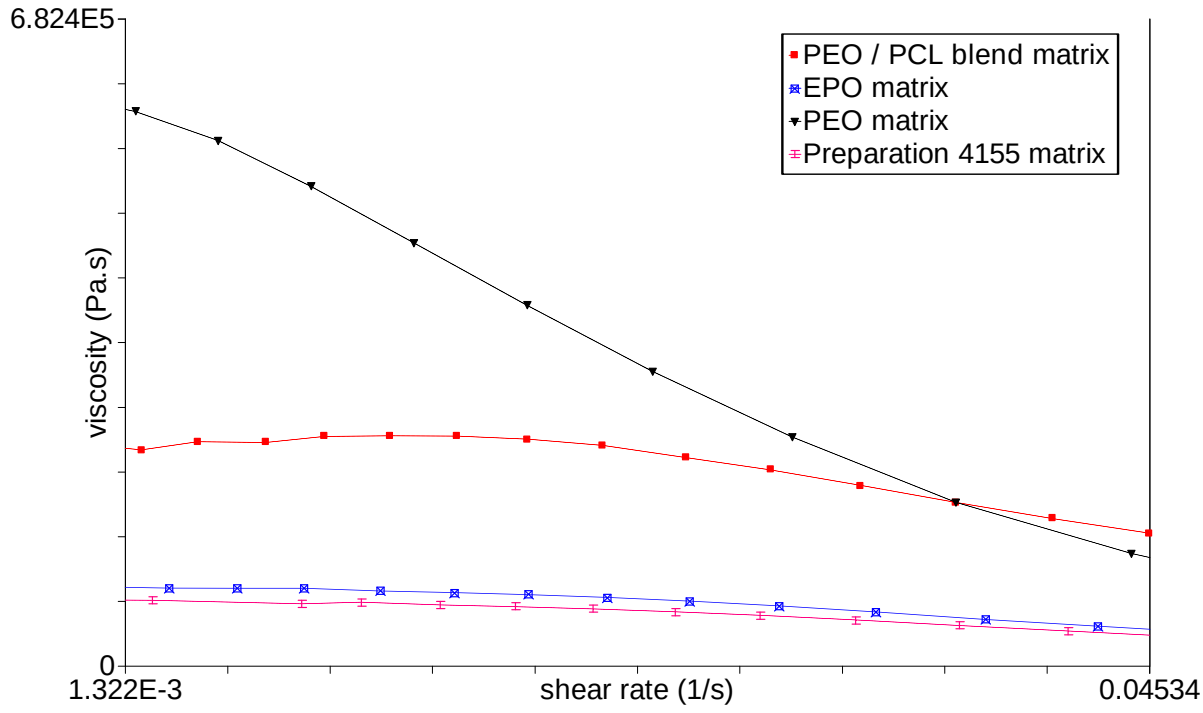

Figure 3.76 *Steady state data for the materials used in the moulding trials.*

The viscosity curves also demonstrate the reduction in viscosity when PCL is blended with PEO. This was also noted in sections 3.2.1.2 and 3.2.1.4.

3.4.4 Surface analysis

The PEO / PCL blend was analysed using AFM. The blend was analysed in each of the manufactured forms, i.e. extrudate, ram-type moulded sample, micro-moulded sample 1 and micro-moulded sample 2. The resultant topographical scans are presented in Figures 3.77, 3.78, 3.79 and 3.80.

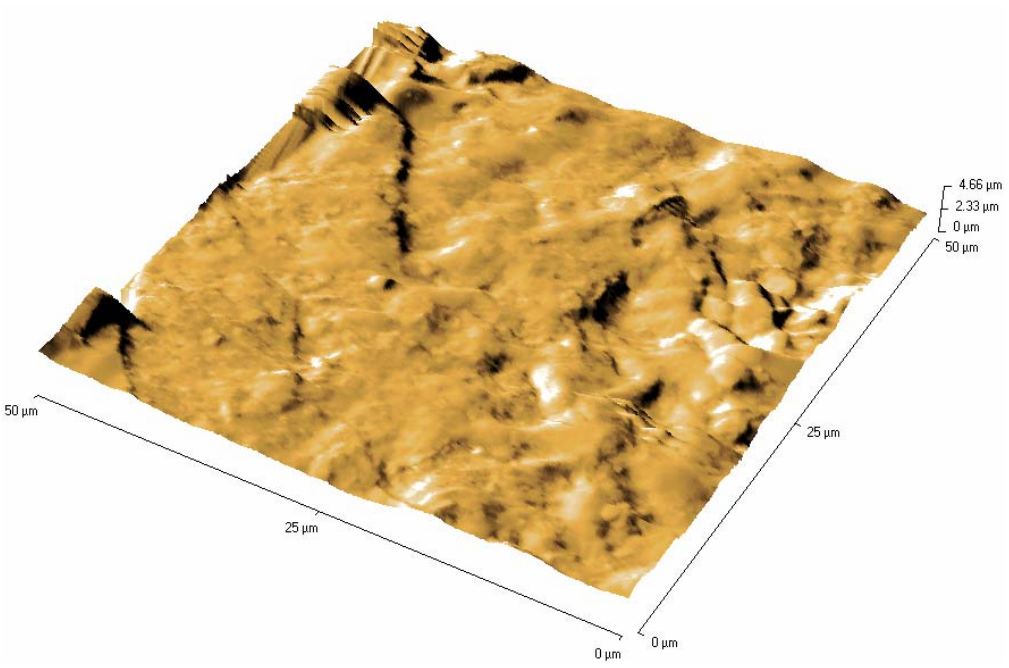

Figure 3.77 *Topographical image of PEO / PCL blend extrudate.*

Each of the topographical areas were also analysed for roughness, the results of which are detailed in Table 3.13.

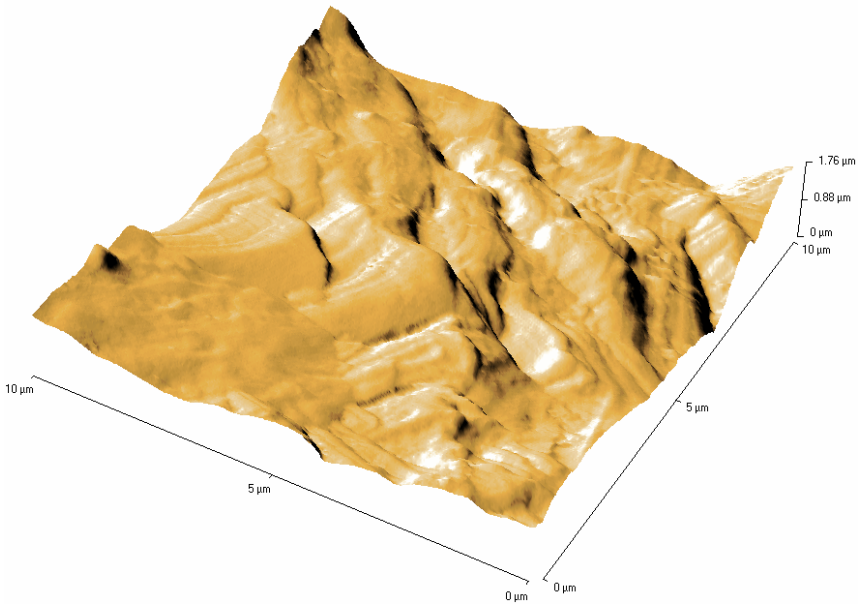

Figure 3.78 *Topographical image of PEO / PCL blend ram-type moulded sample.*

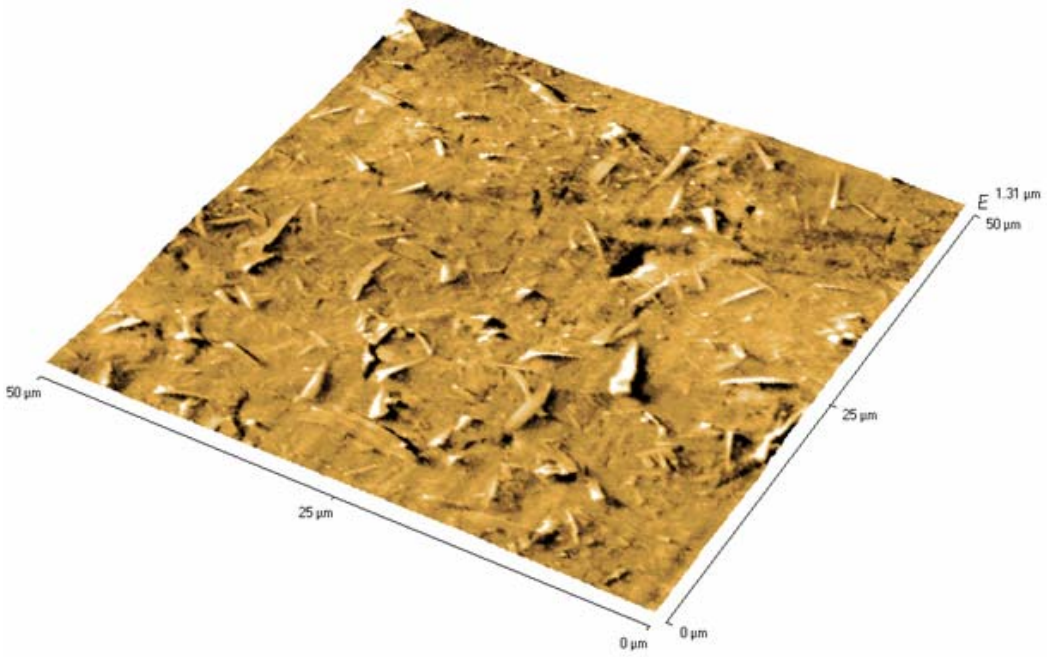

Figure 3.79 *Topographical image of PEO / PCL blend micro-moulded tablet type 1.*

Table 3.13 *Calculated roughness values for topographical images.*

Surface	Area R_a (nm)	Area RMS (nm)	Average height (nm)	Maximum range (nm)
Extrudate	293.3410	391.1184	2625.2053	4657.2540
Ram-Type moulded sample	174.1947	224.8062	877.5261	1763.5590
Micro-moulded tablet type 1	60.6211	88.7572	628.8189	1174.4040
Micro-moulded tablet type 2	73.0296	102.0727	661.3703	1310.4630

Where:	
R_a =	Roughness average: the arithmetic average of the absolute values of the measured profile height deviations.
Area RMS =	Root-mean-square roughness: value is defined as the square root of the mean value of the squares of the distance of the points from the image mean value.
Average Height =	An arithmetic mean defined as the sum of all height values divided by the number of data points.
Maximum Range =	Maximum peak-to-valley range in the area.

The AFM scans obtained reinforce the visual observations made during processing. The extrudate is too rough and uneven to be used as a dosage form without further processing operations. The ram-type injection moulded sample is much smoother than the extrudate but has a much rougher texture to either of the micro-moulded samples, as the bench-top equipment used to produce these samples is not capable of the same level of dimensional accuracy as the micro-moulding apparatus.

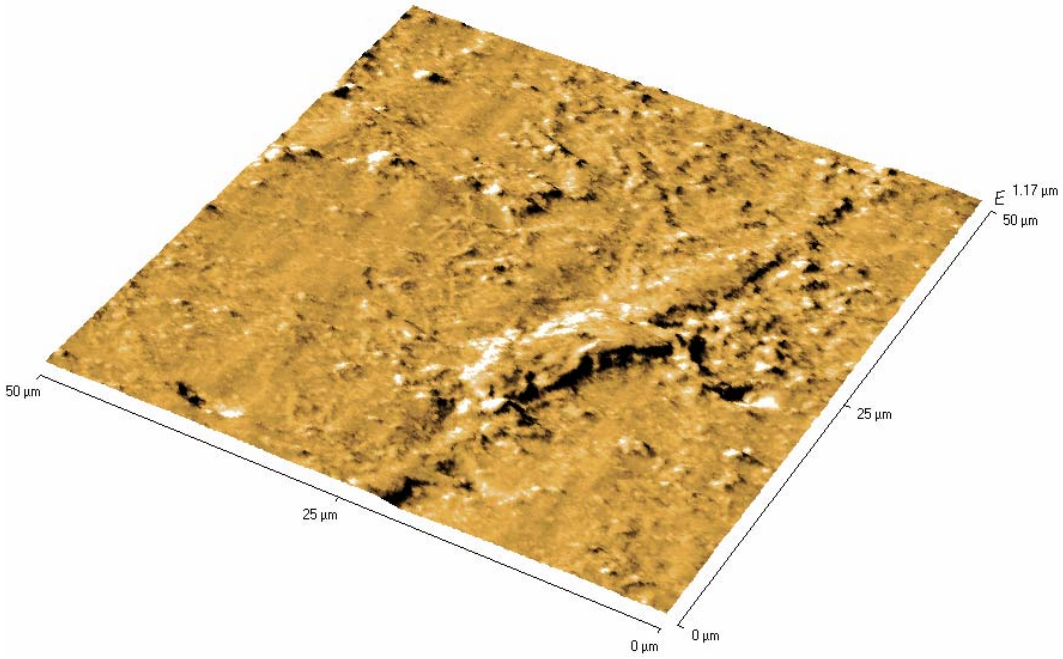

Figure 3.80 *Topographical image of PEO / PCL blend micro-moulded tablet type 2.*

3.4.5 Drug release

It is widely reported that geometric factors play an important role in altering the dissolution rate of an active agent from a monolithic device (Karasulu et al. 2000; Chopra et al. 2002). Particles of irregular shape may be surrounded by a thicker hydrodynamic boundary layer, through which the API must diffuse thus slowing the release of the active agent. Hence for differently shaped particles the boundary conditions are different and thus the drug release kinetics differ in a corresponding manner. To minimise the effect of geometric factors on the drug release from the drug delivery devices studied herein, all of the moulds were designed to make cylindrical matrices.

Figures 3.81 and 3.82 show the overlaid dissolution curves for the matrices moulded using the ram-type injection moulding technique in 0.2M HCl (pH 1.2) and pH 10 buffer respectively.

Drug release data shows that the release from PEO matrices is pH insensitive and proceeds at the same rate regardless of the medium; this was previously noted in section 3.1.1.7. Release of the API from the PEO / PCL blend is also not observed to be affected by the pH of the medium, however, the presence of the more hydrophilic PCL is seen to slow the release of the API when compared to the PEO matrix.

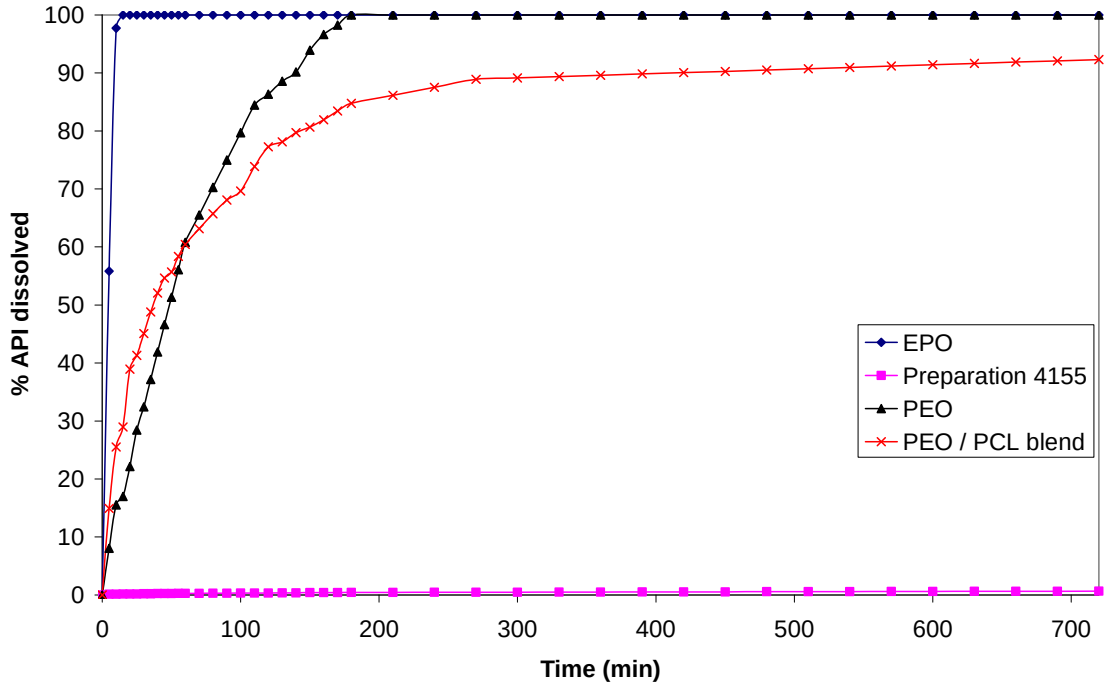

Figure 3.81 *Drug release data in 0.2M HCl (pH 1.2) for the matrices moulded using the ram-type injection moulding technique.*

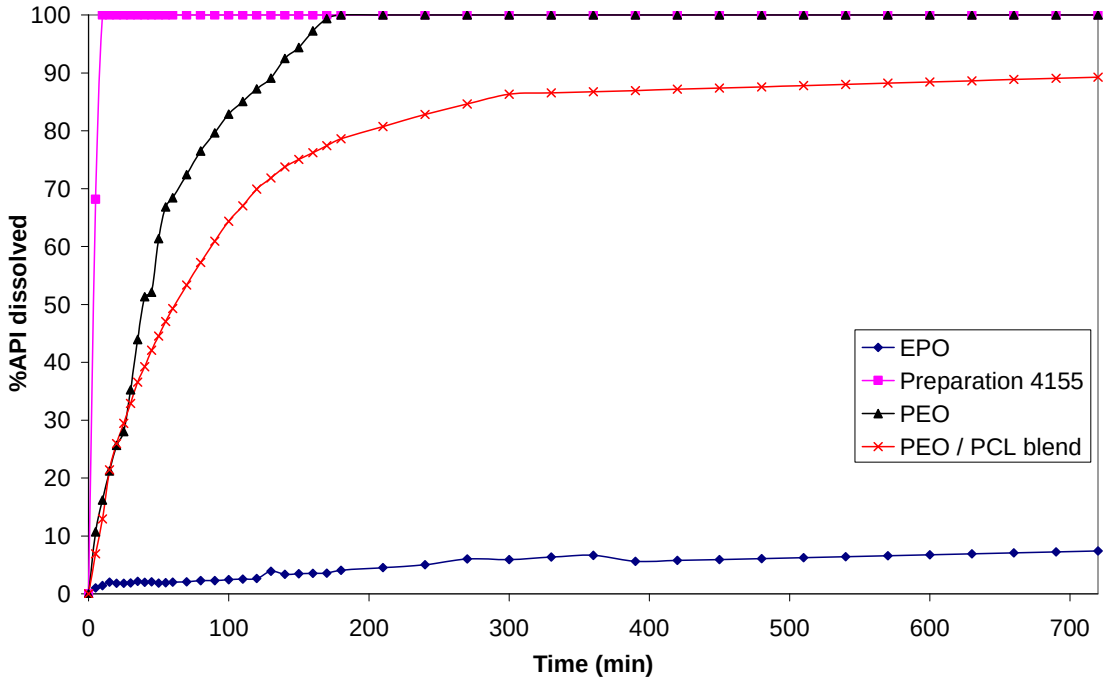

Figure 3.82 *Drug release data in pH 10 buffer for the matrices moulded using the ram-type injection moulding technique.*

The cationic polymer EPO carries amino groups and dissolves quickly by salt formation in the acid environment but as noted earlier, in section 3.2.2.5, EPO does not dissolve above pH 5.5, but swells, resulting in very slow release of the API in pH 10 buffer. However, the purpose of the EPO matrix is to act as a burst release dosage form within the capsule, thus the release rate of the EPO in the higher pH regions is of no consequence. Eudragit preparation 4155 is an experimental polymer from Degussa Ltd, and is not yet commercially available. Preparation 4155 is designed specifically for colonic release. As can be seen from the drug release data obtained in this trial, no API is released in the low pH environment but in the pH 10 buffer preparation 4155 releases the API almost immediately.

Because the PEO / PCL blend matrix was successfully moulded using both the micro-moulding and ram-type injection moulding techniques comparison of the drug release from the different matrix sizes is possible. Figures 3.83 and 3.84 display drug release data for PEO/PCL matrices produced using the Ram type injection moulding process and both tablet types produced using the micro-moulding process.

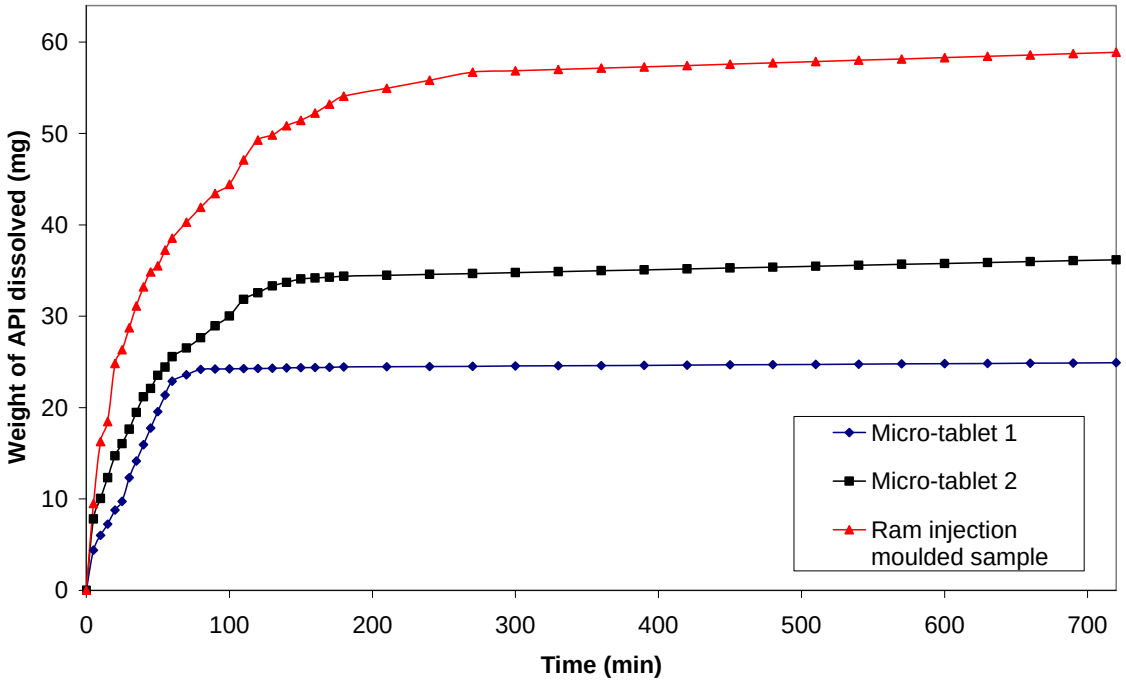

Figure 3.83 *Drug release data in 0.2M HCl (pH 1.2) for the PEO / PCL blend matrices moulded using the ram-type injection moulding technique and the micro-moulding technique.*

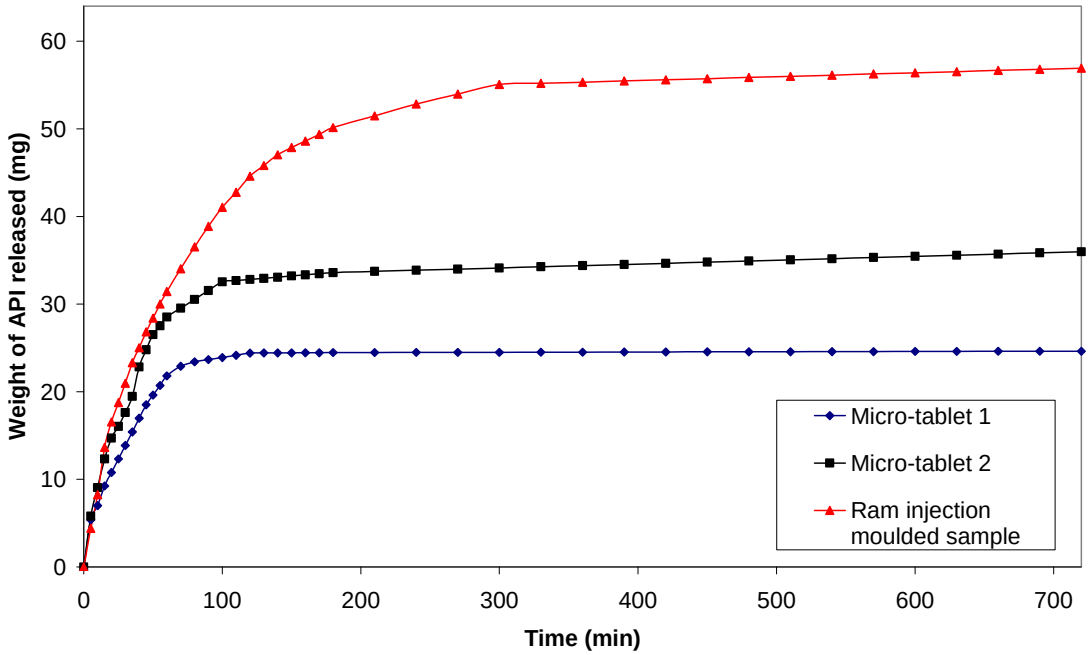

Figure 3.84 *Drug release data in pH 10 buffer for the PEO / PCL blend matrices moulded using the ram-type injection moulding technique and the micro-moulding technique.*

Micro-tablet 1, micro-tablet 2 and the ram injection moulded sample weigh 0.145g, 0.19g and 0.315g respectively. With 20%wt API loading in each matrix that equates to 29mg, 38mg and 63mg diclofenac sodium in micro-tablet 1, micro-tablet 2 and the ram injection moulded sample respectively. These results indicate that release profile for the PEO / PCL matrix is similar regardless of the physical size of the matrix. This is due to the surface area for dissolution increasing as the size of the tablet increases.

3.4.6 Summary

Processing of the matrices selected for this work showed that not all of the materials were capable of being processed in conventional screw-type injection moulding equipment. However, with some difficulty all of the materials could be processed using ram-type injection moulding equipment. Different drug release profiles were successfully achieved using the various materials, including pH sensitive and pH insensitive drug release. These matrices could easily be combined within a single capsule to deliver a range of release profiles for a single API or to deliver more than one API to targeted regions along the GI tract.

Chapter 4

Conclusions

The aim of this study was to produce a range of polymer based monolithic matrices for controlled oral drug delivery using conventional polymer processing equipment. Poly (ethylene oxide) (PEO) was chosen as the primary matrix forming polymer for the work described herein. The molecular weight of the PEO polymers forming the matrix was varied in order to investigate the effect of PEO molecular weight on the processability and drug release characteristics of the matrix. In addition, batches of material were prepared with varying levels of API inclusion to investigate the effect of drug loading on the characteristics of the matrix. Torque and die head pressure measurements taken during the processing of the matrices indicate that at higher percentages of PEO Mw 5 million inclusion the matrix is more difficult to process and was therefore more viscous, this was confirmed by steady state rheometry. Incorporation of PEO Mw 5 million also imparted more strength to the matrix and resulted in longer dissolution times of the active agent. PEO matrices released the API at a rate independent of the pH of the test media. The active agent was observed by thermal analysis and rheometry to have a plasticising effect on the polymer matrix, this was consistent with observations made during processing of the matrix. Higher loading of API was noted to disrupt the PEO crystallisation process using AFM. As the proportion of API inclusion increased the speed of drug release from the polymer matrix increased. This may be due to less rate controlling polymer being present in the matrix at higher API loading.

The stability of PEO (Mw 200,000) when subjected to multiple extrusion operations, both with and without an incorporated active agent, was studied. A significant decrease in the viscosity and by inference, a decrease in the molecular weight of the material, in addition to changes in the morphology of the polymer was noted after the fourth processing step. The results obtained indicate that careful processing of PEO matrices is necessary in order to ensure that extruded material produced is suitable for use in a monolithic matrix for oral drug delivery. Storage conditions have an affect on the molecular weight and crystallinity of PEO. Higher storage temperatures were shown to reduce the molecular weight of PEO matrices quicker than lower storage temperatures. Higher molecular weight PEO matrices were shown to be more vulnerable to decreases in

molecular weight during storage than matrices made up of lower molecular weight material. PEO matrices exposed to UV radiation were shown to have undergone a substantial decrease in molecular weight. An increase in the degree of crystallinity of PEO matrices subjected to UV radiation was also observed. Careful consideration of the storage conditions to which the polymer will be subjected must take place if the polymer is to be useful as a monolithic matrix for oral drug delivery.

PCL / PEO blends were investigated as monolithic dosage forms and in addition the effect of extrusion process variables on the properties of the resultant matrices was studied. The percentage inclusion of PCL in the matrices was altered in order to investigate the effect of PCL inclusion on the properties of the matrix. Both processing temperature and screw speed were varied during the production of the matrices described in this section to ascertain if the process parameters used could affect the end properties of the matrices. Torque and die head pressure measurements taken during processing indicate that inclusion of PCL renders the matrices more easily processable. Higher processing temperatures also resulted in easier processing of the matrices due to lower polymer melt viscosity. Higher screw speeds resulted in higher observed values for torque and die head pressure due to the higher shear being generated during the extrusion process. Thermal analysis of the blends indicated that as the blend composition varied, so too did the melting behaviour. No adverse thermal effects were associated with varying the processing conditions. Steady state rheometry of the matrices indicated that the blends incorporating higher levels of PCL were less viscous than those consisting of higher levels of PEO. Higher screw speed was observed to result in slightly lower matrix melt viscosity when compared with matrices compounded using lower screw speeds. Dissolution testing showed that the incorporation of hydrophobic PCL polymer into a PEO matrix results in a retarded drug release profile. The greater the incorporation of PCL, the slower the drug release. Modulation of drug release from PEO / PCL melt blended matrices was achievable by altering the ratio of PCL to PEO in the matrix. In addition, it was seen that the processing parameters used during the compounding of the matrices had no substantial effect on the end properties of the matrices.

The use of supercritical CO_2 as a plasticiser in the hot melt production of a range of polymer matrices for sustained oral drug delivery was examined. Several batches of matrix material were prepared incorporating an active pharmaceutical ingredient and processed both

with and without supercritical CO_2 incorporation. Torque and die head pressure readings taken from the extruder during processing indicate that supercritical CO_2 acts as a plasticiser during the extrusion process, thus allowing for higher extrusion speeds to be achieved. Characterisation of the resultant matrices revealed that the plasticising effect occurs only in the barrel of the extruder and no viscosity reduction is observed after processing. The matrices were seen to be thermally stable with the incorporation of supercritical CO_2 having no effect on the thermal properties of the matrix when measured post processing. μTA revealed that the incorporation of supercritical CO_2 leads to a higher propensity for crystalisation in PEO. Dissolution analysis showed that the use of supercritical CO_2 during the extrusion process resulted in a faster dissolution of API when compared with unassisted extrusion. The results detailed within this section indicate that supercritical fluid assisted hot melt extrusion is a viable enhancement to conventional hot melt extrusion for the production of monolithic dosage forms.
The use of novel filler materials for hot melt extruded dosage forms was investigated. It was found that the presence of the agar filler in the matrix material led to an increase in the viscosity of the matrix material, thus affecting the hot melt extrusion process. This effect was confirmed by steady state rheometry analysis. The rheometry analysis also confirmed that the increase in matrix viscosity was a direct result of percentage inclusion of filler. However, the increase in viscosity was not so substantial as to rule out the use of agar as a filler material in hot melt produced dosage forms. It would, however, limit the amount of agar filler that could be used in the dosage form. Dissolution studies carried out on the dosage forms produced showed that the agar filler slowed down the release of the pharmaceutical agent in an acidic environment. The extent of the increase in dissolution time increased in proportion to the amount of filler present in the matrix. This effect could be of use for extended release dosage forms. The initial cytotoxic and genotoxic tests showed that cells treated with each of the matrices showed high viability rates with little DNA damage indicating, preliminarily, that the matrices are safe for use in the body. The agar filler system explored in this work proved to be a viable alternative to the commonly used microcrystalline cellulose as a filler system in hot melt extruded dosage forms

The use of an organically modified layered silicate as a novel filler material was also studied. It was confirmed by both steady state rheometry and by direct measurement of the torque on the extruder motor and pressure at the extruder die, that the level of inclusion of

nanoclay examined herein did not have sufficient effect on the melt flow properties of the polymer / API matrix to negatively impact the hot melt preparation of the monolithic matrix. These results were in good agreement with MDSC measurements carried out on the matrices prepared using the nanoclay material at different levels of inclusion, which indicated that the presence of the nanoclay material did not have an effect on the melting behaviour of the polymer / API matrix. The mechanical properties of the polymer / API matrix were seen to show an improvement upon the addition of the nanoclay filler, the degree of the improvement in the mechanical properties was directly proportional to the percentage inclusion of nanoclay particles. The presence of the nanoclay filler was shown to retard the release of the API from the monolithic matrix in an acidic buffer, it was proposed that the mechanism of retardation was similar to the mechanism by which nanoclay incorporation improves the gas barrier properties in conventional nanocomposites. The degree of retardation of the API release from the monolithic matrix was also observed to increase in direct proportion to the percentage inclusion of nanoclay. Lateral force AFM images indicate that the nanoclays were not fully exfoliated in the polymer / API matrix. It is believed that a twin screw extruder with a larger L/D ratio to the equipment used in this trial would more fully exfoliate the nanoclay particles in the polymer / API matrix. The work described herein indicates that nanoclay materials may be of use in the modulation of drug release from sustained release monolithic matrices produced using hot melt extrusion.

Processing of the matrices selected for the micro-moulding trials showed that not all of the materials were capable of being processed in conventional screw-type injection moulding equipment. However, all of the materials could be processed using ram-type injection moulding equipment. Different drug release profiles were obtained using the various materials, including pH sensitive and pH insensitive drug release. These matrices could easily be combined within a single capsule to deliver a range of release profiles for a single API or to deliver more than one API to targeted regions along the GI tract.

References

References

Abuchowski, A., McCoy, J., Palczuk, N., Es, T., Davis, F., 1977. Effect of covalent attachment of polyethylene glycol on immunogenicity and circulating life of bovine liver catalase. *J.Biol. Chem.*, **252**, 3582

Agrawal, C., Athanasiou, K., 1997. Technique to control pH in vicinity of biodegrading PLA-PGA implants. *J. Biomed. Mater. Res.*, **38**, 105

Aikawa, K., Mitsutake, N., Uda, H., Shimamura, H., Aramaki, Y., Tsuchiya S., 1998. Drug release from pH-response polyvinylacetal diethylaminoacetate hydrogel, and application to nasal delivery. *Inter. J. Pharmace.*, **168**, 181

Alderborn, G., Aulton, M.E., (Ed), 2002. Pharmaceutics; the science of dosage form design. Elsevier Science, 397

Alexandre, M., Dubois, P., 2000. Polymer-layered silicate nanocomposites: preparation, properties and uses of a new class of materials. *Mater. Sci. Eng. Res.*, **28**, 1

Aliabadi, H., Mahmud, A., Sharifabadi, A., Lavasanifar, A., 2005. Micelles of methoxy poly(ethylene oxide)-b-poly(q caprolactone) as vehicles for the solubilization and controlled delivery of cyclosporine A. *J. Contr. Rel.*, **104**, 301

Allen, C., Han, J., Yu Y., Maysinger, D., Eisenberg, A., 2000. Polycaprolactone–b-poly(ethylene oxide) copolymer micelles as a delivery vehicle for dihydrotestosterone *J. Contr. Rel.*, **63**, 275

AlNimry, S., Assaf, S., Jalal, I., Najib, N., 1997. Adsorption of ketotifen onto some pharmaceutical excipients, *Int. J. Pharm.*, **149**, 115

Ames, N., McCann, J., Yamasaki, E. 1975. Methods for detecting carcinogens and mutagens with the Salmonella/mammalian microsome mutagenicity test. *Mutation Res.*, **31,** 347

Andrews, R., Wisenberger. M., 2004. Carbon nanotube polymer composites. *Curr. Opin. Solid State Mater. Sc.i,* **8**, 31

Angelova, N., Hunkeler, D., 1999. Rationalizing the design of polymeric biomaterials, *Biomaterials*, **17**, 409

Apicella, A., Capello, B., Del Nobile, M., La Rotonda, M., Mensitieri, G., Nicolais, L., 1993. Poly(ethylene oxide) (PEO) and different molecular weight PEO blends, monolithic devices for drug release. *Biomaterials,* **14**, 83

Armani, D.K., Liu, C., 2000. Microfabrication technology for polycaprolactone, a biodegradable polymer. *J. Micromec. Microeng.*, **10**, 80

Atala, A., Mooney, D., 1997. Synthetic biodegradable polymer scaffolds. Birkhauser Boston

Bae Y., Gulari E., 1997. Viscosity reduction of polymeric liquid by dissolved carbon dioxide. *J. Appl. Polym. Sci.,* **63**, 459.

Barker, S., Murray, D., Zheng, J., Liang, Li. Weinfeld, M., 2005. A method for the isolation of covalent DNA–protein crosslinks suitable for proteomics analysis. *Anal. Biochem*, **344**, 204

Basit, A., Newton, J., Lacey, L., 1999. Formulation of ranitidine pellets by extrusion-spheronization with little or no microcrystalline cellulose. *Pharm. Dev. Technol*., **4**, 499

Bettini, R., Colombo, P., Massimo, G., Catellani, P., Vitali, T., 1994. Swelling and drug release in hydrogel matrices: polymer viscosity and matrix porosity effects. *Eur. J. Pharm. Sci.,* **2**, 213

Bettini, R., Massimo, G., Catellani, P., Peppas, N., Colombo, P., 1995. Zero order release by partial coating of HPMC matrix tablets with permeable and semipermeable films. Proceed. lst World Meeting Pharmaceutics. *Biopharm. Pharm. Technol.*, 288

Bicerano. J., 1996. Prediction of polymer properties (2nd ed), Marcel Dekker, New York

Bickerstaff, G., 1997. Immobilisation of enzymes and cells (methods in biotechnology). Humana press

Biswas, M., Sinha Ray. S., 2001. Recent progress in synthesis and evaluation of polymer montmorillonite nanocomposites. *Adv. Polym. Sci.*, **155**, 167

Blaine G., 1946. The uses of plastics in surgery. *Lancet*, **248**, 525

Bourdon, R., Schneider, W., 1998. A systematic approach to microinjection moulding. *Kunststoffe*, **88**, 1791

Braybrook, J., 1997. Biocompatibility Assessment of Medical Devices and Materials. John Wiley & Sons Ltd, England

Brazel, C., Peppas, N., 1996. On the mechanisms of water transport and drug release from swellable hydrogels. *ACS Polym Mat. Sci. Eng.*, **70**, 370

Breitenbach, J., 2002. Melt extrusion: from process to drug delivery technology. *Eur. J. Pharm. BioPharm.,* **54**, 107

Brown, W., Johnsen, R., 1981. Diffusion in polyacrylamide gels. *Polymer*, **22**, 185

Browne, J.E., Feldkamp, J.R., White, J.L., Hem, S.L., 1980. Characterisation and adsorptive properties of pharmaceutical grade clays. *J. Pharm. Sci.*, **69**, 816

Camilleri, M., Colemont, L., Phillips, S., 1989. Human gastric emptying and colonic filling of solids characterized by a new method. *Am. J. Physiol. Gastrointest. Liver Physiol.*, 257

Carstensen, J.T., Kenneth, S., 1971. Nature of bonding in montmorillonite adsorbates. I: surface adsorption. *J. Pharm. Sci.*, **60**, 733

Chang, J., An, Y., Cho, D., Giannelis, E., 2003. Polylactide nanocomposites: comparison of their properties with montmorillonite and synthetic mica (II). *Polymer,* **44**, 3715

Chang, J., Uk, Y., Sur. G., 2003. Poly(lactic acid) nanocomposites with various organoclays. I. thermomechanical properties, morphology, and gas permeability. *J. Polym. Sci. Part B: Polym. Phys.*, **41**, 94

Chasin, M., Langer R., (Ed), 1990. Biodegradable polymers as drug delivery systems. Marcel Dekker, New York 1

Chen, J., Poliks, M., Ober, C., Zhang, Y., Wiesner, U., Giannelis, E., 2002. Study of the interlayer expansion mechanism and thermal-mechanical properties of surface-initiated epoxy nanocomposites. *Polymer*, **43**, 4895

Chiou J., Barlow J., Paul D., 1985. Plasticization of glassy polymers by CO_2. *J. Appl. Polym. Sci.*, **30**, 2633

Chopra, R., Alderborn, G., Podczeck, F., Newton, J., 2002. The influence of pellet shape and surface properties on the drug release from uncoated and coated pellets. *Int. J. Pharm*, **239,** 171

Claxton, A., Cramer, J., Pierce, C., 2001. A systematic review of the associations between dose regimens and medication compliance. *Clin. Ther.*, **23**, 1296

Coignet, F., 1869. U.S patent no. 93,035

Colombo, P., Bettini, R., Massimo, G., Catellani, P., Santi, P., Peppas, N., 1995. Drug Diffusion Front movement is important in drug release control from swellable matrix tablets. *J. Pharm. Sci.*, **84**, 991

Colucci, W., Packer, M., Bristow, M., Gilbert, E., Cohn, J., Fowler, M., Krueger, S., Hershberger, R., Uretsky, B., Bowers, J., 1996. Carvedilol inhibits clinical progression in patients with mild symptoms of heart failure. *Circulation,* **94**, 2800

Costa, H., Ramos, V., Rocha, M., 2005. Rheological properties of polypropylene during multiple extrusion. *Polym. Test.,* 24, 86

Crowley, M., Zhang, F., Koleng, J., McGinity, J., 2002. Stability of polyethylene oxide in matrix tablets prepared by hot melt extrusion. *Biomaterials,* **23**, 4241

Crowley, M., Zhang, F., Koleng, J., McGinity J., 2002. Stability of Poly (ethylene oxide) in matrix tablets prepared by hot melt extrusion. *Biomaterials*, **23**, 4241

Daneshvar M., Kim S., Gulari E., 1990. High-pressure Phase Equilibria of Poly(ethylene glycol)-Carbon Dioxide Systems. *J. Phys. Chem.,* **94**, 2124

Das, T., 2000. The year 2000: Looking back and looking forward. *Indian J. Ophthalmol.,* **48**, 1

Despa, M., Kelly, K., Collier, J. 1999. Injection moulding of polymeric LIGA HARNs. *Microsyst. Technol.*, 60

Dierickx, P., 1998. Cytotoxicity testing of 114 compounds by the determination of the protein content in HepG2 hepatoma cell cultures. *Toxicology In Vitro,* **3**,189

Dimitriu, S., 1994. Polymeric biomaterials. Marcel Dekker

Dittgen, M., Fricke, S., Gerecke, H., Osterwald, H., 1995. Hot spin mixing: a new technology to manufacture solid dispersions. *Pharmazie,* **50**, 225

Duncan, R., Kopecek, J., 1984. Soluble synthetic polymers as potential drug carriers. *Adv. Polym. Sci.,* **57**, 53

Edwards R., Tao Y., Xu S., Wells P., Yun K., Parcher J., 1998. Chromatographic investigation of the effect of dissolved carbon dioxide on the glass transition temperature of a polymer and the solubility of a third component (additive). *Polym. Sci. Part B Polym. Phys.*, **36**, 2537

Efentakis, M., Koutlis, A., Vlachou, M., 2000. Development and evaluation of oral multiple-unit and single-unit hydrophilic controlled-release systems. *AAPS Pharm. Sci Tech.*, **34,** 1

Egan, J., Waterman, N., 1998. Biomaterials and their contribution to the current and future medical device industry in the UK. Report for the department of trade and industry

Fasset, J., 1995. Thin Wall Moulding: How its processing considerations differ from standard injection moulding. *Plast. Eng.*, 35

Favre, E., Girard, S., 2001. Release kinetics of low molecular weight solutes from mixed cellulose ethers hydrogels: a critical experimental study. *Eur. Polym. J.,* **37**, 1527

Fini, A., Fazio, G., Rosetti, F., Holgado, M., Iruín, A., Alvarez-Fuentes, J., 2005. Diclofenac salts. III. Alkaline and earth alkaline salts, *J. Pharm. Sci.*, **94**, 2416

Fisher, E., 1976. Extrusion of Plastics. The Plastics and Rubber Institute, London

Follonier, N., Doelker, E., and Cole, E., 1994. Evaluation of hot-melt extrusion as a new technique loading for the production of polymer based pellets for sustained release capsules containing high loading of freely soluble drugs. *Drug Develop. Ind. Pharm.*, **20**, 1323

Follonier, N., Doelker, E., and Cole, E., 1995. Various ways of modulating the release of diltiazem hydrochloride from hot-melt extruded sustained-release pellets prepared using polymeric material. *J. Contr. Rel.*, **36**, 342

Fried J., Liu H., Zhang C., 1989. Effect of sorbed carbon dioxide on the dynamic mechanical properties of glassy polymers. *J. Poly. Sci. Part C. Polym. Letters*, **27**, 385

Fukuda, M., Peppas, N., McGinity, J., 2006. Properties of sustained release hot melt extruded tablets containing chitosan and xanthan gum. *Int. J. Pharm.*, **310**, 90

Gad, S., 1988. Product safety evaluation handbook. Marcel Dekker Inc: 15

Gehrke, S., 1993. Synthesis, equilibrium swelling, kinetics, permeability and applications of environmentally responsive gels. *Adv. Polym. Sci.*, **110**, 81

Geng, Y., Discher, D., 2006. Visualization of degradable worm micelle breakdown in relation to drug release. *Polymer*, **47**, 2519

Gerhardt L., Manke C., Gulari E., 1997. Rheology of polydimethylsiloxane swollen with supercritical carbon dioxide. *Polym. Sci.Part B Polym. Phys.*, **35**, 523.

Giannelis, E., 1996. Polymer layered silicate nanocomposites. *Adv. Mater.*, **8**, 29

Giannelis, E., 1998. Polymer-layered silicate nanocomposites: synthesis, properties and applications. *Organomet. Chem.*, **12**, 675

Giannelis, E., Krishnamoorti, R., Manias, E., 1999. Polymer–silicate nanocomposites: model systems for confined polymers and polymer brushes. *Adv. Polym. Sci.*, **138**,107

Gilman, J., 1999. Flammability and thermal stability studies of polymer layered-silicate (clay) nanocomposites. *Appl. Clay Sci.*, **15**, 31

Goosen, M., (Ed) 1993. Fundamentals of animal cell encapsulation and immobilization. CRC Press, USA.

Gourgouillion D., Avelino H., Fareleira J., Nunes da Ponte M., 1998. Simultaneous viscosity and density measurement of supercritical CO_2-saturated PEG 400. *J. Supercrit. Fluids*, **13**, 177

Gourgouillion D., Nunes da Ponte M., 1999. High pressure phase equilibria for poly(ethylene glycol)s + CO_2: experimental results and modeling. *Phys. Chem. Chem. Phys.*, **1**, 5369.

Graham, N., 1990. Controlled drug delivery systems. *Chem Iind.,* 482

Grass, M., Colombo, I., Lapasin R., 2000. Drug release from an ensemble of swellable crosslinked polymer particles. *J. Contr. Rel*, **68**, 97

Gross S., Roberts G., Kiserow D., DeSimone J., 2000. Crystallization and solid state polymerization of poly(bisphenol A carbonate) facilitated by Supercritical CO_2. *Macromol.*, **33**, 40

Gupta, K., Rispin, A., Stitzel, K., Coecke, S., Harbell, J., 2005. Ensuring quality of in vitro alternative test methods: Issues and answers. *Regulatory toxicology and pharmacology***, 43**, 219

Herman, M., 1986. Encyclopedia of Polymer Science and Technology, 6, 3rd Edition. John Wiley and sons.

Hill, S. 2001. Micromolding – a small injection of technology. Mater. World (June):24

Hiroi, R., Sinha Ray, S., Okamoto, M., Shiroi. T., 2004. Organically modified layered titanate: a new nanofiller to improve the performance biodegradable polylactide. *Macromol*. *Rapid Commun.,* **25**,1359

Hodgson E., Richard B., Mailman E., Janice E., 2000. Dictionary of Toxicology. Macmillan Reference Ltd

Hoffman, D., in: Okano, T., (Ed.), 1998. Biorelated Polymer and Gels, Academic Press, 231

Holy, E., Fialkov, J., 2003. Use of a biomimetic strategy to engineer bone. *J. biomed. Mat. Res. part A*, **15**, 447

Houde Y., Kulkarni S., Kulkarni M., 1992. Permeation and plasticization behaviour of glassy polymers: a WASD interpretation. *J. Membr. Sci.*, **71**, 117

Hülsmann, S., Backenfeld, T., and Bodmeier, R., 2001 Stability of extruded 17 ss-estradiol solid dispersions. *Pharma. Devel. Tech.*, **6**, 223

Hülsmann, S., Backenfeld, T., Keitel, S., and Bodmeier, R., 2000. Melt extrusion an alternate method for enhancing the dissolution rate of 17 beta-estradiol hemihydrate. *Eur. J. Pharm. Biopharm.*, **49**, 237

Iskedjian, M., Einarson, T., MacKeigan, L., Shear, N., Addis, A., Mittmann, N., Ilersich, A., 2002. Relationship between daily dose frequency and adherence to antihypertensive pharmacotherapy: evidence from a meta-analysis. *Clin. Ther.*, **24**, 302

Janssen, L., 1978. Twin Screw extrusion. *Chem. Eng. Mon.,* **7**, 150

Janssen, L., 1987. Twin Screw Extrusion. Elsevier Scientific Publishing Company Inc., 6

Jaruga, P., Speina, E., Gackowski, D., Tudek, B., Olinski, R., 2000. Endogenous oxidative DNA base modifications analysed with repair enzymes and GC/MS technique. *Nucleic Acids Res.*, **28**, E16

Jung, J., Yoo, S., Lee, S., Kim, K., Yoon, D., Lee, K., 1999. Enhanced solubility and dissolution rate of itraconazole by a solid dispersion technique. *Int. J. Pharm.*, **187**, 209

Kaczmarek, H., Sionkowska, A., Kaminska, A., Kowalonek, J., Swiatek, M., Szalla, A., 2001. The influence of transition metal salts on photo-oxidative degradation of poly(ethylene oxide). *Polym. Deg. Stab.*, **73**, 437

Kaminska, A., Kaczmarek, H., Kowalonek J., 1999. Cobalt(II) chloride catalysed oxidative degradation of poly(ethylene oxide) by a short wavelength UV-radiation. *Polymer,* **40**, 5781

Karasulu, H., Ertan, G., Kose T., 2000. Modeling of theophylline release from different geometrical erodible tablets. *Eur. J. Pharm. Biopharm.*, **49** 182

Kappas, A., 1990. Mechanisms of environmental mutagenesis-carcinogenesis. New York. Plenum Press

Kazarian, S., 2000. Polymer processing with supercritical fluids. *Polymer Sci.*, **42**, 78

Kazarian, S., Vincent M., Bright F., Liotta C., Eckert C., 1996. Specific Intermolecular interaction of carbon dioxide with polymers. *J. Am. Chem. Soc.*, **118**, 1729

Kendall, M., Thornhill, D., Willis, J., 1979. Factors affecting the pharmacokinetics of diclofenac sodium. *Rheumatol. Rehabilitation Suppl.,* **2**, 38

Kenneth, S., Carstensen, J.T., 1972. Nature of bonding in montmorillonite adsorbates II: bonding as an ion-dipole interaction. *J. Pharm. Sci.*, **61**, 420

Kim, C., 1995. Drug release from compressed hydrophilic polyox-WSR tablets. *J. Pharm. Sci.*, **84**, 303

Kim, C., 1998. Effects of drug solubility, drug loading, and polymer molecular weight on drug release from Polyox tablets. *Drug Dev. Ind. Pharm.*, **24**, 645

Kiran E., Sen Y., 1993. Viscosity of polymer solutions in near critical and supercritical polystyrene and n-Butane. Washington. *ACS Polym Mat. Sci. Eng*, **514**, 104

Kishida, A., Ikada,Y., Dumitriu S., (Ed), 2002. Hydrogels for biomedical and pharmaceutical applications. *Polym. Biomaterials,* **2**,133

Korsmeyer, R., Peppas, N., Roseman T., and Mansdorl Z., (Ed.), 1983. Macromolecular and modelling aspects of swelling-controlled systems. Marcel Dekker, Inc

Krawiec, W., Scanlon, L., Fellner, J., Vaia, R., Vasudevan, S., Giannelis, E., 1995. Polymer Nanocomposites: A new strategy for synthesizing solid electrolytes for rechargeable lithium batteries. *J. Power Sources*, **54**, 310

Krishnamoorti, R., Giannelis, E., 1997. Rheology of end-tethered polymer layered silicate nanocomposites. *Macromol.*, **30**, 4097

Krishnamoorti, R., Ren, J., Silva., A., 2001. Shear response of layered silicate nanocomposites. *J. Chem. Phys.*, **15**, 4968

Krishnamoorti, R., Vaia, R., Giannelis, E., 1996. Structure and dynamics of polymer layered silicate nanocomposites. *Chem. Mater.*, **8**, 1728

Kukla, C., Loibl, H., Detter, H., 1998. Micro-injection moulding – the aims of a project partnership. *Kunststoffe Plast. Europe*, 1331

Kuo, S., Lin, C., Chang, F., 2002. Phase behavior and hydrogen bonding in ternary polymer blends of phenolic resin/poly(ethylene oxide)/poly(ε-caprolactone). *Macromol.*, **35**; 278

Kwag C., Manke C., Gulari E., 1999. Rheology of molten polystyrene with dissolved supercritical and near-critical gases. *J. Polym. Sci. Part B Polym. Phys.*, **37**, 2771

Lagaly, G., 2001. Pesticide–clay interactions and formulations. *Appl. Clay Sci.*, **18**, 205

Lagassé, P. 2001, Columbia Encyclopedia, Columbia university press

Langer R., 1990. New methods of drug delivery. *Science*, **249**, 1527

Lead, J., Starchev, K., Wilkinson, K., 2003. Diffusion coefficients of humic substances in agarose gel and in water. *Environ. Sci. Technol.,* **37**, 482

LeBaron, P., Wang, Z., Pinnavaia. T., 1999. Polymer-layered silicate nanocomposites: an overview. *Appl. Clay Sci.*, **15**, 11

Lee M., Park C., Tzoganakis C., 1999. Measurements and modeling of PS/supercritical CO_2 solution viscosities. *Polym. Eng. Sci*, **39**, 99

Lee M., Tzoganakis C., Park C., 1998. Extrusion of PE/PS blends with Supercritical Carbon Dioxide. *Polym. Eng. Sci.*, **38**, 1112

Lee, J., Park, T., Park, H., Lee, D., Lee, Y., Yoon, S., 2003. Thermal and mechanical characteristics of poly(L-lactic acid) nanocomposite scaffold. *Biomaterials,* **24**, 2773

Lee, P., In Levis D., (Ed.), 1981. Controlled drug release from polymeric matrices involving moving boundaries. Controlled release of pesticides and pharmaceuticals, Plenum Publishing Corporation, 39

Lee, T., Robinson, J., 2000. The science and practice of pharmacy. Lippincott Williams and Wilkins, **2**, 903

Lim, L., Khang, J., Rhees, J., Lee, H., 2000. Monolithic osmotic tablet system for nifedipine delivery. *J. Contr. Rel.*, **67**, 309

Lin, W., Flanagan, D., Linhardt, R., 1999. a novel fabrication of poly(e-caprolactone) microspheres from blends of poly(e-caprolactone) and poly(ethylene glycol)s. *Polymer*, **40** 1731

Liu, J., Zhang, F. and McGinity, J., 2001. Properties of lipophilic matrix tablets containing phenylpropanolamine hydrochloride prepared by hot melt extrusion. *Eur. J. Pharm. Biopharm.*, **52**, 181

Loeb, L., Preston, B., 1986. Mutagenesis by apurinic/apyrimidinic sites. *Annual Review Genetics,* **20,** 201

Lopez A., Gourgouillion D., Pereira P., Ramos A., Nunes da Ponte M., 2000. On the effect of polymer fractionation on phase equilibria in carbon dioxide + poly(ethylene glycol)s systems. *J. Supercrit. Fluids*, **16**, 261

Ma, P., Zhang, R., 2001. Microtubular architecture of biodegradable polymer scaffolds. *J. Biomed. Mat. Res.,* **15**, 469

Maclaine, J., Booth, C., 1975. Effect of molecular weight on crystallization isotherms of high molecular weight polyethylene oxide fractions. *Polymer*, **16**, 680

Maeda, H., Seymour, L., Miyamoto, Y., 1992. Conjugates of anticancer agents and polymers: advantages of macromolecular therapeutics in vivo. *Bioconj. Chem.*, **3**, 351

Maggi, L., Segale, L., Torre, M., Ochoa Machiste, E., Conte, U., 2002. Dissolution behavior of hydrophilic matrix tablets containing two different polyethylene oxides (PEOs) for the controlled release of a water-soluble drug: dimensionality study. *Biomaterials,* **23**, 1113

Mandorsky, L., Straus, S., 1959. Thermal degradation of polyethylene oxide and polypropylene oxide. *J. Polym. Sci.,* **36**, 183

Mank, R., Kala H., Richter, M., 1989. Preparation of extrusion pellets containing drugs on the base of thermoplastics .1 Investigation of drug release. *Pharmazie*, **44**, 773

Mank, R., Kala H., Richter, M., 1990. Preparation of extrusion pellets containing drugs on the base of thermoplastics. 2. Investigations on the improvement of the drug release on the base of thermoplastics. *Pharmazie*, **45**, 592

Martelli, F., 1982. Twin-Screw Extruders: A Basic Understanding. Springer.

McGary, C., 1960. Degradation of poly(ethylene oxide). *J. Polym. Sci.*, **42**, 51

McGinity, J.W., Harris, M.R., 1980 a. Optimization of slow-release tablet formulations containing montmorillonite I. Properties of tablets. *Drug Dev. Ind. Pharm.*, **6**, 399

McGinity, J., Koleng, J., 1997. Preparation and evaluation of rapid-release granules using novel hot melt extrusion technique. *16th Pharmaceutical technology Conference, Athens Greece*, **2**, 153

McNair, A., 1996. Using hydrogel polymers for drug delivery. *Med. Device Tech.*, 16

Mertsch, R., Wolf, B., 1994. Solutions of Poly(dimethyl siloxane) in supercritical CO_2: viscometric and volumetric behavior. *Macromol.*, **27**, 3289

Michaeli, W., Rogalla, A., Ziegmann, C., 1999. Mass-production of microstructures. *Kunststoffe*, **89**, 80

Miller, C., Shanks, H., 2001. Oriented Schwann cell growth on micropatterened biodegradable polymer substrates. *Biomaterials*, **22**, 1263

Mitchell, C., Bahr, J., Arepalli, S., Tour, J., Krishnamoorti, R., 2002. Dispersion of functionalized carbon nanotubes in polystyrene. *Macromol.,* **35**, 8825

Miyagawa, Y., Okabe, T., Yamaguchi, Y., 1996. Controlled release of diclofenac sodium from wax matrix granules. *J. Pharm. Sci.*, **138**, 215

Modak, M., Shanta, M., Sampath, Lester, A., 1990. US Patent 5133090

Moes, A., 1993. Gastroretentive dosage forms. *Crit. Rev. Therap. Drug Carrier Systems*, **10**, 143

Mohanty, A., Drzal, L., Misra, M., 2003. Nano-reinforcement of bio-based polymers—the hope and reality. *Polym. Mater. Sci. Eng.*, **88**, 60

Mohanty, A., Misra, M., Drzal. L., 2001. Surface modifications of natural fibres and performance of the resulting biocomposites: An Overview. *Comp. Interf.*, **8**, 313

Mosharraf, M., Nystrom, C., 1995. The effect of particle size and shape on the surface specific dissolution rate of micronized practically insoluble drugs. *Int. J. Pharm.,* **122**, 35

Nakamichi, K., Yasuura, H., Fukui, H., Oka, M. Izumi, S., 2001. Evaluation of a floating dosage form of nicardipine hydrochloride, and hydropropylmethylcellulose acetate succinate prepared using a twin-screw extruder. *Int. J. Pharm*., **218**, 103

Nalawade S., Picchioni F., Janssen L., 2006. Supercritical carbon dioxide as a green solvent for processing polymer melts: processing aspects and applications. *Prog. Polym. Sci.*, **31**, 19

National Lead Co. 1950. U.S. Patent No. 2531396,

Nguyen, K., West J., 2002. Photopolymerizable hydrogels for tissue engineering applications. *Biomaterials*, **23**, 4307

Nozawa, Y., Mizumoto, T., Higashide, F., 1986. Improving dissolution rate of practically insoluble drug kitasamycin by forcibly roll mixing with additives. *Pharm. Ind.,* **8**, 967

Nozawa, Y., Mizumoto, T., Higshide, F., 1985. Roll-mixing of formulations. *Pharm. Acta Helv.,* **60**, 175

Okada, S., Nakahara, H., Isaka, H., 1987. Adsorption of drugs on microcrystalline cellulose suspended in aqueous-solutions. *Chem. Pharm. Bull.*, **35**, 761

Okamoto, M., in: Nalwa, H., (Ed.), 2004. Polymer/Clay Nanocomposites, Encyclopedia of Nanoscience and Nanotechnology. American Scientific

Oya, A., Pinnavaia, T., Beall, G., (Ed). 2000. Polymer clay nanocomposites. Wiley; London

Ozeki T., Yuasa H., Kanaya Y., 1997. Application of the solid dispersion method to the controlled release of medicine. Difference in the controlled release of flurbiprofen from solid dispersions with PEO and HPMC. *Int. J. Pharm.*, **155**, 209

Ozeki, T., Yuasa H., Kanaya, Y., 1999. Control of medicine release from solid dispersion composed of the poly(ethylene oxide)—carboxyvinylpolymer interpolymer complex by varying molecular weight of poly(ethylene oxide). *J. Contr. Rel.*, **58**, 87

Packer, M., 2003. Do β-blockers prolong survival in heart failure only by inhibiting the β1-receptor? A perspective on the results of the COMET trial. *J. Card. Fail.*, **9**, 429

Packer, M., Coats, A., Fowler, M., Katus, H., Krum, H., Mohacsi, P., Rouleau, J., Tendera, M., Castaigne, A., Roecker, E., Schultz, M., DeMets, D., 2001. Effect of carvedilol on survival in severe chronic heart failure. *N. Engl. J. Med.,* **344**, 1651

Packer, M., Colucci, W., Sackner-Bernstein, J., Liang, C., Goldscher, D., Freeman, I., Kukin, M., Kinhal, V., Udelson, J., Klapholz, M., 1996. Double-blind, placebo-controlled study of the effects of carvedilol in patients with moderate to severe heart failure: the PRECISE trial. *Circulation,* **94**, 2793

Palmskog, G., 1997. In: Proceedings of the 1997 international conference on solid-state sensors and actuators. 1415

Pandey, J., Kumar, P., Misra, M., Mohanty, A., Drzal, L., Palsingh, R., 2005. Recent Advances in Biodegradable Nanocomposites. *J. Nanosci. Nanotech.,* **5**, 497

Park C., Suh N., 1996 a. Filamentary extrusion of microcellular polymers using a rapid decompressive element. *Polym. Eng. Sci.*, **36**, 34.

Park C., Suh N., 1996 b. Rapid polymer/gas solution formation for continuous production of microcellaur plastics. *J. Manuf. Sci. Eng.*, **118**, 639.

Park, S., Kim, K., Kim, S., 2005. Effect of poly(ethylene oxide) on the release behaviors of poly(e-caprolactone) microcapsules containing erythromycin. *Colloids and surfaces B: Biointerfaces,* **43**, 238-244

Park J., Lakes R., 1992. Biomaterials: an introduction. Springer Inc.1

Paul, D., 1978. Polymer Blends. **1** Academic press

Peppas, L., 1997. Polymers in controlled drug delivery. Medical plastics and biomaterials magazine.

Perissutti, B., Newton, M., Podczeck, F., Rubessa, F., 2002. Preparation of extruded carbamazepine and PEG 4000 as a potential rapid release dosage form. *Eur. J. Pharm. Biopharm.,* **53**, 125

Pinto J., Wunder, K., Okoloekwe, A., 2004. Evaluation of the Potential Use of Poly(ethylene oxide) as Tablet- and Extrudate-Forming Material. *AAPS Pharm. Sci.*, **6**, 1

Piskin, E., Hoffman, A., 1986. Polymeric biomaterials, Nijhoff publications

Potschke, P., Bhattacharyya, A., Janke, A., Goering, H., 2003. Melt-mixing of polycarbonate/multi-wall carbon nanotube composites. *Compos. Interfaces,* **10**, 389

Qiu, Z., Ikehara, T., Nishi, T., 2003. Miscibility and crystallization of poly(ethylene oxide) and poly(e-caprolactone) blends. *Polymer*, **44**, 3101

Rabek, J., 1987. Mechanisms of photophysical processes and photochemical reactions in polymers. John Wiley and Sons, 28.

Rabek, J., 1995. Polymer Photodegradation. Mechanisms and experimental methods. Chapman and Hall

Ranga Rao, K., Padmalatha Devi, K., 1988. Swelling controlled-release systems: recent developments and applications. *Int. J. Pharm.*, **48**, 1

Ratner, B., 1996. Biomaterials science, an introduction to materials. Elsevier

Rauwendaal C., 1986. Polymer Extrusion, Hanser publishers

Recum, A. 1998. Handbook of Biomaterials evaluation – Scientific, Technical, and Clinical Testing of Implant Materials – 2nd edition. Taylor and Francis

Rehman, I., Andrews, E., Smith, R., 1996. In vitro degradation of poly(ester-urethanes) for biomedical applications. *J. Mat. Sci. Mat. Med.*, **7**, 17

Repka, M., McGinity, J., 2000. Influence of Vitamin E TPGS on the properties of hydrophilic films produced by hot-melt extrusion. *Int. J. Pharm.*, **202**, 63

Rippie, E., Johnson J., 1969. Regulation of dissolution rate by pellet geometry. *J. Pharm. Sci.*, **58**, 428

Risbud, M., Hardikar, A., Bhat, S., Bhonde, R., 2000. pH-sensitive freeze-dried chitosan-polyvinyl pyrrolidone hydrogels as controlled release system for antibiotic delivery. *J. Contr. Rel.*, **68**, 23

Rivera, S., Ghodbane, S., 1994. In-vitro adsorption-desorption of famotidine on microcrystalline cellulose. *Int. J. Pharm.*, **108**, 31

Ruel-Gariépy, E., Chenite, A., Chaput, C., Guirguis, S., Leroux, J., 2000. Characterization of Thermosensitive chitosan gels for the sustained delivery of drugs. *Inter. J. Pharm.*, **203**, 89

Russel, W., Burch, R., 1959. The Principle of Humane Experimental Technique. Methuen. 238

Sato, H., Miyagawa, Y., and Okabe, T., 1997. Dissolution mechanism of diclofenac sodium from wax matrix granules. *J. Pharm. Sci.*, **86**, 929

Savas, H., Guven, O., 2001. Investigation of active substance release from poly (ethylene oxide) hydrogels. *Int. J. Pharm.,* **224**, 151

Scheirs, J., Bigger S., Delatycki, O., 1991. Characterizing the solid state thermal oxidation of poly(ethylene oxide) powder. *Polymer*, **32**, 2014

Schenkel, G., 1966. Plastics Extrusion Technology & Theory. Iliffe Books Ltd

Schroeder, M., Kleinebudde, P., 1995. Development of disintegrating pellets obtained from extrusion/spheronisation. *Pharm. Sci.*, 415

Sekikawa, H., Arita, T., Nakano, M., 1978. Dissolution behaviors and gastrointestinal absorption of phenytoin in phenytoin-polyvinylpyrrolidine coprecipitate. *Chem. Pharm. Bull.*, **26**, 118

Sekikawa, H., Fukyda, W., Takada, M., Ohtani, K., Arita, T., Nakano, M., 1983. Dissolution behavior and gastrointestinal absorption of dicumarol from solid dispersion systems of dicumarol-polyvinylpyrrolidine and dicumarol-beta-cyclodextrin. *Chem. Pharm. Bull.*, **31**, 1350

Seymour, L., in: Dimitriu, S., (Ed.), 2002. Polymeric Biomaterials, Marcel Dekker, 843

Shia, D., Hui, C., Burnside, S., Giannelis. E., 1998. An interface model for the prediction of Young's modulus of layered silicate–elastomer nanocomposites. *Polym. Compos.,* **19**, 608

Sinha, R., Islam, M., Bhadra, K., Kumar, G., Banerjee, K., Maiti, M., 2005. The binding of DNA intercalating and non-intercalating compounds to a-form and protonated form of poly(rC)Epoly(rG): Spectroscopic and viscometric study. *Bioorg. Med. Chem.*, **14**, 800

Sinha Ray, S., Bousmina, M., 2005. Biodegradable polymers and their layered silicate nanocomposites: In greening the 21st century materials world. *Prog. Mat. Sci.*, **50**, 962

Sinha Ray, S., Okamoto, M., 2003. Polymer/layered silicate nanocomposites: a review from preparation to processing. *Prog. Polym. Sci.,* **28**, 1539

Sinha Ray, S., Yamada, K., Okamoto, M., Ogami, A., Ueda, K., 2003. New polylactide/layered silicate nanocomposites. 3. High performance biodegradable materials. *Chem. Mater.*, **15**, 1456

Sinha Ray, S., Yamada, K., Okamoto, M., Ueda, K., 2002. Polylactide-Layered Silicate Nanocomposite: A Novel Biodegradable Material. *Nano. Letts.*, **2**. 1093

Sprockel, O., Sen, M., Shivanand, P., and Prapaitrakul, W., 1991. Release of chlorpheniramine maleate from fatty acid ester matrix disks prepared by melt extrusion. *J. Pharm. Pharmac.*, **43**, 377

Sprockel, O., Sen, M., Shivanand, P., Prapaitrakul, W., 1997. A melt extrusion process for manufacturing matrix drug delivery systems. *Int. J. Pharm.*, **155**, 191

Sumathi, S., Ray, A., 2002. Release behavior of drugs from tamarind seed polysaccharide tablets. *J. Pharm. Pharm. Sci.*, **5**, 12

Tabata, Y., Ikada, Y., 1998. Protein release from gelatin matrices. *Adv. Drug Delivery Rev.*, **31**, 287

Tarcha, P., 1991. Polymers for controlled drug delivery. CRC press

Thommes, M., Kleinebudde, P., 2006. Use of k-carrageenan as alternative pelletisation aid to microcrystalline cellulose in extrusion/spheronisation. I. Influence of type and fraction of filler. *Eur. J. Pharm. Biopharm.,* **63**, 59

Timbrell, J., 1991. Principles of biochemical toxicology. Taylor & Francis: 190

Tolls, J., 2001. Sorption of veterinary pharmaceuticals in soils: a review. *Environ. Sci. Technol.,* **35**, 3397

Tuan D., Zollweg J., Harriot P., Rizvi S., 1999. Measurement and modeling of viscosity of supercritical carbon dioxide/biomaterial(s) mixtures. *Ind. Eng. Chem. Res.*, **38**, 2129

Uhrich, K., 1999. Polymeric systems for controlled drug release. *Chem. Rev.*, **99**. 3181

Union Oil Co. 1963. U.S. Patent No. 3084117

Vaia, R., Giannelis. E., 1997. Polymer melts intercalation in organically-modified layered silicates: model predictions and experiment. *Macromol.,* **30**, 8000

Vaia, R., Vasudevan, S., Krawiec, W., Scanlon, L., Giannelis, E., 1995. Synthesis and properties of two Dimensional nanostructues by direct intercalation of polymer melts in layered silicates. *Adv. Mater.*, **7**, 154

Vamvakas, S., Vock, E., Lutz W., 1997. On the role of DNA double-stand breaks in toxicity and carcinogenesis. *Crit. Rev. Tox.*, **27,** 155

Varshosaz, J., Koopaie, N., 2002. Cross-linked poly (vinyl alcohol) hydrogel: study of swelling and drug release behaviour. *Iranian Polym. J.,* **11**, 123

Verhoeven, E., Vervaet, C., Remon, J., 2006. Xanthan gum to tailor drug release of sustained release ethylcellulose mini-matrices prepared via hot melt extrusion: *in vitro* and *in vivo* evaluation. *Eur. Jour. Pharm. Biopharm.*, **63**, 320

Verreck, G., Chun, I., Li, Y., Kataria, R., Zhang, Q., Rosenblatt, J., Decorte, A., Heymans, K., Adriaensen, J., Bruining, M., Remoortere, M., Borghys, H., Meert, T., Peeters, J., Brewster, M., 2005. Preparation and physiochemical characterization of biodegradable nerve guides containing the nerve growth agent abeluzole. *Biomaterials,* **26**, 1307

Verreck, G., Brewster, M., 2004. Melt extrusion-based dosage forms: excipients and processing conditions for pharmaceutical formulations. *Bull.Tech. Gattefosse*, **97**, 85

Verreck, G., Decorte, A., Li, H., Tomasko, D., Arien, A., Peeters, J., Rombaut, P., Van den Mooter, G., Brewster, M., accepted 1 November 2005. The effect of pressurized carbon dioxide as a plasticizer and foaming agent on the hot melt extrusion process and extrudate properties of pharmaceutical polymers. *J. Supercrit. Fluids*, In press Corrected proof

Vervaet, C., Baert, L., Remon, J., 1995. Extrusion–spheronisation – a literature review, *Int. J. Pharm.,* **116**, 131.

Wai, K.N., Banker, G.S., 1966. Some physicochemical properties of the montmorillonites. *J. Pharm. Sci.*, **55**, 1215

Washburn, N., Simon. C., Tona, A., Elgendy, H., Karim, A., Amis, E., 2002. Co-extrusion of biocompatible polymers for scaffolds with co-continuous morphology. *J. Biomed. Mater. Res.*, **60**, 20

Weidner, E., Weismet, V., Knez, Z., Skerget, M., 1997. Phase Equilibrium (solid-liquid-gas) in Poly(ethylene glycol) - carbon dioxide systems. *J. Supercrit. Fluids*, **10**, 139.

Weiner, M., Kotkoskie, L., 2000. Excipient toxicity and safety: drugs and the pharmaceutical sciences. 1**03,** Marcel Dekker.

Wetzels, G., Nelemans, P., Schouten, J., Prins, M., 2004. Facts and fiction of poor compliance as a cause of inadequate blood pressure control: a systematic review. *J Hypertens.,* **22**, 1849

Willaims, D., 1987. Definitions in biomaterials, Progress in biomaterials. **4**, Elsevier press

Williams, D., (Ed.), 1990. An Introduction to Medical and Dental Materials. Concise Encyclopedia of Medical & Dental Materials. Pergamon Press and The MIT Press

Williams, D., Cunningham, J., 1979. Materials in clinical dentistry. Oxford university press

Willis, J., Kendall, M., Jack, D., 1981. The influence of food on the absorption of diclofenac after single and multiple oral doses. *Eur. J. Clin. Pharmacol*., **19**, 33

Willis, J., Kendall, M., Flinn, R., Thornhill, D., Welling, P., 1979. The pharmacokinetics of Diclofenac sodium following intravenous and oral administration. *Eur. J. Clin. Pharmacol.,* **16**, 405

Witt, C., Mader, K., Kissel, T., 2000. The degradation, swelling and erosion properties of biodegradable implants prepared by extrusion or compression moulding of poly(lactide-co-glycolide) and ABA triblock copolymers. *Biomaterials*, **21**, 931

Xiong, Y., Kiran, E., 1995. Miscibility, density and viscosity of polydimethylsiloxane in supercritical carbon dioxide. *Polymer*, **36**, 4817

Yano, K., Usuki, A., Okada, A., Kurauchi, T., Kamigaito, O., 1993. Synthesis and properties of polyimide-clay hybrid. *J. Polym. Sci. A: Polym. Chem.*, **31**, 2493

Yasuura, K., Nakano, H., Hiroyuki, T., Izumi, S. Yoshiaki, K., 2002. The role of kneading paddle and effects of screw revolution speed and water content on the preparation of solid dispersions using a twin-screw extruder. *Int. J. Pharm.*, **241**, 203

Young, C., Koleng, J., McGinity, J., 2002. Production of spherical pellets by hot melt extrusion and spheronization process. *Int. J. Pharm.*, **242**, 87

Young, M., 1988. Bioreactor immobilised enzymes and cells. Elsevier applied science.

Yuan, J., Cao, H., Hellmuth, E., Jean, Y., 1998. Subnanometer hole properties of CO2-exposed polysulfone studied by positron annihilation lifetime spectroscopy. *J. Polym. Sci. (B) Polym. Phys.*, **36**, 3049.

Zhang, F., McGinity, J., 1998. Properties of sustained release tablets prepared by hot-melt extrusion. *Pharm. Develop. Tech.*, **14**, 242

Zhang, F., McGinity, J., 2000. Properties of Hot-melt extruded theophylline tablets containing poly (vinyl acetate). *Drug Develop. Ind. Pharm.*, **26**, 931

Zhong, Z., Zheng, S., Mi, Y., 1999. High-pressure DSC study of thermal transitions of a poly(ethylene terephthalate)/carbon dioxide system. *Polymer*, **40**, 3829

Zimm, K., Schwartz, J., O'Connor, R., 1996. Drug release from a multiparticulate pellet system. *Pharm. Dev. Technol.*, **1**, 37

Appendices

Appendix I

Selected solution viscometry data.

PEO 180,000 (20 degrees)		**PEO 180,000 (40 degrees)**		**PEO 900,000**		**PEO Mw 900,000 (720 hours UV exposure)**	
Percentage viscosity loss	days	Percentage viscosity loss	days	Percentage viscosity loss	days	Percentage viscosity loss	days
0	1	0	1	0	1	0.5	1
0.02	2	0.038	2	0.023	2	0.888	2
0.04	3	0.076	3	0.046	3	1.276	3
0.06	4	0.114	4	0.069	4	1.664	4
0.08	5	0.152	5	0.092	5	2.052	5
0.1	6	0.19	6	0.115	6	2.44	6
0.12	7	0.228	7	0.138	7	2.828	7
0.14	8	0.266	8	0.161	8	3.216	8
0.16	9	0.304	9	0.184	9	3.604	9
0.18	10	0.342	10	0.207	10	3.992	10
0.2	11	0.38	11	0.23	11	4.38	11
0.22	12	0.418	12	0.253	12	4.768	12
0.24	13	0.456	13	0.276	13	5.156	13
0.26	14	0.494	14	0.299	14	5.544	14
0.28	15	0.532	15	0.322	15	5.932	15
0.3	16	0.57	16	0.345	16	6.32	16
0.32	17	0.608	17	0.368	17	6.708	17
0.34	18	0.646	18	0.391	18	7.096	18
0.36	19	0.684	19	0.414	19	7.484	19
0.38	20	0.722	20	0.437	20	7.872	20
0.4	21	0.76	21	0.46	21	8.26	21
0.42	22	0.798	22	0.483	22	8.648	22
0.44	23	0.836	23	0.506	23	9.036	23
0.46	24	0.874	24	0.529	24	9.424	24
0.48	25	0.912	25	0.552	25	9.812	25
0.5	26	0.95	26	0.575	26	10.2	26
0.52	27	0.988	27	0.598	27	10.588	27
0.54	28	1.026	28	0.621	28	10.976	28
0.56	29	1.064	29	0.644	29	11.364	29
0.58	30	1.102	30	0.667	30	11.752	30

Solution viscometry data from PEO stability testing (continued on the next page)

Peo 180,000 (20 degrees)		**PEO 180,000 (40 degrees)**		**PEO 900,000**		**PEO Mw 900,000 (720 hours UV exposure)**	
Percentage viscosity loss	days	Percentage viscosity loss	days	Percentage viscosity loss	days	Percentage viscosity loss	days
0.6	31	1.14	31	0.69	31	12.14	31
0.62	32	1.178	32	0.713	32	12.528	32
0.64	33	1.216	33	0.736	33	12.916	33
0.66	34	1.254	34	0.759	34	13.304	34
0.68	35	1.292	35	0.782	35	13.692	35
0.7	36	1.33	36	0.805	36	14.08	36
0.72	37	1.368	37	0.828	37	14.468	37
0.74	38	1.406	38	0.851	38	14.856	38
0.76	39	1.444	39	0.874	39	15.244	39
0.78	40	1.482	40	0.897	40	15.632	40
0.8	41	1.52	41	0.92	41	16.02	41
0.82	42	1.558	42	0.943	42	16.408	42
0.84	43	1.596	43	0.966	43	16.796	43
0.86	44	1.634	44	0.989	44	17.184	44
0.88	45	1.672	45	1.012	45	17.572	45
0.9	46	1.71	46	1.035	46	17.96	46
0.92	47	1.748	47	1.058	47	18.348	47
0.94	48	1.786	48	1.081	48	18.736	48
0.96	49	1.824	49	1.104	49	19.124	49
0.98	50	1.862	50	1.127	50	19.512	50
1	51	1.9	51	1.15	51	19.9	51
1.02	52	1.938	52	1.173	52	20.288	52
1.04	53	1.976	53	1.196	53	20.676	53
1.06	54	2.014	54	1.219	54	21.064	54
1.08	55	2.052	55	1.242	55	21.452	55
1.1	56	2.09	56	1.265	56	21.84	56
1.12	57	2.128	57	1.288	57	22.228	57
1.14	58	2.166	58	1.311	58	22.616	58
1.16	59	2.204	59	1.334	59	23.004	59
1.18	60	2.242	60	1.357	60	23.392	60

Solution viscometry data from PEO stability testing (continued from the previous page)

Appendix II

Selected DSC thermograms of the materials used in this work.

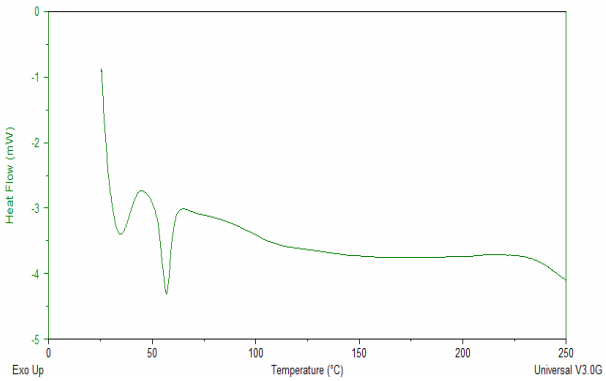

Eudragit EPO

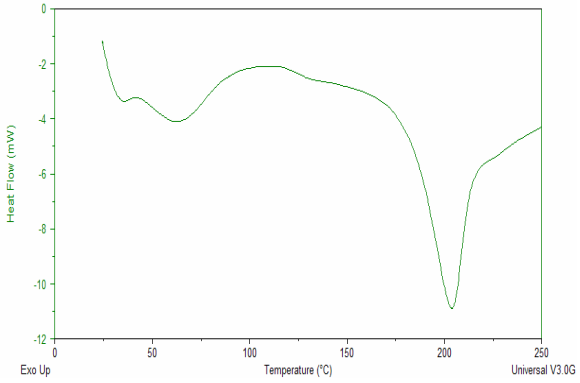

Eudragit L100

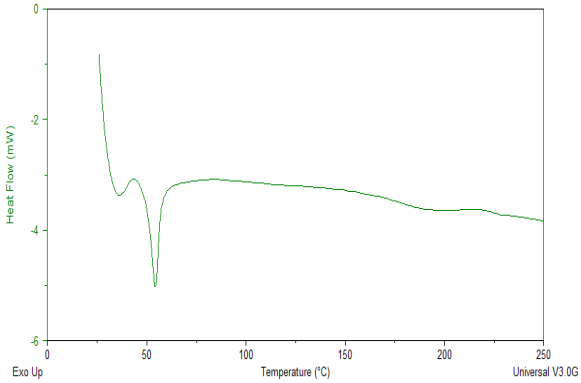

Eudragit Preparation 4155 F

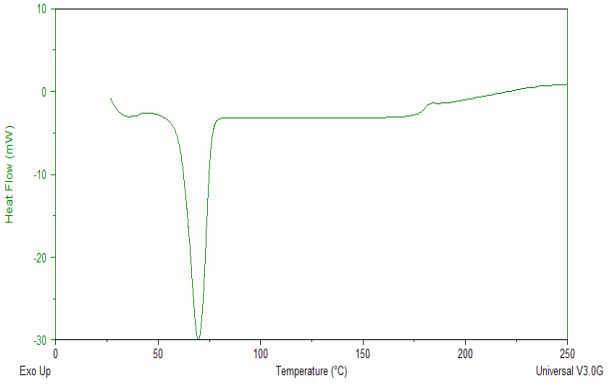

PEO (Mw 1 million)

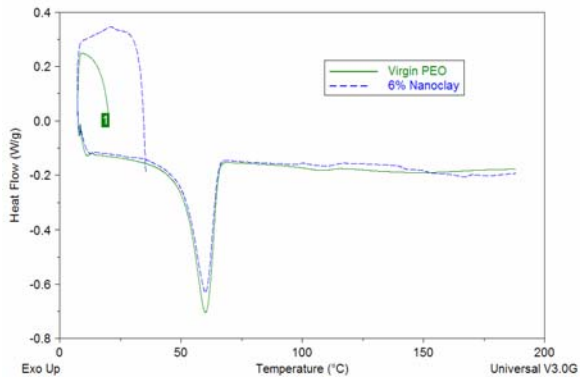

Comparison of virgin PEO polymer and PEO with 6% nanoclay incorporation

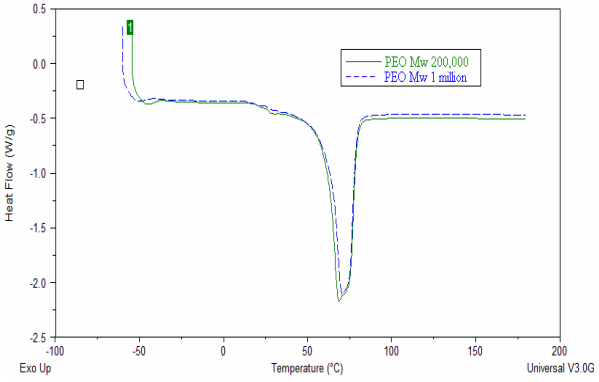

Comparison of PEO (Mw 200,000 and Mw 1 million)

Appendix III

Atomic force images of drug loaded PEO matrices.

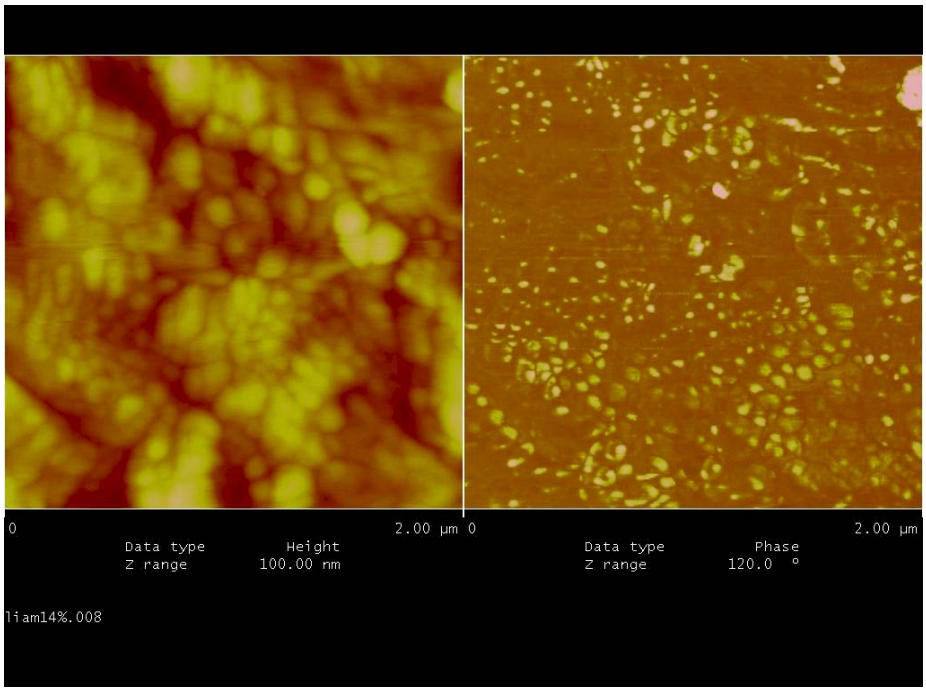

Non-contact AFM analysis of sample containing 10% Carvedilol

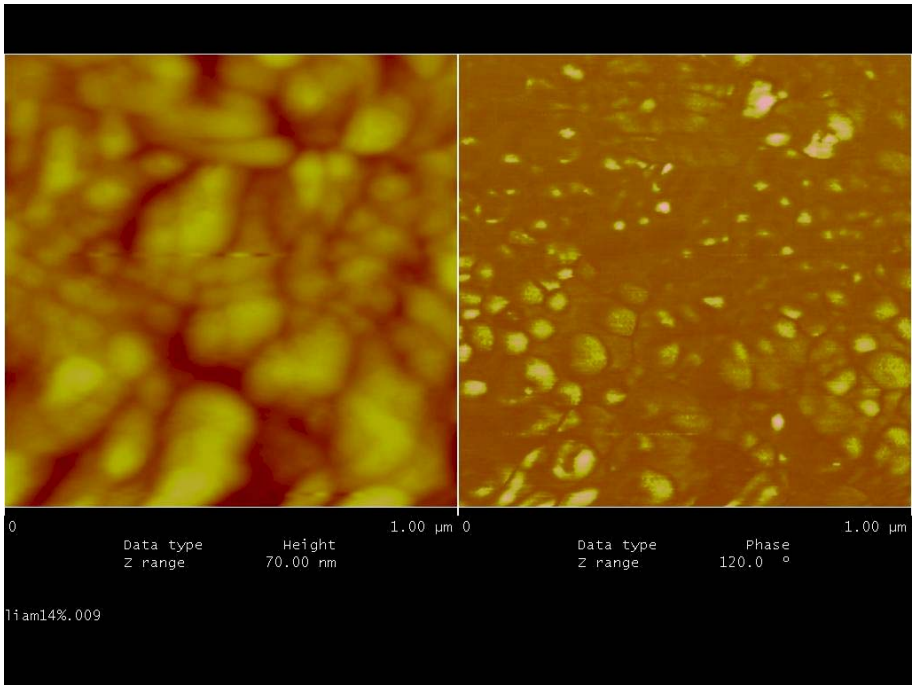

Non- contact AFM analysis of sample containing 30% Carvedilol

Appendix IV

Rheological data for the materials used in this work.

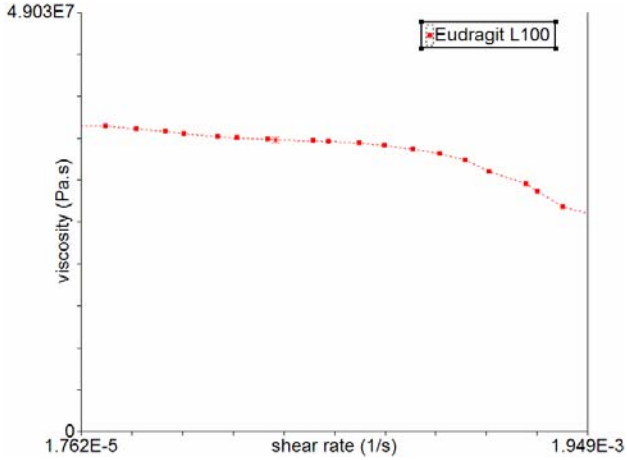

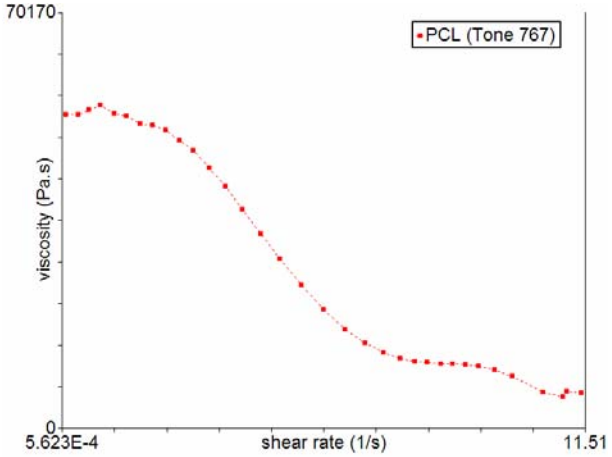

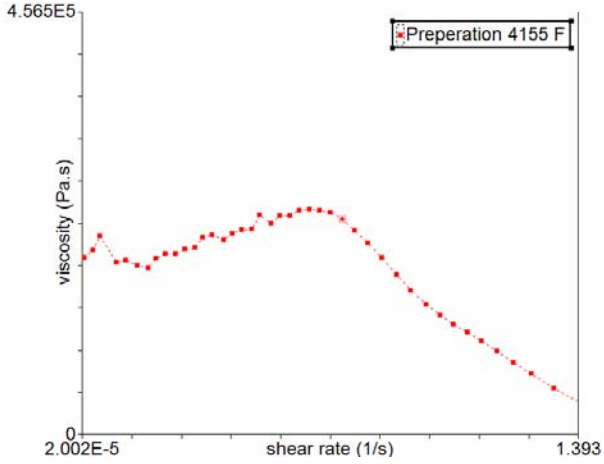

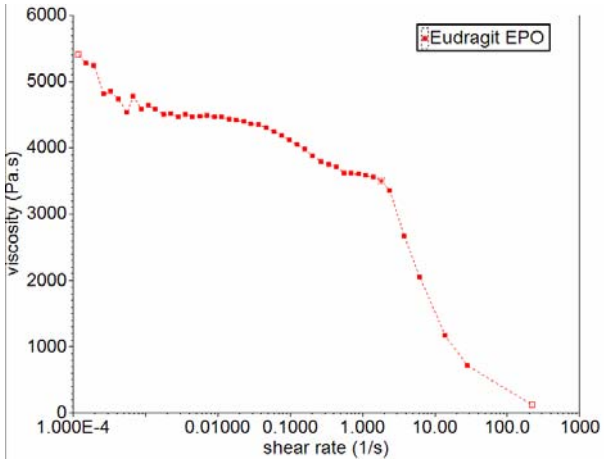

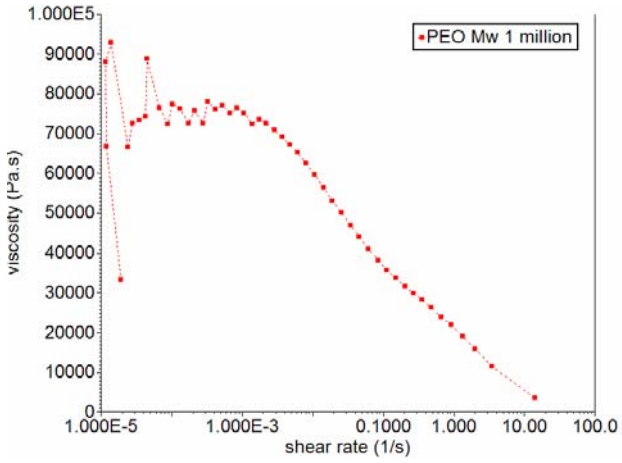

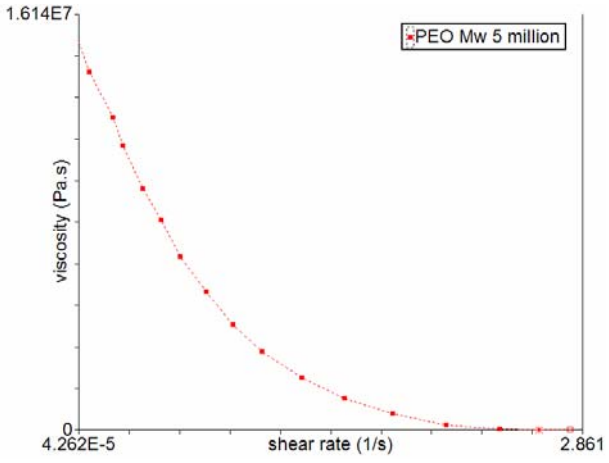

Appendix V

Solid models of the micro-moulding tool generated during the design phase.

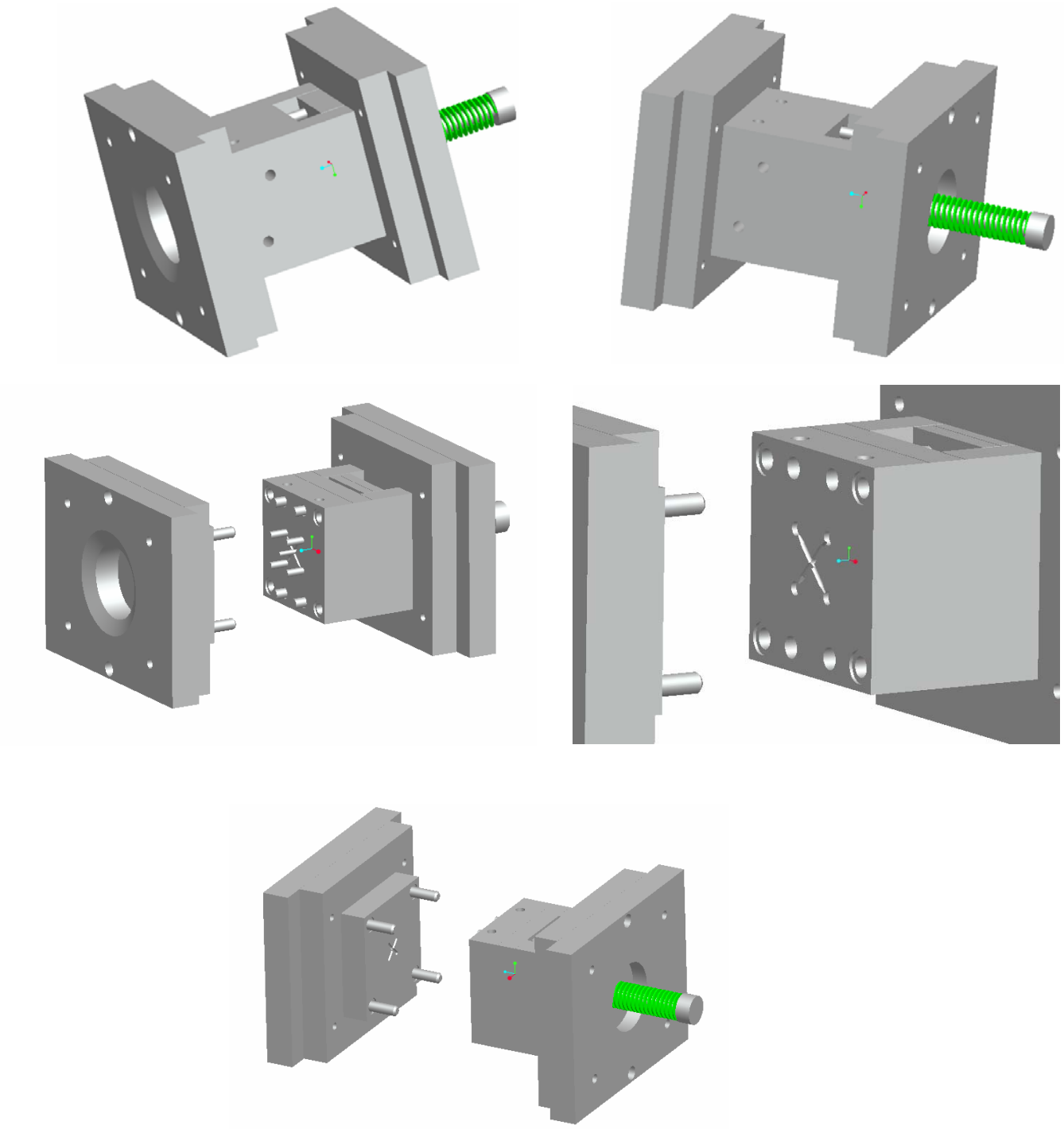

Appendix VI

Theoretical moldflow data generated during the design of the micro-moulding tool.

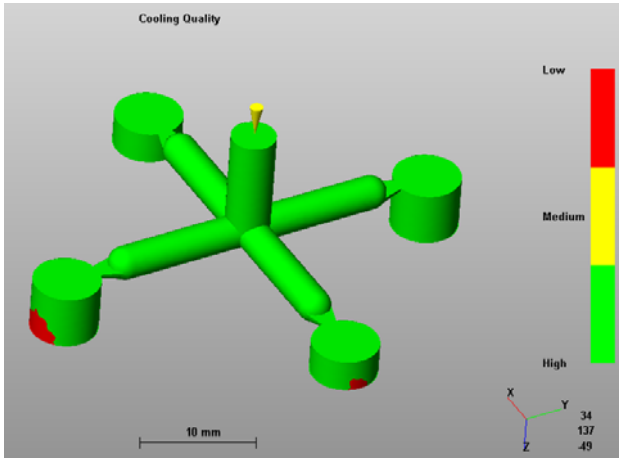

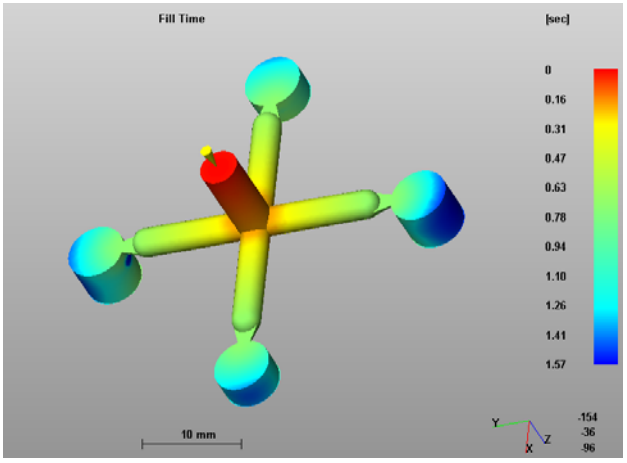

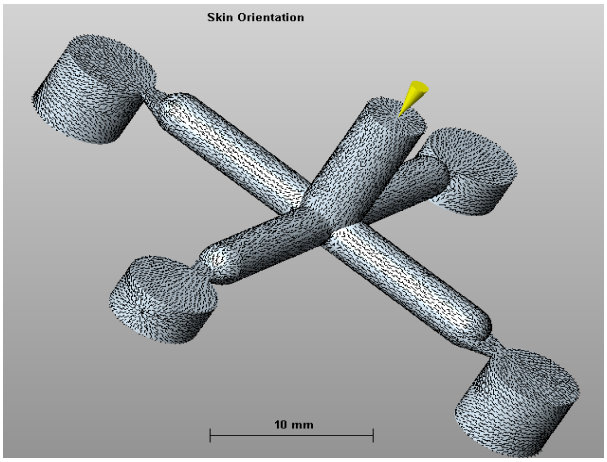

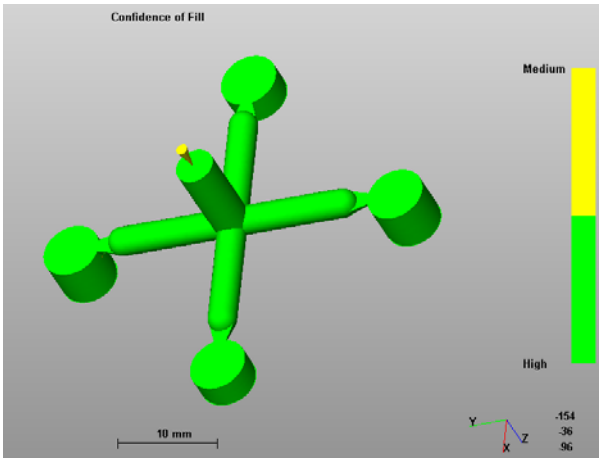

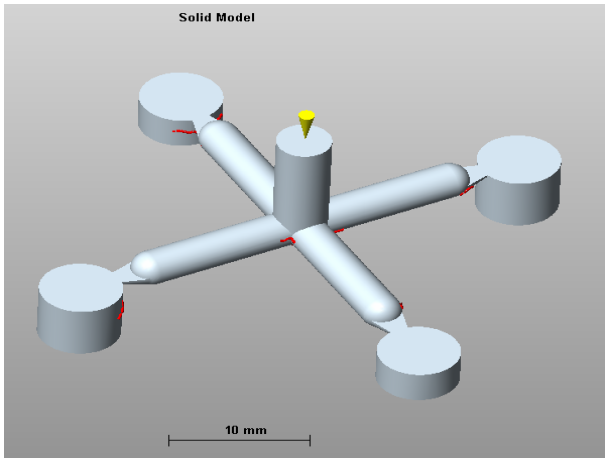
Solid Model
10 mm

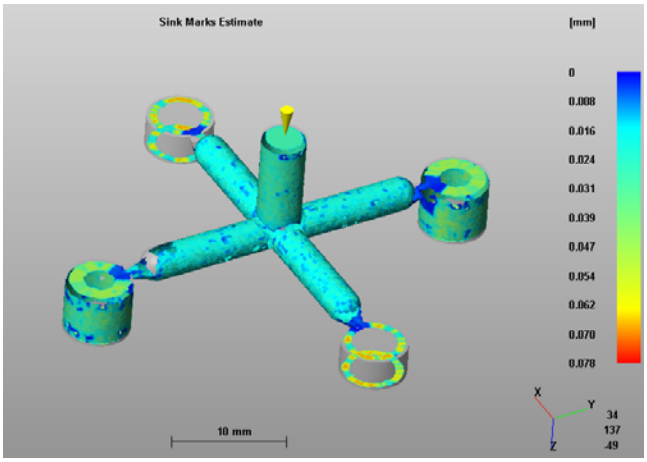
Sink Marks Estimate
[mm]
0
0.008
0.016
0.024
0.031
0.039
0.047
0.054
0.062
0.070
0.078
10 mm
X
Y
Z
34
137
-49

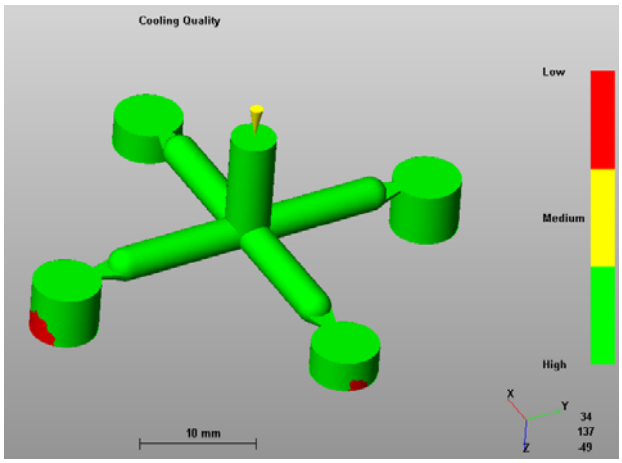
Cooling Quality
Low
Medium
High
10 mm
X
Y
Z
34
137
-49

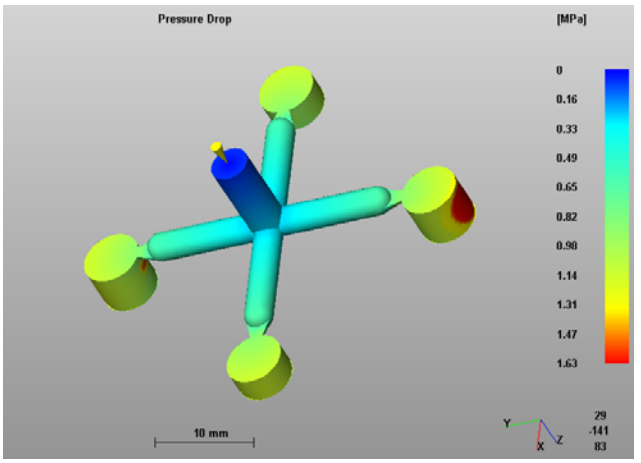
Pressure Drop
[MPa]
0
0.16
0.33
0.49
0.65
0.82
0.98
1.14
1.31
1.47
1.63
10 mm
Y
X
Z
29
-141
83

Relevant Publications